POLITECNICO DI MILANO
ENERGY DEPARTMENT
DOCTORAL PROGRAMME IN ELECTRICAL ENGINEERING, XXVIII-CYCLE

OPTIMAL PLANNING OF HYBRID MICROGRIDS

Doctoral Dissertation of:
Godfrey Gladson Moshi

Supervisor:
Prof. Alberto Berizzi

Co-supervisor:
Dr. Leonardo Taccari

Tutor:
Prof. Castelli Dezza

The Chair of the Doctoral Program:
Prof. Alberto Berizzi

2015 – XXVIII

Abstract

Microgrids stand as the best approach for integration of Distributed Energy Resources (DERs), Energy Storage Systems (ESSs) and conventional generators in order to electrify rural or remote areas in least developed countries (LDCs). Statistics show that 97% of population without access to electricity live in LDCs in sub-Saharan Africa and developing Asia. Studies have also shown that by 2030 only 30% of these un-electrified areas can be reached by grid extensions. In most cases, grid extensions are infeasible due to large distances from the main grids, difficult terrains, and low population with highly dispersed settlements patterns. However, most of un-electrified regions, such as sub-Saharan Africa, are rich of fossil fuels, natural gas, and important renewable resources such as solar, wind, hydro, and geothermal. The remaining challenge is on the planning of rural off-grid electrification systems. Proper planning is of paramount importance in order to realise all technical, economical, and environmental benefits of various types of DERs and ESSs applied for off-grid electrification. In particular, this thesis addresses the problem of optimal planning of hybrid microgrids with solar Photovoltaic (PV) arrays, Wind Turbines (WTs), Storage Battery Banks (SBBs), and conventional Diesel Generators (DGs).

Microgrid planning requires joint optimization of operation and selection of capacities, quantities, and combination of components of different types and technologies. Integration of renewable energy based generation technologies, storage systems, and conventional generators presents technical and economic challenges that must be considered in the planning of hybrid microgrids. Economically, conventional generators such as DGs have lower investment costs but higher operation costs, whereas renewable energy based generators such as solar PVs and WTs have higher investment costs but lower operation costs. Technically, generation from PVs and WTs, are subject to uncertainties and variations of weather conditions, and thus they are not fully dispatchable. These uncertainties and high variations in microgrid demand make Battery Energy Storage System (BESS) necessary, particularly for stand-alone microgrids. One of the main challenges in microgrid planning is to ensure that the components to be installed will offer minimum life cycle operational cost while fulfilling all required technical constraints. Consequently, hourly dispatching of DGs, BESS and other sources, which determine the overall life cycle operational cost, must be considered in the planning of hybrid microgrids.

This thesis applies mathematical programming and optimization approach in planning of hybrid microgrid considering long-term operational constraints. The aim is to obtain the optimum capacities, combination, and number of components to install in a microgrid in order to ensure reliable and continuous supply of its demand at minimum cost. A novel Mixed Integer Linear Programming (MILP) deterministic model for microgrid planning is proposed. The overall microgrid long-term operation is

integrated in this planning model. A technique called Clustered Unit Commitment (CUC) is applied in order to reduce the number of discrete variables required to model DGs operation. In addition, in order to make the model computationally tractable, K-medoids clustering algorithm is applied to select typical representative days with profiles of renewable resources and demand data. Piecewise Linear Approximation (PWLA) of components nonlinear characteristics is carried out to enable the use of CPLEX and GUROBI solvers in General Algebraic Modeling System (GAMS). The deterministic planning model is extended to include uncertainties in renewable resources and electric demand in microgrid planning, based on Two-Stage Stochastic Integer Programming (2SSIP) and Robust Optimization (RO) frameworks. Applicability of the proposed models are demonstrated by using microgrid planning case studies.

Acknowledgements

This dissertation would not have been possible without the help and support of many overlapping communities and individuals. Firstly, I would like to express my sincere gratitude to my advisor Prof. Alberto Berizzi for the continuous support of my Ph.D study and related research, for his patience, motivation, and immense knowledge. His guidance helped me in all the time of research and writing of this thesis. I could not have imagined having a better advisor and mentor for my Ph.D study. Besides my advisor, I would like to thank the rest of my thesis committee: Prof. Dario Zanielli, Prof. Edgardo Castronuovo, and Prof. Renato Rizzo for agreeing to spend their time to assess this thesis. Special thanks to the opponent, Prof. Claudio A. Cañizares, for reading and commenting this thesis.

My sincere thanks also goes to my tutor, Prof. Castelli Dezza, for his guidance and advices. Special thanks to my co-supervisor Dr. Leonardo Taccari, for his guidance and support, particularly on mathematical modelling and computational aspects of this research. Special thanks also goes to Prof. Cristian Bovo, who guided me into the field of power system modeling and optimization by using GAMS. In particular, I am gretful to Prof. Edoardo Amaldi who provided me an opportunity to join his operational research team, and for his valuable ideas and support in the modelling issues. Without their precious support it would not be possible to conduct this research.

This research was funded by the Politecnico di Milano. Thanks to all the university management, particularly the PhD school office, for their support and guidance throughout my studies at Politecnico di Milano. Special thanks to Prof. Emanuela Colombo and Prof. Fabio Inzoli who were the pioneers of the collaboration between my home country institute, The Dar-es-Salaam Institute of Technology, and Politecnico di Milano. This PhD is one of the fruits of their laborious work to support development of local institution in third world countries. Without this collaboration I would have not come to Politecnico di Milano. Also my sincere thanks to all colleagues who work in the research group under Prof. Emanuela Colombo and Prof. Fabio Inzoli guidance. Also I thank my friends and colleagues at the Electrical Engineering section of Energy Department for their support along the way.

Special thanks to my fellow officemates for the stimulating discussions, encouragements, and for all the fun we have had in the last three years. I am very grateful to Dr. Valentin Ilea and Dr. Dinh-Duong Le for encouraging me throughout this journey.

Thanks to my family and relatives for their encouragements and prayers. In particular, special thanks to my wife, Hobokela, and my children, Joel and Elizabeth, for putting up with loneliness when "daddy" was away for three years whilst pursuing this PhD research in Italy. Last but not the least, I am grateful to Pastor, Jim Kutnow, and his wife, Lynda, for supporting me spiritually throughout my stay in Milano. I thank God that he has used Pastor Jim Kutnow to enlighten my life and prepare me to serve others using my professional. Non con la potenza né con la forza, ma con il mio spirito, dice il Signore degli eserciti!

Dedications

To my wife Hobokela, my son Joel, and my daughter Elizabeth.

Queste dunque le tre cose che rimangono: la fede, la speranza e la caritá;
ma di tutte piú grande é la caritá!
And now these three remain: Faith, Hope, and Charity,
but the greatest of these is Charity.

Contents

List of Figures

List of Tables

Acronyms

ANN	Artificial Neural Network.
FL	Fuzzy Logic.
CERTS	Consortium for Electric Reliability Technology Solutions.
DER	Distributed Energy Resource.
DSM	Demand Side Management.
ROI	Return On Investment.
RES	Renewable Energy Resources.
PSO	Particle Swarm Optimization.
SA	Simulated Annealing.
ACA	Ant Colony Algorithm.
AWA	Annual Worth Analysis.
PV	Photovoltaic.
DG	Diesel Generator.
SB	Storage Battery.
SBB	Storage Battery Bank.
WT	Wind Turbine.
BESS	Battery Energy Storage System.
HOMER	Hybrid Optimization of Multiple Energy Resources.
DER-CAM	Distributed Energy Resources Customer Adoption Model.
iHOGA	improved Hybrid Optimization by Genetic Algorithms.
SOC	State of Charge.
MILP	Mixed Integer Linear Programming.
NLP	Nonlinear Programming.
LP	Linear Programming.
MINLP	Mixed Integer Nonlinear Programming.
MPP	Maximum Power Point.
LCCA	Life Cycle Cost Analysis.
LCCA	Life Cycle Cost.

Acronyms

NPC	Net Present Cost.
NPV	Net Present Value.
LCOE	Levelized Cost of Energy.
LFDS	Load Following Dispatch Strategy.
CCDS	Cycle Charging Dispatch Strategy.
IDS	Ideal Dispatch Strategy.
GAMS	General Algebraic Modeling System.
AMPL	A Mathematical Programming Language.
PWLA	Piecewise Linear Approximation.
LDCs	least developed countries.
LDC	Load Duration Curve.
SC	Screening Curve.
ESS	Energy Storage System.
2SSIP	Two-Stage Stochastic Integer Programming.
UC	Unit Commitment.
SCUC	Security Constrained Unit Commitment.
CUC	Clustered Unit Commitment.
PSHP	Pumped Storage Hydroelectric Power Plant.
CF	Capacity Factor.
GA	Genetic Algorithms.
NSGA-II	Non-dominated Sorting Genetic Algorithm-II.
DP	Dynamic Programming.
LPSP	Loss of Power Supply Probability.
STRONG	Trust-Region Response Surface Method.
MCS	Monte Carlo Simulation.
DIRECT	Dividing RECTangles.
DFT	Discrete Fourier Transform.
HOGA	Hybrid Optimisation by Genetic Algorithms.
WASP-IV	Wien Automatic System Planning.
MARKAL	MARKet ALlocation.
EGEAS	Electric Generation Expansion Analysis System.
CGP	Capacity Generation Planning.
LBNL	Lawrence Berkeley National Lab.
NREL	National Renewable Energy Laboratory.
CHP	Combined Heat and Power.
PEV	plug-in electric vehicle.
BD	Bender's Decomposition.
GBD	Generalized Bender's Decomposition.
CAES	Compressed Air Energy Storage.
EFOM	Energy Flow Optimization Model.
TIMES	The Integrated MARKAL/EFOM System.
ESP	energy shortfall probability.
SO	Stochastic Optimization.

RO	Robust Optimization.
BC	Biderectional Converter.
PDF	Probability Distribution Function.
CCG	Column-and-Constraint Generation.
RC	Robust Counterpart.
FC	Fuel Cell.
LHS	Latin Hypercube Sampling.
SOCPs	Second Order Cone Problems.
KiBaM	Kinetic Battery Model.
PAM	Partitioning Around Medoids.
CLARA	Clustering LARge Applications.
CLARANS	Clustering Large Applications based on RANdomized Search.
SSE	Sum of Squared Error.
EDC	Error in Duration Curve.
PCC	Point of Common Coupling.
MCC	Microgrid Central Controller.
LC	Local Controller.
EMM	Energy Management Module.
PCM	Protection Co-ordination Module.
AWEA	American Wind Energy Association.
IEC	International Electrotechnical Commission.
BSI	British Standards Institution.
DOD	depth of discharge.
BMS	Battery Management System.
DSO	Distribution System Operator.
MO	Market Operator.
EMS	Energy Management System.
SOCSDS	Load Following Dispatch Strategy.
FPMRTDS	Full Power/Minimum Run Time Dispatch Strategy.
FDS	Frugal Dispatch Strategy.
MODS	Modified Optimal Dispatch Strategy.
NASA	National Aeronautics and Space Administration.

CHAPTER 1

Introduction

1.1 Motivation and Relevance

Microgrid has emerged as an important paradigm for electrification of rural or remote areas and as a platform for integration of DERs in the existing power grids. A microgrid can be defined as a group of loads connected to DER and and ESS within clearly defined electrical boundaries that can act as a single controllable entity with respect to the main grid [1]. The Consortium for Electric Reliability Technology Solutions (CERTS) considers a microgrid as an aggregation of loads and microsources operating as a single system providing both power and heat. The majority of the microsources must be power electronic based to provide the required flexibility to insure operation as a single aggregated system. This control flexibility allows the microgrid to present itself to the bulk power system as a single controlled unit that meets local needs for reliability and security [2], [3]. The ability to operate in connection to the main grid *(grid-connected mode)* or in disconnection with the main grid *(island, off-grid, or stand-alone mode)* makes microgrid the best option to manage a cluster of local DERs and ESS while maximizing reliability, flexibility and economic benefits which would be impossible to achieve by individual decentralized microsources or load.

The main drivers for microgrid deployment arise from its two features, namely the integration of DERs of different technologies and the ability to operate in stand-alone or grid-connected mode. These two features enhance reliability, efficiency, security, quality, and sustainability of power supply [4]. Using several small DERs may lower power outage probability, thus increasing supply reliability. Since the DERs in microgrids are located close to the end users, there is a significant decrease in distribution losses. The use of energy storage and energy efficiency technologies in microgrid may also lead to increased efficiency. Microgrid can be a solution to postpone huge investment in new transmission and distribution lines required to cope with the growing demand in most electrified areas. For grid-connected microgrids, their ability to seamlessly disconnect from the main grid and continue to supply the demand in stand-alone mode decreases the vulnerability to acts of terrorism, natural disasters and other risks which may happen in large power system and results in cascaded outages. This is particularly important for critical sites such as military bases and hospitals. Integration of Renewable Energy Resources (RES) in remote microgrids offers independence from imported fossil fuel and reduction in fuel consumption [5]. Furthermore, the use of RES increases sustainability by reducing production of greenhouse gas emissions and mitigating climate change. Other drivers for microgrids are: lower energy costs, environmental incentives from the governments, and advancements in DER technologies.

In developed countries, where electricity distribution grids are already in place, microgrids are seen as a “bottom-up” transition towards the so-called Smart Grids. The aims are to be able to provide increased reliability to end users and to maximize the use of primary renewable energy sources for electricity generation. A key study developed by Zprýme and commissioned by the IEEE, found three main benefits of microgrids: to meet local demand, to enhance grid reliability, and to ensure local control of supply [6]. This study indicates that challenges from both DERs and ESSs are transferable to microgrid planning. Several studies have confirmed the important role of microgrids in improving reliability of distribution grids, considering that 80% to 90% of all grid failures start in these networks [7]. It is required that, in case of a fault in neighbouring feeder or a perturbation in the main grid, the microgrid disconnects and continue the operation without any particular problem. These technical requirements must be considered in microgrid planning.

Statistics show that 97% of population without access to electricity live in LDCs in sub-Saharan Africa and developing Asia [8]. In these areas, microgrids are the only way to provide electricity to small remote villages, as connections to the main grids are not available yet. In most cases grid extensions are infeasible due to large distances from the main grids, difficult terrains, and low population with highly dispersed settlements patterns. So far, there has been slow progress in rural electrification particularly due to low end user Return On Investment (ROI) and thus long payback period [9]. This is one of the biggest obstacles towards adoption of microgrids for electrification of rural and remote areas and has been hindering the involvement of private investors. One of the solutions for this problem is to link microgrid development with productive use of energy for poverty reduction. In addition to the above solution, optimal microgrid planning can play a key role here too. The planning should arrive at the optimal solution which fulfills the current end user requirements. Taking advantage of shorter construction time for most microgrid DERs, the planning should consider various scenarios for the future demand growth. In this case, the planning should also consider operation in standing-alone *(off-grid)* mode, but the microgrid should be designed in a way that will allow interconnection to the neighbouring microgrids or to the future extension from the main grid. Again, this can be viewed as "bottom-up" framework that depicts the growth of future active electric distribution systems as a step-by-step aggregation of many small microgrids.

Integration of conventional and renewable based DERs presents new operational and planning challenges in microgrids that needs to be addressed in detail. In this thesis, DER refers to small and modular energy resources, including generation, storage and Demand Side Management (DSM) equipments, that provide energy or storage capacity locally [10], [11]. Different types of DERs that can be found in microgrids include: microturbines, PV generators, WTs, SBB, small hydroelectric turbines, fuel cells, heat recovery systems, and reciprocating engines (commonly DGs). These DERs have different technical and economic specifications. As a results, a mix of these DERs allows them to complement each others' technical and economical limitations and thus results to an optimal system. However, combination of traditional and modern DERs, presents economic and technical challenges in microgrid planning.

Economically, conventional units such as DGs have lower investment costs but higher operation costs, whereas renewable energy based generating units such as Solar PVs and WTs have higher investment costs but lower operation costs. Technically, generation from renewable energy based technologies such as PVs and WTs, which are the main focus of this thesis, are subject to uncertainties and variations of weather conditions. In additional to microgrid's resources uncertainties and variations which make PVs and WTs nondispatchable, microgrid demand is highly variable. Compared to large power systems, microgrids experience much severe effects from uncertainties and variations of resources and demand, particularly due to the reduced number of loads, lower system inertia, and high penetration of RES. These variations and uncertainties make SBB necessary, particularly for stand-alone microgrids. Variations and uncertainties in renewable resources and demand, and dynamics of SBB, require operational flexibility which has significant impact on the microgrid planning. As a result, the overall operation of microgrid becomes very strongly coupled to its planning decisions, and vice versa. Therefore, unlike conventional power system, microgrid planning must consider hourly operation of all components for the complete planning period. A block diagram of microgrid planning approach adopted in this research is shown in Fig.1.1.

Planning a microgrid requires joint optimization of operation and selection of capacities, quantities, and combination of components of different types and technologies. One of the main challenges in planning a microgrid is to solve the resulting model which combines capacity planning and system operational in a single optimization problem. As explained above, the strong coupling between microgrid operation and its capacity planning problem makes it necessary to integrate the two problems in order to obtain optimal planning decisions. Integration of operation and the capacity planning is crucial since inter-hour and intra-hour dynamics can not be neglected in planning microgrids or modern power systems, particularly in the presence of RES and ESS [12]. This is the major difference between microgrid planning and conventional power system planning in which the Load Duration Curve (LDC) model, with the assumptions that ignore inter-hour and intra-hour dynamics, is applied. Techniques which employ LDC model or planning the system based on peak demand data are too conservative and may result in an oversized components or a completely infeasible microgrid plan.

Furthermore, the nonlinear characteristics of microgrid components, time dependent variables for tracking the operation of SBB, and discrete design decisions make microgrid planning model a Mixed Integer Nonlinear Programming (MINLP) problem. The size of design search space and long time required for the planning study make the resulting problem very large and in most cases numerically intractable. To simplify this model it is necessary to adopt PWLA and decomposition techniques. Existing design softwares and most of previous researches on microgrid planning have only focused on simulations to approximate system lifetime operational cost. This enables evaluation of cost and performance of design or planning alternatives which must be specified by the designer. However, simulation approach does not guarantee global optimality thus posing the need to apply mathematical programming method. So far, few studies have applied mathematical programming to plan new microgrids [13]–[16]. Most of these studies adopt very simplified models which can not capture important operational constraints which affect the planning decisions. The research presented in this thesis is aiming at filling the above

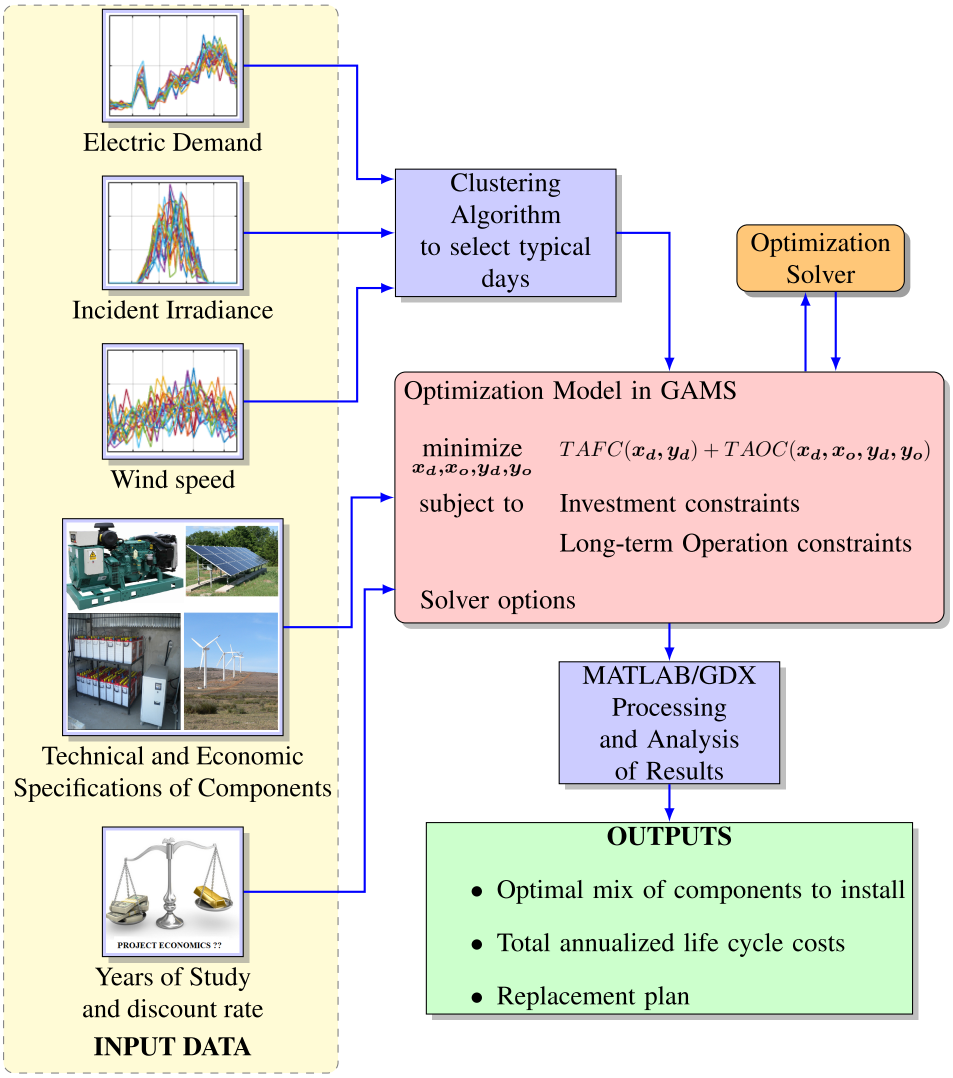

Figure 1.1: *Block diagram of microgrid planning*

gap.

1.2 Research Objectives

The main aim of this research is to apply mathematical programming and optimization approach in the planning of microgrids considering key operational constraints which affect the planning decisions. The underlying hypothesis is that with the advancements in the performance of mathematical optimization solvers, it is possible to apply mathematical optimization approach to find global or near optimum solution for the microgrid planning problem. This is important, since the existing simulation based planning tools still adopt many simplifications but can not guarantee finding the global solution. It will be demonstrated that applying mathematical optimization even on the same microgrid planning model and with the same assumptions and level of simplifications adopted in most of the simulation based tools gives better planning results. Further investigations to improve the simplified model and add more details and constraints in order to get to a new complete planning model are presented. The main advantage of this approach is that it can offer global optimum or near optimum solution with the possibility to assess the quality of the obtained solution. Therefore, this research seeks to answer two questions:

1. Given available demand and renewable resources data, what is the optimum capacities, quantities, and combination of microgrid components which will ensure reliable and continuous supply of its demand at minimum cost?

2. How can (1) above be fulfilled taking into account uncertainties in renewable resources and electric demand?

1.3 Main Contribution

The main contributions from this research are as follows:

1. A new MILP deterministic model for microgrid planning is presented. The overall microgrid long-term operation is integrated in this planning model. A technique called CUC is applied in order to reduce the number of discrete variables required to model DGs operation. In addition, in order to make the model computationally tractable, K-medoids clustering algorithm is applied to select typical representative days with profiles of renewable resources and demand data. To adopt linear formulation, components nonlinear characteristics are approximated by using PWLA methods. This makes it possible to use powerful solvers, such as CPLEX and GUROBI, which are available in GAMS.

2. Two formulations to include uncertainties in renewable resources and electric demand in microgrid planning, based on 2SSIP and RO frameworks are presented. Applicability of the proposed models are demonstrated by using microgrid planning case studies.

1.4 The Structure of This Thesis

The rest of this thesis is structured as follows: Chapter 2 presents a review of deterministic planning techniques in microgrids. The chapter starts by a broader view of power systems Capacity Generation Planning (CGP) and extends it to microgrid planning. Fundamental problems facing the planning of conventional power systems which are inherent to microgrid planning are discussed. Particular features of microgrid planning problem, techniques, and tools which have been applied in planning of microgrids are presented.

Chapters 3, 4, and 5 constitute the main body of this work. Although these chapters are related to each other, they can be read independently. Chapter 3 discusses microgrid architecture, components characteristics and modelling. This chapter lays the foundation of a mathematical model of the complete planning problem and explains PWLA of nonlinear characteristics of microgrid components.

Chapter 4 describes the deterministic microgrid planning model and presents case studies to validate the model and demonstrate its applicability.

Chapter 5 covers microgrid planning under uncertainties. Techniques to model uncertainties in renewable resources and demand are discussed, followed by extended formulation of the deterministic planning model to include uncertainties using stochastic optimization and robust optimization frameworks. The proposed 2SSIP and RO models models are applied to plan microgrid using manageable instances of the problem.

Finally, the thesis concludes in Chapter 6 by presenting the main conclusion of this research and suggesting directions for future research work.

1.5 List of publications

The following is a list of the publications arising from the work presented in this thesis:

[1] G. G. Moshi, A. Berizzi, and C. Bovo, "Grid connected systems for access to electricity: From microgrid to grid extension," English, in *Renewable Energy for Unleashing Sustainable Development*, E. Colombo, S. Bologna, and D. Masera, Eds., Springer International Publishing, 2013, pp. 99–132, ISBN: 978-3-319-00283-5. DOI: 10.1007/978-3-319-00284-2_5. [Online]. Available: http://dx.doi.org/10.1007/978-3-319-00284-2_5 (cit. on pp. 27, 28).

[2] G. G. Moshi, M. Pedico, C. Bovo, and A. Berizzi, "Optimal generation scheduling of small diesel generators in a microgrid," in *Energy Conference (ENERGYCON), 2014 IEEE International*, 2014, pp. 867–873. DOI: 10.1109/ENERGYCON.2014.6850527.

[3] G. G. Moshi, C. Bovo, and A. Berizzi, "Optimal operational planning for pv-wind-diesel-battery microgrid," in *PowerTech, 2015 IEEE Eindhoven*, 2015, pp. 1–6. DOI: 10.1109/PTC.2015.7232461.

[4] G. G. Moshi, C. Bovo, and A. Berizzi, "Optimization of combined planning and operation of pv-wind-diesel-storage microgrid," *To be submitted*, 2016.

[5] N. Nguyen, D. Le, G. Moshi, C. Bovo, and A. Berizzi, "Sensitivity analysis on locations of energy storage in power systems with wind integration," in *Environment and Electrical Engineering (EEEIC), 2015 IEEE 15th International Conference on*, 2015, pp. 1115–1119.

[6] G. G. Moshi, L. Taccari, C. Bovo, and A. Berizzi, "Optimization of integrated design and operation of microgrid under uncertainties," *Submitted to: Power Systems Computation Conference (PSCC)*, 2016.

[7] N. Nguyen, D. Le, G. Moshi, C. Bovo, and A. Berizzi, "Optimal siting and sizing of energy storage in power system with high wind integration," *To be submitted*, 2016.

CHAPTER 2

Literature Review

2.1 Introduction

Microgrids have received significant attention in recent years due to their prominent features appropriate for electrification of rural and remote areas. In already electrified areas, microgrids are viewed as a stepping stone towards the full realisation of smart grids. This transition is aiming at accommodating DERs, improving reliability and quality of power, increasing system efficiency, security of supply, and autonomy from the main grid. As explained in the Introduction, microgrids consist of interconnection of loads, mix various DERs, and ESS operating as as autonomous systems or in connection with the main grid. A major challenge in planning a microgrid is to select optimum capacities, quantities, and combination of components of different types and technologies while optimizing their combined operation in the full planning horizon. The aim is to obtain a installation plan which will offer continuous and reliable supply of power at minimum cost, minimum emissions or both. The plan should adopt a scalable and flexible architecture to allow future connection with the main grid or neighboring microgrid as well as ability to operate in stand-alone mode.

This chapter presents a detailed review on deterministic planning and optimization of microgrids. It will be argued that mathematical programming and optimization techniques are the best methods for planning hybrid microgrids, albeit with some limitations. To this end, first the planning problem is reviewed from CGP aspects of conventional power systems in order to introduce main challenges and differences between conventional power system planning and microgrid planning. This will answer the question, "Why planning techniques applied in conventional power systems cannot be directly adopted for planning microgrids?". Then, microgrid planning techniques adopted by researchers are discussed under four broad classifications: trade-offs curves, simulation based planning, heuristic planning techniques, and mathematical programming and optimization techniques. Finally, a review on the current state of the art for microgrid planning softwares, their capabilities and limitations, is presented.

2.2 Capacity Generation Planning in Conventional Power Systems

2.2.1 Capacity Generation Planning Methods

CGP is one of the most important planning aspect in power systems. The aim of CGP is to find a mix of generators by technologies and sizes and the period to install each of them in order to ensure reliable and cost-effective supply of the current and future system demand and reserve. CGP consider investment cost, power generation cost, and operation and maintenance costs. Under monopoly system, CGP and transmission planning decisions are carried out by a single organisation. On the contrary, under deregulated system, CGP and transmission planning involve various organisations with different objectives. Consequently, each generation company has to consider its own CGP problem to see if is profitable to make a new investment. Since microgrid planning is primarily related to the micro CGP, it is reasonable to assume a case in which CGP is carried out independent of transmission system planning as illustrated in Fig.2.1.

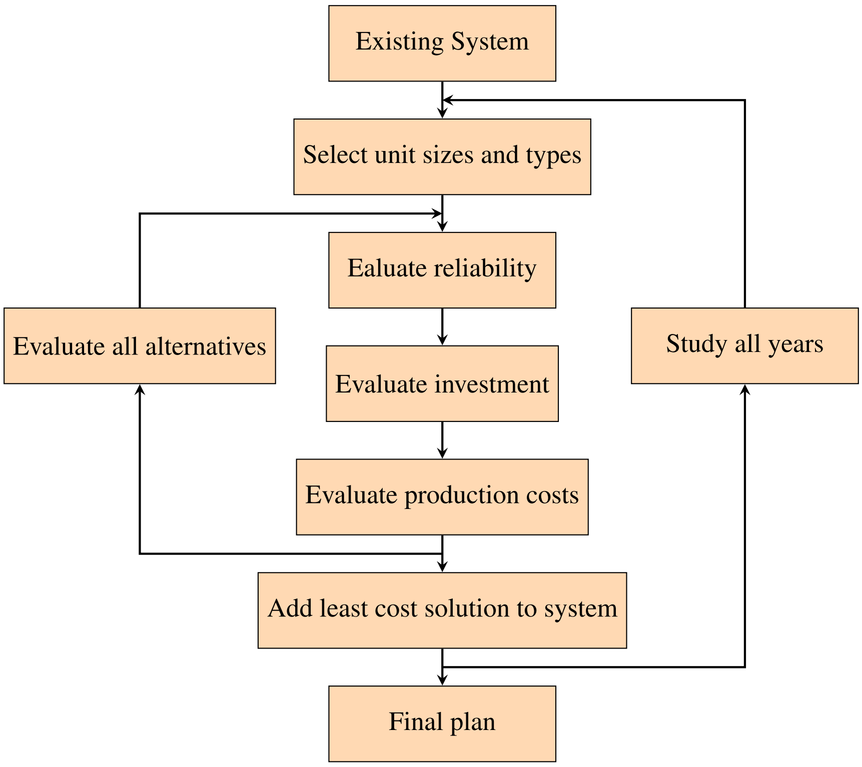

Figure 2.1: *Flowchart for the basic capacity generation planning process [17]*

Traditional methods for CGP in power systems involve the use of Screening Curve (SC) and LDC [18]. SC is a plot of average cost of a megawatt-hour of plant generating capacity as a function of its Capacity Factors (CFs) .CF is the ratio of average annual load to the plant rated capacity. This factor accounts for the fact that the plant will not always operate at its rated power. To obtain SCs, total annualized costs, which consist of fixed and variable costs, of each type of generator are plotted against their corresponding CFs. In order to apply SCs to approximate energy to be supplied by each plant and thus their production costs, a construction of LDC is required. The LDC is obtained by rearranging hourly data in the load curve from chronological order into an order based on magnitude. The area under the resulting LDC is still equal to the total annual energy required by the system. To determine the generation mix, a straight line connecting intersection points from the SC are extended to LDC as shown in Fig.2.2.

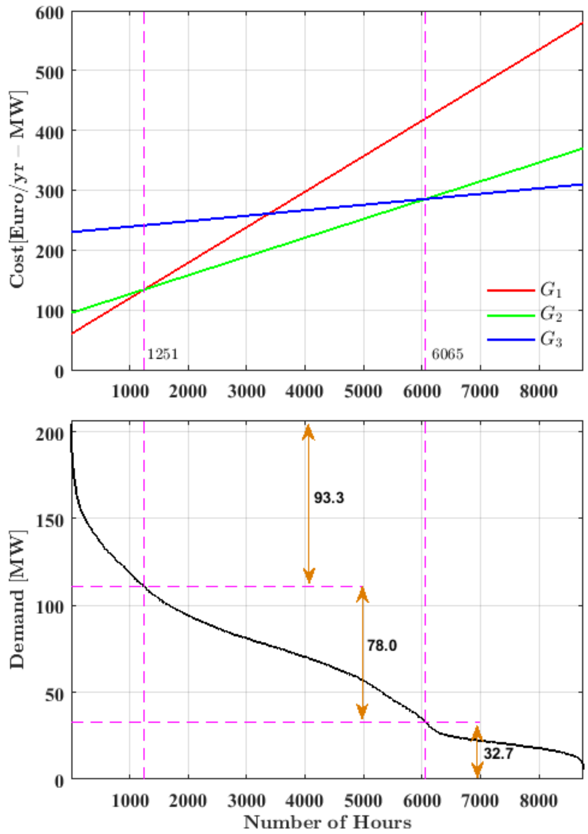

Figure 2.2: *Screening Curve (SC) and Load Duration Curve (LDC) method*

In Fig.2.2, the intersection point between generator type G_1 and G_2 occurs at 1251 hours of operation whereas the intersection between between generator type G_2 and G_3, occurs at 6065 hours of operation. These intersection points correspond to the transition points at which the use of a generator with higher fixed cost is more cost effective due to lower operation costs. These intersections are entered into the LDC shown below the screening curve plots. The screening curve tells us that generator G_3 is the best option as long as it operates for more than 6065 h/yr, and the load–duration curve indicates that the demand is at least 32.7 MW for 6065 h/y. Therefore, generator G_3 is regarded as a baseload generator. Generator G_2 needs to operate at least 1251 h/y and less than 6065 h to be most cost-effective. The screening curve shows that required operation capacity of generator G_2 is about 78 MW. Generator G_1 is the most cost effective as long as it does not operate more than 1251 h/y. Since during this period the load is between 110.7 MW and 204 MW, the generation mix should contain at least 93.3 MW of generator G_1. In this example G_2 is regarded as intermediate generator and G_1 as a peaking generator.

This method gives a very simplified solution of CGP problem as it does not include forced outages of generators, variability, and system reliability. However it presents the basic foundation of the power system CGP problem.

There is a large body of literature on improvement and application of SC and LDC method for power system planning [19], [20]. Each of these studies attempts to capture some operational details in order to approximate the production cost more precisely. In fact, most of commercial power system CGP tools, which are still in use today, were developed based on the principle of SC and LDC. Some of them, e.g. MARKet ALlocation (MARKAL) model, which is formulated as Linear Programming (LP) model, is an extension of SC with additional constraints such as emission reduction and market penetration [21]. Electric Generation Expansion Analysis System (EGEAS) is another tool which can model discrete planning decisions and detailed system operation [22]. This tool performs Fourier transform of the LDC and employs Dynamic Programming (DP) algorithm. Similar tool which adopts LP formulation of the planning problem and employs DP algorithm is Wien Automatic System Planning (WASP-IV) package [23]. This package approximate system production by using equivalent LDC with 12 subperiods for each of which probabilistic simulation is applied. However, the use of LDC implies that production cost is approximated based on magnitude of the demand without considering when this demand occurs.

A growing need to incorporate more operation details in power system CGP led to the development of planning programs with two main functions: operational simulation and generation capacity optimization. Due to computation limitations, the two functions were decoupled but still had to complement each other. Hence, production simulation programs, with finer temporal granularity, were applied to analyse results from generation capacity planning studies. This approach is still applied even in today's power system planning tools. For example, PLEXOS is an integrated energy model which combines several modules for simulation and optimization of power system CGP and expansion. This tool adopts MILP formulation of CGP problem in competitive market environment. In PLEXOS, more temporal characteristics can be captured by approximating the LDC using large number of blocks. However, increasing the blocks makes the computational more intensive to the extent that may require the use of supercomputers, particularly for large systems [24]. To avoid long computation time, commercial planning tools adopt typical representative days or one week for each season, for example, GTmax [25]. Available commercial production simulation tools include: GE-MAPS, PROMOD-IV [26], PCI GenTrader [27], and PROSYM [28]. A combination of these tools, e.g. MARKAL and Energy Flow Optimization Model (EFOM) to The Integrated MARKAL/EFOM System (TIMES), can be used to perform long-term CGP studies [29].

Integrating RES in power system generation planning poses a need to consider two important aspects. First is that RES generators have variable and intermittent production but have minimum marginal cost. Based on the SC and LDC planning approach, these generators should be dispatched first as the base load generators whenever they produce power. Second, dispatching of conventional thermal generators should be able to follow the variations in the net demand (i.e. difference between the peak demand and renewable generation). This would require a mix of various medium size generators with appropriate technical specifications or employing large ESS to balance the system. Large scale storage can be provided by matured technology such Pumped Storage Hydroelectric Power Plant (PSHP) and large SBBs, or by adopting new technology such as Compressed Air Energy Storage (CAES). In spite of the ESS deployment, significant changes in the dispatching of conventional generators must be considered in CGP. Therefore, in order to model operation of thermal generators and approximate system operation costs more accurately, it is necessary to adopt high temporal resolution in power system CGP, particularly when the penetration of RES is high.

Initially, CGP was carried out based on the peak demand and renewable generation was considered in order to modify dispatching of conventional generators [30]. This traditional approach ignores dynamics introduced by RES generators and thus results in sub-optimal system operation in which most of time conventional generators operate below their rated power and thus at lower efficiency, higher emissions, and higher operation costs. Later, a modern planning approach which includes renewable generation in the initial planning stage and thus plan for net demand, was adopted. The key issue here is to ensure that conventional generators have enough operational flexibility to cope with net demand variations which are proportional to the penetration of renewable generation. However, these approaches rely on iterative simulations to compare alternatives plans but do not optimize generators' selection and system operation at the same.

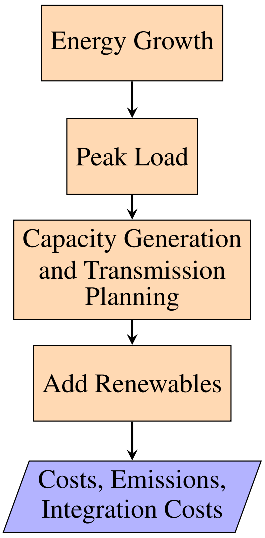

(a) Traditional CGP

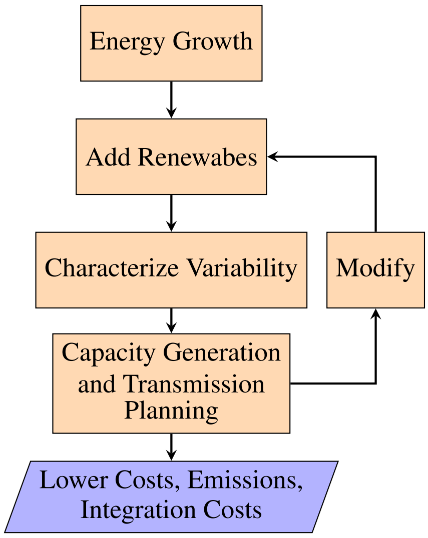

(b) Modern CGP

Figure 2.3: *Traditional and emerging practice in capacity planning*

Simultaneous optimization of selection and operation of all generators in CGP requires the problem be recast to MILP model. MILP offers possibility to model discrete planning decisions. The drawback of MILP model is higher computation time which increases exponentially with the number of integer variables. However, with advancement in computation power and heuristic searching techniques, larger system CGP problem formulated as MILP can be solved. Note that most of the nonlinear constraints in CGP problem are linearized in order to avoid difficulties encountered in solving MINLP models. This is necessary for purely mathematical optimization approach, particularly due to limitations of MINLP solvers. However, heuristic techniques can solve MINLP model of CGP.

Heuristic techniques have been applied even in commercial tools such EGEAS and WASP-IV. In these tools, heuristic tunneling technique is combined with DP routine in order to achieve sequential improvement of local optimum solution [31], [32]. A study which compares nine classical heuristic techniques for solving CGP problem is presented in [33]. Results of this study found that for short planning horizon of 6 years, DP outperformed all other techniques, whereas for long planning horizon of 14 and 24 years, DP required very long computation time. Among all techniques, hybrid Genetic

Algorithms (GA) was found to perform better with ability to avoid trapping in local minima even for larger dimension problems. Park, et al. presented a study which compares solutions of CGP problem obtained by using simple GA, improved GA, DP, and the combined heuristic tunneling and DP method employed in WASP-IV [34]. The improved GA is a modified version of conventional GA to include artificial creation of initial population and stochastic crossover strategy. This study found that improved GA provided better solutions than the conventional GA and the other two methods. Another study presents application of Non-dominated Sorting Genetic Algorithm-II (NSGA-II) for multi objective optimization of CGP [35]. The study proposed virtual mapping procedure which modifies representation of decision vector in order to reduce sensitivity of capacity vector to changes in decision vector and thus improve convergence of NSGA-II. That study compares a tradeoff between investment cost and violations of soft constraints as well as a tradeoff between investment and outage system reliability. Although heuristic methods can handle CGP problem, they only provide an approximation solution but cannot guarantee the optimal solution, but with nonlinear problems, this can not be avoided (apart from particular cases).

Advancements in capability of mathematical optimization solvers make them very promising technique for solving CGP problem. The main advantage of this technique is that it guarantees optimal solution to the planning problem, though with some simplifications. Bakirtzis, et al. present MILP model for centralized CGP which includes generator sizes, reliability constraints, maintenance scheduling and reservoir management constraints [36]. This work uses CPLEX 12.0 solver in GAMS to solve CGP model in 20 years planning horizon using monthly steps. Load profile of each month is approximated by a stepwise LDC in order to capture monthly peak load. This allows modeling medium term operation decisions, such as generator maintenance scheduling and reservoir management, to be considered in the optimization of investment decisions. The study found that unit maintenance periods were selected mostly when the system load is low. Authors in [37] consider medium term generation planning over a yearly horizon for a generation company with PV, WT and PSHP. The work adopts a probabilistic model of LDC matching in order to account for uncertainties in RES and random unit outages of conventional generators. Compared to the previous work which uses monthly LDC, this work use annual LDC with 6 subperiods of daily step. The optimization is carried out by using IPOPT 3.9.3 solver in A Mathematical Programming Language (AMPL). Other authors, applied Bender's Decomposition (BD) method [38], and its variant, Generalized Bender's Decomposition (GBD) [39], [40], to solve CGP problem. However, BD requires either master-problem or sub-problem but not both to have complicating integer variables and thus it is not easy to model discrete decisions in both investment and operation problem.

Another interesting work which assess the role of wind generation in desirable generation portfolios for Ireland in 2020 is presented in [41]. The problem is formulated as LP model. This study optimize both capacities of various types of generations and their production while considering generation from WTs and its impact on the net demand profile. A LDC with 18 bins is adopted to perform sensitivity analysis using different scenarios for wind generation capacities. The study found that for a large range of scenarios, wind generation played a significant role in desirable generation mix. In contrary to some studies which suggest that wind generation displaces higher merit order generators, analysis of this study found that, in the least cost solution, wind generation displaced base load generators. However, authors admit that further analysis using detailed operational model, which can fully and fairly accounts for wind generation, energy storage, and wind energy curtailment, is required.

2.2.2 Detailed Operation Constraints in Capacity Generation Planning

As discussed in above subsection, most of CGP models and techniques adopt low temporal resolution using stepwise LDC and thus do not preserve chronological variations of RES and electric demand. Most of these models do not plan based on technical and economic specifications of individual generators but rather they work on specifications of different types of technologies considered in the planning. In conventional power systems, ignoring operational details in CGP was acceptable due to low variations of demand and high accuracy in forecasting the demand growth. However, this planning approach has recently been challenged by many researchers particularly due to the need to include renewable energy generation technologies in the CGP [12], [42]–[45].

In [42], extension of an open source energy system model (OSeMOSYS) to include short term operational constraints is presented. A comparison of CGP results obtained by original version of OSeMOSYS and its extended version with results obtained by a combination of TIMES and PLEXOS models are reported in [43]. The study found that results of the extended OSeMOSYS model converge to the same results obtained by a combination of TIMES-PLEXOS model. Collectively, these study concluded that introducing short-term operational constraints in long-term planning models may considerably influence the dispatch of power plants, capacity investments, and, ultimately, the policy recommendations derived by such models. Similar conclusion was obtained by Vithayasrichareon, et al. [46] who assessed impacts of incorporating short term generation dispatch in CGP model which is presented in [44]. The results show that the extent to which short-term operation constraints affect CGP results depends on dispatch strategies, carbon price, and the mix of technologies within the planning. These impacts are likely to be more significant in systems with high fraction of renewable sources due to increased cycling of thermal generators.

Another study which characterizes and quantifies limitations of conventional CGP models which do not consider chronological sequence of resource and demand data, and the mixed-integer nature of generating units is presented in [12]. The study shows that the use LDC in planning model does not allow accurate representation of dynamic constraints in the system and hence fails to properly model variability from RES. Again, to what extent these limitations are significant depends on the type of the system, its resource and demand profile, generation mix and penetration of generation from RES generators. Palmintier, et al. investigate the effect of Unit Commitment (UC) constraints on CGP with presence of WTs [45]. The findings of that study suggest that incorporating UC in the CGP has significant effect in the optimal planning of system generation mix. However, the remaining challenges are how to make the model tractable considering the size of the problem, and to identify which UC constraints are necessary to be considered in the CGP models.

The discussion to this point has placed emphasis on fundamental approaches adopted in power system CGP. Standard techniques such SC and LDC method, simulation and optimization programs, and mathematical programming have been reviewed. In conventional power system, large size of the system, long planning horizon, long construction periods, large number of technologies to be considered, and additional environmental constraints made it impossible to use time series demand and resources data in CGP. Because of this, the hourly load profile of the complete year has been approximated by using stepwise LDC with few number of subperiods. However, it has shown that this approach is being replaced by the use of typical representative days or weeks which preserve the chronological nature of load and resource data. This approximates the complete year operational costs by weighted sum of typical days or weeks, but system planning is optimized considering actual hourly operational dynamics. It is clear that how to bridge the gap between short-term operation planning problem and the long-term planning problem is a challenging research question which has been considered by many researchers. The same question is to be faced when planning microgrids.

2.3 Microgrid Planning Methods and Techniques

Compared to the conventional power systems, microgrids planning considers small system size, sometime short planning period, fewer technologies, and shorter construction time. However, variations in renewable generation and electric demand have much more adverse effects on microgrid stability particulary due to its small size and lower system inertial. This makes BESS essential for microgrid, particularly stand alone microgrid, and thus need to be considered in its planning. Introducing SBB requires additional dynamic constraints to model the control of its charging and discharging processes. Nevertheless, microgrid planning must consider operation of individual generators in order to get optimal plan. Most of the challenges of conventional power system CGP problem are inherently found in in microgrid planning. The need to combine short-term operational planning in microgrid generation mix planning model is addressed in [47]. The study shows that considering short term operational volatility affects the investment decisions in microgrid planning. Therefore, it is necessary to incorporate modelling of overall microgrid operation in its planning model. For this reasons, LDC are not appropriate for microgrid planning. This section section presents a review of microgrid planning techniques and their limitations.

2.3.1 Trade-off Curves

Cost versus reliability trade-offs curves have been applied for microgrid planning, particularly for existing systems which require additional of RES, SBB, or both. Borowy, et al. proposed a method for optimal sizing of PV and SBB combination in a microgrid with WT [48]. Given demand and resource data, capacity of WT, and desired reliability criteria, which in this case is the Loss of Power Supply Probability (LPSP), simulations are run to calculate series of possible combinations of number of PV modules and Storage Batteries (SBs). Assuming that the total cost of the system is linearly related to both the number of PV modules and SBs, the minimum system cost is determined by a point of tangency between cost function line and the curve that relates the number of PV modules and SBs for the desired reliability. Authors in [49] adopt similar approach in which system reliability is defined by energy shortfall probability (ESP). This approach starts by generating cost versus reliability curve in which the cost for each reliability represents the optimal combination of PV and SBB capacities which achieve that reliability. The planning is preformed by choosing a point on the cost versus reliability curve and conducting hourly performance analysis for months with the lowest reliability. If the performance and cost are acceptable the planning configuration is accepted otherwise the procedures are repeated. The trade-off curves approach has mainly being applied for microgrid expansion planning which considers only a subset of the complete planning problem, i.e. addition of RES generators or SBB in an existing microgrid.

2.3.2 Simulations Based Planning

If only few alternative plans are to be considered in the planning of a microgrid, then the planning solution can be obtained by applying simulation technique. Simulation-based planning has been applied to study the integration of PV, WT, and ESSs, or their combinations, in order to realize hybrid microgrid. The main objective in most cases is to minimize fuel cost for existing systems with already installed conventional DGs. For example, [50] adopts simulation approach to optimize sizes of PVs, WTs, and SBB for a microgrid in which the DG is sized based on the peak electric demand. A work in [51] considers hybrid PV,WT, and SBBs off-grid system without DGs. Simulation planning approach offers the following advantages:

- Flexible formulation which can accurately model system behaviour
- Use procedural statements which allows detailed modelling of system operation constraints
- Easy implementation of complex algorithms for dispatching DGs and ESSs
- Allows quantitative and qualitative assessment of different alternatives

Figure 2.4 shows the general flow chart for microgrid simulation planning method.

Simulation planning are preferred for techno-economic analysis and feasibility studies of small hybrid systems. Authors in [52] presents a study on investigation of economic and environmental feasibility of microgrid in two Australian islands. Simulations were performed in HOMER software which considers system operation for 8760 hours of the year. In the same vein, Tanaka et al., proposed a microgrid simulation planning method which includes battery management algorithm in a time step of 30 minutes for the planning horizon of 1 year [53]. This method is applied to plan a resort microgrid in Okinawa, Japan. Such a detailed resource field data applied in that study are not easy to find in most cases, particularly for 30 minutes time step. Although most of these work do not comment on the simulation time, it is generally high due to small simulation time steps and many system alternative configurations to be covered.

Another application of simulation-based method in microgrid planning is to assess effects of various system dispatching strategies. Barley, et al. present a significant analysis to planning an optimal dispatching strategy for hybrid power system [54]. The analysis was carried out on the results obtained by using a simple time series model applied to minimize fuel cost, number of DG start up, and SB erosion, based on present worth life cycle analysis. Simulations considered Load Following Dispatch Strategy (LFDS), Cycle Charging Dispatch Strategy (CCDS), and Ideal Dispatch Strategy (IDS). The study found that optimal dispatch strategy closely depends on the demand and wind speed profiles, component costs, and more important on the sizing of WTs. The study concluded by emphasizing the need to perform joint optimization of components sizing and dispatching strategy when planning a microgrid. In [55], a simulation approach is applied to size components in a stand-alone microgrid for large remote community. This work adopt enumeration of the planning search space to obtain feasible combinations for the simulations. The model considers nonlinear fuel characteristics of DGs, reliability index, and minimization of Net Present Value (NPV) based on Life Cycle Cost Analysis (LCCA). Compared to other simulation studies which consider single dispatch strategy with generation balance constraint for active power only, this study consider four power management strategies which include both active and reactive power balance constraints [56].

Simulation planning technique can consider only system combinations which are specified as inputs in the planning search space. Increasing the planning search space requires exhaustive enumeration of all possible combinations and thus long simulation time. One solution to this problem is to combine simulation planning with sampling algorithm to aid in exploring the planning domain. In [57], a Dividing

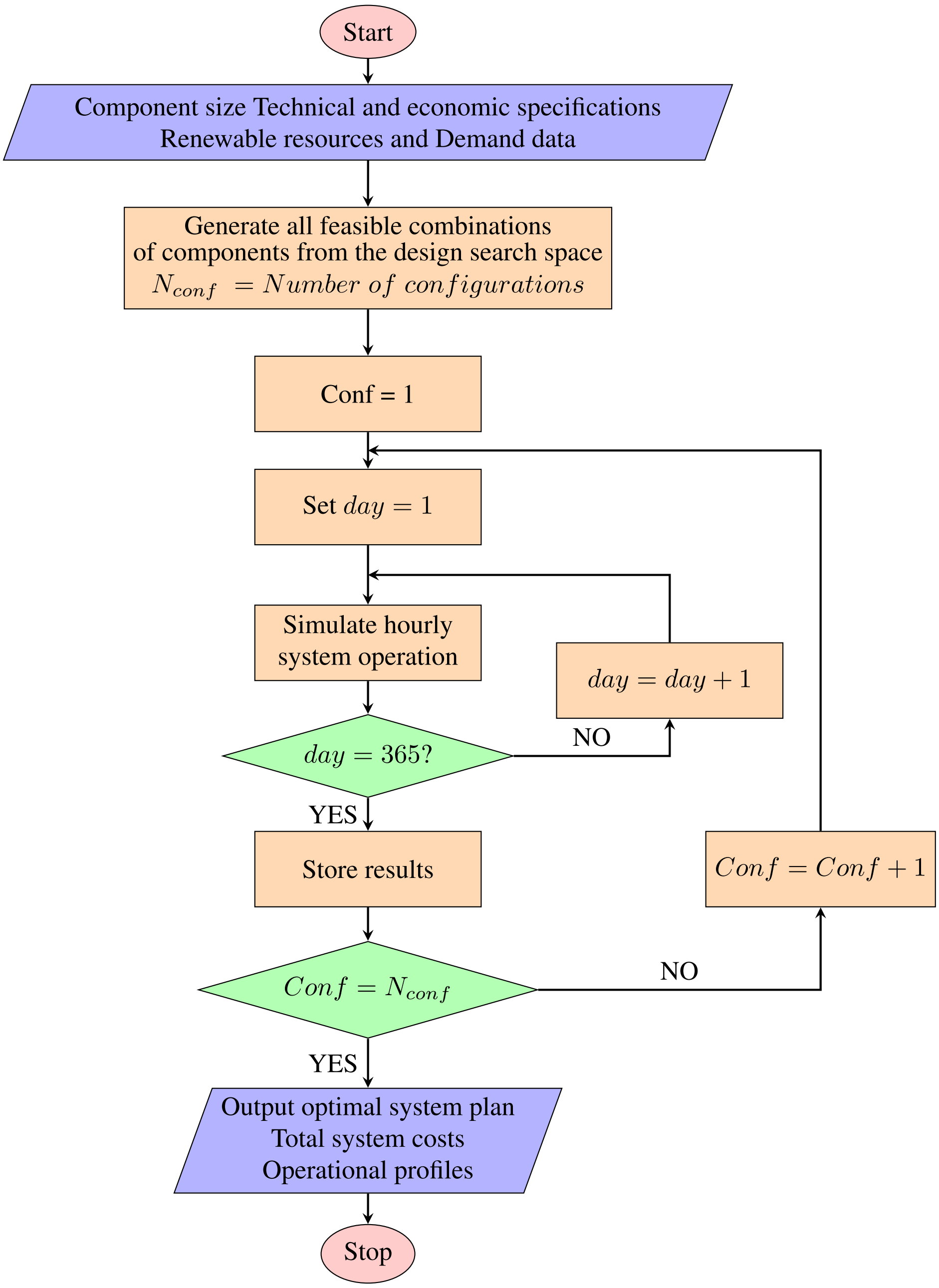

Figure 2.4: *General flowchart for microgrid simulation based planning*

RECTangles (DIRECT) algorithms is applied to optimize the planning of hybrid system with PV array, WTs, DGs and SBB in Le Havre, France. In this approach, DIRECT algorithm performs sampling of the planning domain whereas the simulation approach is employed to calculate the value of objective function at each sampled point. This method can locate a solution whch were not specified the planning search space and thus would not be possible to determine by purely simulation approach. However, location of global solution may require exhaustive search over the planning domain and thus very long time. Another work by Chang et al. apply simulation optimization method based on stochastic Trust-Region Response Surface Method (STRONG) together with Monte Carlo Simulation (MCS) in order to avoid exhaustive enumeration of planning domain [58]. In that paper, STRONG is applied to build metamodel to characterize the behavior of objective function in a local region and MCS is applied to approximate the value of objective function. The drawback of this method is that it is not suitable for MILP problem and thus requires some modifications. Also, depending on the size of the problem, MCS may need long time to approximate the value of objective function. Another limitation of this method is availability of historical data needed to build the distributions of input data.

Using different simulation planning approach, researchers in [59] apply multi-period Discrete Fourier Transform (DFT) to size DGs and SBB for an isolated microgrid. The DFT is applied to allocate power balance between DG and SBB. Capacities of DG and SBB are then determined based on their allocated power. This method requires historical data to determine a cut-off frequency for the DFT. This frequency has significant effect on the sizing of DGs and SBB. For example, in the sizing case adopted in [59], it seems that the cut-off frequency is too small and thus the algorithm favor installation of large SBB and small DGs. Also, that paper adopt gradient search method which require high computation time and may be trapped at local solution.

Simulation planning can be performed using time series resource and demand data. This approach can partially capture the coupling between the planning and operation problem. Due to the high level of operational details considered in this technique and the use hourly time steps, most of simulation planning studies are run for one typical planning year. Simulation approach depends on the planning alternatives specified by the user as inputs in the planning search space, but it can not generate new alternatives. This limitation can be overcome by combining simulation planning models with global searching algorithms or adopting simulation optimization approach [58]. Still, to achieve global convergence requires exhaustive searching of the planning domain and long simulation time. Therefore, solution provided by these approaches may not necessarily be the optimal solution. The following subsection presents a review of heuristic algorithms which offer efficient global searching strategies.

2.3.3 Heuristic Based Planning

Heuristic algorithms have been widely applied in optimizing the planning of hybrid microgrids. These methods start with randomly generated initial solution and, based on some rules, iteratively produce new solutions and evaluate them until the best solution is found. The main advantage of these methods is that they do not completely rely on the mathematical form of the problem. They are therefore useful to solve complex problems such as microgrid planning problem which fall under MINLP. GAs are one of the most widely used heuristic methods particularly due to their ability to model complex objective function with many variables. Specific features which distinguish GAs from the normal optimization and searching algorithms are [60]:

1. GAs work with a coding of the parameter set, not the parameters themselves.
2. GAs search from a population of points, not a single point.
3. GAs use payoff (objective function) information, not derivatives or other auxiliary knowledge.
4. GAs use probabilistic transition rules, not determinists rules.

Figure 2.5 shows the flowchart illustrating how GA can be adopted to solve microgrid planning problem.

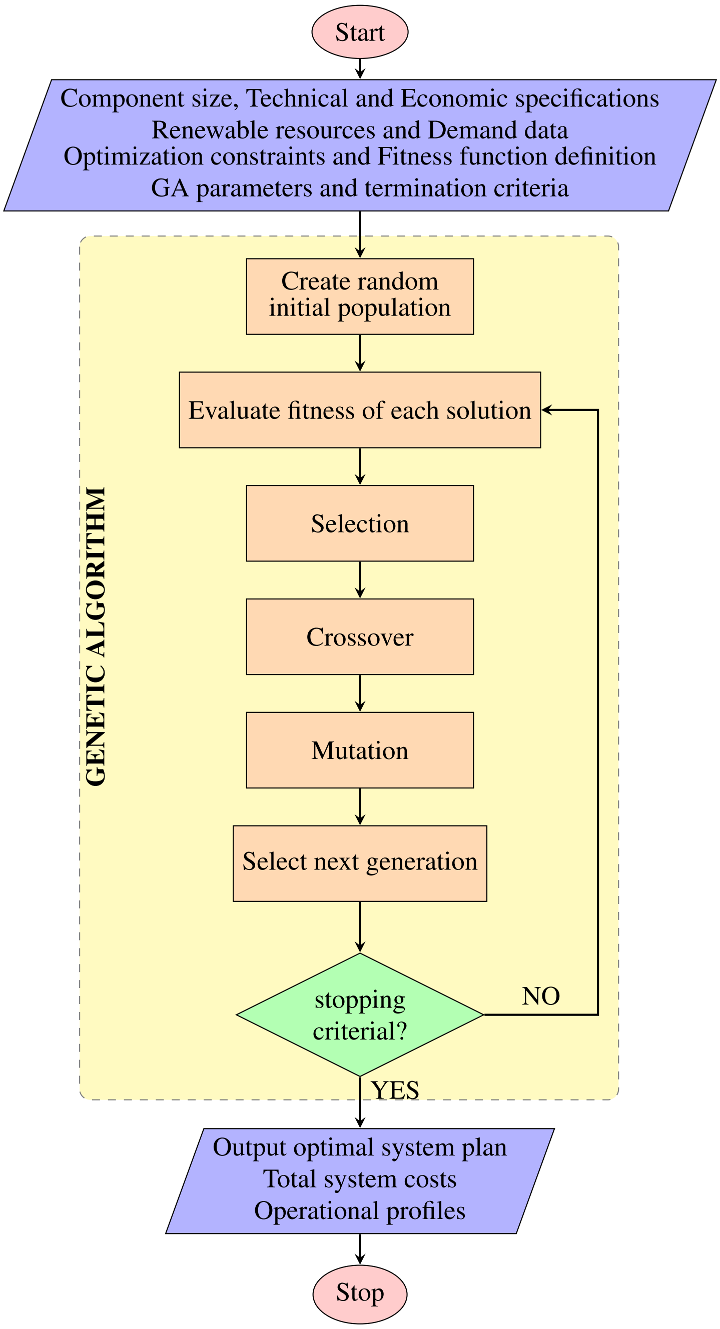

Figure 2.5: *Genetic algorithm flowchart for microgrid planning*

Dufo-López et al. developed a Hybrid Optimisation by Genetic Algorithms (HOGA) program and applied it to planning a hybrid system with PV array, SBB, and DGs [61]. The program, implemented in C++, optimizes the planning of microgrid considering the number, types, and sizes of all components in it together with the control strategy. This program offers the possibility to perform multi-objective optimization, probabilistic analysis, and advanced modelling of SB aging effect [62].

Another work adopts real coded GA for planning of hybrid PV/WT/DG/ and SB system [63]. In that paper, pre-evaluation and repair mechanisms are applied to ensure that the GA process only feasible solutions. This approach improves convergence of the algorithm and has been adopted in other recent work [64]. Arriaga, et al. propose a technique, called *Renewable Energy Reduced Search Space*, to perform pre-selection of PV and WT in order to reduce computational time of the main optimization problem [65]. For each type of PV and WT considered, the cost effective configurations are those with minimum Levelized Cost of Energy (LCOE) calculated based on equipment economic specifications and their expected power generation. These studies adopt long-term hourly resource and demand data to evaluate system operation under various scenarios. Also, these studies model dispatch strategies with dynamic and nonlinear constraints. Apart from the time spent to compute the values of these constraints for each individual solution, the nonlinearities do not affect searching of the optimal solution. A recent study in [66], compares planning with high temporal resolution resource and demand data and the planning based on hourly data. The study applies NSGA-II to perform multi-objective optimal planning in order to minimize total system cost and its availability. Results show that using high resolution data could help to avoid oversized planning. However, obtaining high resolution data may not be possible, particularly for remote areas which are not electrified.

Another heuristic method which has been applied in microgrid planning is Particle Swarm Optimization (PSO). This method is similar to GA in that they both of them work on populations which are randomly updated until the best solution is obtained. However, PSO does not have genetic operators such as crossover and mutation, and each particle in PSO is associated with a velocity. Despite the claim by some authors that PSO can outperform GA, it is generally agreed that the performance of these algorithms is problem-dependent. Figure 2.6 summarize PSO algorithm in the context of microgrid planning.

Navaeefard et al. applied PSO for capacity sizing of hybrid microgrid with PV/WT/DG/ and SB [67]. In that work, uncertainty in WTs power is modelled by using forecasting errors assumed to follow normally distribution. Another approach which applies PSO for multi-objective optimization of hybrid system with PV, SB and hydrogen storage is presented in [68]. That study considers grid connected system and thus the objective functions to be minimized are total system cost and the maximum energy exchange with the grid. PSO gives good performance for model with less variables such as small hybrid systems or when considering optimization of only a subset of the microgrid components [69], [70]. For complex systems with many variables PSO suffers low performance in locating the optimal solution as compared to GA.

GA and PSO are the two most commonly heuristic methods used for optimizing the planning of microgrids. Other heuristic algorithms such as Simulated Annealing (SA) and Ant Colony Algorithm (ACA) are seldom applied for microgrid planning. During the time of this review only few main contributions were found in literatures [71], [72]. As discussed above, heuristic methods have advantages such as ability to handle complex nonlinear model and improved exploration of planning search space. However, these methods do not guarantee obtaining global optimal solution. Due to this reason it is not possible to assess relative accuracy of the obtained solution because the optimum solution is not known and cannot be approximated. The next section discusses applications of mathematical programming and optimization methods which are capable to determine optimal solution for microgrid planning problem.

2.3.4 Mathematical Programming and Optimization Planning Techniques

Planning a microgrid requires combined optimization of operation problem and the capacity planning problem. Operational problem implements energy management strategy, commitment and dispatching

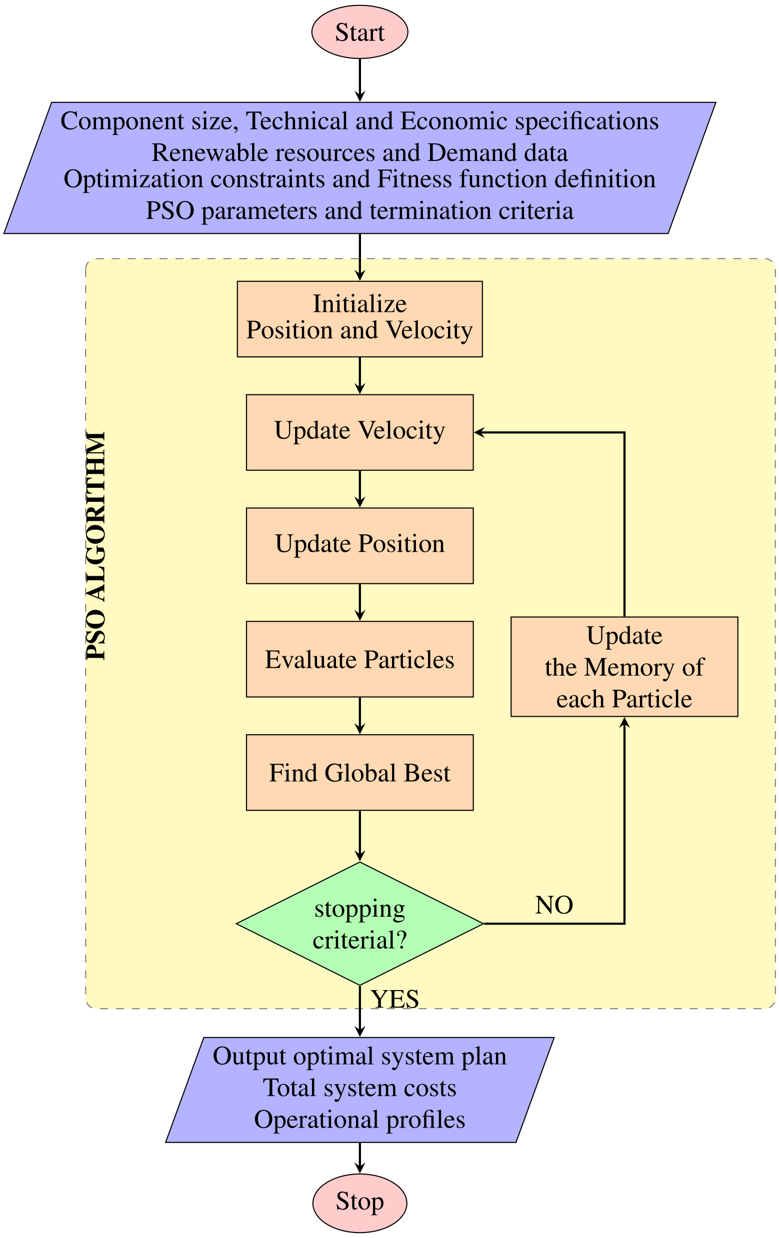

Figure 2.6: *PSO based microgrid planning*

of DGs, and operation of SBB. The operation problem in its original form is a MINLP due to nonlinear characteristics of DGs, discrete variables required to describe commitment of DGs and to control charging and discharging of SBB, and dynamic constraints governing the evolution of State of Charge (SOC) of the SBB. The capacity planning problem features itself as integer combinatorial problem since for the case of microgrids the planning involves sizes, quantities, and combination of components of different types and technologies. Therefore, microgrid planning problem is originally one of the challenging MINLP problems. In describing the mathematical formulation of hybrid power system planning model, Kuznia, et al. observed that under special circumstances, the model is equivalent to capacitated lot sizing problem and thus it is in general NP-hard[1]. To approximate the solution of this model in its original form, i.e. MINLP model, one should adopt heuristic techniques such as GA [65]. However, as discussed in the previous subsection, heuristic techniques does not guarantee the quality of the obtained solution and thus offers limited insight on the optimal planning solution.

The general form of MINLP problem is defined as [74]:

$$\begin{aligned}\min_{x,y} \quad & f(x,y) \\ \text{s. t.} \quad & h_i(x,y) = 0,\ i = 1,\ldots,n. \\ & g_j(x,y) \le 0,\ j = 1,\ldots,m. \\ & x \in \mathbf{X}, y \in \mathbf{Z}\end{aligned} \tag{2.1}$$

where i is the index of set of equality constraints, j is the index of set of inequality constraints, n is the number of equality constraints, m is the number of inequality constraints, x are integer variables, and y are continuous variables. In most cases set $\mathbf{Y}$ corresponds to a convex compact set of the form: $\mathbf{Y} = \{y \mid y \in \mathbf{R^n}, \mathbf{D}y \le d, y^{lo} \le y \le y^{up}\}$, and the discrete set $\mathbf{X}$ corresponds to a polyhedral set of integer points, $\mathbf{X} = \{x \mid x \in \mathbf{Z^m}, \mathbf{A}x \le a\}$. In the case of microgrid planning problem, y are continuous variables such as output power from DGs, PVs, WTs and SBBs charging and discharging power, whereas x is a union of integer planning variable and integer or discrete commitment and control variables for DGs and SBBs operation. As it will be shown in the following chapter, nonlinearity in (2.1) occur in both the objective function and constraints. In this thesis, any nonlinear term arising in the model formulation will be approximated by using PWLA technique. Thus, the model is formulated as a MILP in order to allow the use of powerful linear solvers. However, a challenging part of the planning problem is a large number of variables which can easily make the problem computationally intractable. One of the contribution of this thesis is to propose a technique to cluster commitment variables in order to reduce the number of discrete variables required to model DGs operation.

Study in [75] discuss applications of MILP in energy system engineering which includes polygeneration energy systems. In [76] a MILP model for integrated planning and evaluation of distributed energy system is presented. That paper mention three levels of optimization required in planning of DER systems: synthesis optimization to decide a mix of components, design optimization to imply the technical characteristics of the components, and operation optimization to obtain optimal operational schedule. These three levels cannot be considered in complete isolation from the others because operational strategy affects the selection of specific equipments and vice versa. Zhou, et al. adopt aenergy system engineering optimization approach to plan energy system in China. The authors formulated MILP model with six different technologies and main grid connection. Similar to the above two papers, this work use superstructure based modelling and mathematical optimization. All these studies adopt energy planning approach which does not model detail operation of electric power generation and storage [77], [78]. This gap is covered in this thesis in which the focus is on microgrid planning for electrification of rural or remote areas. The overall microgrid long term operation problem is integrated in microgrid planning model.

A common feature of MILP planning models is that they use time series hourly data for the selected typical days which represents all 365 days of the planning year. This simplification is necessary in

[1] NP: Nondeterministic Polynomial time. A problem is NP-hard if there is an NP-complete problem that can be polynomially reduced to it [73].

order to make the model tractable and is applied even in the planning studies which optimize only the subset of the problem. For example, [79] considers optimal selection of DGs in order to minimize fuel consumption in the microgrid by adopting hourly data for 13 typical representative weeks. Typical representative daya approach still has loss of temporal information but not as much as compared to the LDC method. One of the gap which will will be addressed in this thesis is to propose a method to select typical representative days.

Chen, et al. proposed MILP model for optimal sizing of SBB in a microgrid based on the unit commitment formulation with spinning reserve [80]. This work employs time series analysis and forward neural networks to forecast hourly wind speed and irradiation data. The optimization minimizes total cost of the microgrid in grid connected and stand-alone mode. The model was implemented in AMPL and solved by CPLEX solver of which its results were confirmed by KNITRO solver. The results show that optimal size of SBB in stand-alone mode is significantly different from the optimal size of SBB selected in the grid connected mode, as expected. The work further analyses the roles of SBB in the microgrid: increasing operational flexibility, smoothing variations introduced by RES, stabilizing DGs operation by reducing the number of start-up, enabling efficient operation of DGs, and supplying part of system reserve. However, this work considers only the subset of the problem, i.e. only optimizing SBB for the system with already installed DGs, WTs and PVs, and the optimization is run for only one typical day with 24 hours. Similar work which considers a subset of the hybrid system by optimizing the size of electrolyser and fuel cell for a system with fixed sizes of DG and WT is presented in [81]. This work starts by fixing the size of DGs and then calculates the number of required WTs based on the system average demand and CF of the type of WT under consideration, as proposed in [82]. Next, system optimization is carried out for two scenarios: full renewable in which the demand is supplied by WTs and fuel cell and the DGs run only as a back-up in case the demand can not be full covered, and partial renewable scenario in which DGs run in parallel with other sources to supply the demand. The model is implemented and solved in GAMS and MATLAB environments, and results are compared with those of the base case system with only DGs.

Work in [83] presents a Nonlinear Programming (NLP) model for optimizing capacities of biomass generators, WTs, PVs and SBBs to be allocated in 12 candidate buses of a medium voltage microgrid having 31 bus bars. The model considers two separate objective functions which minimize annual energy loss and total cost of energy under grid connected and stand-alone operation modes. Each season of the year is represented by three typical days. The first day captures profiles for minimum hourly resource and demand data, the second second day for average hourly resource and demand data, and the third day for maximum hourly resource and demand data. The model is implemented in GAMS and solved by using sequential quadratic programming algorithm in SNOPT solver. The main limitation of this model is that it does not consider the integrality of the planning variables. It is possible that some of the continuous capacities in the obtained solution will not match with sizes of the standard off-the-shelf components.

Another recent study by Malheiro, et al. presents MILP model for optimal sizing of PV, WT, DG, and SBB in isolated industrial microgrid [16]. The model selects and sizes optimal system components considering hourly long-term operation for one year. The objective function minimizes LCOE subject to power balance constraint, installed capacity limits, and only maximum and minimum power constraints for DGs and SBB. This study adopts a simplified formulation of operational problem in order to make the model tractable. Indeed, the aim here is not to perform a detailed long-term operational planning, but rather to approximate operational cost and capture system dynamics that can significantly affect planning decisions. Also, in order to reduce number of integer variables, only the number of WTs, PV panels, and DGs are considered to be integer variables and SBB capacity is continuous variable. Another simplifying assumption in this work is that the model considers only one type of each components in the planning. Regarding the input data, the study adopt a well defined demand profile which is constant for all hours of the day except from 8:00 to 19:00. Furthermore, this profile is considered constant throughout the year. This presents a special case of demand profile which is reasonable for industrial microgrids. However, similar assumptions can not be adopted when considering village microgrids in which the demand profile may be highly variable.

2.4 Microgrid Planning Softwares

There are several comercial software tools that can be applied in the optimization of microgrids planing. Hybrid Optimization of Multiple Energy Resources (HOMER), developed by the U.S. National Renewable Energy Laboratory (NREL) and maintained by HOMER Energy, is the standard and most commonly used tool for planning of microgrids [84]. This tool can consider all types of systems such as single house system, industrial, village, island, campus and military base microgrids, in stand alone or grid connected mode. HOMER works by enumerating the planning search space and performs simulations to create a list of feasible system configurations based on NPV. Besides economic minimization, HOMER can perform system planning based on fuel or weight minimization. HOMER combines three planning functions: simulation, optimization, and sensitivity analysis. These functions are nested as illustrated in Fig.2.7. This relationship means that to perform sensitivity analysis several optimizations, which consists of many simulations of feasible system configurations, are performed. A description of each function is as follows [84]:

1. **Simulation:** simulate microgrid operation for an entire year in time steps from one minute to one hour.

2. **Optimization:** examine all possible combinations of system types in a single run and rank them according to the optimization variable of choice.

3. **Sensitivity analysis:** perform "What if?" analysis to enable comparison of importance of a particular variable or option in a single run.

Several studies have applied this tool for planning microgrids [85], [86]. In [85], HOMER is applied to find optimal microgrid planning on Ontario area in Canada. The study applies sensitivity analysis to examine the effect of uncertainties in diesel price and average wind speed in a long term planning. Researchers in [86] applied HOMER to optimize hybrid microgrid planning considering minimization of life cycle cost and environmental emissions. Four different cases including DGs-only microgrid, fully renewable-based microgrid, mixed DGs and renewable microgrid, and an external grid-connected microgrid configurations were planned and compared. Also, the study presents analysis to determine the break-even economics for a grid-connected microgrid. Continuously improvement of HOMER makes its current version, HOMER Pro 3.3, able to consider a large number of equipments, operation strategies, improved demand and resource modelling, and additional operation constraints. However, the software does not offer flexibility to add user-defined constraints and the planning search space is limited and has to be pre-specified by the user.

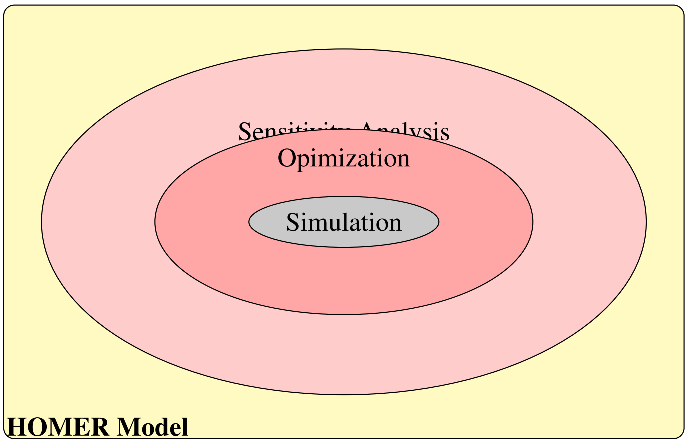

Figure 2.7: *Relationship between simulation, optimization, and sensitivity analysis in HOMER.*

Distributed Energy Resources Customer Adoption Model (DER-CAM) is a decision support tool for investment and planning DERs in buildings and microgrids. DER-CAM adopts MILP model of microgrid planning problem which is implemented in GAMS and use CPLEX solver for its optimization [87], [88]. The model finds optimal DERs investments while minimizing total energy costs, carbon dioxide (CO_2) emissions, or a weighted sum that simultaneously considers both criteria. This tool has been developed and maintained at the Lawrence Berkeley National Lab (LBNL) since 2000. Currently, there are two major branches of DER-CAM:

- **Investment and Planning:** determines optimal equipment combination and operation based on historic load data, weather, and tariffs.

- **Operations:** determines optimal week-ahead scheduling for installed equipment and forecasted loads and weather, tariffs. Due to the complexity of different optimization goals not all features are bundled in one of the two major branch versions and different versions within a branch exist.

Figure 2.8 show the block diagram of DER-CAM.

DER-CAM has been successfully applied to plan systems with Combined Heat and Power (CHP) applications [85], [89]. A study in [90] extends DER-CAM model application to include optimization of plug-in electric vehicle (PEV) storage in its objective function. The study analyzes possibility to extend the life cycle of PEV batteries for a secondary stationary application. Researchers in [91] compare HOMER with WebOpt which is a free, non-commercial, limited web-accessible version DER-CAM. The study concludes that DER-CAM is suitable tool for planninging microgrids with CHP applications. HOMER also has ability to model CHP strategies, but for heating loads only. However, HOMER has more constraints than DER-CAM and can consider each technology independently. The main advantages of DER-CAM is that it can obtain true optimal planning solution whereas HOMER relies on the user specified search space to find the best system configuration. Since HOMER considers only the search space input by the user, there could be an optimal planning configuration that is not being considered.

Improved Hybrid Optimization by Genetic Algorithms (iHOGA) is an improved version of of the HOGA described in Section 2.3.3 above. The software, which is developed in C++, can simulate and optimize various systems sizes in stand alone or grid-connected mode and with different cases of net metering. Also, iHOGA allows multi-objective optimization considering minimization of cost, emissions,

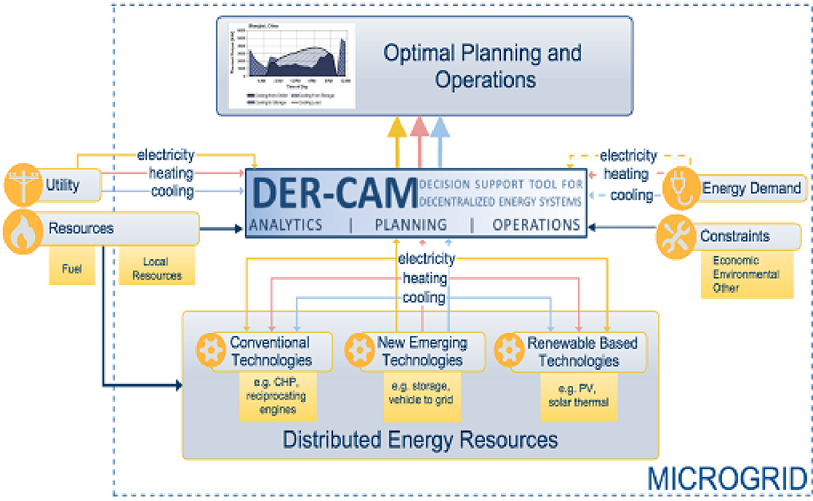

Figure 2.8: *Block diagram of DER-CAM [88].*

or unmet demand. Different technologies such as PV system, WTs, SBB, DGs, hydroelectric turbines, fuel cells, H_2-tanks, and electrolyzers, as well as several dispatch strategies can be considered in the planning. However, a full version of this software is not free, and its student version is very limited for practical studies.

Hybrid2 is a comprehensive probabilistic time series model, developed by NREL, which use statistical methods to account for inter time step variations. A detailed modelling of the system may include alternating current (AC) DGs, direct current (DC) DGs, an AC distribution system, a DC distribution system, loads, renewable power sources, ESS, power converters, rotary converters, coupled diesel systems, dump loads, load management options, or a supervisory control system. Hybrid2 allows the user to include manufacturer specified parameters, such as the wind power curve for a wind turbine, or the I–V curve of a solar PV panel. Figure 2.9 shows the block diagram of system configuration adopted in Hybrid2 model. A new version of Hybrid2 is not yet released to public users and its old version is somewhat difficult to use, particularly in processing the outputs [92], [93]. However, the simulations are very precise (time intervals from 10 min to 1 h).

A free access software which has been applied to perform simple feasibility studies for several renewable energy projects in LDCs is RETScreen [94].. RETScreen can be applied to asses the feasibility of energy efficient technologies and clean energy technologies such as solar, wind, small hydro, CHP, solar heating, biomass heating, ocean-thermal power, tidal power, waves power, and current power. The model is implemented in excel with very user friendly graphical interfaces. This tool, which is accessible in more than 30 languages, is developed and maintained by Ministry of Natural Resources, Canada. The main limitation of RETScreen is that there is no flexibility to define alternative operational strategies. Other software tools for microgrids planning include: INSEL, TRNSYS, iGRHYSO, HYBRIDS, RAPSIM, SOMES, SOLSTOR, HySim, HybSim, IPSYS, HySys, PVsyst, Dymola/Modelica, ARES, SOLSIM, and HYBRIDDESIGNER [95].

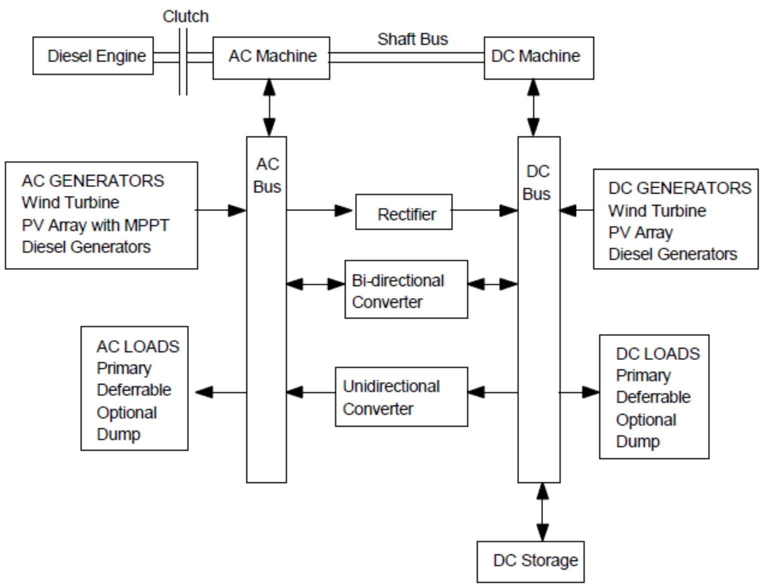

Figure 2.9: *Block diagram of Hybrid2 Model*

2.5 Summary

This chapter presents a review of deterministic planning techniques in microgrids. First, a broader view of power systems CGP is presented and extended to microgrid planning. Trends in the research literature indicate that CGP is a challenging problem because of the large-scale, long-term, non-linear, and discrete nature of generation investment. It is shown that fundamental problems facing the planning of conventional power systems are inherent to microgrid planning. However, compared to the conventional power systems, microgrids planning considers small system size, sometime short planning period, fewer technologies, and shorter construction time. In addition, variations in renewable generation and electric demand have much more adverse effects on microgrid stability due to its small size and lower system inertial. Particular features of microgrid planning problem, mainly the integration of long-term operation into the planning problem, is discussed. Techniques and tools which have been applied for microgrid planning such trade-off curves, simulation based planning, heuristic based planning, and mathematical programming and optimization techniques are discussed. This thesis adopts mathematical programming and optimization techniques mainly because of the ability to obtain optimal solution for microgrid planning problem. The following chapter discusses microgrid architecture, components characteristics and modelling.

CHAPTER 3

Microgrid Architecture and Long Term Operational Planning

3.1 Introduction

This chapter presents a general review of microgrids, their advantages, modeling of different types of DERs employed in microgrids, and operational planning for the stand-alone mode. Nonlinear models of DERs considered in this study and their linearized characteristics are presented. Two basic dispatch strategies, namely LFDS and CCDS, are presented followed by the Modified Optimal Dispatch Strategy (MODS) adopted in this research. The concept of CUC is then introduced and adopted for the operational planning in microgrid. Finally, a case study on operational planning problem which will be extended to the long term planning model in Chapter 4 is presented.

3.2 Microgrid Architecture

A typical Microgrid configuration is shown in Figure 3.1 [1]. In this thesis, the focus is on rural electrification, which envision a microgrid as a standalone system capable of being connected to the distribution system when grid extension will arrive in future. The generic architecture of microgrid consists of electrical loads and various types of DERs connected through a LV distribution network. The main distinguishing features of a microgrid include: its ability operation in both island mode or grid-connected, the presence of power electronic interfacing converters, the use of medium and small size DERs, localized generation and consumption of power, installation of DERs and other sources of energy close to the consumers, power generation at low voltage, and in some cases, the use of modern communication channels for data management and system automation. Installing the DERs close to the loads offers an efficient way to generate and use energy locally at a satisfactory voltage and frequency profile and with negligible losses [7], [1], [96].

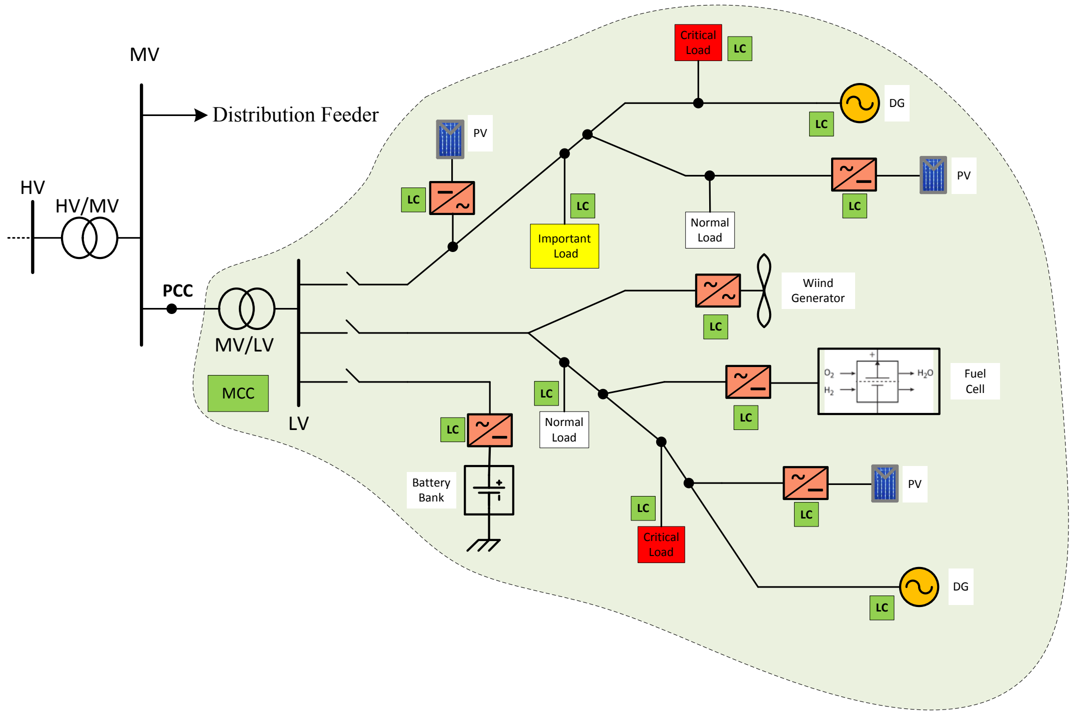

Figure 3.1: *A general microgrid configuration*
LC: Local controller, MCC: Microgrid Central Controller

A point in the electrical network where the microgrid is connected to the main distribution grid is called Point of Common Coupling (PCC). This point is very important, because it determines the grid equivalent impedance as seen by DGs in the microgrid and it is the main location to monitor the dynamic behaviour of a grid connected microgrid. Normally, the PCC is located on the primary side of the transformer. From the PCC, the microgrid can be considered by the main grid as a single controllable unit [97]. At this point, the microgrid must fulfil all interfacing requirements in standards the defined by distribution system operator.

The Microgrid Central Controller (MCC), shown in Fig. 3.1, executes the overall control of operation and protection of the microgrid. The main objectives of MCC are twofold: first, to maintain overall microgrid voltage and frequency within the specified limits; and secondly, to ensure energy optimisation for the microgrid. In addition, MCC performs protection co-ordination and optimization to provide power dispatch and voltage set points for all DERs. MCC should be designed to operate in automatic mode with provision for manual intervention as and when necessary. Two main functional modules in the MCC are Energy Management Module (EMM) and Protection Co-ordination Module (PCM). These controllers are manufactured by companies such as ELVI SPA and ABB S.A. [98], [99].

Figure 3.1 shows that a microgrid can include various types of DERs such as internal combustion engines (commonly DGs), PVs, WTs, and SBBs. These DERs and SBBs are the main components considered in this planning study. Other DERs such as fuel cells, microturbines, and gas turbines, can also be considered in microgrid planning. Each DER is controlled by its own Local Controller (LC) which implements all functionalities that are local and performed by a single DER, SBB or controllable load. These functionalities include: protection functions, primary voltage and frequency control, primary active and reactive power control, and control of charging and discharging of SBBs or fuel cells [7], [96]. The main required feature for the LC is the ability to quickly control the DERs independently, with minimum dependence or completely no dependence on communication links. Since the operation of DERs depends on other DERs and ESSs, it is necessary to consider the flexibility and limitation of these components when optimizing microgrid planning. The following subsections present mathematical modeling of the components considered in this study.

3.3 Component Modelling

This section presents modelling of microgrid components which are considered in this planing study. These components include DGs, PVs, WTs, SBBs and Biderectional Converters (BCs).

3.3.1 Diesel Generator

The main characteristics of DGs which are considered in the long-term planning of hybrid microgrid are fuel consumption curve and efficiency curves. The fuel curve describes the amount of fuel the generator consumes to produce electric power. Fuel consumption curves for DGs are usually modeled by using quadratic function:

$$FC_g = C_g P_g^2 + B_g P_g + A_g \tag{3.1}$$

where FC_g is fuel consumption of DG of type g, C_g, B_g, and A_g, are coefficients of quadratic fuel consumption function for DG of type g, and P_g is the output power from the DG of type g. The coefficients of quadratic fuel consumption curve are derived from the manufactures data sheet. In order to incorporate the quadratic cost function into the MILP planning model, (3.1) is linearised and replaced by a PWLA function with three linear segments. Since the fuel consumption and hence the cost of DG is minimized, and the fuel consumption characteristic is monotonically increasing convex function, the PWLA is formulated without using binary variable:

$$FC_g = \max_{q=1,2,3} \{B_{q,g} P_g + A_{q,g}\} \tag{3.2}$$

where q, is the index of segments of the PWLA fuel consumption curve. However, standard microgrid planning tools such as HOMER and iHOGA, use a linear fuel consumption curve given by:

$$FC_g = B_g P_g + A_g P_g^{rated} \tag{3.3}$$

where in this case, B_g is the fuel curve slope in $[L/kWh]$, P_g is the output power from the DG in $[kW]$, A_g is the fuel curve intercept coefficient in $[L/kWh]$, P_g^{rated} is the rated capacity of the generator in $[kW]$. The coefficients can be obtained by curve fitting of manufactures data or adopting default values for A and B as proposed by Skarstein and Ullen [100]. Figure 3.2 shows PWLA of the quadratic fuel consumption curve of a 16 kW DG.

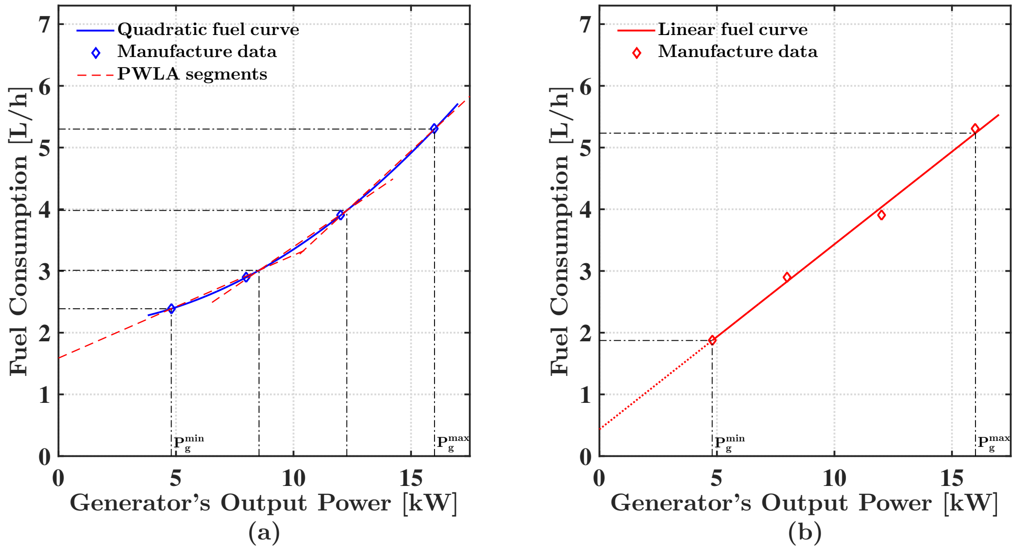

Figure 3.2: *Fuel consumption curve for 16 kW diesel generator (a) Quadratic and PWLA curves (b) Linear curve*

Electrical efficiency of DG depends on characteristic of the diesel fuel, and is related to the generator's output power by:

$$\eta_g = \frac{3600 P_g}{\rho_{diesel} LHV_{diesel} FC_g(P_g)} \tag{3.4}$$

where η_g is electrical efficient of the DG, P_g is the DG output power in kW, ρ_{diesel} is the density of diesel fuel usually 832 kg/m^3, LHV_{diesel} is the lower heating value of diesel in $43.2MJ/kg$, and $FC_g(P_g)$ is the fuel consumed to generate output power P_g. Figure 3.3 shows the efficiency curve for 16 kW DG obtained by using quadratic and linear approximations.

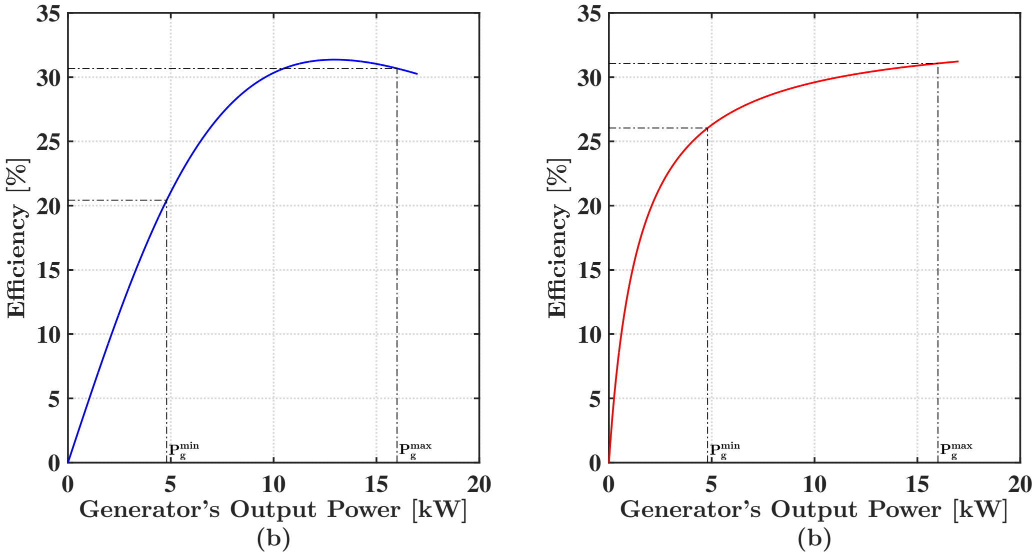

Figure 3.3: *Efficiency curves for 16 kW diesel generator obtained by (a) Quadratic fuel consumption (b) Linear fuel consumption*

As it can be seen in Fig.3.3, the generator efficiency is poor for low output power levels and increases with generation. For quadratic fuel consumption curve, efficiency increases to some optimum level after which it begins to diminish as the output power approaches the maximum ratings of the generator. Most DG are designed so that the range in which the generator is most efficient is at or close to the rated output power. DGs manufactures do not recommend operating the generators at less than 30% of its rated output power. The reason for this, as revealed in Fig.3.3, is that the generator efficiency is significantly reduced with a reduction in its output power. Operating the DG at lower output power has adverse effects on the diesel engine operation: lower cylinder pressure, lower temperature, ignition problems, poor combustion, soot formation, and aggregation of unburned fuel in the cylinder. These conditions deteriorate the engine efficiency allowing hot combustion gases, soot particles and unburned fuel to leak past the piston rings. As a results, the DG maintenance will be frequent thus increasing the maintenance costs. This situation is common in systems with oversized DG, thus justifying the need to optimize the mix, number and capacities of DG to be installed in microgrid.

A constraint to limit the minimal power output of the DG to 30% of its rated capacity is included to model the minimum operation limit. In additional, the DG cannot generate more power than its rated capacity. These two conditions are specified by the upper and lower bounds to enforce the technical limits for the DG as in (3.5).

$$\underline{P_g} \leq P_g \leq \overline{P_g} \tag{3.5}$$

where $\underline{P_g}$ is the minimum power specified as 30% of the maximum power $\overline{P_g}$ of the generator.

3.3.2 Photovoltaic Array

Output power of a PV array depends on the solar irradiance, environmental temperature, panels characteristics and efficiency. The output power is nonlinearly related to the incident irradiance and temperature of the surface of the PV panel (the PV cell temperature). This temperature is the same as the ambient temperature during the night but in full sun it can exceed the ambient temperature by great amount. The cell temperature, T_h^c, in any period h is calculated from the ambient temperature T_h^a, the incident irradiance G_h and the Nominal Operating Cell Temperature, NOCT, by [101]:

$$T_h^c = T_h^a + \frac{NOCT_p - 20}{800} G_h \tag{3.6}$$

The maximum output power from the PV panel at any irradiance and cell temperature is given by [102]:

$$\overline{P}_{h,p} = f_{der} \frac{G_h}{G^{STC}} \overline{P}_p^{STC} \left[1 + \gamma_p \left(T_h^c - T^{STC}\right)\right] \tag{3.7}$$

where $\overline{P}_p^{STC}$ is the maximum power output under standard testing conditions with $G^{STC} = 1000\ W/m^2$, $T^{STC} = 25\,°\mathrm{C}$ and the air mass value $AM = 1.5$, while γ_p is the maximum power correction factor for temperature and f_{der} is the derating factor. Substituting (3.6) in (3.7) gives,

$$\overline{P}_{h,p} = f_{der} \frac{G_h}{G^{STC}} \overline{P}_p^{STC} \left[1 + \gamma_p \left(T_h^a + \frac{NOCT_p - 20}{800} G_h - T^{STC}\right)\right] \tag{3.8}$$

The PV array constists of parallel and series connection of PV panels. The number of installed PVs is defined as $N_p = N_p^{par} N_p^{ser}$ where N_p^{par} is the variable representing the number of parallel connected PV panels and N_p^{ser} is the parameter representing the number of series strings of PV panels of type

p. Therefore, assuming that the PV panel is operated at Maximum Power Point (MPP) for all solar irradiance and ambient temperatures, then the total array output power is given by 3.9.

$$P_{h,p}^{pv} = \sum_{\forall p} N_p \overline{P}_{h,p} \tag{3.9}$$

Note that the planner can model power mismatching, power losses due to dust and dirt, and partial shading effects, by setting the value of derating factor. The $(NOCT)$ values can be obtained from the PV module datasheet while T_h^a and G_h can be obtained from the weather forecast data. It is important to mention that the parameter G_h, i.e. solar irradiation, refers to the incident irradiation to the surface of the PV panel (for detailed calculation of this parameter see Ch.2 of [103]).

3.3.3 Wind Turbine

Small WTs industry has been growing rapidly due to the market expansion for small power producers and microgrids customers who needs to employ this technology. Currently, there are about 229 manufacturers of small WTs worldwide [104]. Manufacturing and deployment of small wind turbines is governed by a number international standards such as American Wind Energy Association (AWEA), International Electrotechnical Commission (IEC), and British Standards Institution (BSI) [105]. Generally most small wind turbines need an average speed of at least $4.5\ m/s$ to be able to generate useful power. Power from the wind turbine is related to the wind speed V_w, the area swept by the turbine's rotor A, and the air density ρ_{air}, the rotor power coefficient C_p and the drive train efficiency (i.e. generator power/rotor power) η [105].

$$P_W = \frac{1}{2}\rho_{air} A C_p \eta V_w^3 \tag{3.10}$$

The most useful characteristic of WT required for the planning purposes is its power curve. The power curve relates electrical output power of the WT to the wind speed at hub height incident to the rotor in the ambient flow field. The shape of the power curve depends on the speed control strategy. Since the power in the wind is a cube of the wind speed, as shown in (3.10), it is necessary to control and limit the converted mechanical power at higher wind speed. The following are three main control techniques for small wind turbines:

- Stall control, the blade position is fixed but stall of the wind appears along the blade at higher wind speed,
- Active stall, the blade angle is adjusted in order to create stall along the blades, and
- Pitch control, the blades are turned out of the wind at higher wind speed.

Figure 3.4 shows the typical power curve of the active stall or pitch controlled WT. Generally, output power output the stall-controlled WT decreases slightly after the WT exceeding the nominal wind speed. The overshoot which appears for the stall control WT depends on its aerodynamic design. For the active stall or pitch-controlled WT, the controller adjusts the orientation of the blades in the WT to maintain a close-to-optimal angle and rotor speed. These turbines can maintain a constant output power output after the WT nominal wind speed is reached, and continues until the cut-off speed is reached.

In this thesis, generation from WTs is obtained by interpolating the power curve of each type of turbine considered in the planning. Hub height wind speed used in the interpolation is calculated by

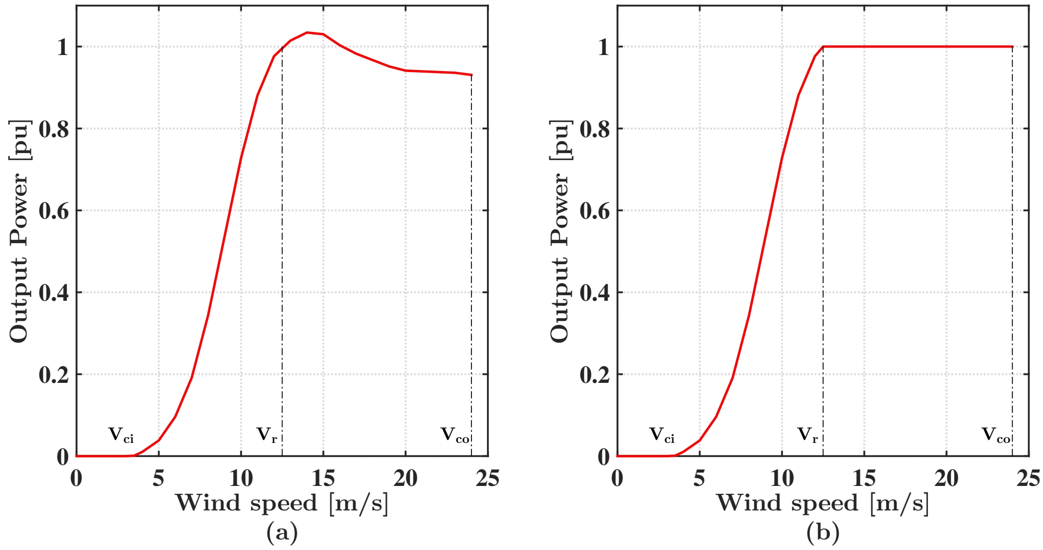

Figure 3.4: *Typical power characteristics of fixed speed wind turbines [2]. (a) Stall control, (b) active stall control, and (c) pitch control.*

using logarithmic law and the effect of air density is modelled by using the air density ratio. Hourly average wind speed at the anemometer height can be obtained from the site measurement data or from the meteorological database. The anemometer wind speed $V^r_{h,w}$ measured at reference height z_r is converted to the hub wind speed corresponding to the turbine hub height z_h by (3.11):

$$V^{hub}_{h,w} = \left(\frac{z_h}{z_r}\right)^{\alpha} V^r_{h,w} \tag{3.11}$$

where $V^{hub}_{h,w}$ is the hub wind speed, α is the shear exponent which varies nonlinearly with the surface roughness of the terrain over which the wind blows. The WT output power is obtained by referring the power corresponding to the hub wind speed (3.11) in the power curve. To correct for the altitude of the site, the turbine output power determined determined from its power curve is multiplied by the air density ratio (3.12) [106].

$$\overline{P}_{h,w} = \left(\frac{\rho}{\rho_0}\right) P^0_{h,w}(V^{hub}_{h,w}) \tag{3.12}$$

where $\overline{P}_{h,w}$ is the calculated output power of WT of type w in hour h, $P^0_{h,w}$ is the measured power at the standard air density $\rho_0 = 1.225\ kgm^{-3}$, and ρ is the air densities at the site location. The air density ratio is assumed to be constant throughout a year and is calculated as shown below in (3.13) [107].

$$\frac{\rho}{\rho_0} = \left(1 - \frac{\beta z_h}{T_0}\right)^{\frac{g}{RB}} \left(\frac{T_0}{T_0 - \beta z_h}\right) \tag{3.13}$$

where ρ and ρ_0 are as defined above, B is the lapse rate $(0.00650K/m)$, z_h is the turbine hub altitude in (m), T_0 is the standard temperature in (K), g is the acceleration due to gravity $(9.81m/s^2)$, and R is is the gas constant $(287J/kg.K)$.

Total power generated by multiple WTs may be obtained by adding the individual power generated by each type of turbine. However, similar turbines may not produce same power due to the variability resulted from their relative spacing, characteristics of the site and wake effect. To simplify the model, all turbines are assumed to operate at their corresponding MPP and the the above variations are considered negligible particularly for the microgrid case in which only few turbine may be installed. Therefore, the total power from the wind turbines by (3.14) is given by:

$$P_{h,w}^{wt,tot} = \sum_{w} N_w \overline{P}_{h,w} \tag{3.14}$$

where N_w is an optimization variable representing the total number of wind turbines of given type.

3.3.4 Energy Storage in Microgrid

When a microgrid is operating in islanding mode, the balance between generation and demand becomes crucial. Power generated from distributed renewable resources in a microgrid is highly intermittent. Matching power generated with electricity demand of end-users makes it necessary the use of reliable, efficient and cost-effective energy storage systems. The power balance requirement is still important even when the microgrid is connected to a distribution system with the possibility of import or export power from/to the grid. However, from the technical and economical point of view, energy storage plays a paramount role in microgrid. A classification of energy storage technologies in microgrids includes the following:

- Mechanical (pumped hydro, compressed air, flywheels);
- Electrochemical (Secondary batteries: Lead acid / NiCd / NiMh / Li / NaS and Flow batteries: Redox flow / Hybrid flow);
- Chemical (hydrogen);
- Electrical (capacitors, super-capacitors, Super-conducting Magnetic Energy Storage (SMES));
- Thermal (Sensible, latent and thermochemical storage).

The choice of the economically viable technology for particular application depends on the factors such as: required level of power and energy to be stored, power and energy density, and storage characteristics. The latter includes: life time, operation cycle, charging and discharging performance and environmental impact. For purposes of comparison, Figure 3.5 summarises characteristics of various energy storage technologies and their possible application ranges, based on the duration of discharge and photovoltaic system power rating [108]. Of all storage technologies, secondary batteries, particularly lead acid batteries, are widely applied in rural electrification system, mainly to provide short-term power balancing and/or long-term energy management.

3.3.5 Storage Battery Bank Model

The performance of battery storage system is affected by factors such as the SOC, storage capacity, rate of charge/discharge, environmental temperature and age/shelf life of the SBs [109]. The SBB has power and energy constraints which must be fulfilled during the optimization process. The main parameters of a SB are:

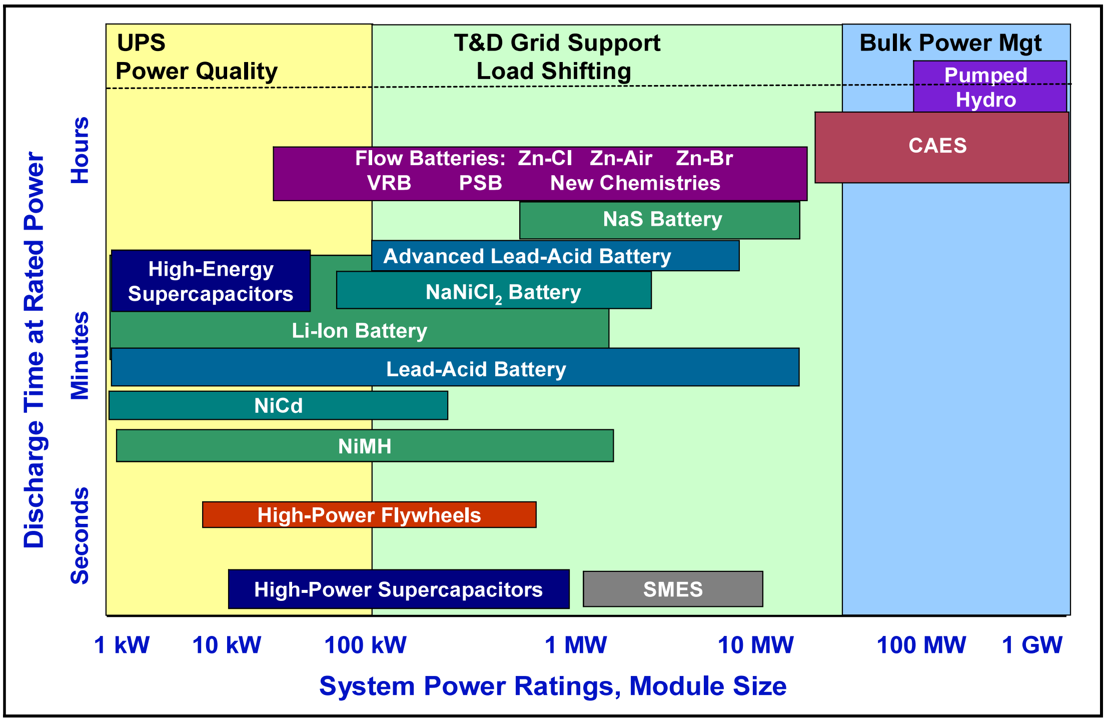

Figure 3.5: *Energy storage technologies and their applications*

- Nominal rated capacity
  The nominal capacity defines the total charge that can be stored in a battery. The capacity of a battery, expressed in Ampere-hours [Ah], is the total charge expressed in [Ah] that can be obtained from a fully charged battery under specified discharge conditions specified by the manufacturer. In this thesis it is preferred to convert the Ah units to units of energy in order to specify the total energy that can be supplied by the battery from full charge to cut-off voltage. This conversion is given by:
  $$C_{b,n}[Wh] = C_{b,n}[Ah]\ V_{b,n}[V] \tag{3.15}$$
  where $V_{b,n}$ is the nominal voltage of the battery. The capacity of the battery depends on its charging and discharging rates as shown in the next item.

- C-rate or Charging and Discharging rates
  C-rate specifies the charge or discharge current equal in Amperes to the rated capacity in Ah. Multiples larger or smaller than the C-rate are used to express larger or smaller currents. For example, the C-rate is 600 mA in the case of a 600 mAh battery, whereas the C/2 and 2C rates are 300 mA and 1.2 A, respectively. These rates provides a convenient way to compare currents at which batteries are discharged or charged independently of their capacities.

- Cycle Life:
  The number of cycles that a cell or battery can be charged and discharged under specific conditions, before the available capacity in [Ah] fails to meet specific performance criteria. This will usually be 80% of the rated capacity.

- Battery State of Charge:
  SOC is the fraction or percentage of the capacity that is still available in the battery. It indicates the quantity of electricity which is still available in the battery relative to its nominal capacity with the given past and future discharging rates.

$$SOC_{h,b} = \frac{Q^{rem}_{h,b}}{C^n_b} = \frac{C^n_b - Q_{h,b}}{C^n_b} = 1 - \frac{Q_{h,b}}{C^n_b} \tag{3.16}$$

where $Q^{rem}_{h,b}$ is the quantity of charge remaining in the battery at hour h, C^n_b the capacity of the battery and $Q_{h,b}$ the quantity of charge which has been drawn from the battery of type b at hour h. This quantity of charge, already delivered by the battery at hour h, is given by:

$$Q_{h,b} = \int_0^h i_{dch}(h)dh \tag{3.17}$$

where $i_{dch}(h)$ is the is the discharging current.

A complementary parameter that defines the fraction or percentage of the capacity which has been removed from the fully charged battery is called the depth of discharge (DOD).

$$DOD = \frac{Q_{h,b}}{C^n_b} \tag{3.18}$$

Therefore

$$DOD = 1 - SOC \tag{3.19}$$

Even though the SOC and DOD values are unit less parameters, the calculations involved here express them in units of energy (i.e. Wh) to specify the energy remaining in the battery bank and the energy already delivered by the battery bank at a given time. The initial state of charge SOC_0 [Wh] is specified to indicate the amount of energy available in the battery bank before the beginning of any optimization process.

3.3.5.1 Simple Battery Model

The simple battery model energy in the SBB in in each hour by using an energy balance equation given by:

$$E_{h,b} = E_{h-1,b} + \Delta h \left(\eta^{ch}_b P^{ch}_{h,b} - P^{dch}_{h,b}/\eta^{dch}_b\right) \qquad \forall h, b \tag{3.20}$$

where $E_{h,b}$ is the energy in the SBB of type b in the current hour h, $E_{h-1,b}$ is the energy in the SBB of type b in the previous hour $h-1$, Δh is the time step, $P^{ch}_{h,b}$ is the charging power to the SBB of type b, η^{ch}_b is the charging efficiency of SB of type b, $P^{dch}_{h,b}$ is the discharging power from the SBB of type b, and η^{ch}_b is the discharging efficiency of SB of type b. This model considers different charging and discharging efficiencies and splits the net SBB power into two positive variables for charging and discharging power in order to: identify the charging and discharging cycles separately, and apply the corresponding efficiencies. Hourly self-discharging rate is considered negligible. Maximum and minimum storage energy limits are modeled by constraint (3.21).

$$\underline{E}_b \leq E_{h,b} \leq \overline{E}_b \qquad \forall h, b \tag{3.21}$$

where $\overline{E}_b$ is the maximum energy limit of SBB of type b, and $\underline{E}_b$ is the minimum energy limit for SBB of type b. The charging and discharging power are limited by the maximum charging and discharging power which depend on SOC, maximum charging and discharging currents and the charging and discharging rates, respectively.

$$0 \leq P^{ch}_{h,b} \leq \overline{P}^{ch}_{h,b} \qquad \forall h, b \qquad (3.22a)$$

$$0 \leq P^{dch}_{h,b} \leq \overline{P}^{dch}_{h,b} \qquad \forall h, b \qquad (3.22b)$$

where $\overline{P}^{ch}_{h,b}$ is the maximum charging power for the SB of type b, $\overline{P}^{dch}_{h,b}$ is the maximum discharging power for the SB of type b, Capacity of installed SBB is an auxiliary variable which depends on the number of installed SBs.

$$\overline{C}_b = N_b \, C^{sb,n}_b \, V^{sb,n}_b \qquad \forall b \qquad (3.23a)$$

where $\overline{C}_b$ is the total total capacity of SBB of type b, N_b is the number of installed SBs, $C^{sb,n}_b$ is the nominal capacity of a single SB of type b, and $V^{sb,n}_b$ is the nominal voltage of a SB of type b. The number of installed SBs is defined as $N_b = N^{par}_b N^{ser}_b$, where N^{par}_b is the number of parallel connected batteries in a string of SB of type b and N^{ser}_b is the number of series strings of SB of type b. Number of battery in series is determined by the required input voltage of the bidirectional charger converter. Initial energy level, and minimum and maximum energy levels in the SBB are defined by:

$$E_{0,b} = SOC_{0,b}\overline{C}_b \qquad \forall b \qquad (3.24a)$$

$$\overline{E}_b = \overline{C}_b \qquad \forall b \qquad (3.24b)$$

$$\underline{E}_b = (1 - DOD_b)\overline{C}_b \qquad \forall b \qquad (3.24c)$$

where $E_{0,b}$ is the initial energy in the SBB of type b, $SOC_{0,b}$ is the relative initial SOC of SBB of type b, $\overline{E}_b$ is the minimum energy limit for SBB of type b, $\underline{E}_b$ is the minimum energy limit for SBB of type b, and DOD_b is the depth of discharge of SBB of type b.

A straightforward way to enforce the complementarity condition which requires that the charging and discharging power cannot be greater than zero at the same time, is to use the big M formulation (3.25a) to (3.25c).

$$P^{ch}_{h,b} \leq x^{ch}_h M \qquad \forall h, b \qquad (3.25a)$$

$$P^{dch}_{h,b} \leq x^{dch}_h M \qquad \forall h, b \qquad (3.25b)$$

$$x^{ch}_h + x^{dch}_h \leq 1 \qquad \forall h, b \qquad (3.25c)$$

The big M formulation increases the size of the planning problem since it requires at least one more binary variable for each hour of the planning horizon. Alternatively, replacement cost of the SBB, as a function of charging and discharging power, charging and discharging efficiencies, and replacement cost per hour, is included in the objective function. Since the objective function minimizes the Life Cycle Cost (LCCA) of the system, in most cases the optimal solution will not contain charging and discharging power at the same time, thus fulfill the complementarity condition without using binary variables [110].

3.3.5.2 Kinetic Battery Model (KiBaM)

The Kinetic Battery Model (KiBaM), introduced by Manwell and McGowan, models the SBB as a two tank electrical storage device [111], [112]. Total energy, E^{tot}, in the SBB is distributed over these two tanks into the available-energy E^a, and the bound-energy, E^b,. Figure 3.6 illustrates the KiBaM.

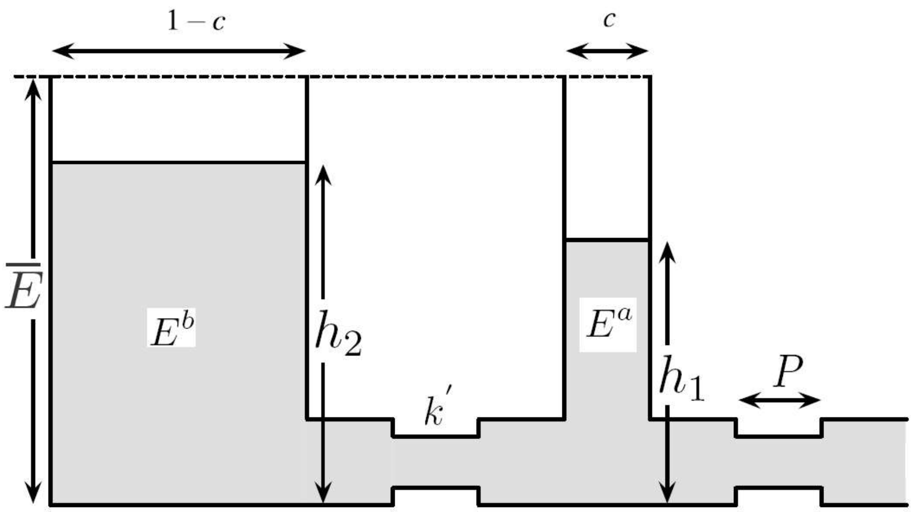

Figure 3.6: *The Kinetic Battery Model (KiBaM)*

Each tank has a unit depth, but different widths, corresponding to different volumes. The width of tank 1 ("available") is c whereas that of tank 2 ("bound") is $1-c$. The combined width of the two tanks is thus equal to 1, and gives the combined tank area of unit. The combined volume of the tanks is $\overline{E}$. Since the area is unit, when both tanks are full, the maximum head $\overline{h}$ is also equal to the maximum energy $\overline{E}$. The valve between the two tanks has a fixed conductance $k^{'}$ which model the first order rate constant of a chemical reaction/diffusion process by which the bound energy becomes available. The rate at which the bound energy becomes available is proportional to the difference in "head" of the two tanks. It is assumed that the power flow during the time step of interest is maintained constant by the output valve.

In summary, the capacity section of the KiBaM, which is of interest for the planning studies, is characterized by three parameters: capacity ratio c, maximum (theoretical) capacity of the SBB which is equal to the maximum energy $\overline{E}$, and the overall rate constant defined by $k = k^{'}/c(1-c)$. It is assumed that the same parameters apply to both charging and discharging. The total amount of energy stored in the SBB in any hour h is the given by the sum of the available and bound energy. Note that lower subscript b stand for index of types of SBs, whereas when similar letter appear as superscript represent "bound" energy.

$$E^{tot}_{h,b} = E^a_{h,b} + E^b_{h,b} \qquad \forall h, b \tag{3.26}$$

where $E^{tot}_{h,b}$ is the total energy in the SBB of type b, $E^a_{h,b}$ and $E^b_{h,b}$ are available and bound energy in SBB of type b in hour h. The available and chemically bound energy at the end of any hour are defined by:

$$E^a_{h,b} = E^a_{h-1,b}\, e^{-k_b \Delta h} + \frac{(E^{tot}_{h-1,b}\, k_b\, c_b + P^{net}_{h,b})(1-e^{-k_b \Delta h})}{k_b} + \frac{P^{net}_{h,b}\, c_b\, (k_b\, \Delta h - 1 + e^{-k_b \Delta h})}{k_b} \qquad \forall h, b \tag{3.27a}$$

$$E^b_{h,b} = E^b_{h-1,b}\, e^{-k_b \Delta h} + \left(E^{tot}_{h-1,b}\,(1-c_b)\,(1-e^{-k_b \Delta h}\right) + \frac{P^{net}_{h,b}\,(1-c_b)\,(k_b\,\Delta h - 1 + e^{-k\Delta h})}{k_b} \qquad \forall h,b \qquad (3.27b)$$

where $E^a_{h,b}$ is the available energy in the SBB of type b, $E^b_{h,b}$ is the bound energy in the SBB of type b, $P^{net}_{h,b}$ is the net power of the SBB of type b, Δh is the time step, c_b is the capacity ratio parameter for the SBB of type b, and k_b the rate constant parameter for the SBB of type b. In this formulation, the net power is defined by:

$$P^{net}_{h,b} = \eta^{ch}_b P^{ch}_{h,b} - P^{dch}_{h,b}/\eta^{dch}_b \qquad (3.28)$$

In KiBaM, maximum charging and discharging power are formulated as the functions of the stored energy.

$$\overline{P}^{ch}_{h,b} = \frac{-k_b\; c_b\; \overline{E}_b \;+\; k_b\; E^a_{h,b}\; e^{-k_b \Delta h} \;+\; E^{tot}_{h,b}\; k_b\; c_b\; (1-e^{-k_b \Delta h})}{[1-e^{-k_b \Delta h} \;+\; c_b\; (k_b\; \Delta h - 1 \;+\; e^{-k_b \Delta h})]\; \eta^{ch}_b} \qquad \forall h,b \qquad (3.29a)$$

$$\overline{P}^{dch}_{h,b} = \frac{\left[k_b\; E^a_{h,b}\; e^{-k_b \Delta h} + E^{tot}_{h,b}\; k_b\; c_b\; (1-e^{-k_b \Delta h})\right]\; \eta^{dch}_b}{1-e^{-k_b \Delta h} + c_b\; (k_b\; \Delta h - 1 \;+\; e^{-k_b \Delta h})} \qquad \forall h,b \qquad (3.29b)$$

where $\overline{E}_b$ is the maximum energy limit of SBB of type b, $\overline{P}^{ch}_{h,b}$ is the maximum charging power for the SB of type b, and $\overline{P}^{dch}_{h,b}$ is the maximum discharging power for the SB of type b.

In this model, the SOC of a SBB is defined by:

$$SOC_{h,b} = \frac{E_{h,b}}{\overline{E}_b} \qquad (3.30)$$

The parameter c, k and $\overline{E}$ can be obtained by using the SB parameter finding programmes[1]. Alternative approach to obtain these parameters can be implemented by using nonlinear curve fitting function based on Levenberg-Marquardt algorithm [111]. The method requires data for the SB capacity curve shown in Figure 3.7. In this case, $c = 0.273$, $k = 0.3441\ h^{-1}$ and $\overline{E} = 540.43\ Ah$.

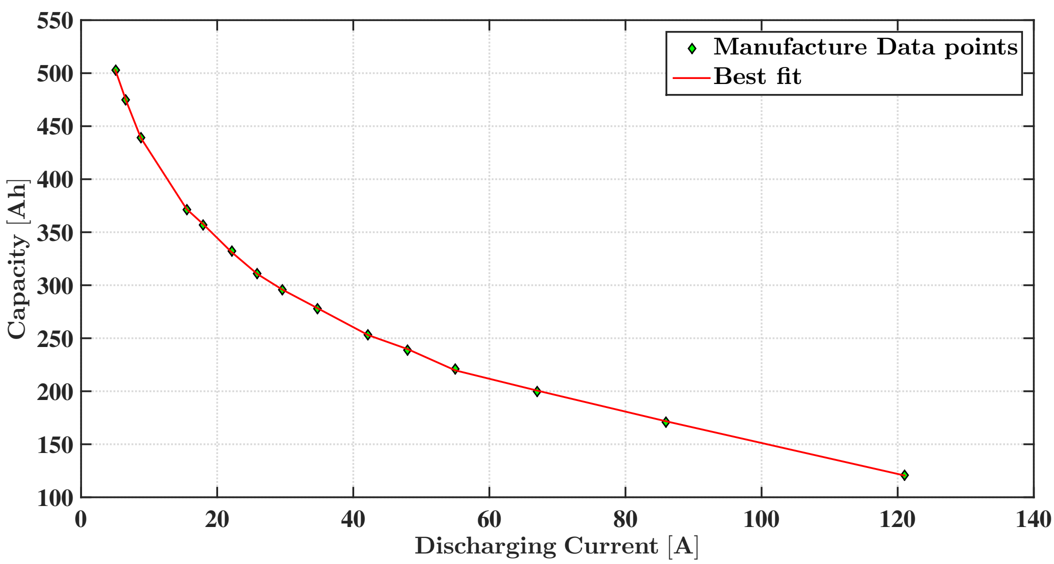

Figure 3.7: *Typical capacity versus discharge current curve for 357 Ah, 12V Storage Battery*

[1] https://www.umass.edu/windenergy/research/topics/tools/software/kibam

3.3.5.3 Lifetime Model for the Storage Battery Bank

The SBB lifetime model is one of the key part of the planning model as is used to assess the impact of the desired operation strategy on the expected lifetime of all types of SBs considered in the planning. Two main types of lifetime models for lead acid batteries are: (i) post processing models and (ii) performance degradation models [113]. The post processing lifetime models are pure lifetime models that do not contain any performance measure. They are often used to analyse measured data from real systems. The performance degradation lifetime models combines performance measures with the lifetime indicators such that the performance of the SB degrades with time, depending on its utilisation pattern. Obtaining the utilization pattern involves calculation of lifetime consumption or wearing of the SB which depends on factors: charge rate, discharge rate, temperature, acid stratification, SOC and DOD, time at low SOC, cycle duration, overall energy transfer (throughput), charge factor, time between full charge, and partial cycling [114]. Two common methods for calculating the lifetime consumption of the SB are [115]:

- Ah-throughput counting, and
- Cycle counting

The Ah-throughput model simply counts the amount of charge through the battery. In this model, it is assumes that there is a fixed amount of energy that can be cycled through a SB before it requires replacement, regardless of the DOD of the individual cycles or any other parameters specific to the way the energy is drawn in or out of the battery. On the other hand, the cycle counting model mainly rely on the current and SOC to model lifetime of SB. The main assumption of the cycle counting model is that the magnitude of a charge cycle determines the fraction of lifetime that is consumed. This implies that even though the charge throughput is the same, the lifetime consumption can be different depending on whether the battery is cycled at large or small magnitudes of SOC.

This thesis adopts the Ah-throughput model due to its simplicity, especially from a modelling perspective, and the possibility to perform throughput calculations using either Ah or kWh unit. The estimated throughput is derived from the DOD versus cycles to failure curve data provided by the manufactures. For each set of DOD and number of cycles to failure, the lifetime throughput is calculated by:

$$Q_b^{lifetime} = f_i DOD_i \left(\frac{Q_b^{max} V_b^n}{1000} \right) \tag{3.31}$$

where $Q_b^{lifetime}$ is the lifetime throughput in kWh, f_i is the number of cycles to failure, DOD_i is the depth of discharge in $\%$, Q_b^{max} is the maximum capacity of the battery in Ah, and V_b^n is the nominal voltage of the battery in V. Figure 3.9 shows the plot of manufacture data for DOD, cycles to failure, and the calculated lifetime throughput for a flooded deep cycle, 357 Ah, 12V SB by Rolls.

If the minimum SOC is specified as 40%, then the range of allowable DOD is between 0% and 60%. In this case, the expected throughput is obtained by averaging all the lifetime throughput values in the DOD range between 0% and 60%, thus giving a value of 7977.3 kWh This procedure implies linearization of the SB lifetime model, i.e. it is assumed that the value of battery throughput is constant for the above range of DOD. However the actual throughput varies as can be seen in Fig. 3.9

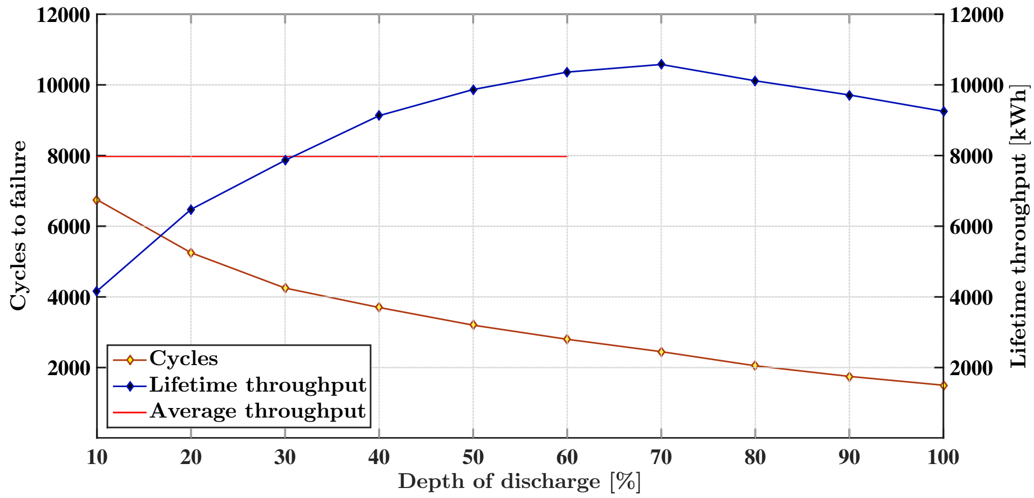

Figure 3.8: *Lifetime curve of 357 Ah, 12 V Storage Battery*

3.3.6 Power Electronic Interfacing Converters and Inverters

Power electronic converters play important role of interfacing and power conversion to enable components of different specification and technologies to be connected to a common AC or DC bus bar. For the planning purpose, the most important characteristics of the interfacing converters are their conversion efficiencies and maximum capacity limit. Inverters are DC to AC interfacing converters which are employed to connect components which generate AC power to the DC bus bar. Special types of inverter capable of operating in rectification and inversion mode can be employed for interfacing the main DC and AC bus bars in a microgrid.

Transformation efficiency of power inverter is defined by:

$$\eta = \frac{P_{AC}}{P_{DC}} = \frac{P_{DC} - P_{loss}}{P_{DC}} \tag{3.32}$$

where P_{AC} is the output AC power, P_{DC} the input DC power and P_{loss} are inverter losses. To establish the operation point of the inverter, it is necessary to relate its efficiency to the input power.

$$\eta = \frac{P_{AC}}{P_{DC}} = \frac{P_{DC} - P_{loss}}{P_{DC}} \tag{3.33}$$

where P_{AC} is the output AC power, P_{DC} the input DC power and P_{loss} are inverter losses. Power losses in a converter can be divided into two distinct parts: static and dynamic losses. The first is constant and involves the power to supply the control unit and the other auxiliary parts only. The second part of power losses is load-dependent and consists of: switching losses on power switches, ohmic losses and the losses caused by temperature variation. Therefore, the total loss of the converter is not constant, and the efficiency is dependent mainly on the load current .

Power converters employed for interfacing the SBB are required to be able to offer bidirectional power flow to enable energy transfer during charging and discharging cycle. These converter are automatically controlled by a Battery Management System (BMS) which monitors the charging and discharging profiles as per technical specifications of the SBB. In modern systems, the BMS can have a

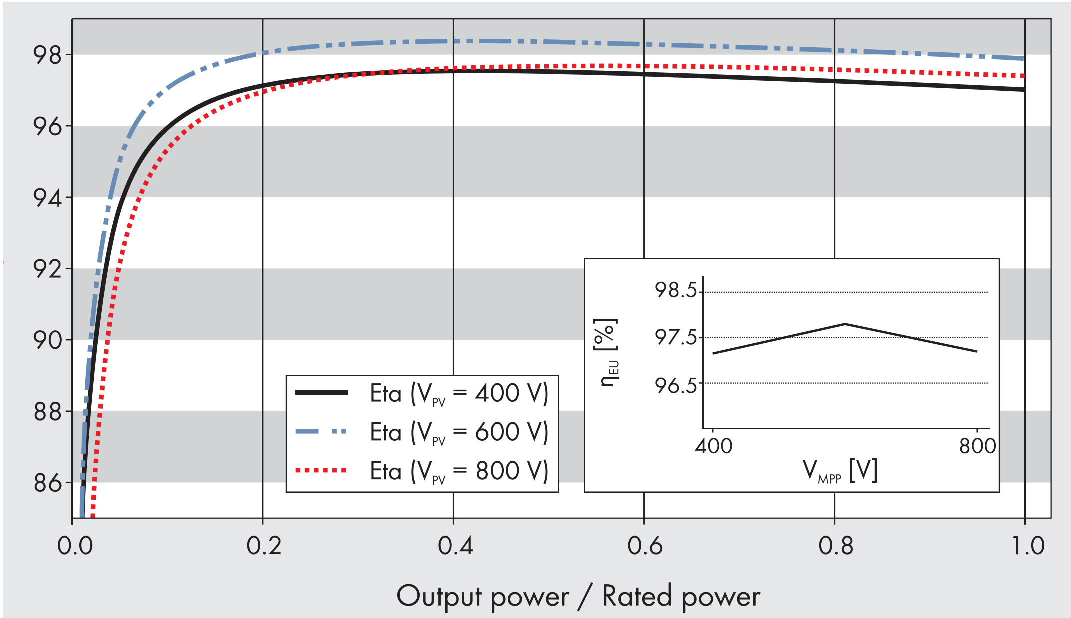

Figure 3.9: *Efficiency curve of Sunny Tripower 10000TL inverter*

provisional to communicate with the MCC system in order to ensure that the battery operates within its buffer range in order to allow short-term or long-term energy management. Similar to inverters, the efficiency of DC to DC converters are non linear function of its input power. In this study, efficiencies of power converters are assumed to be constant values set to 90%. Conversion limit is imposed on the main system interfacing converters which connect the DC and AC bus bar.

3.4 Energy Management System

Proper control of hybrid microgrid with multiple DERs and SB is critical to achieve stable, efficient, and reliable system operation [116]. The management and control of microgrid is achieved by using an intelligent supervisory control system which ensures proper operation in all conditions. For grid-connected microgrids, Distribution System Operator (DSO) standards require a robust control responsible for smooth transferring of the microgrid from grid-connected to island operation. These system management rules, or operational logics, must be considered in the planning of hybrid microgrid, albeit with some simplification as the real time operational logics will make the planning model untractable. Common control strategies for microgrids include: centralized, decentralized and hybrid control strategy [117]. The use of these strategies depends on the ownership and regulatory policies applied to a specific microgrid. So far, the centralised Energy Management System (EMS) is the most widely adopted approach. Figure 3.10 shows the architecture of centralised EMS. Note that although this thesis does not cover grid connected microgrid planning, the control architecture are illustrated using a generic microgrid concept with interconnection to the distribution system.

The centralized control system for microgrid can adopt hierarchical-type three-level management and control [108], [117]:

(i) Distribution System Operator (DSO) and Market Operator (MO);

(ii) Microgrid Central Controller (MCC);

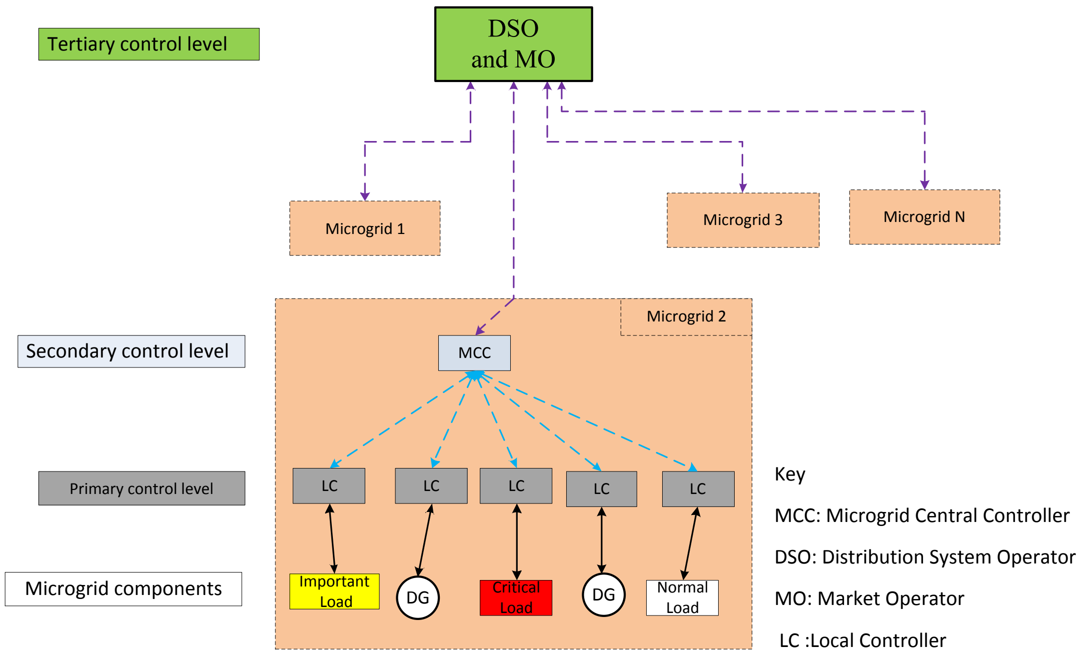

Figure 3.10: *Centralised energy management system*

(iii) Local Controllers (LC) .

In the grid-connected mode, the DSO and Market Operator (MO) determine the operational and market requirement for the distribution network in which more than one microgrids might be in operation. In this mode, the MCC performs optimization based on reliability, economics of local generation versus grid supply and demand, so as to continuously determine appropriate set points for the individual generators, storage elements, and loads in the microgrid. These set points are transferred to the LCs which control the operation of DGs, storage devices and dispatchable loads. The LCs interact with the MCC to exchange information on the current local operational constraints and conditions. Depending on the technology, the LCs may have a certain level of intelligence to enable some control operations to take effect independently of the MCC. The following control functions are incorporated within the LC:

- Active and reactive power control;
- Voltage control;
- Charging and discharging of storage devices;
- Load sharing through P-f control.

These functions enable each DER in the microgrid to adopt new operating conditions based on the operational mode of the microgrid. This include fast adoption of new generation set points during the transition from the grid connected to islanding operation mode. The above control functionalities are implemented through power electronic inverters, the dominating interfacing converters for renewable based DERs. In the islanded mode, the MCC optimizes the set points for generators, storage devices, and loads based on balance requirement between load and generation. Often, renewable energy based DERs will be operated at maximum power point to maximize their generation. Dispatchable DERs, which are capable of producing controlled active and reactive power on demand, are assigned the task of regulating the voltage and frequency. With this reference, the LCs of each DGs performs frequency-droop and voltage-droop control to enable sharing of real and reactive power components among all DGs, whenever possible depending on the primary source and on the technology.

Decentralized EMSs adopts a strategy in which a microgrid component is controlled by its own LC. This LC derives its control decision after communicating to the nearby LCs instead of being governed by the MCC. The neighbouring LCs communicate and reach a consensus on optimal set points of the parameter under consideration before effecting the control action [118]. In this scheme, LCs have the intelligence to make operational decisions without the central master controller. Decentralized EMS avoids single point failures and guarantee stable operation, system re-configuration and replication following availability of primary sources of energy [119]. Figure 3.11 illustrates the architecture and flow of information in decentralised EMS [108].

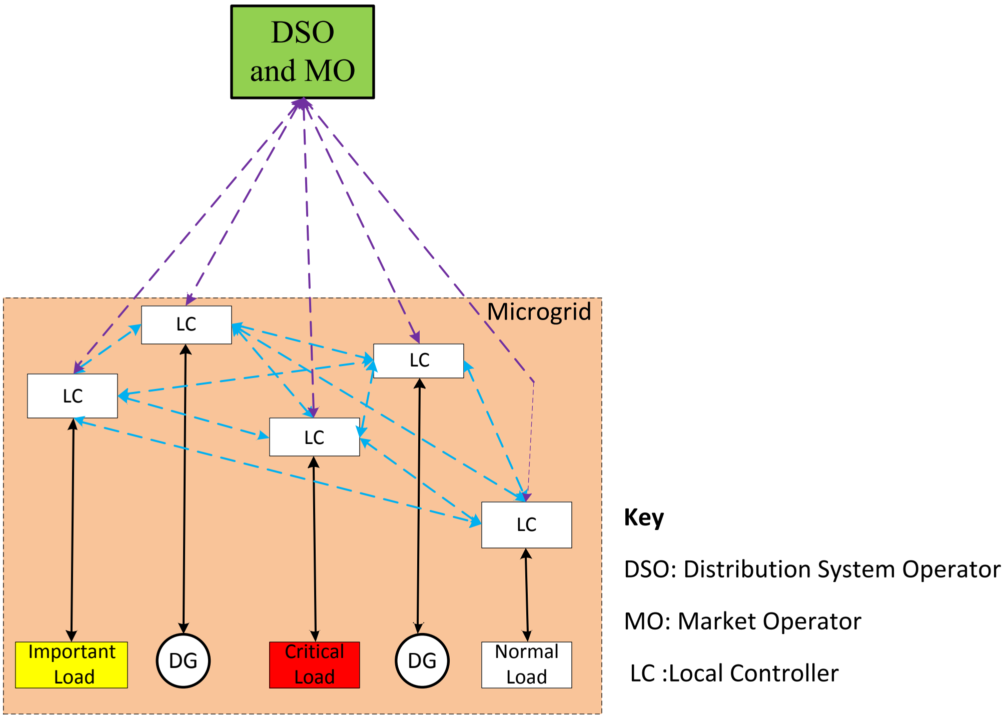

Figure 3.11: *Decentralised energy management system*

Another scheme for EMS, known as hybrid control paradigm, combines the centralized and distributed EMS. [116]. The DERs are grouped within a microgrid; MCC is used within each group, while distributed control is applied to a set of groups. With such a hybrid EMS, local optimization is achieved via centralized control within each group, while global coordination among the different groups is achieved through distributed control. This way, the computational burden of each controller is reduced, and single-point failure problems are mitigated.

3.5 Hybrid System Dispatching Strategies

Central to the operational planning and energy management in microgrid is the concept of dispatching strategy. These are rules which control the flow of energy among microgrid components. The foundation of this work is set on the quest for a joint optimization of the number of components in the microgrid and their operation. Optimal operation of these components depends on the selected dispatching strategy. Dispatching, commonly referred to as Economic Dispatching (ED), is one of the most important and a well established study in power system operations. ED dates back to early 1920's, when engineers were concerned with the problem of economic allocation of generation or the proper division of the load among the generating units available [120],[121]. The main objective is to schedule the available (or committed) generating units outputs so as to meet the required load demand at minimum operating cost while satisfying all units and system equality and inequality constraints. Microgrids consist of a mix of conventional and non conventional generating units and storage system. Therefore, a microgrid's dispatching strategy is basically an algorithm which governs how to economically schedule generation from the available microgrid conventional units taking into consideration the presence of renewable generation sources and storage system. In particular, exchange of energy with the storage system is subject to fulfilling the dynamic constraints which links its overall current and previous state of charge. It is the dispatching strategy which determines the flow of energy to and from various sources in the microgrid.

Selection of the dispatching strategy has a significant effect on the overall cost of a microgrid. Based on the available resources and technologies to be applied in the design of the hybrid generation system for a microgrid, its optimal planning is often faced by conflicting objectives. For example, it is always required to minimize the fuel cost, component costs, number of startup and shutdown of diesel generators, sometimes to maintain the operating point of the diesel generators constant and at high efficiency, and to maximize the utilization of renewable resources. These objectives have led to several dispatching strategies for controlling energy flow in microgrids with renewable sources, diesel generators and storage batteries. The most common strategies are:

- Battery Charging and Discharging Strategy
- Load-Following Strategy
- Cycle Charging Strategy
- Peak Shaving Strategy
- Predictive Dispatching Strategy

In the following some of these strategies are described.

3.5.1 Load-Following Strategy

The LFDS is also known as "zero charge strategy". Diesel generators are set to match the instantaneous load. It is required not to use the diesel generator output power to charge the batteries at any time. Whenever renewable power exceeds the gross electrical, demand the storage batteries are charged by the excess power until the bank becomes full charged. If the storage bank is fully charged, the excess power is dumped. The difference between the gross load and available renewable power is the net load to be supplied by either the storage batteries or diesel generators. This net load is shared among diesel generators and storage batteries, with the batteries use given preference (“Load following Battery Preference”). In case of deficit, when the storage batteries are not able to meet the net load, then the diesel generators run to produce only enough power to meet the load. However, to ensure the efficient use of fuel, minimum output power limit is set for the diesel generators. In this case, if the load is less than the minimum operating power of the diesel generators then the excess power is used to charge the batteries. If the net load can not be met by both diesel generators operating at their maximum capacities and storage batteries delivering their maximum available capacity, then the deficit will be treated as unmet load which may be penalised in the objective function. Figure (3.13) presents a flowchart for the LFDS.

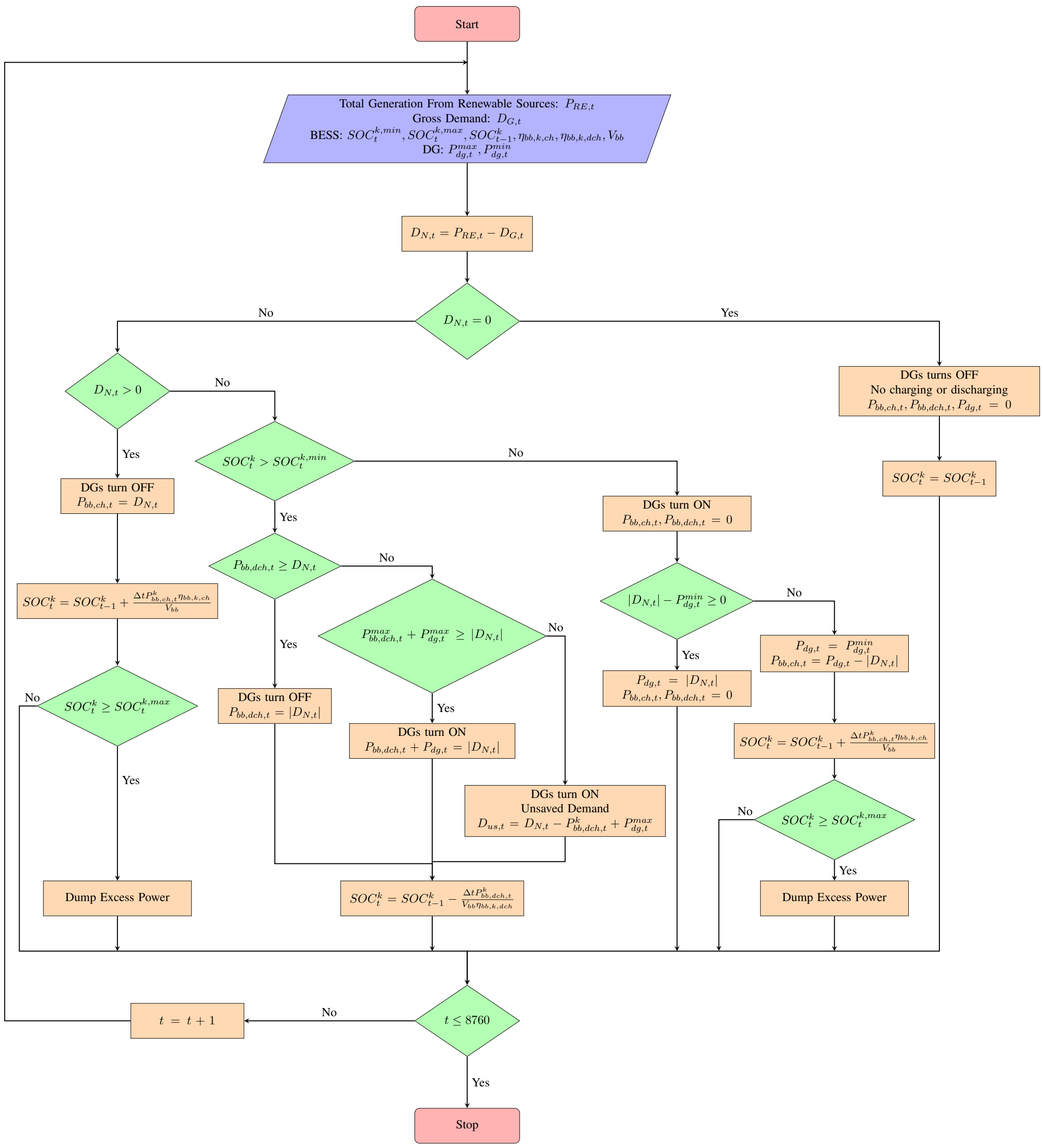

Figure 3.12: *Load Following Dispatching Strategy*

3.5.2 Cycle Charging Strategy

CCDS is one of the controversial dispatching strategy which explore the possibility of using DGs to charge the SBB in the microgrid. Under the CCDS strategy, whenever DGs are needed they are operated at (or very close to) rated capacities without dumping power. The difference between total power from DGs and the net load is used to charge the SBB. Generators may continue running beyond the minimum run time until: the prescribed overall state of charge SOC of the storage batteries is reached, the net load is zero, or when the excess power from renewable is sufficient to continue charging the SBB. This strategy aimed at optimizing the DGs operating points exactly at (or very close to) their rated power and at minimizing the number of DGs startup. However, its disadvantages includes shortening of battery wear life, electrical losses in storage system and the lost opportunity to store renewable energy in the storage battery.

3.5.3 Other Dispatching Strategies

There are many other dispatching strategies reported in the literature. For off-grid or stand-alone microgrid, the dispatching strategies mainly focus on the optimal use of DGs and SBBs in order to to achieve diesel savings, minimizing number of start-up and shut-down, minimize SBB replacement costs, and minimizing emissions. Detailed and extensive investigations of various dispatching strategies has been carried out by authors in [122] and [123]. In addition to the LFDS and CCDS, work in [122] considered other strategies such as Load Following Dispatch Strategy (SOCSDS), Full Power/Minimum Run Time Dispatch Strategy (FPMRTDS), Frugal Dispatch Strategy (FDS)FDS, and IDSIDS. Another work which considered both real and reactive power and analysed different dispatching strategies for the sizing of islanded microgrid is presented in [56].

In this thesis, a MODS proposed in [124] is adopted. The statergy allows the use of excess renewable generation or excess power from DGs to charge SB bank, thus the CCDS constraint to always operate DGs at their rated power is relaxed. This strategy combines LFDS and CCDS. The optimization algorithm is given freedom to choose when and how long to use either LFDS or CCDS. Figure 3.14 presents operation planning results obtained by the MODS when applied to plan a small microgrid with four DGs, PV array, WTs and SBBs [124]. It can be seen that with the MODS, dispatching of DG in hour 2 is shifted to hour 15 at which it this DG is operated at high efficiency to supply the net demand and recharge the SBB. Compared to the LFDS and CCDS, the MODS gave minimum number of start-up and shut-down for DGs. In summary, the study found that MODS gives optimal operational plan because it maximizes the use of renewable generation, operates DGs at high efficiencies, and minimizes number of start-up and shut-down for DGs. This strategy assumes perfect knowledge of future renewable resources input data and electrical demand. However, uncertainty in the input data can be considered as demonstrated in Chapter 5.

3.6 Clustered Unit Commitment Problem

Since the the planning problem addressed in this thesis does not consider distribution network constraints, and since microgrids have small distribution networks with various DERs and storage system, it is reasonable to allow the planning model to consider clusters of components to be installed instead of treating each individual component. The main benefit of this formulation is on the reduction of number

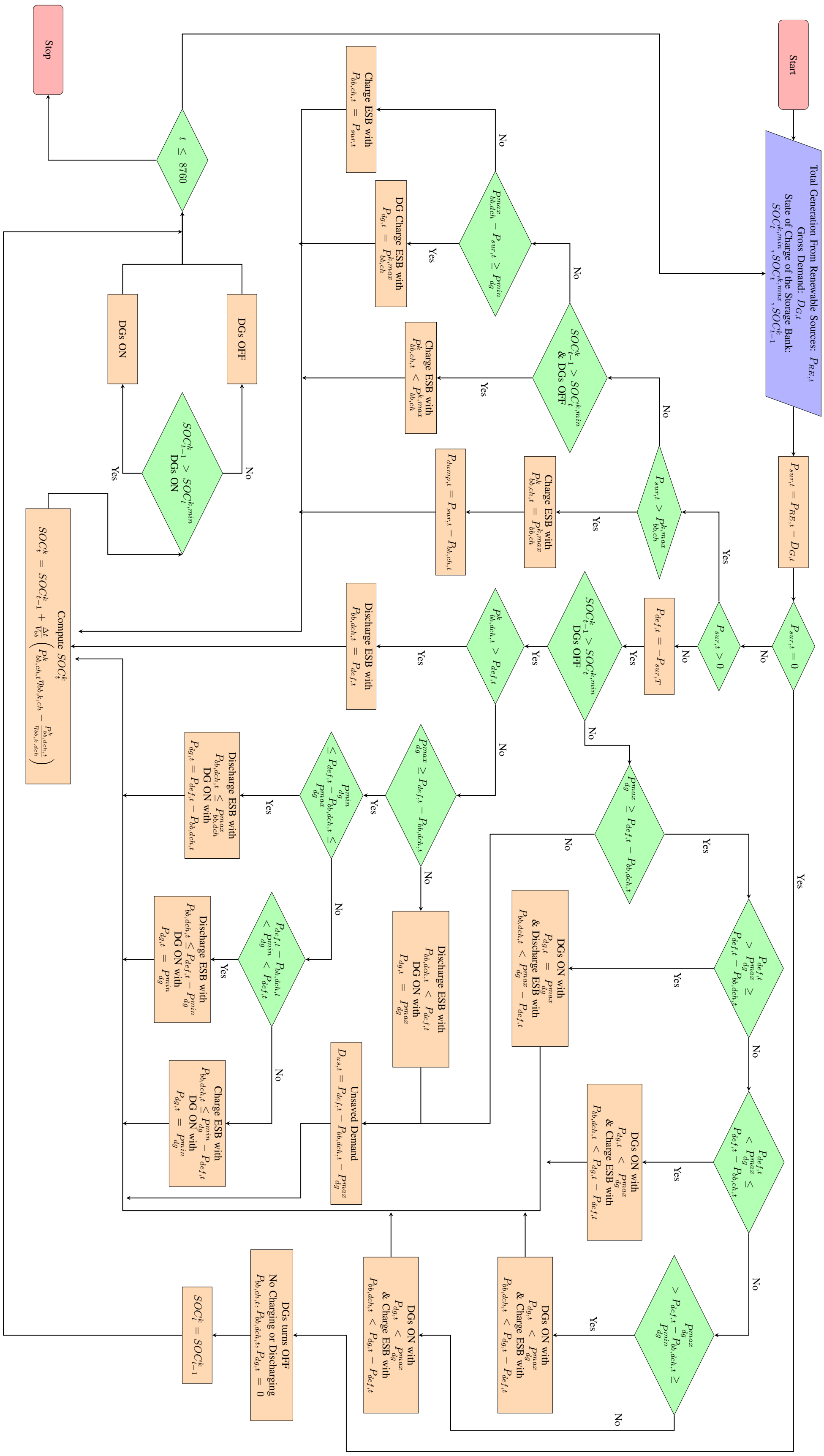

Figure 3.13: *Load Following Dispatching Strategy*

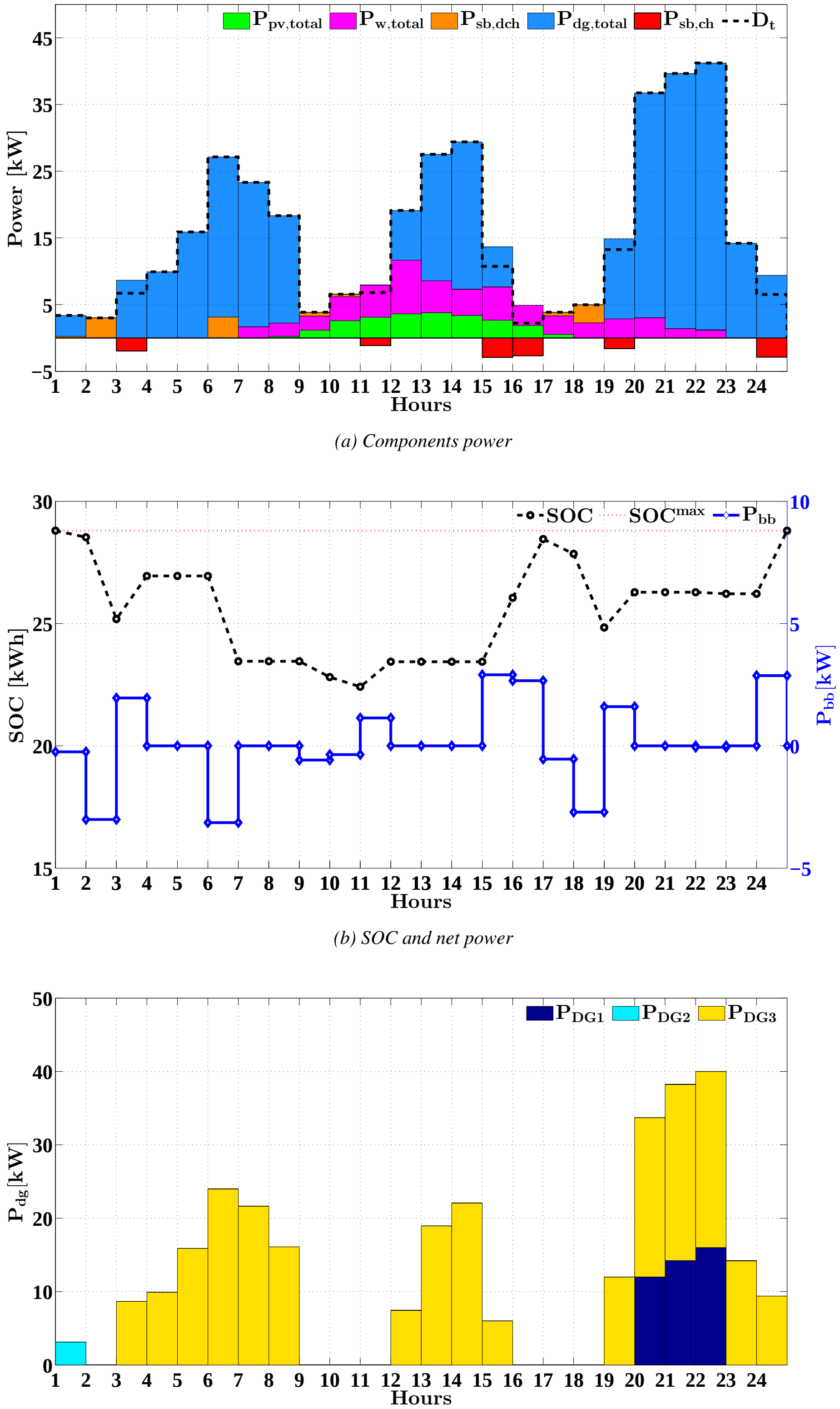

(a) Components power

(b) SOC and net power

(c) DGs dispatching

Figure 3.14: *Operational planning under MODS*

of variables for the operational part of the planning problem. This technique replaces a large number of binary variables required by the conventional unit commitment by fewer integer variables which enable modelling the operation of groups of generators of the same type [45], [125]. CUC offers an accurate approximation of operational costs while significantly reduces the size of the operational problem. This technique is suitable for microgrid planning applications which usually consider small number and several different types of DERs. Figure 3.15 illustrate the concept of CUC.

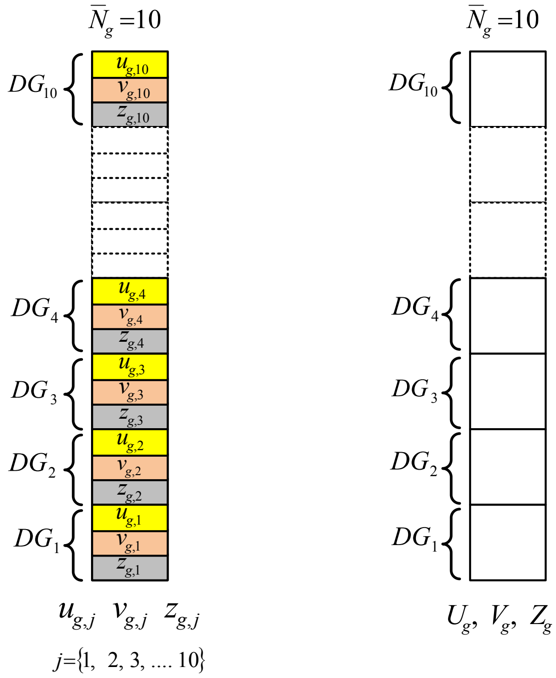

Figure 3.15: *Conceptual diagram of the clustered unit commitment(CUC) of DG of type g where j is the index of generator. Note that the conventional unit commitment requires 30 binary variables, whereas the CUC requires 3 integer variables only.*

The basic CUC model is described as following: The objective function minimizes the total operational costs for DGs which includes: fuel consumption cost, total start up and shutdown costs of DGs, maintenance costs, penalty costs for unmet demand and operating the DGs with excess power.

$$\begin{aligned} \min \quad TOC = & \sum_h \sum_g C_{fuel} FC_{h,g} \; + \sum_h \sum_g U_{h,g} OMC_g \; + \\ & \sum_h \sum_g \left(V_{h,g} SUC_g + Z_{h,g} SDC_g \right) \; + \\ & \sum_h \left(C_{exc} P^{exc}_{h,g} \; + \; C_u D^u_h \right) \end{aligned} \tag{3.34}$$

where C_{fuel} is the fuel cost, $FC_{d,h,g}$ is fuel consumption for DGs of type g in hour h of day d, $U_{h,g}$is the number of online DGs, $V_{h,g}$ is the number of DGs started-up, SUC_g is start-up cost for DG of type g, $Z_{h,g}$ is number of DGs shut-down, and SDC_g is shut-down cost for DG of type g. OMC_g is operational and maintenance cost for DG of type g, C_{exc} is penalty cost for excess DG power, $P^{exc}_{h,g}$ is the total excess power from DGs, C_u is the penalty cost for unmet demand, and D_h^u is the unmet demand in hour h of the planning horizon. This formulation results to a MILP model because the decision variables $U_{h,g}$ $V_{h,g}$ and $Z_{h,g}$ are integer variables, whereas the remaining variables are continuous variables, and all the constraints are linearized.

The minimization is subject to the power balance constraint expressed by:

$$\sum_g P_{h,g} - \sum_g P_{h,g}^{exc} + D_h^u = D_h \quad \forall h \tag{3.35}$$

where $P_{h,g}$ is the power from group of DG of type g, $P_{h,g}^{exc}$ is the total excess power from DGs, D_h^u the unmet demand, and D_h the electric demand in hour h. Input-output characteristics of DGs are formulated by using PWLA function with maximum of three segments.

$$FC_{h,g} = \max_{q=1,2,3}\{B_{q,g}P_{h,g} + U_{h,g}A_{q,g}\} \qquad \forall h, g \tag{3.36}$$

where $FC_{h,g}$ is the fuel consumption for DGs of type g in hour h of day d, $B_{q,g}$ is the slope of linear segment q of PWLA of input-output characteristic of DG of type g, $P_{h,g}$ is the generation from a group of DGs of type g, $U_{h,g}$ is the number of online DGs, and $A_{q,g}$ is the y-intercept of linear segment q of PWLA of input-output characteristic of DG of type g. Upper and lower bounds to enforce technical limits for DGs are specified in (3.37).

$$U_{h,g}\underline{P_g} \le P_{h,g} \le U_{h,g}\overline{P_g} \qquad \forall h, g \tag{3.37}$$

where $\underline{P}_g$ is the minimum power from DG of type g, and $\overline{P}_g$ is the maximum power from DG of type g. Excess DG power is defined by (3.38) in order to avoid infeasibility in case the demand is supplied by DG only and it is lower than the DG minimum output power.

$$P_{h,g}^{exc} \le U_{h,g}\underline{P_g} \qquad \forall h, g \tag{3.38}$$

where $P_{h,g}^{exc}$ is the excess power from online DG of type g and the remaining symbols are as defined before.

Standard modern DGs are equipped with automatic transfer switch (ATS) and they can supply the load within 10 seconds. If the DG is manually controlled it may be useful to consider minimum up and down time to model the time required for the operator to switching on and connect the DG into the system. Another reason to consider min up and down constraints is to limit frequent starts and stops of the generator. These reduces wearing of the DG and minimizes its maintenance costs. Minimum-up time constraint (3.39) requires that the number of DGs which are started up in hour h remain ON for at least $(UT_g - 1)$ hours, whereas minimum-down time constraint (3.40) requires that the number of DGs shut down in hour h remain OFF for at least $(DT_g - 1)$ hours [126].

$$U_{h_1,g} \ge V_{h,g},\ h_1 \in [h+1, min\{h + UT_g - 1, H\}] \qquad \forall g, h > 1 \tag{3.39}$$

$$N_g - U_{h_1,g} \ge Z_{h,g},\ h_1 \in [h+1, min\{h + DT_g - 1, H\}] \qquad \forall g, h > 1 \tag{3.40}$$

where $U_{h,g}$ $V_{h,g}$ $Z_{h,g}$ are number of online, started-up, and shut-down generators, UT_g and DT_g are minimum up-time and down-time for DG of type g respectively, and H is the time length of a day, i.e.

hour 24.

Relationship between the number of started up generators, number of shut down generators and number of online generators is given by (3.41).

$$V_{h,g} - Z_{h,g} = U_{h,g} - U_{h-1,g} \qquad \forall g, h > 1 \tag{3.41}$$

For each type of DG, the number of online generators must be less than or equal to the number of selected generators to install (3.42).

$$U_{h,g} \leq N_g \qquad \forall g, h \tag{3.42}$$

where $U_{h,g}$ is the number of online DGs, and N_{g,n_g} is the number of DG of type g specified in the n_g^{th} solution of the search space. For the planning problem both of these variable are not known a priori.

The number of DGs that can be started-up in the current hour cannot exceed the number of DGs kept off-line in the previous hour, whereas the number of DGs that can be shut-down in the current hour cannot exceed the number of DGs that were online in the previous hour.

$$V_{h,g} \leq N_g - Z_{h-1,g} \qquad \forall g, h \tag{3.43a}$$

$$Z_{h,g} \leq U_{h-1,g} \qquad \forall g, h \tag{3.43b}$$

If the planning will consider medium size or large DGs, then the ramping limits must be considered. These constraints require the most extensive changes since hour-to-hour output for the entire cluster must account for the number of DGs that start up, $V_{h,g}$, and shut down, $Z_{h,g}$. The ramp rates for on-line DGs also need to be scaled by the number of DGs that are actually on-line, $U_{h,g}$, thus,

$$P_{h-1,g} - P_{h,g} \leq (U_{h,g} - V_{h,g})RD_g - V_{h,g}\underline{P_g} + min(\underline{P_g}, RD_g)Z_{h,g} \qquad \forall g, h \tag{3.44a}$$

$$P_{h,g} - P_{h-1,g} \leq (U_{h,g} - V_{h,g})RU_g - Z_{h,g}\underline{P_g} + min(\underline{P_g}, RU_g)S_{h,g} \qquad \forall g, h \tag{3.44b}$$

In both constraints (3.44a) and (3.44b), the first term on the right includes DGs that run in both time periods, the second term corrects for startup and shutdowns to prevent artificial inflation of the ramping limits for the DGs that run in both time periods, and the third term captures the allowable extra change in cluster generation due to shutdown and startup respectively.

3.7 Summary

This chapter has presented the general architecture of hybrid microgrid and mathematical modelling of the components in it. It is shown that characteristics of microgrid components are mainly nonlinear and the approximation of these characteristics to enable formulation of MILP planning model is discussed. To achieve optimal planning one can not proceed by using blind optimization approach. Normally practical planning studies are subject to many investment and operational constraints. For this reason, a general discussion on energy management and dispatching strategies is presented. The dispatching strategies has directly effect on the optimal planning decisions and thus has to be considered carefully. To ensure tractability of the long-term operational planning problem which will be integrated in the main microgrid planning model, the CUC unit commitment formulation is adopted. In the CUC, DGs are grouped into clusters depending on their types and or technologies. This way, binary commitment variables are replaced by integer commitment variables which reduces the computing times considerably. This approach shows that CUC formulation is suitable for integration in microgrid planning model,as it will be shown in the following chapters.

CHAPTER 4

Deterministic Planning of Hybrid Microgrids

4.1 Introduction

This chapter presents a MILP model for microgrid planning problem. The proposed model combines joint optimization of component selection and long-term operation of the microgrid. The model allows optimal selection of multiple components of various fixed sizes and of different types under each technology. MILP formulation is adopted in order to capture discrete planning and operational decisions. Nonlinearities in the components characteristics are approximated by using PWLA. Long-term operation for DGs are included in the planning model through CUC technique. The CUC offers more accurate approximation of operational costs while significantly reduces the size of the operational problem and at the same time allows to model the operation of multiple DGs of the same type. This technique is suitable for microgrid planning applications which usually consider small number and several different types of DGs. Economic analysis of microgrid components is performed using LCCA method adopting system lifetime of 20 years. However, operation of the system is optimized over one year with its results assumed to be a representation of all other years in the project lifetime.

The remainder of this chapter is organised as follows: Section 4.2 presents the topology of microgrid under consideration and the description of the planning problem. Section 4.3 discuss economic analysis approach adopted in in this study. The proposed model formulated using integer planning variables is presented in Section 4.4 followed by explanation on the formulation of the binary planning model, presented in Section 4.5. Selection of typical representative days is discussed in Section 4.6. Components specifications are presented in Section 4.7. Then, a case study used for validation of the MILP model on the planning of a small village microgrid in Philippines is presented in Section 4.8. Further application of the MILP model and its two formulations are demonstrated in and 4.9. Finally, the chapter summary is presented in Section 4.10.

4.2 Microgrid Topology

Before introducing mathematical models, architecture of the microgrid considered in developing the model is presented. This work considers a generic parallel hybrid microgrid topology with AC and DC bus bars, as shown in Fig. 4.1. It is assumed that WTs, PVs, and SBBs are connected to the DC bus bar, whereas DGs and electric loads are connected to the common AC bus bar. The DC bus bar is connected to the AC bus bar via BCs, capable of operating in inversion and rectification mode. Charger controller block represents bidirectional DC/DC converters which control charging and discharging of the SBBs.

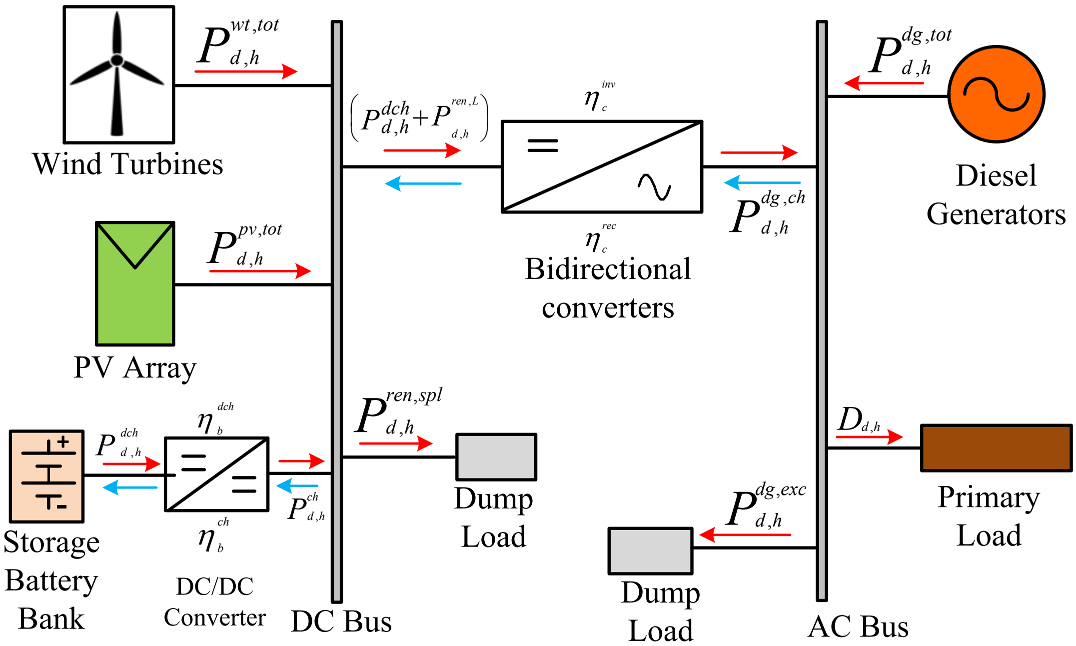

Figure 4.1: *Topology of a parallel AC-and-DC bus microgrid* (arrows represent flow of power from or to the components*)*.

Diesel generators block represents a combination of multiple small or medium size DGs. The use of such combination in an isolated microgrid ensures high reliability, availability, and maintainability while offering optimal operational flexibility [127]. This topology offers superior performance over other topologies, such as single bus DC or AC topologies, because it enables all or part of electric demand to be supplied directly by any combination of PV arrays, WTs, SBBs and DGs [128].

At this planning stage, the focus is only on the planning of a new microgrid, i.e. to obtain optimal generation mix, number of generation equipment to install, and their capacities considering the topology shown in Figure 4.1. Therefore, network constraints are not considered in the formulation of the model. However, these constraints may be necessary when considering generation expansion plan in which distribution network structure is known, e.g. when planning additional of RESs in an existing remote system powered by DGs only.

4.3 Life-Cycle Cost Analysis Rationale

This section explains the conversion of fixed costs of each component into annualized costs to be used as inputs in the optimization process. We adopted LCCA approach which is similar to Annual Worth Analysis (AWA) with positive sign associated to the costs and negative sign to the revenues and salvage value at the end of the project life. Note that replacement cost for DGs and SBBs depends on the total hours of operation and are considered as variable costs. Their equivalent annualized costs are calculated in the post optimization stage. The following costs are calculated for each type of component.

- The annualized capital and installation cost, $ACIC_\ell$ is given by:

$$ACIC_\ell = (CC_\ell + IC_\ell)CRF(r_{real}, Y_{proj}) \tag{4.1}$$

where CC_ℓ is the capital cost, IC_ℓ the Installation costs, and CRF is the capital recovery factor. The capital recovery factor, CRF, is calculated using

$$CRF(r_{real}, Y_{proj}) = \frac{r_{real}(1 + r_{real})^{Y_{proj}}}{(1 + r_{real})^{Y_{proj}} - 1} \tag{4.2}$$

where Y_{proj} is the project lifetime and r_{real} is real interest rate which is defined by [129]:

$$r_{real} = \frac{r_{nom} - r_{infl}}{1 + r_{infl}} \tag{4.3}$$

where r_{nom} and r_{infl} are the nominal interest rate and inflation rate respectively.

- Annualized replacement cost, ARC_ℓ of the component is calculated by

$$ARC_\ell = RC_\ell f_{rep,\ell} SFF(r_{real}, Y_\ell) - SV_\ell SFF(r_{real}, Y_{proj}) \tag{4.4}$$

where RC_ℓ is the replacement cost of the component, $f_{rep,\ell}$ is the replacement factor accounting for the difference between the component lifetime and project lifetime [130], SV_ℓ the Salvage value, and SFF_ℓ the sinking fund factor which is defined by [131]:

$$SFF(r_{real}, Y) = \frac{r_{real}}{(1 + r_{real})^Y - 1} \tag{4.5}$$

The replacement factor is given by:

$$f_{rep,\ell} = \begin{cases} CRF(r_{real}, Y_{proj})/CRF(r_{real}, Y_{rep}) & Y_{rep} > 0 \\ 0 & Y_{rep} = 0 \end{cases} \tag{4.6}$$

where $Y_{rep,\ell}$ is the number of replacement of component of type ℓ:

$$Y_{rep,\ell} = Y_\ell \, INT\left(\frac{Y_{proj}}{Y_\ell}\right) \tag{4.7}$$

in which $INT(.)$ is a function which rounds a number down to the nearest integer. Remaining lifetime of the component is determined by

$$Y_{rem,\ell} = Y_\ell - (Y_{proj} - Y_{rep,\ell}) \tag{4.8}$$

Salvage value, SV_ℓ, of the component is given by [84]:

$$SV_\ell = RC_\ell \left(\frac{Y_{rem,\ell}}{Y_\ell} \right) \tag{4.9}$$

where RC_ℓ is the replacement cost, $Y_{rem,\ell}$ the remaining lifetime, and Y_ℓ the lifetime of component.

- Annuallized operation and maintenance cost, $AOMC_\ell$, for each type of component except DG is assumed to be fixed for the whole project lifetime.

Using the annualized costs calculated above, the total annualized cost for each component installed in the microgrid is given by:

$$\begin{aligned}
AC_p &= ACIC_p + AOMC_p + ARC_p - SV_p && \forall p && \text{(4.10a)}\\
AC_w &= ACIC_w + AOMC_w + ARC_w - SV_w && \forall w && \text{(4.10b)}\\
AC_c &= ACIC_c + AOMC_c + ARC_c - SV_c && \forall c && \text{(4.10c)}\\
AC_c &= ACIC_c && \forall b && \text{(4.10d)}\\
AC_g &= ACIC_g && \forall g && \text{(4.10e)}
\end{aligned}$$

where AC_ℓ is annualized cost of component of type ℓ and the remaining parameters are as defined before.

4.4 MILP Microgrid Planning Model

4.4.1 Objective Function

The objective function minimizes the total annualized LCCA of the system, which includes the total annualized investment cost for installed PVs, SBBs, BC, DGs, and WTs, annual replacement costs for DGs and SBBs, annual fuel cost of DGs, total operational and maintenance costs of DGs, total start up and shutdown costs of DGs, and the total annualized penalty costs for spilling power from renewable sources.

$$
\begin{aligned}
\text{Min} \quad TACS = & \sum_p N_p AC_p \ + \ \sum_c N_c AC_c \ + \ \sum_w N_w AC_w \ + \\
& \sum_b N_b AC_b \ + \ \sum_g N_g AC_g \ + \\
& \sum_d \sum_h \sum_g f_d U_{d,h,g} RC_g \ + \ \sum_d \sum_h \sum_b f_d C_{bw_b} P^{dch}_{d,h,b} \ + \\
& \sum_d \sum_h \sum_g f_d C_{fuel} FC_{d,h,g} \ + \ \sum_d \sum_h \sum_g f_d U_{d,h,g} OMC_g \ + \\
& \sum_d \sum_h \sum_g f_d \left(V_{d,h,g} SUC_g + Z_{d,h,g} SDC_g \right) \ + \\
& \sum_d \sum_h f_d \left(C_{exc} P^{exc}_{d,h,g} \ + \ C_{spl} P^{ren,spl}_{d,h} \right)
\end{aligned} \tag{4.11}
$$

where N_p is the number of installed PVs of type p, N_c the number of installed BCs of type c, N_w the number of installed WTs of type w, N_b the number of installed SBs of type b, and N_g the number of installed DGs of type g. AC_ℓ is the annualized cost of component of type ℓ, where ℓ is the index set of components and types to be considered $\ell \in \{g, p, w, b, c\}$. f_d is the weight of the typical day d, $U_{d,h,g}$ is the number of online DGs, and RC_g is the replacement cost for DG of type g. $C_{bw,b}$ is the SBB wear cost, $P^{dch}_{d,h,b}$ is the discharging power from the SBB of type b, C_{fuel} is the fuel cost, and $FC_{d,h,g}$ is fuel consumption for DGs of type g in hour h of day d. OMC_g is operational and maintenance cost for DG of type g, $V_{d,h,g}$ the number of DGs started-up, SUC_g the start-up cost for DG of type g, $Z_{d,h,g}$ the number of DGs shut-down, and SDC_g the shut-down cost for DG of type g. C_{exc} is the penalty cost for excess DG power, $P^{dg,exc}_{d,h}$ is the total excess power from DGs, C_{spl} the penalty cost for spilling RES generation, and $P^{ren,spl}_{d,h}$ is the total spilled power from RESs,

Replacement cost for the SB is modelled by the battery wear cost, C_{bw_b}, defined as the cost per kWh of cycling energy through the SBB [84], [132].

$$
C_{bw_b} \ = \ \frac{RC_b}{N_b Q_{life_b} \sqrt{\eta^{rt}_b}} \quad [€/kWh] \tag{4.12}
$$

where RC_b is the replacement cost of a SB of type b, Q_{life_b} is the lifetime throughput of a single battery, and η^{rt}_b is the round trip efficiency of SB of type b. The round trip efficiency is defined as the ratio of energy recovered from the SBB to the energy put into it.

$$
\eta^{rt}_b \ = \ \frac{Energy\ Recovered}{Energy\ Input} 100\% \ = \ \eta^{ch}_b \eta^{dch}_b \tag{4.13}
$$

where η^{ch}_b and η^{ch}_b the charging and discharging efficiencies of SB of type b.

Annualized costs for WTs can be modeled to consider economies of scale. This requires PWLA of concave capital and installation cost functions:

$$
AC_w = \sum_q \left(B_{w,q} N_{w,q} + C^0_{w,q} y_q \right) \tag{4.14a}
$$

$$N_w = \sum_{q \in Q} N_{w,q} \qquad \forall w \qquad (4.14b)$$

$$\lambda_{w,q} y_{w,q} \leq N_{w,q} \leq \lambda_{w,q+1} y_{w,q} \qquad \forall w, q \qquad (4.14c)$$

$$\sum_{q \in Q} y_{w,q} \leq 1 \qquad \forall w \qquad (4.14d)$$

$$y_{w,q} \in \mathbb{Z}_2 \qquad \forall w, q \qquad (4.14e)$$

where $B_{w,q}$ and $A_{w,q}$ defines the slope and fixed cost of a linear segment q of the PWLA cost function for WTs of model w. $N_{w,q}$ is the umber of wind turbine from segment q and y_q is the binary variable to indicate the selection of segment q. Minimum and maximum number of WTs in each segment of PWLA curve are given by $\lambda_{w,q}$.

Planning variables are positive integers specifying the number of parallel strings of PV panels in the array, and SBs in SBB, number of WTs, BCs, and DGs to instal in the microgrid.

$$0 \leq N_\tau \leq \overline{N_\tau} \qquad \tau = \{p, w, b, c, g\} \qquad (4.15a)$$

Number of PV panels connected in series to form a string is a parameter determined by string voltage and the panel MPP voltage. Similarly, number of SB in series is determined by DC bus bar voltage.

4.4.2 Power Balance Constraint and Dispatching Strategy

Power balance constraint at the AC bus bar of Fig. 4.1 is expressed by:

$$P_{d,h}^{dg,tot} + \left(P_{d,h}^{dch} + P_{d,h}^{ren,L} \right) \eta_{inv} - P_{d,h}^{dg,ch} - P_{d,h}^{dg,exc} + D_{d,h}^{u} = D_{d,h} \quad \forall d, h \qquad (4.16)$$

where $P_{d,h}^{dg,tot}$ is the total power from online DGs, $P_{d,h}^{dch}$ the total discharging from the SBBs, $P_{d,h}^{ren,L}$ the total power from RES supplied directly to the load, η_{inv} the BC inversion efficiency, $P_{d,h}^{dg,ch}$ the total charging power from DGs, $P_{d,h}^{dg,exc}$ the total excess power from DGs, $D_{d,h}^{u}$ the unmet demand, and $D_{d,h}$ the electric demand in hour h of typical day d. Constraint (4.16) implies that that the demand can be supplied by any combination of DGs, SBBs, PV array, and WTs.

Part of the total generation from RESs which is supplied directly to the load is equal to the difference between the total RESs generation and the sum of charging and spilled power from RESs, (4.17).

$$P_{d,h}^{ren,L} = P_{d,h}^{ren,tot} - P_{d,h}^{ren,ch} - P_{d,h}^{ren,spl} \quad \forall d, h \qquad (4.17)$$

where $P_{d,h}^{ren,tot}$ is the total generation from RESs, $P_{d,h}^{ren,ch}$ the total charging power from RESs, and $P_{d,h}^{ren,spl}$ the total spilled power from RESs in hour h of typical day d.

The total RESs generation is given by sum of generation from PV array and WTs (4.18a)-(4.18c).

$$P_{d,h}^{ren,tot} = P_{d,h}^{pv,tot} + P_{d,h}^{wt,tot} \qquad \forall d, h \qquad (4.18a)$$

$$P_{d,h}^{pv,tot} = \sum_{p} N_p \overline{P}_{d,h,p} \qquad \forall d, h \qquad (4.18b)$$

$$P_{d,h}^{wt,tot} = \sum_{w} N_w \overline{P}_{d,h,w} \qquad \forall d, h \qquad (4.18c)$$

where $P_{d,h}^{pv,tot}$ is the total generation from PV arrays, $\overline{P}_{d,h,p}$ is the per unit MPP generation from PV panel of type p, and $\overline{P}_{d,h,w}$ is the per unit MPP generation from WT of type w in hour h of typical day d. Variables N_p and N_w represent number of installed PVs and WTs respectively.

The total power from the DGs is the sum of generation from all types of DGs which are online at a particular period (4.19a). Similarly, the total discharging power power is the sum of discharging power from all types of SBBs installed (4.19b).

$$P_{d,h}^{dg,tot} = \sum_{g} P_{d,h,g} \qquad \forall d,h \tag{4.19a}$$

$$P_{d,h}^{dch} = \sum_{b} P_{d,h,b}^{dch} \qquad \forall d,h \tag{4.19b}$$

where $P_{d,h,g}$ is the generation from a group of DGs of type g, and $P_{d,h,b}^{dch}$ is the discharging power from the SBB of type b in hour h of typical day d.

Total charging power to the SBBs is the sum of charging power from RESs and DGs.

$$\sum_{b} P_{d,h,b}^{ch} = P_{d,h}^{ren,ch} + P_{d,h}^{dg,ch}\eta_{rec} \qquad \forall d,h \tag{4.20}$$

where $P_{d,h,b}^{ch}$ is the charging power to the SBB of type b, $P_{d,h}^{ren,ch}$ and $P_{d,h}^{dg,ch}$ are the total charging power from RESs and DGs in hour h of typical day d respectively, and η_{rec} is the BC rectification efficiency.

Total amount of power which can flow from the DC bus to the AC bus during the inversion mode is limited by the total inversion capacity of the installed BCs (4.21a). Similarly, the amount of charging power from DGs flowing from the AC to the DC bus bar during the rectification mode is limited by the total rectification capacity of installed BCs (4.21b).

$$\left(P_{d,h}^{dch} + P_{d,h}^{ren,L}\right) \le \sum_{c} N_c \overline{P}_c^{inv} \qquad \forall d,h \tag{4.21a}$$

$$P_{d,h}^{dg,ch} \le \sum_{c}\sum_{n_c} N_c \overline{P}_c^{rec} \qquad \forall d,h \tag{4.21b}$$

where $\overline{P}_c^{inv}$ and $\overline{P}_c^{rec}$ are the maximum inversion and rectification capacities of a single BC of type c and other variables are as defined before.

Power flow from the AC bus bar to the DC bus bar occurs only during the rectification mode, whereas power flow from the DC to AC bus bar occurs only during the inversion mode. This complementarity condition is enforced by (4.22a) and (4.22b) respectively.

$$\left(P_{d,h}^{dch} + P_{d,h}^{ren,L}\right) \le w_{d,h}^{inv} M \qquad \forall d,h \tag{4.22a}$$

$$P_{d,h}^{dg,ch} \le w_{d,h}^{rec} M \qquad \forall d,h \tag{4.22b}$$

where $w_{d,h}^{inv}$ is the binary variable equal to 1 when the BCs operate as inverters and 0 otherwise, and $w_{d,h,s}^{rec}$ is the binary variables equal to 1 when the BCs operate as rectifiers and 0 otherwise. Parameter M is a big number which is set to enforce the complementarity constraint. The BCs cannot operate in inversion and rectification mode at the same time (4.23).

$$w_{d,h}^{inv} + w_{d,h}^{rec} \le 1 \quad \forall d, h \tag{4.23}$$

The rectification mode can occur only when at least one DG is online (4.24).

$$w_{d,h}^{rec} \le \sum_g U_{d,h,g} \quad \forall d, h \tag{4.24}$$

Any online DGs may charge the SBB only when they operates at their minimum limits and the demand is less than these DGs minimum limits (4.25).

$$P_{d,h}^{dg,ch} \le \sum_g U_{d,h,g}\underline{P}_g - P_{d,h}^{dg,exc} - w_{d,h}^{rec} D_{d,h} \quad \forall d, h \tag{4.25}$$

where $P_{d,h}^{dg,ch}$ is the total charging power from DGs, $U_{d,h,g}$ is the number of online DGs, $\underline{P}_g$ is the minimum power from DG of type g, $P_{d,h}^{dg,exc}$ is the total excess power from DGs, $w_{d,h}^{rec}$ is the binary variable indicating the BCs rectification mode, and $D_{d,h}$ is the electric demand in hour h of typical day d.

Unsaved demand is limited by maximum allowable unsaved energy (4.26a) whereas installed capacity for renewable sources is limited by setting renewable penetration factor (4.26b).

$$\sum_d \sum_h f_d D_{d,h}^u \le MAUE \tag{4.26a}$$

$$\sum_d \sum_h \sum_g f_d \left(P_{d,h,g} - P_{d,h,g}^{exc}\right) / E_{total} \ge f_{ren} \tag{4.26b}$$

where $D_{d,h}^u$ is the unmet demand, $MAUE$ the maximum allowable unmet energy, E_{total} the total energy energy, f_{ren} the renewable fraction, and the remaining variables are as defined before.

4.4.3 Constraints Related to Diesel Generators

Operational constraints for DGs are formulated using CUC approach described in Chapter 3. This approach reduces the number of decision variables and allows the model to select planning solution with combinations of multiple DGs of the same type. Input-output characteristics of DGs are formulated by using PWLA function with maximum of three segments.

$$FC_{d,h,g} = \max_{q=1,2,3} \{B_{q,g} P_{d,h,g} + U_{d,h,g} A_{q,g}\} \qquad \forall d, h, g \tag{4.27}$$

where $FC_{d,h,g}$ is the fuel consumption for DGs of type g in hour h of day d, $B_{q,g}$ is the slope of linear segment q of PWLA of input-output characteristic of DG of type g, $P_{d,h,g}$ is the generation from a group of DGs of type g, $U_{d,h,g}$ is the number of online DGs, and $A_{q,g}$ is the y-intercept of linear segment q of PWLA of input-output characteristic of DG of type g.

Upper and lower bounds to enforce technical limits for DGs are specified in (4.28).

$$U_{d,h,g}\underline{P_g} \le P_{d,h,g} \le U_{d,h,g}\overline{P_g} \qquad \forall d, h, g \tag{4.28}$$

where $\underline{P}_g$ is the minimum power from DG of type g, and $\overline{P}_g$ is the maximum power from DG of type g.

Excess DG power is defined by (4.29) in order to avoid infeasibility in case the demand is supplied by DG only and it is lower than the DG minimum output power.

$$P^{exc}_{d,h,g} \leq U_{d,h,g}\underline{P_g} \qquad \forall d,h,g \qquad (4.29)$$

where $P^{exc}_{d,h,g}$ is the excess power from online DG of type g and the remaining symbols are as defined before.

Minimum up time constraint (4.30) requires that the number of DGs which are started up in hour h remain ON for at least $(UT_g - 1)$ hours, whereas minimum down time constraint (4.31) requires that the number of DGs shut down in hour h remain OFF for at least $(DT_g - 1)$ hours [126].

$$U_{d,h_1,g} \geq V_{d,h,g},\ h_1 \in [h+1, min\{h+UT_g-1, H\}] \qquad \forall g,d,h>1 \qquad (4.30)$$

$$N_g - U_{d,h_1,g} \geq Z_{d,h,g},\ h_1 \in [h+1, min\{h+DT_g-1, H\}] \qquad \forall g,d,h>1 \qquad (4.31)$$

where $U_{d,h,g}$ $V_{d,h,g}$, and $Z_{d,h,g}$ are number of online, started-up, and shut-down generators, UT_g and DT_g are minimum up-time and down-time for DG of type g respectively, and H is the time length of a day, i.e. hour 24. Relationship between the number of started up generators, number of shut down generators and number of online generators is given by (4.32).

$$V_{d,h,g} - Z_{d,h,g} = U_{d,h,g} - U_{d,h-1,g} \qquad \forall g,d,h>1 \qquad (4.32)$$

For each type of DG, the number of online generators must be less than or equal to the number of selected generators to install (4.33).

$$U_{d,h,g} \leq N_g \qquad \forall g,d,h \qquad (4.33)$$

where $U_{d,h,g}$ is the number of online DGs, and N_{g,n_g} is the number of DG of type g specified in the n_g^{th} solution of the search space. Both of these variable are not known a priori.

The number of DGs that can be started-up in the current hour cannot exceed the number of DGs remained off-line in the previous hour, whereas the number of DGsthat can be shut-down in the current hour cannot exceed the number of DGs that were online in the previous hour.

$$V_{d,h,g} \leq N_g - Z_{d,h-1,g} \qquad \forall g,d,h \qquad (4.34a)$$

$$Z_{d,h,g} \leq U_{d,h-1,g} \qquad \forall g,d,h \qquad (4.34b)$$

4.4.4 Constraints Related to Storage Battery Bank

4.4.4.1 Simplified Model of Storage Battery Bank

SBB is modelled by using two main variables, energy level and the net power. The net power is decomposed into two positive variables (*i.e. charging and discharging powers*) in order to capture the charging and discharging cycles [110]. For the simplified model, SBB lifetime is assumed to be constant and hourly self-discharging rate is considered negligible. The energy conservation equation is given by (4.35).

$$E_{d,h,b} = E_{d,h-1,b} + \Delta h(\eta^{ch}_b P^{ch}_{d,h,b} - P^{dch}_{d,h,b}/\eta^{dch}_b) \qquad \forall d,h,b \qquad (4.35)$$

where $E_{d,h,b}$ is the energy in the SBB of type b, Δh is the time step, $P^{ch}_{d,h,b}$ is the charging power to the SBB of type b, η^{ch}_{b} is the charging efficiency of SB of type b, $P^{dch}_{d,h,b}$ is the discharging power from the SBB of type b, and η^{ch}_{b} is the discharging efficiency of SB of type b. Maximum and minimum storage energy limits are enforced by using constraint (4.36).

$$\underline{E}_b \leq E_{d,h,b} \leq \overline{E}_b \qquad \forall d,h,b \tag{4.36}$$

where $\overline{E}_b$ is the maximum energy limit of SBB of type b, and $\underline{E}_b$ is the minimum energy limit for SBB of type b.

Maximum charging and discharging power are enforced through constraints (4.37a) to (4.37e).

$$0 \leq P^{ch}_{d,h,b} \leq \overline{P}^{ch}_{d,h,b} \qquad \forall d,h,b \tag{4.37a}$$
$$0 \leq P^{dch}_{d,h,b} \leq \overline{P}^{dch}_{d,h,b} \qquad \forall d,h,b \tag{4.37b}$$
$$P^{ch}_{d,h,b} \leq x^{ch}_{d,h} M \qquad \forall d,h,b \tag{4.37c}$$
$$P^{dch}_{d,h,b} \leq x^{dch}_{d,h} M \qquad \forall d,h,b \tag{4.37d}$$
$$x^{ch}_{d,h} + x^{dch}_{d,h} \leq 1 \qquad \forall d,h,b \tag{4.37e}$$

where $\overline{P}^{ch}_{b}$ is the maximum charging power for the SB of type b, $\overline{P}^{dch}_{b}$ is the maximum discharging power for the SB of type b, $x^{ch}_{d,h}$ is the binary variable indicating that the SBB is charging, $x^{ch}_{d,h}$ is the binary variable indicating the discharging of SBBs, and M is the Big number. Constraints (4.37c) to (4.37e) ensures that the charging and discharging power cannot both be greater than zero at the same time. Capacity of installed battery banks is an auxiliary variable which depends on the number of installed SBs.

$$\overline{C}_b\ [Wh] = N_b\ C^{sb,n}_{b}\ [Ah]\ V^{sb,n}_{b}\ [V] \qquad \forall b \tag{4.38a}$$

where $\overline{C}_b$ is the total capacity of SBB of type b, N_b is the number of installed SBs, C_b is the nominal capacity of a single SB of type b, and V_b is the nominal voltage of a SB of type b. Constraints to define the initial energy level, minimum and maximum energy level in SBB are:

$$E_{0,b} = SOC_{0,b}\overline{C}_b \qquad \forall b \tag{4.39a}$$
$$\overline{E}_b = \overline{C}_b \qquad \forall b \tag{4.39b}$$
$$\underline{E}_b = (1 - DOD_b)\overline{C}_b \qquad \forall b \tag{4.39c}$$

where $E_{0,b}$ is the initial energy in the SBB of type b, $SOC_{0,b}$ is the relative initial SOC of SBB of type b, and $\underline{E}_b$ is the minimum energy limit for SBB of type b. DOD_b is the depth of discharge of SBB of type b.

To avoid that the model installs large number of SBs due to their free initial energy content, a cost term in the objective function which is associated to this initial energy can be specified. Since it is not easy to approximate the cost of energy initially found in the SBBs, the second possibility could be to enforce the final energy in the SBB to be equal to the initial energy. Such constraint impose heavy computational burden as it requires linking all hours in the planning horizon. A simple technique which is adopted in this research is to set the initial energy level to its minimum limit. It is found that with this constraint the SBB is mainly used as a buffer and all energy stored in it is recharged leaving the final energy level at the minimum limit. Note that the number of installed SBs is defined as $N_b = N_b^{par} N_b^{ser}$, where N_b^{par} is the number of parallel connected batteries in a string of SB of type b and N_b^{ser} is the number of series strings of SB of type b.

4.4.4.2 Kinetic Battery Model

The second formulation of SBB model adopt the KiBaM. The KiBaM represents the SBB with two connected tanks. The first tank models a capacity which is directly available, whereas the second tank contains chemically bound energy which may become available at a limited rate. This model takes into account capacity reduction with increased charging or discharging power, as well as the recovery effect [111], [112]. Constraints for SBB are summarised as follow:

The maximum capacity of SBB to be installed is specified by (4.40).

$$\overline{C_b} = N_b\, C_b^{sb,n}\, V_b^{sb,n} \qquad \forall b \qquad (4.40)$$

where all symbols are as defined before. The total, available, and bound energy of SBB before the beginning of the planning horizon are defined by (4.41a) - (4.41c).

$$E_{1,0,b}^{tot} = \overline{C_b}\; SOC_{0,b} \qquad \forall b \qquad (4.41a)$$
$$E_{1,0,b}^{a} = c_b\, \overline{C_b}\; SOC_{0,b} \qquad \forall b \qquad (4.41b)$$
$$E_{1,0,b}^{b} = (1 - c_b)\, \overline{C_b}\; SOC_{0,b} \qquad \forall b \qquad (4.41c)$$

where $E_{1,0,b}^{tot}$ is the total initial energy in the SBB of type b, $E_{1,0,b}^{a}$ the available initial energy in the SBB of type b, $E_{1,0,b}^{b}$ the bound initial energy in the SBB of type b, and c_b the capacity ratio parameter for the SBB of type b. For the KiBaM, net power of the SBB of type b, $P_{d,h,b}^{net}$, is given by

$$P_{d,h,b}^{net} = \eta_b^{ch} P_{d,h,b}^{ch} - P_{d,h,b}^{dch} / \eta_b^{dch} \qquad \forall b \qquad (4.42)$$

where all other symbols are as defined in the simplified battery model.

The energy balance constraints for any hour are defined by (4.43a) - (4.43c).

$$E_{d,h,b}^{tot} = E_{d,h-1,b}^{tot} + \Delta h P_{d,h,b}^{net} \qquad \forall d,h,b \qquad (4.43a)$$
$$E_{d,h,b}^{a} = E_{d,h-1,b}^{a}\, e^{-k_b \Delta h} + \frac{(E_{d,h-1,b}^{tot}\, k_b\, c_b + P_{d,h,b}^{net})(1 - e^{-k_b \Delta h})}{k_b} + \frac{P_{d,h,b}^{net}\, c_b\, (k_b\, \Delta h - 1 + e^{-k_b \Delta h})}{k_b} \qquad \forall d,h,b \qquad (4.43b)$$
$$E_{d,h,b}^{b} = E_{d,h-1,b}^{b}\, e^{-k_b \Delta h} + \left(E_{d,h-1,b}^{tot}\, (1 - c_b)\right)\left(1 - e^{-k_b \Delta h}\right) + \frac{P_{d,h,b}^{net}\, (1 - c_b)\, (k_b\, \Delta h - 1 + e^{-k \Delta h})}{k_b} \qquad \forall d,h,b \qquad (4.43c)$$

where $E_{d,h,b}^{tot}$ is the total energy in the SBB of type b, $E_{d,h,b}^{a}$ the available energy in the SBB of type b, $E_{d,h,b}^{b}$ the bound energy in the SBB of type b, $P_{d,h,b}^{net}$ the net power of the SBB of type b, Δh the time step, c_b the capacity ratio parameter for the SBB of type b, and k_b the rate constant parameter for the SBB of type b. In any period, the sum of available and bound energy must be equal to the total energy in SBB (4.44).

$$E_{d,h,b}^{tot} = E_{d,h,b}^{a} + E_{d,h,b}^{b} \qquad \forall d,h,b \qquad (4.44)$$

The total energy in the SBB must be greater than or equal to the minimum energy limit (4.45).

$$(1 - DOD_b)\overline{C}_b \;\leq\; E^{tot}_{d,h,b} \;\leq\; \overline{C_b} \qquad \forall d, h, b \tag{4.45}$$

In any period, maximum charging power must be less than or equal to the smallest of the three limits: KiBaM maximum charging power limit determined by the total energy stored in the SBB (4.46a), maximum charging power limit determined by the SBB maximum charging rate (4.46b), and maximum charging power limit determined by the maximum charging current of SBB (4.46c).

$$P^{ch}_{d,h,b} \leq \frac{-k_b\ c_b\ \overline{E}_b\ +\ k_b\ E^{a}_{d,h,b}\ e^{-k_b \Delta h}\ +\ E^{tot}_{d,h,b}\ k_b\ c_b\ (1 - e^{-k_b \Delta h})}{[1 - e^{-k_b \Delta h}\ +\ c_b\ (k_b\ \Delta h - 1\ +\ e^{-k_b \Delta h})]\ \eta^{ch}_b} \qquad \forall d, h, b \tag{4.46a}$$

$$P^{ch}_{d,h,b} \leq \left(1 - e^{-\overline{Chr}_b\ \Delta h}\right)\left(\overline{E}_b - E^{tot}_{d,h,b}\right) / \ \Delta h \eta^{ch}_b \qquad \forall d, h, b \tag{4.46b}$$

$$P^{ch}_{d,h,b} \leq N_b \bar{I}^{ch}_b\ V^{sb,n}_b / \ \eta^{ch}_b \qquad \forall d, h, b \tag{4.46c}$$

where $\overline{E}_b$ is the maximum energy limit of SBB of type b, $\overline{Chr_b}$ is the maximum charging rate for the SB of type b, $\bar{I}^{ch}_b$ is the maximum charging current of the SBB of type b, and the remaining symbols are as defined before. On the other hand, the maximum discharging power is given by (4.47a)

$$P^{dch}_{d,h,b} \leq \frac{\left[k_b\ E^{a}_{d,h,b}\ e^{-k_b \Delta h} + E^{tot}_{d,h,b}\ k_b\ c_b\ (1 - e^{-k_b \Delta h})\right]\ \eta^{dch}_b}{1 - e^{-k_b \Delta h} + c_b\ (k_b\ \Delta h - 1\ +\ e^{-k_b \Delta h})} \forall d, h, b \tag{4.47a}$$

The complementarity condition for charging and discharging power described in the simplified model remain unchanged for the KiBaM, that is,

$$P^{ch}_{d,h,b} \leq x^{ch}_{d,h} M \qquad \forall d, h, b \tag{4.48a}$$

$$P^{dch}_{d,h,b} \leq x^{dch}_{d,h} M \qquad \forall d, h, b \tag{4.48b}$$

$$x^{ch}_{d,h} + x^{dch}_{d,h} \leq 1 \qquad \forall d, h, b \tag{4.48c}$$

Note that it is assumed that charging losses occur before energy enters the SBB and discharging losses occur after energy leaves the SBB.

4.4.5 Renewable Generation

Generation from PV array is modelled as a function of solar irradiance and ambient temperature [102].

$$\overline{P}_{d,h,p} = f_{der} \tfrac{G_{d,h}}{G^{STC}} \overline{P^{STC}_p} \left[1 + \gamma_p \left(T^{a}_{d,h} + \tfrac{NOCT_p - 20}{800} G_{d,h} - T^{STC}\right)\right] \tag{4.49}$$

where the parameters f_{der} is the derating factor, $G_{d,h}$ the irradiance at hour h of typical day d, G^{STC} the irradiance at STC, P^{STC}_p the output power of PV of type p at STC, T^{STC} the temprature at STC, NOCT the Nominal Operating Cell Temperature, and γ_p the temperature coefficient for output power from PV of type p. The number of installed PVs is defined as $N_p = N^{par}_p N^{ser}_p$ where N^{par}_p is the variable representing the number of parallel connected PV panels and N^{ser}_p is the parameter representing the number of series strings of PV panels of type p. Generation from WTs, $\overline{P}_{d,h,w}$, is obtained by interpolating the power curve of each type of turbine considered in the planning. Hub height wind speed used in the interpolation is calculated by using Logarithmic law and the effect of air density is modelled by using the air density ratio.

4.4.6 Reserve Requirements

Reserve requirements are determined by setting the forecast errors for demand and renewable resources (4.50a). In this study, reserve can be provided by online DGs and the SBB (4.50b). Reserve requirements and constraints to include it in the model are given by:

$$R_{d,h}^{sys} = \alpha^l \hat{D}_{d,h} + \alpha^{pv} P_{d,h}^{pv,tot} + \alpha^{wt} P_{d,h}^{wt,tot} \qquad \forall d,h \qquad (4.50a)$$

$$\sum_{g\in G} R_{d,h,g} + \sum_{b\in B} R_{d,h,b} \geq R_{d,h}^{sys} \qquad \forall d,h,g,b \qquad (4.50b)$$

$$E_{d,h,b}^{tot} \geq \underline{E_b} + R_{d,h,b}/\ \eta_b^{dch} \qquad \forall d,h,b \qquad (4.50c)$$

$$P_{d,h,g} + R_{d,h,g} \leq U_{d,h,g}\overline{P_g} \qquad \forall d,h,g \qquad (4.50d)$$

$$P_{d,h,b}^{dch} + R_{d,h,b} \ \leq \ \overline{P_{d,h,b}^{dch}} \qquad \forall d,h,b \qquad (4.50e)$$

where constraint (4.50c) ensures that sufficient amount of minimum energy is stored in the SBB in order to provide a part of reserve during under frequency events, whereas (4.50e) limits the sum of discharging power and reserve from the SBB below or equal to the maximum discharging power. The upper limit for the output power from DGs and and the discharging power from SBBs are updated to include their reserve contributions as in (4.50d) and (4.50e) respectively.

4.5 Binary Formulation of Microgrid Planning Model

The binary formulation of the planning model is a simplified version of the MILP model in which alternative planning solutions, specified in a table of search space, are provided as an input to the planning model. Still, the planning problem aims at obtaining the optimal installation plan for the microgrid considering the search space made of different types, combinations, capacities, and number of components with different technical and economic specifications. In this case, instead of purely integer planning decisions, the planning vector consists of binary variables representing the selection, 1, or rejection, 0, of a planning alternative. The planning problem presented in this thesis considers multiple types of components with the planning search space defined as explained in the following subsection.

4.5.1 Redefinition of the Planning Search Space

Consider a planning search space which consists of several alternatives which specify quantities of PV panels of type p to be considered in optimizing the installation plan of the microgrid. The design search space for PV panels is described as follow: The index for types or model of PV panels is defined by (4.51),

$$p = \{PV1,\ PV2\} \qquad (4.51)$$

The indices of alternative planning solution in the search space are specified by (4.52),

$$n_p = \{n_{p1},\ n_{p2},\ n_{p3}\} \qquad (4.52)$$

Binary variables which indicate selection of n_p^{th} alternative solution in the search space are defined by (4.53),

$$x_{p,n_p} = x_{PV1,n_{p1}},\ x_{PV1,n_{p2}},\ x_{PV1,n_{p3}},\ x_{PV2,n_{p1}},\ x_{PV2,n_{p2}},\ x_{PV2,n_{p3}} \tag{4.53}$$

The planning solution search space for the PV panels is shown in Table 4.1.

		p	
		$PV1$	$PV2$
n_p	n_{p1}	1	2
	n_{p2}	2	4
	n_{p3}	3	6

Table 4.1: *Planning search space for PV panels to be considered in the optimization*

For the search space presented in Table 4.1, if $x_{PV1,n_{p1}} = 1$, then the n_{p1} design alternative for the PV panel of type $PV1$ with specified number of panels to install in the microgrid, $N_{PV1,n_{p1}} = 2$, is selected. Using this formulation, constraints to allow either single type or multiple types of component be installed can be included in the model.

4.5.2 Objective Function in the Binary Planning Model

Objective function of the binary planning model is similar to the objective function of the integer planning model except for the planning variables.

$$\begin{aligned}
\text{Min} \quad TACS = & \sum_{p}\sum_{n_p} x_{p,n_p} N_{p,n_p}^{par} N_p^{ser} AC_p \ + \sum_{w}\sum_{n_w} x_{w,n_w} N_{w,n_w} AC_w \ + \\
& \sum_{b}\sum_{n_b} x_{b,n_b} N_{b,n_b}^{par} N_b^{ser} AC_b \ + \sum_{c}\sum_{n_c} x_{c,n_c} N_{c,n_c} AC_c \ + \\
& \sum_{g}\sum_{n_g} x_{g,n_g} N_{g,n_g} AC_g \ + \\
& \sum_{d}\sum_{h}\sum_{g} f_d U_{d,h,g} RC_g / Y_g \ + \sum_{d}\sum_{h}\sum_{b} f_d C_{bw,b} P_{d,h,b}^{dch} \ + \\
& \sum_{d}\sum_{h}\sum_{g} f_d U_{d,h,g} OMC_g \ + \sum_{d}\sum_{h}\sum_{g} f_d C_{fuel} FC_{d,h,g} \ + \\
& \sum_{d}\sum_{h}\sum_{g} f_d \left(V_{d,h,g} SUC_g + Z_{d,h,g} SDC_g\right) \\
& \sum_{d}\sum_{h} f_d \left(C_{exc} P_{d,h,g}^{exc} \ + \ C_{spl} P_{d,h}^{ren,spl}\right)
\end{aligned} \tag{4.54}$$

where x_{p,n_p} is the binary variable indicating the selection of n_p^{th} solution from search space of PV of type p, x_{w,n_w} is the binary variable indicating selection of n_w^{th} solution from search space of WT of type w, x_{w,n_w} is the binary variable indicating selection of n_w^{th} solution from search space of WT of type w, x_{b,n_b} is the binary variable indicating the selection of n_b^{th} solution from search space of SB of type b, x_{c,n_c} is the binary variable indicating selection of n_c^{th} solution from search space of BC of type c, and x_{g,n_g} is the binary variable indicating the selection of n_g^{th} solution from search space of DG of type g. The solution search space is defined by the following parameters: N_p^{par} is the number of parallel connected PV panels, N_{p,n_p}^{par} is the number of parallel connected PV panels of type p specified in the n_p^{th} solution of the search space, N_p^{ser} is the number of series strings of PV panels of type p, N_{w,n_w} is the number of WTs of type w specified in the n_w^{th} solution of the search space, N_b^{par} is the number of parallel connected batteries in a string of SB of type b, N_{b,n_b}^{par} is the number of parallel connected SB of type b specified in the n_b^{th} solution of the search space, N_b^{ser} is the number of series strings of SB of type b, N_{c,n_c} is the number of BC of type c specified in the n_c^{th} solution of the search space, and N_{g,n_g} is the number of DG of type g specified in the n_g^{th} solution of the search space. The remaining variables are as defined in (4.11)

4.5.3 Reformulation of Constraints with Integer Planning Variables

Most of the constraints in the integer planning model remain unchanged except those in which the integer planning decisions appear. The integer planning decisions are replaced by the following:

$$N_p = x_{p,n_p} N_{p,n_p}^{par} N_p^{ser} \qquad \forall p \tag{4.55a}$$
$$N_w = x_{w,n_w} N_{w,n_w} \qquad \forall w \tag{4.55b}$$
$$N_b = x_{b,n_b} N_{b,n_b}^{par} N_b^{ser} \qquad \forall b \tag{4.55c}$$
$$N_c = x_{c,n_c} N_{c,n_c} \qquad \forall g \tag{4.55d}$$
$$N_g = x_{g,n_g} N_{g,n_g} \qquad \forall g \tag{4.55e}$$

Since the discrete search space for each type of component is made by different alternatives n_ℓ, where the binary variable x_{ℓ,n_ℓ} defines if the n_ℓ^{th} alternative is selected or not, it is possible to enforce the choice of only one alternative for each type of component, so:

$$\sum_{n_\ell} x_{\ell,n_\ell} \leq 1 \qquad \forall \ell \in \{g,p,w,b,c\} \tag{4.56}$$

Another formulation to enforce selection of only one alternative in all types of particular component can be used:

$$\sum_{\ell}\sum_{n_\ell} x_{\ell,n_\ell} \leq 1 \qquad \forall \ell \in \{g,p,w,b,c\} \tag{4.57}$$

4.6 Selection of Typical Days

Due to computational limits, planning models which use discrete operation decisions to model detailed operational constraints use a small number of typical representative days with hourly profiles of input data [13]. Representative days are selected based on the seasons and weighted based on the number of days in each season. In most cases, there are no clear explanations of the selection of typical representative days. Study in [133] adopted 12 typical days, each representing one months of the year, whereas in [134], 24 typical days (one working day and one weekend day for each month) were adopted. Both studies divide a day in 24 hours and assume that each day in the month has the same pattern of the typical day profiles. A graphical method to select typical energy demand days based on iterative selection of a number of days which closely approximate the cumulated demand curve of the raw data is presented in [135]. Another work in [136], proposes an exhaustive searching algorithm to select representative weeks which yield minimum error for the reconstructed net LDC. This study found that 4 representative weeks give a reconstructed net LDC which closely match the original net LDC.

In order to obtain a reduced representation of input data for the planning model, it is necessary to apply clustering technique. The integrated planning technique adopted in this thesis models discrete operational decisions which require the use of integer variables for all 8760 hours of the planning year. It is well known that for MIP problem, the number of feasible integer solutions grows exponentially with the number of integer variables which is also exponential to the number of time periods. This results in a computational difficulty called the *curse of dimensionality* making it difficult to solve the model in acceptable computation time for the real world application [137]. Therefore, to solve this problem, clustering algorithm is applied to reduce a full year data to a number of typical representative days with profiles of input data which retains some of the main characteristic of the original raw data. For the planning problem at hand, it necessary to ensure that sampled typical days retains the peak demand profile and accurately approximate total electric energy to be supplied as well as total energy from RESs.

The main objective of the clustering algorithm is to find clusters, that is the objects of which show a high degree of similarity, while objects belonging to different clusters are as dissimilar as possible [138]. For the planing problem, input data is classified into number of groups or clusters which together satisfy the requirements of a partition:

- Each group must contain at least one object.
- Each object must belong to exactly one group.
- The peak demand days must be unconditionally selected a representative objects.

The third requirement is imposed because the peak-demand days determine the overall capacity of the generation components installed in the microgrid. Without that condition, there is a high possibility to miss the peak demand values, particularly due to the fact that the peak demand days are rare objects which might appear to the clustering algorithm as outliers.

There are many data clustering algorithms proposed in the literature [138], [139]. Hard (or crisp) clustering algorithms are either hierarchical, where a nested sequence of partitions is generated, or partitional where a partition of the given data set is generated. Fuzzy (or soft) clustering algorithms are based on fuzzy sets, rough sets, artificial neural nets, or evolutionary algorithms, specifically GA. Figure 4.2 shows a general classification of clustering algorithms.

Generally, conventional clustering algorithms can be classified into two categories, namely hierarchical algorithms and partitional algorithms. Hierarchical algorithms are further classified into: divisive hierarchical algorithms and agglomerative hierarchical algorithms. Divisive hierarchical algorithm perform clustering from the top to the bottom, i.e., the algorithm starts with one large cluster containing all the data points in the data set and continues splitting clusters; whereas agglomerative hierarchical algorithm proceeds from the bottom to the top, i.e., the algorithm starts with clusters each containing one data point and continues merging the clusters. Hierarchical clustering methods are less robust and therefore only suitable to less noisy data. Due to memory and CPU time limitations, hierarchical methods become impractical for large data sets, unless other techniques are incorporated.

Unlike hierarchical algorithms, partitioning algorithms create a one-level non-overlapping partitioning of the data points. Partitional clustering assigns a set of data points into a number of clusters without any hierarchical structure. Clustering of the data is accompanied by minimization or maximization of

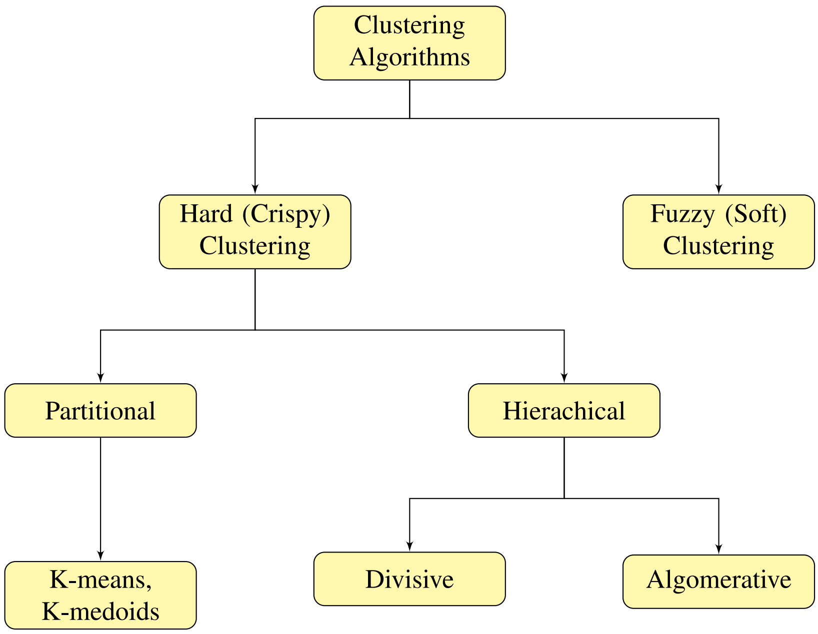

Figure 4.2: *Classification of conventional clustering techniques*

a pre-specified criterion function. For example, a criterion function which is most widely used in partitional clustering algorithm is the Sum of Squared Error (SSE) criterion.

4.6.1 K-Medoids Clustering Algorithm

K-medoids is an iterative clustering algorithm similar in approach to k-means clustering technique, but instead of using the mean, the most centrally located data or medoids are used to represent a set of data. Note that the medoids are taken from the data set itself making the new cluster center the nearest data point to the mean of the cluster points. In the K-medoids clustering, a medoid is a point that has the minimal average distance to all other objects in the same cluster. The K-medoids algorithm is more robust than the K-means algorithm in the presence of noise and outliers because a medoid is less influenced by outliers or other extreme values than a mean. However, its processing is more costly than the K-means algorithm. Three most common versions of K-medoids algorithm are Partitioning Around Medoids (PAM), Clustering LARge Applications (CLARA), and Clustering Large Applications based on RANdomized Search (CLARANS). Compared to PAM, the last two algorithms, CLARA, and CLARANS are more efficient for large data sets. Mathematical formulation of the K-medoid clustering can be summarized in form of MILP optimization problem:

$$\min \quad \sum_{i}^{n} \sum_{j}^{n} C_{ij} z_{ij} \tag{4.58a}$$

$$\text{s.t.} \quad \sum_{i}^{n} z_{ij} = 1 \qquad j = 1, 2, \ldots, n \tag{4.58b}$$

$$z_{ij} \leq y_i \qquad i = 1, 2, \ldots, n \tag{4.58c}$$

$$\sum_{i}^{n} y_i = k \qquad k = \text{Number of clusters} \tag{4.58d}$$

$$z_{ij},\ y_i \in 0,1 \qquad i,j = 1,2,\dots,n \tag{4.58e}$$

where C_{ij} is the clustering criterion to be minimized, i and j are indices of objects, y_i is a binary variable equal to 1 if and only if object i, $(i = 1, 2, ..., n)$ is selected as a representative object, z_{ij} is a binary variable equal to 1 if and only if object j is assigned to the cluster of which i is the representative object (medoid). The objective function (4.58a) minimizes the sum of the clustering criterion, e.g. distance from all objects to their representative objects. Constraint (4.58b) enforces that each object j must be assigned to a single representative object. Constraint (4.58c) ensures that each object j can only be assigned to an object i if this last object is a representative object. Constraint (4.58d) implies that exactly k objects are to be selected as representative objects. Constraint (4.58e) set the type of variables y_i and z_{ij} to be binary variables. The general implementation of K-medoids clustering algorithm, known as PAM, is summarized in Algorithm 4.1.

Algorithm 4.1 K-Medoids Algorithm

INPUT: A set of data objects to be clustered, and the number k of desired clusters.

OUTPUT: Partition of input data into k clusters.

```
procedure BUILD PHASE
    Sequentially select k centrally located objects as the initial medoids.
end procedure
procedure SWAP PHASE
    repeat
        Assign each object to the cluster represented by the most similar medoid.
        for each medoid i do
            for each non-medoid example j do
                calculate the change in clustering criterion C_ij when swapping j and i
                if C_ij has improved then
                    swap i and j
                end if
            end for
        end for
    until there is no change in clusters
end procedure
```

In the PAM algorithm, the minimized clustering criterion C_{ij} is the sum of dissimilarities between an object and the representative object of the cluster to which it belongs. To ensure that the peak days are retained in the selected medoids, days (i.e. objects) with the peak demand can be removed from the input matrix, then apply the PAM algorithm to select $k - 1$ clusters, and after this, returning the object with peak demand as a shielded cluster. Another alternative is to fix one of the day (object) with peak demand as a medoid and leave the clustering algorithm to assign objects for this fixed medoid. Note that the number of clusters k has to be specified as an input to the algorithm. For this reason, the algorithm has to be run repeatedly with different values of k until the required quality of representative sample is met.

4.6.2 K-Medoids Clustering for Selection of Typical Days Profiles

This subsection demonstrates application of the K-medoids clustering technique to select typical representative days. Input data is made up of 365×72 matrix with the first block elements 1:24 represent hourly demand data for each day, second block elements 25:48 represent hourly insolation data for each day, and third block elements 49:72 represent hourly wind speed data for each day. Since elements in the three blocks are in different scales, i.e. Demand is in kW, solar irradience in kW/m^2, and wind speed in m/s, min-max normalisation is applied before applying the clustering algorithm. The output of algorithm is k medoids, in this case k representative days, each with 72 elements (first 24 for demand data, second 24 for solar irraidence, and the remaining 24 data points for wind speed).

$$\left[\begin{array}{cccc|cccc|cccc} D_{1,1} & D_{1,2} & \cdots & D_{1,24} & G_{1,1} & G_{1,2} & \cdots & G_{1,24} & V_{w,1,1} & V_{w,1,2} & \cdots & V_{w,1,24} \\ D_{2,1} & D_{2,2} & \cdots & D_{2,24} & G_{2,1} & G_{2,2} & \cdots & G_{2,24} & V_{w,2,1} & V_{w,2,2} & \cdots & V_{w,2,24} \\ \vdots & & \ddots & \vdots & \vdots & & \ddots & \vdots & \vdots & & \ddots & \vdots \\ \vdots & & \ddots & \vdots & \vdots & & \ddots & \vdots & \vdots & & \ddots & \vdots \\ D_{365,1} & D_{365,2} & \cdots & D_{365,24} & G_{365,1} & G_{365,2} & \cdots & G_{365,24} & V_{w,365,1} & V_{w,365,2} & \cdots & V_{w,365,24} \end{array}\right] \tag{4.59}$$

The above technique is implemented in MATLAB and GAMS. The current version of Statistics and Machine Learning Toolbox in MATLAB provides implementation of PAM, CLARA, and other two types of K-medoids clustering algorithms presented in [140]. For simplicity, this work does not apply scaling factors on the selected medoids as proposed in [141] An index called Error in Duration Curve (EDC) compares the original duration curve DC_h^0 for the input data with the duration curves reconstructed from the sampled typical days profiles DC_h^{typ}.

$$EDC = \frac{\sum_{h=1}^{8760} |DC_h^0 - DC_h^{typ}|}{\sum_{h=1}^{8760} DC_h^0} \tag{4.60}$$

After obtaining typical representative days with their weights, each data point in the profiles of typical day is reproduced by the corresponding weight of that day and from these, duration curve for the input data are plotted. Wind speed duration curve has a shape which gives simple description of the kind of wind regime. The flatter the duration curve, i.e. the longer one specific wind speed persists, the more constant the wind regime is. The steeper the duration curve, the more irregular the wind regime is. Similar interpretation applies for the annual duration curve for solar irradiance which also describes the solar irradiation potential and regime of the site. The LDC is defined in Chapter 2. Using the information above, EDC index (4.60) can be calculated for each type of input data. Note that solar irradiance data available from meteorological database mainly consists of *global horizontal radiation*. This quantity must be converted to the global solar incident radiation which is used to calculate power output from the PV panels [142].

4.7 Technical and Economic Specifications of the Components

Two types of DGs, a 16 kW, 404D-22G generator (DG1) and a 7.2 kW, 403D-11G generator (DG2), both of 400 Series by Perkins are considered in this study. Table 4.2 summarises the technical and economic input data for DGs.

Table 4.2: *Specifications of diesel generators*

Type	$\overline{P_g}$	$\underline{P_g}$	B_1	A_1	AC_g	RC_g	OMC_g	Y_{dg}^g	SUC	SDC
	$[kW]$	$[kW]$	$[L/h/kW]$	$[L/h]$	[€]	[€]	[€/h]	[h]	[€]	[€]
DG1	16.0	4.80	0.3000	0.4336	949.89	11000	0.2080	15000	0.4	0.20
DG2	7.2	2.16	0.3611	0.3830	335.99	3890.88	0.1008	8200	0.2	0.10

For the PVs, a 1 kWp array (PV1) and 0.3 kWp panels (PV2) with specifications given in Table 4.3 are considered.

Table 4.3: *Specifications of PV panels*

Type	$\overline{P_p^{STC}}$	T^{STC}	G^{STC}	f_{der}	$V_p^{pv,n}$	$NOCT$	γ	AC_p	Y_{pv}^p
	[kW]	$[^oC]$	$[kW/m^2]$	$[^oC]$	[V]	$[^oC]$	$[\%/^oC]$	[€]	[yr]
PV1	1	25	1	1	6	47	-0.509	355.73	25
PV2	0.3	25	1	1	12	45	-0.440	126.12	25

Table 4.4 summarises technical and economic specifications for two types of WTs: 10 kW, XZERES, 442SR wind turbine(WT1), and 3 kW, WWCD-3016, Ampair® wind turbine (WT2), respectively.

Table 4.4: *Specifications of wind turbine models*

Type	$P_w^{wt,n}$	$V_w^{wt,n}$	V_w^{ci}	V_w^{co}	AC_g	Y_w^{wt}
	$[kW]$	$[m/s]$	$[m/s]$	$[m/s]$	[€]	[yr]
WT1	10	12.5	3.0	25.0	3052.09	15
WT2	3	12.0	3.0	20.0	1277.88	15

The SBBs considered are: 820 Ah, 20 HR, 6V, deep cycle battery, model 6 CS 25P by Rolls (SB1), and 357 Ah, 20 HR, 12V, flooded deep cycle battery, model 12 CS 11P by Rolls (SB2).

Table 4.5: *Specifications of storage battery models*

Type	C_n	$\overline{C_b^{sb}}$	V_{bn}	DOD	η_{ch}	η_{dch}	$\overline{I_{ch}}$	$\overline{I_{dch}}$	$\overline{Ch_{rb}}$	AC_b	$C_{bw,b}$	Y_b^{sb}
	$[Ah]$	$[Ah]$	$[V]$	$[\%]$	$[\%]$	$[\%]$	$[A]$	$[A]$	$[A/Ah]$	[€]	[€/kW]	[yr]
SB1	820	1151.56	6	60	90.0	90.0	164.0	500	1	153.62	0.1275	12
SB2	357	514.00	12	60	90.0	90.0	71.4	500	1	147.24	0.2052	10

The BC represents rectifier and inverter of 10 kW with the specifications summarised in Table 4.6.

Table 4.6: *Specifications for the bidirectional converter*

Type	$\overline{P^{inv}}$	$\overline{P^{rec}}$	η_{inv}	η_{rec}	AC_c	Y_c^{bc}
	$[kW]$	$[kW]$	$[\%]$	$[\%]$	[€]	[yr]
BC1	10	10	90.0	90.0	1179.4	20

4.8 Case Study 1: Validation of the Planning Model

This case study applies the MILP planning model for planning of Sicud village microgrid in Philippine. The aim is to validate the accuracy of model, particularly the long-term operation, by comparing its results with results obtained by using a standard microgrid planning software, HOMER Pro 3.3. To this end, the Philippine village of Sicud model, which is available from HOMER Energy's sample files page is selected [143]. It is assumed that all days of the year have the same profiles of electric demand, irradiation and wind speed. The MILP model is solved for 36 days, each having the same weighting factor of 365/36. Integer planning variables for the proposed MILP model are bounded by maximum number of each type of component to be considered as specified in Section 4.7. The model, formulated by adopting the KiBaM, is solved while relaxing minimum up and down time and reserve constraints and setting start up and shut-down costs to zero. This is done so to ensure similar constraints are in the proposed models as those in HOMER Pro. In this case, the MILP model found optimal microgrid plan with two DGs, DG1(16 kW) and DG2(7.2 kW), three PVs (PV1 3 kW), one WT(WT1 10 kW), seven SBs (SB1 34.44 kWh), and one INV (INV1 10 kW).

Next, results from the proposed MILP model were set as inputs to HOMER Pro planning search space. Then, HOMER Pro was run to simulate the system for the whole year with the same hourly data under similar assumption that all days of the year have the same profiles with average electric demand, irradiation and wind speed. System control options in HOMER Pro were set to allow LFDS, planning configurations with multiple components, and simultaneous operation of multiple DGs. Architecture of the system implemented in HOMER Pro is shown in Fig.4.3.

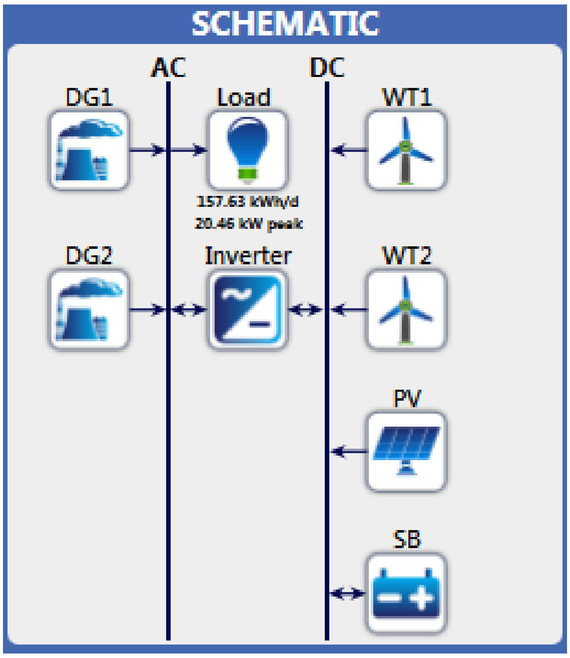

Figure 4.3: *Microgrid architecture in HOMER Pro*

Results from HOMER show that the optimal system, i.e. the one with minimum Net Present Cost (NPC), has the same components as those found by the MILP model. Figure 4.4 and 4.5 show results obtained by the proposed MILP model and HOMER Pro respectively. Figure 4.4a and 4.5a show output power from DG , part of power from renewable sources, in this case WTs, which is supplied directly to the load, the part this power which goes to charge the SBB, discharging power from SBB, and electric demand. Net SBB power and SOC ere shown in Figure 4.4b and 4.5b.

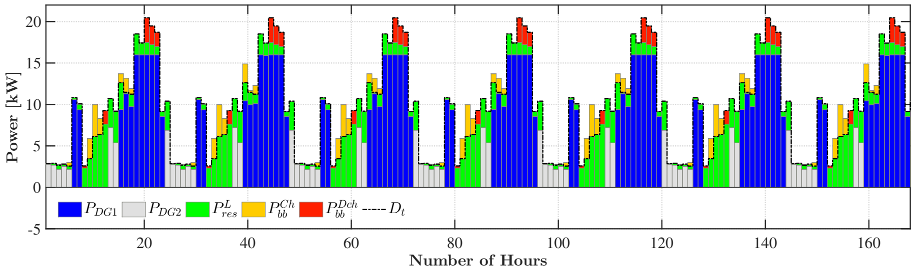

(a) *Dispatching of DGs and SBB obtained by MILP planning model*

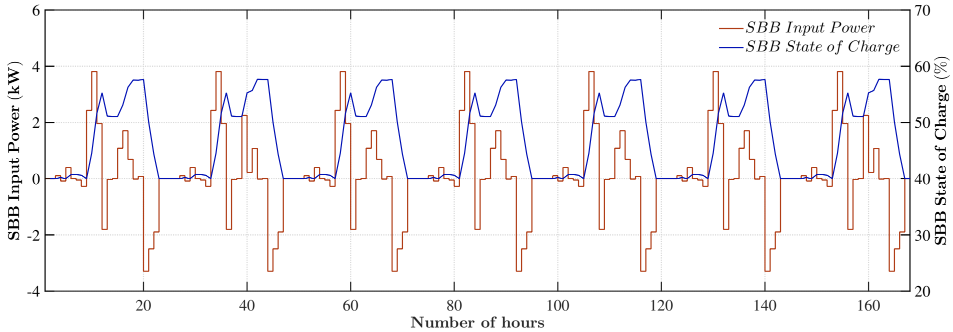

(b) *Input power and SOC of SBB obtained by MILP planning model*

Figure 4.4: *System operation obtained by MILP planning model*

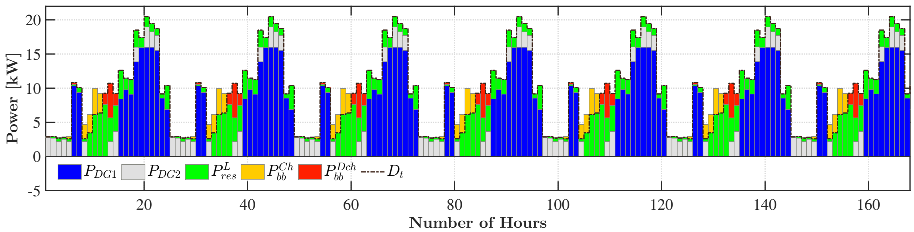

(a) *Dispatching of DGs and SBB obtained by HOMER Pro*

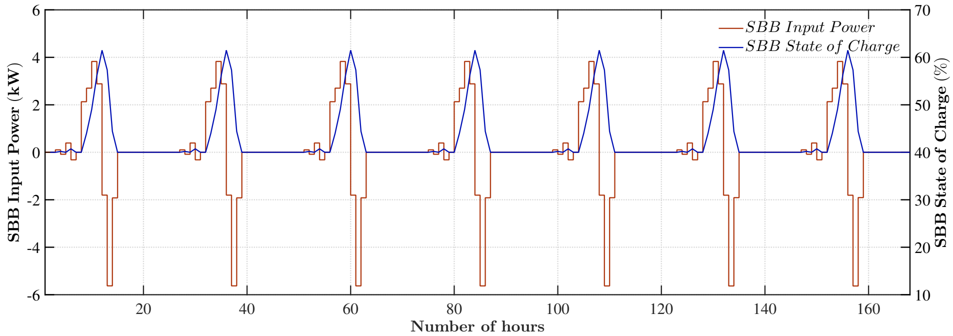

(b) *Input power and SOC of SBB obtained by HOMER Pro*

Figure 4.5: *System operation obtained by HOMER Pro*

Comparing Fig.4.4a and 4.5a indicates that the MILP model dispatch DG in a very similar way as HOMER Pro. However, there is a noticeable difference in the charging and discharging of SBB as can be seen in Fig.4.4b and 4.5b. The main reason for such difference is that mathematical optimization approach, which was applied to solve the MILP model, optimizes operational variables for all hours concurrently, whereas HOMER, which uses simulation approach, finds the solution based on the current and previous system operation state. For this reason, HOMER maximizes the use of available power from renewable resources or discharging of SBB for the current period without considering time shifting of this energy to the other periods. On the contrary, the proposed MILP model operate DG at high output range while charging the SBB and then use the stored energy during peak hours. As a results the total operational cost and number of operational hours for DG are minimized as compared to HOMER (see Table 4.7). These results confirm that the proposed model implements operational constraints correctly.

Table 4.7: *Comparison of results from MILP model and HOMER Pro*

Description			**Case 1 Results**	
Variable	**Symbol**	**Unit**	**MILP Model**	**HOMER Pro**
Annualized fuel cost	AFC_{DG1}	€	17139.87	172884
	AFC_{DG2}	€	5328.90	5700
Annualized O&M cost	$AOMC_{DG1}$	€	867.66	911.04
	$AOMC_{DG2}$	€	315.98	440.60
Hours of Operation	h_{DG1}	h	4015.0	4380
	h_{DG2}	h	2920	4371
Annualized Replacement cost	ARC_{DG1}	€	2486.0	2693.55
	ARC_{DG2}	€	1263.0	1916.68
SBB annualized Replacement cost	ARC_{SBB}	€	264.22	264.22
Total annualized cost of system	$TACS$	€	36207.21	37994
Total annualized operation cost	$TAOC$	€	28479.0	30266.0
Levelized cost of energy	$LCOE$	€	0.4278	0.449
Renewable energy fraction	f_{ren}	%	26.4	26.2

Results in Table 4.7 confirm that the proposed MILP model can approximate the system long-term operational planning accurately. As expected, almost all indices are the same except for the slight difference in the operation of DGs and SBBs which is mainly caused by differences between the solution methods employed.

4.9 Case Study 2: Comparison of MILP and Binary Planning Models

4.9.1 Input Data

In this section, another planning case study for a microgrid, located in $5.5°S,\ 34.5°E$, Singida, Tanzania. The aim is to apply the proposed MILP model to obtain optimal combination and number of components to be installed in this village microgrid consisting of 150 households, a small milling machine, primary school, and 4 small shops. The peak load of this microgrid is 78.6 kW. One year electric demand data are from the demand data developed in the study reported in [144], [145]. Solar irradiance and wind speed data were obtained from the National Aeronautics and Space Administration (NASA) database, and processed by HOMER Pro. 3.3 [146]. First, the K-medoids clustering algorithm is applied to select typical representative days. It is found that 36 representative days are sufficient to approximate the input data profiles, available energy from renewable resources and annual energy to be supplied with errors of less than 4%. Table 4.8 summarises indices of typical representative days d_{typ} and their weights f_d obtained after applying the clustering algorithm to sample 36 typical representative days from the input data.

Table 4.8: *Typical representative days d_{typ} and their occurrence weights f_d*

n_d	1	2	3	4	5	6	7	8	9	10	11	12
d_{typ}	346	243	188	155	48	324	179	75	148	33	19	260
f_d	12	18	12	17	1	22	32	1	14	3	9	6
n_d	13	14	15	16	17	18	19	20	21	22	23	24
d_{typ}	8	325	109	315	15	4	47	165	343	320	9	55
f_d	3	4	35	9	2	5	1	41	13	22	1	4
n_d	25	26	27	28	29	30	31	32	33	34	35	36
d_{typ}	264	78	49	51	85	252	191	140	332	241	341	158
f_d	14	1	1	7	9	13	5	8	12	4	3	1

Profiles of typical representative days with their corresponding duration curves compared to the duration curves of raw data for electric demand, solar irradiance, and wind speed, are shown in Figure 4.6, 4.7, and 4.8 respectively.

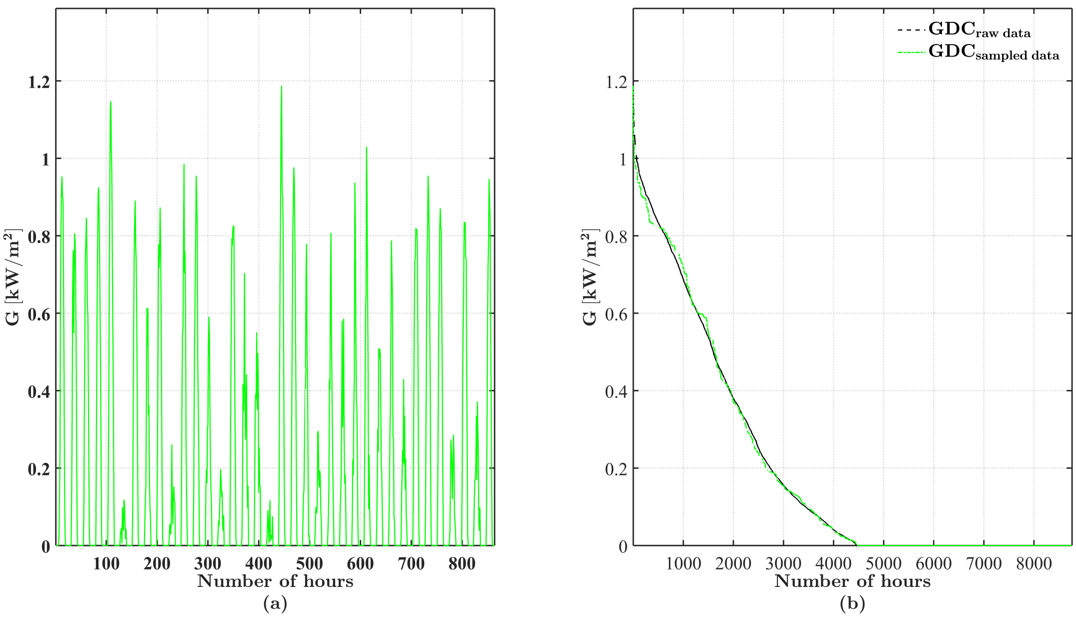

Figure 4.7: *(a) Profiles of solar irradiance for 36 representative days (b) Comparison of duration curves from sampled and raw data*

H]

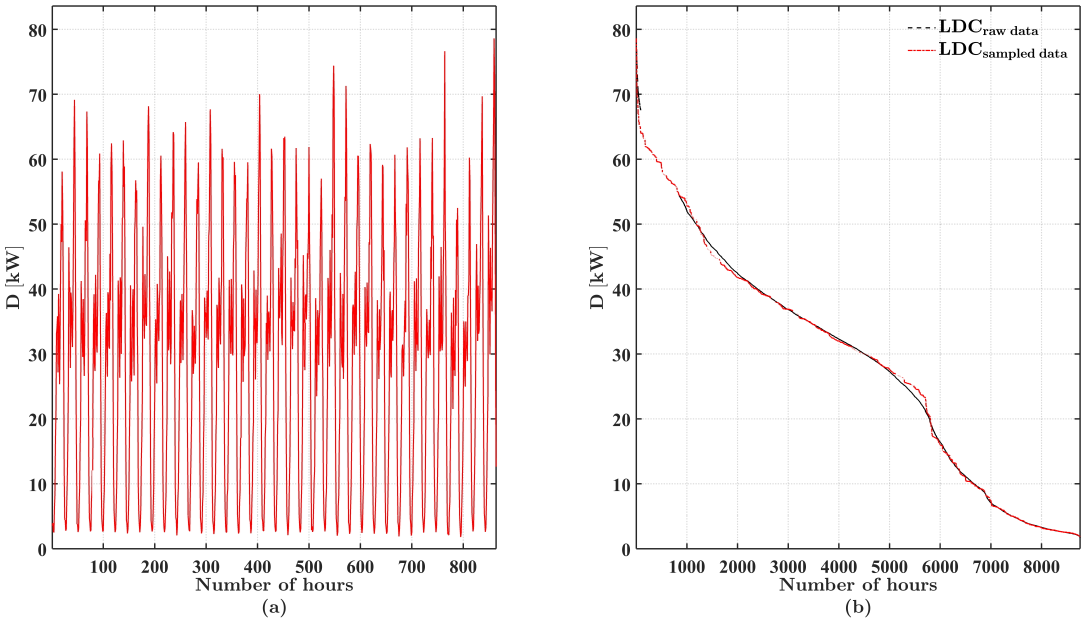

Figure 4.6: *(a) Profiles of electric demand for 36 representative days (b) Comparison of duration curves from sampled and raw data*

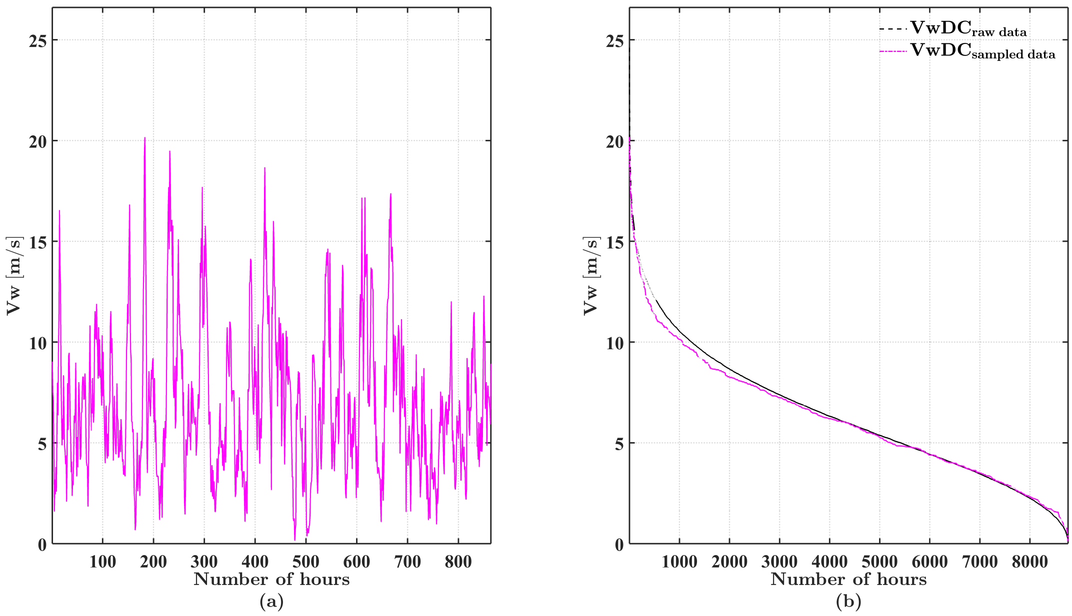

Figure 4.8: *(a) Profiles of wind speed for 36 representative days (b) Comparison of duration curves from sampled and raw data*

In this case, the EDC for electric demand, solar irradiance, and wind speed, were found to be 1.4484%, 3.0691%, and 3.1792% respectively.

4.9.2 Results from the MILP Planning Models

Table 4.9 summarised the optimal number of components to be installed in the microgrid obtained by applying the the MILP planning model.

Table 4.9: *Optimal number of components to install as obtained by MILP planning model*

Description			Case 1 Results		
Component	**Symbol**	**Capacity**	**Maximum Number Considered**	**Optimal Number to Install**	**Installed Capacity**
PV panels	$PV1$	1.0 kWp	10	5	5.6
	$PV2$	0.3 kWp	10	2	
Wind Turbines	$WT1$	10.0 kW	10	6	60
	$WT2$	3.0 kW	10	0	
Storage Batteries	$SB1$	4.92 kWh	50	16	78.72
	$SB2$	4.284kWh	50	0	
Diesel generators	$DG1$	16.0 kW	5	3	69.6
	$DG2$	7.2 kW	5	3	
Bidirectional Converters	$BC1$	10.0 kWh	10	5	50

The breakdown of total annualized system cost obtained by applying the MILP planning model is shown in Figure 4.9.

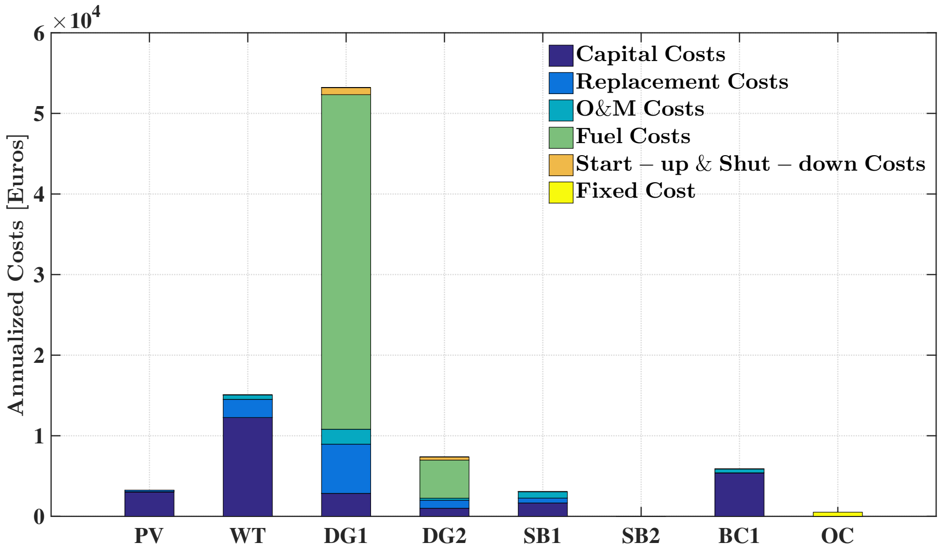

Figure 4.9: *Breakdown of total annualized costs of the system for case study 1*

The results summarised in Figure 4.9 show that the annual fuel cost makes a significant part of the overall annualized cost of the microgrid. In this case, the annual fuel cost is €41596.87, which is equal to 46% of the total annualized cost of the microgrid, i.e €90075.31. The total installed capacity of DGs is 69.6 kW, equivalent to 88.5% of the peak system demand, 78.64 kW. On the other hand, the total installed capacity of PVs and WTs is 65.6 kW while the SBB capacity is 78.72 kWh. In this case the renewable fraction, that is, the fraction of the energy delivered to the load that originated from renewable power sources, is found to be 46.1% and the LCOE is 0.3596.

Another important information which can be obtained from the model is the long-term operational scheduling of all components in the microgrid. Figure 4.10 summarises system operation schedule which consists of: output power from DGs, part of the total generation from PVs and WTs which is supplied directly to the load, part total generation from PVs and WTs and charging power from DGs which makes the total charging power to the SBBs, discharging power from the SBBs, and the electricity demand. As shown in Figure 4.10, all constraints for the long-term system operational model are fulfilled. Supplying the demand by using generation from RESs is prioritized while DGs are dispatched when there is no enough power from PV array, WTs and SBB. Figure 4.11 shows the operation SBBs.

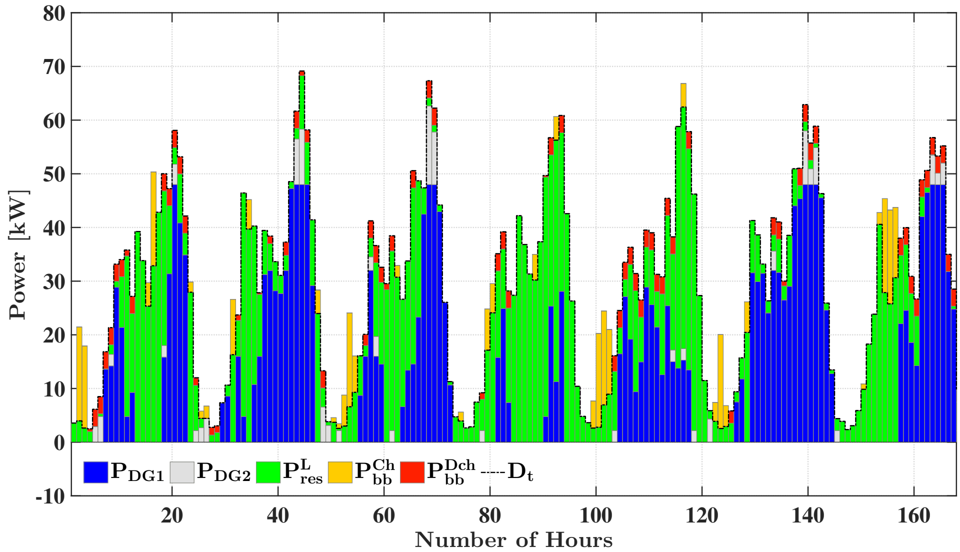

Figure 4.10: *Overall system operation schedule from the MILP planning model*

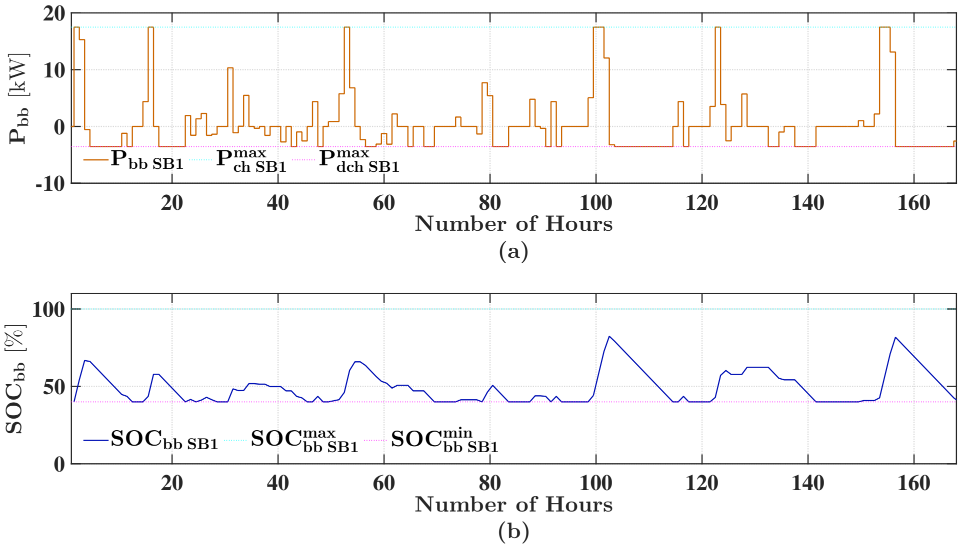

Figure 4.11: *(a) Net hourly SBB power $P_{bb} = P_{ch} - P_{dch}$ (b) Profile of hourly SBB overall SOC*

From Figure 4.11, charging and discharging power are maintained within their maximum limits. Also, the SOC of is maintained above its minimum limit.

Figure 4.12 summarises the results obtained from the operation planning model run over one year in order to assess the overall microgrid operation with the results from the MILP planning model. In particular, the assessment focuses on the daily operation cost and unmet demand. Since it is not clear how to obtain the value of unmet demand, a very big penalty cost, $5500 \text{ €}/kW$, was set in order to enforce the model to avoid unmet demand. The microgrid operation in the days with unmet demand iss shown in Figure 4.13.

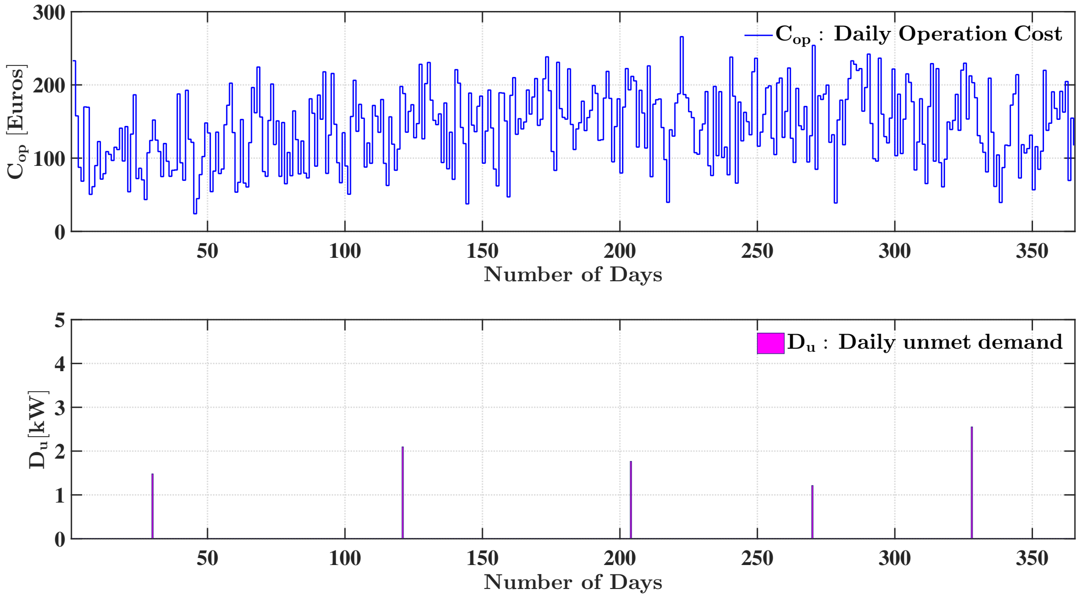

Figure 4.12: *Results obtained by running the operation planning model with fixed MILP planning results (a) Daily operational cost (b) Daily unmet demand*

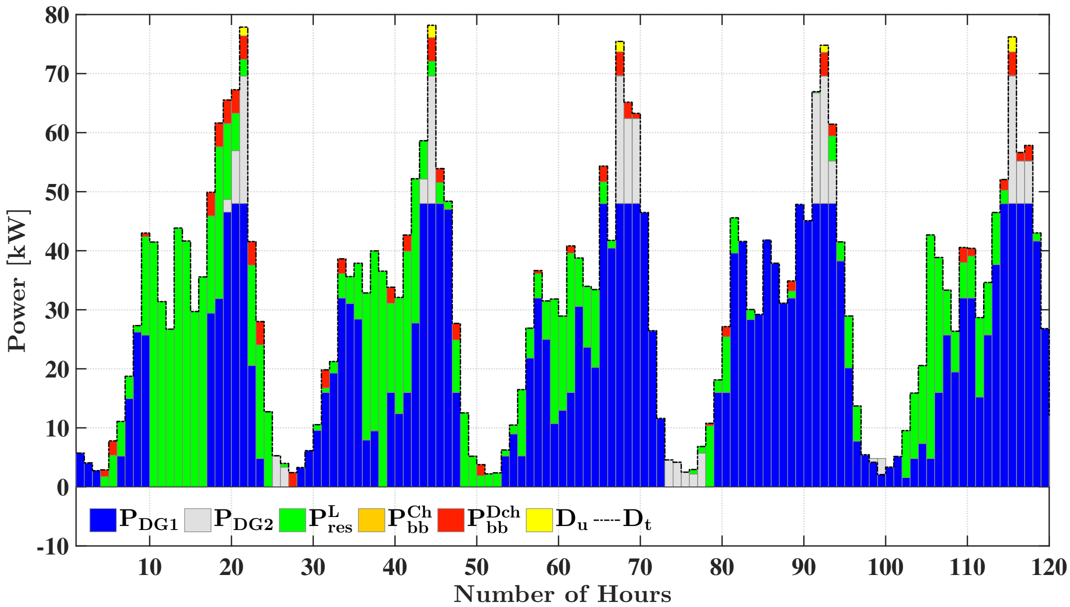

Figure 4.13: *System Operation for the days with unmet demand*

As it can be seen from Figure 4.12, there are only five days in a year with unmet demand, days with index d which stands for day number, equal to: 30, 121, 204, 270, and 328. The total annual unmet demand is found to be $9.106\ kWh$ and the total cost of unmet demand is €55084.23. The magnitude of this cost is even larger than the total annual operation cost, €41596.87, meaning that the penalty was high enough to ensure all possibilities to avoid the unmet demand are explored by the solver. It is interesting to note that unmet demand occurs in the peak hour of the days in which the net demand was greater than the total installed capacity of DGs 4.13. Operation of the SBB in the days with unmet demand is shown in Figure and 4.14.

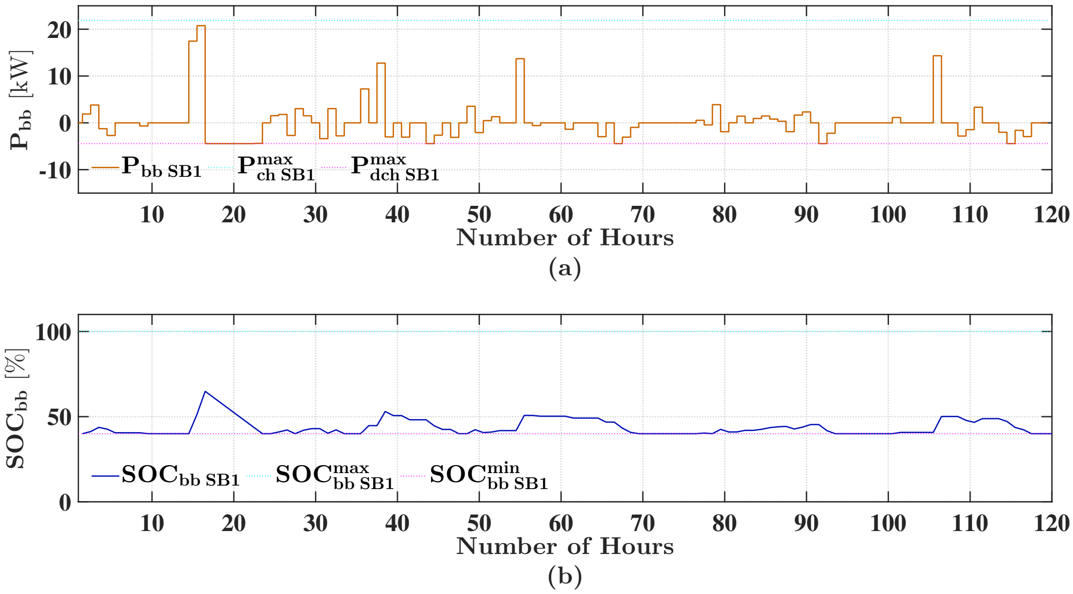

Figure 4.14: *SBB net power and SOC for the days with unmet demand*

It can be observed from Figure 4.13 and 4.14 that the unmet demand occurs in the peak hours. In this case, the model dispatched all available power from the installed component in order to supply the demand, that is, all DGs are operated at maximum capacity $69.6\ kW$, the charging power from SBB is at maximum limit, and the total available generation from PVs and WTs is directly supplied to the load. These results demonstrate the usefulness of setting the reliability criteria, i.e. the maximum allowable unmet energy, $MAUE$. If this criteria is set to zero and the peak demand is among the sampled typical days, then the model will install components with total generation sufficient to supply the peak demand. However, this will depend on the availability of renewable energy resources during the peak demand hours. If the peak demands and higher RES generations coincide, the model can determine a solution with lower total capacity of conventional DGs, but which fulfils the $MAUE$ criteria. One option to avoid this case is to include a constraint which requires the total installed capacity of conventional DGs to be greater or equal to a specified percentage of the peak demand. Another way is by assuming forecasting errors and use them to determine the required capacity reserve. In this case, forecasting errors lower the total generation from RES and increase the demand in each hour of planning horizon. These approach work very well, with obvious results that the model install more DGs and SBB, thus increasing the total annualized cost of the system. However, it is the task of the planner to decide if such an increase in the system cost is worthy for the sake of supplying a small amount of unmet demand as demonstrated above.

Note that it may be necessary to enforce these reliability constraints if it the expected allowable load shedding limit is known during the planning stage.

Alternative model in which the SBB replacement cost is formulated in the objective function as a function of its wear cost, charging power, and discharging power, in order to avoid the use of binary variables to enforce the complementarity condition for the charging and discharging of SBB was considered. The aim was to investigate if by avoiding the binary variables, the computational time would improve. Interestingly, this model obtains similar results as those obtained by the MILP model with binary variables to enforce the complementarity condition for SBB operation. For sake of brevity, the results are not presented here again. However, regarding the computational time, it is found that this formulation, which uses charging and discharging costs to enforce the complementarity constraints for SBB operation, does not result in any significant improvement in the computation time as compared to the MILP planning model with binary variables. This finding suggested that the difficult in solving the optimal planning model does not necessarily depend on the SBB operational control variables, but rather on the complex interaction between system planning and operation constraints (computational times and model sizes are summarised in the next subsection, see Table 4.12).

4.9.3 Results from the Binary Planning Models

This section summarises the results and the findings obtained by applying the binary planning model proposed in Section 4.5 for planning a microgrid under consideration. The model was run by using the same input data as for the previous case study. The main change for this case is that the planning search space is specified to the model as a table containing different planning alternatives which specify the number of components of each type to be considered in the optimization. The planning search space is presented in Table 4.10. Note that there is no need to include zeros in the search space as this is the condition when the binary variables corresponding to a particular type of components are all equal to zero.

Table 4.10: *Search space for the Binary planning model*

Alternative		**Components and the types to consider for each**								
		PV		**WT**		**SBB**		**DG**		**BC**
		p		w		b		g		c
		$PV1$	$PV2$	$WT1$	$WT2$	$SB1$	$SB2$	$DG1$	$DG2$	$BC1$
n_ℓ	1	1	1	1	4	4	4	1	1	3
	2	2	2	2	8	8	6	2	2	4
	4	4	4	8	12	12	8	3	3	5
	5	5	6	6	16	16	10	4	4	6
	6	6	8	8	20	20	12	5	5	8
							15			

Using Gurobi 6 solver, the binary model solved to optimal solution with a gap of 1% while giving the same solutions as obtained with the previous formulation, in only 2.43 hours. The results found by the binary model are summarised in Table 4.11. This is a significant reduction in the computation time as compared to the MILP model which took more than 48 hours to obtain the solution with optimality gap

Table 4.11: *Optimal solution obtained by the Binary planning model*

	Components and the types to consider for each								
	PV		WT		SBB		DG		BC
	$PV1$	$PV2$	$WT1$	$WT2$	$SB1$	$SB2$	$DG1$	$DG2$	$BC1$
Installed components	6	0	6	0	16	0	3	3	5

of 1.64%. The reason for this is that the binary formulation simplifies the MILP planning model, leaving the solver with the task of optimal selection of the planning solutions among the specified planning alternatives which have already fixed the number of components to install. This approach is acceptable, particulary when the particular alternatives are already known to the planner. For example, if the DC bus voltage is known and fixed, for some technical reasons, then it is possible to specify SBBs alternatives based on the multiple number of their series connections as per standard input voltage of the off the shelf bidirectional DC/DC interfacing converters. The same approach may be applied for series connection of PV panels. In some cases this approach can be repeated while refining the search space until an optimal solution is found. This finding confirmed the applicability of the proposed planning models real system planning.

Table 4.12: *Size and computational time of MILP planning models*

Model	Number of Constraints	Number of Variables				CPU Time [h]
		Integer	Binary	Continuous	Total	
MILP^{a}	394,230	52,571	35,044	210,249	297,864	>168.00
MILP*	38,910	5,195	3,460	20,745	29,400	37.00
MILP**	35,520	5,193	1,728	19,885	25,078	22.34
MILP***	47,607	5,184	3,496	18,157	26,837	2.43

^{a}Deterministic MILP model solved for the complete year, *Deterministic MILP model solved for 36 typical days, ** MILP model without complementarity constraints solved for 36 typical days, *** Binary model with complementarity constraints solved for 36 typical days.

4.10 Summary

This chapter presents three formulations for deterministic MILP microgrid planning models. The models are formulated to minimize total annualised cost of system which includes the annualised investment cost and annualised overall system operation cost. Using discrete planning variables makes it possible to model operational flexibilities required to ensure continuous balance of demand and generation despite high variations in demand and the generation from renewable energy sources. Furthermore, a more accurate approximation of overall system operation cost is obtained. Findings from the results of sample planning case studies have important implications for microgrid planning. First, about 50% of the total life cycle cost of a microgrid is made up by the fuel cost for running diesel generators. This justifies the need to consider hourly operation of overall microgrid in order to obtain accurate approximation of fuel cost. Second, the planning proposed MILP can be efficiently applied to plan any microgrid configuration. Thirdly, the binary version of the proposed planning model is very efficient in terms of computational time and can be applied for practical feasibility studies. Lastly, the accuracy of planning results depends mainly on the clustering of resources and electric demand data.

CHAPTER 5

Microgrid Planning under Uncertainties

5.1 Introduction

In order to obtain an optimal planning solution, which ensures operational feasibility for the microgrid under a range of plausible operation scenarios, uncertainties in renewable energy resources and electricity demand must be considered. The deterministic model presented in Chapter 4 assumes fixed profiles for electricity demand, solar irradiance, and wind speed. The assumption is that these profiles are fixed representation of the input data. However, actual profiles which will be revealed in different days and seasons may differ significantly from the deterministic profile used during planning. As a result, the microgrid may either fail to supply the demand or supply it at a very high operational cost. This makes it necessary to include uncertainties in the microgrid planning model. Clearly, it is not possible to represent profiles of all possible realization of input data as this will make the model very large and computationally intractable. Therefore, proper techniques for modeling uncertainties should be adopted. This chapter starts by discussing sources of uncertainties in microgrid planning, Section 5.2. Next, Section 5.3 presents frameworks for modeling uncertainty in microgrid planning problem. These frameworks are: Stochastic Optimization (SO) and RO. Afterwards, a 2SSIP model for microgrid planning is presented in Section 5.4; following Section 5.5 presents Γ-robust optimization model for microgrid planning. A case study to demonstrate the applicability of these models is presented in Section 5.6. Results and the discussion from the two models are presented in Section 5.7. Finally the chapter summary is presented in Section 5.8.

5.2 Uncertainties in Microgrid Planning

The main sources of uncertainties in microgrid planning can be classified as [147]:

- uncertainties in energy demand,
- uncertainties in weather input data (Wind speed and solar irradiation),
- uncertainties in technological parameters,
- uncertainties in economic parameters (fuel or natural gas cost, electricity price),
- operational uncertainties (contingencies).

Uncertainties in energy demand arise from the long-term forecasting of electricity demand. Microgrid electricity demand cannot be forecasted easily because of the small number of users which makes the the total load profile, seasonal variations in electricity demand, difficulties in identification of the peak demand hours, and many exogenous variables such as weather conditions and social events. Compared to the demand profiles of large conventional power system, microgrid demand profiles are characterised by high disaggregation of power consumption and thus high variability. As a result, the demand profiles for microgrid do not always conform to the standard demand profile as for the case of large power system. Typical microgrid demand profile is therefore much noisier and thus harder to forecast by using traditional methods employed in large power systems. Electric demand forecasting models can be classified in two major branches: (1) parametric methods such as regression methods, time series prediction methods, and grey dynamic methods, which employ statistical techniques on historical demand data, (2) artificial intelligence methods such as Artificial Neural Networks (ANNs) and Fuzzy Logic (FL) [148], [149]. Despite their ability to automatically learn from experience and adapt themselves, these forecasting techniques are prone to forecasting errors particularity when considering long-term demand forecasting as required by planning studies [150]. Existing microgrid planning softwares use algorithms to synthesize hourly electricity demand based on some input parameters which take into account hourly and seasonal variations. Since this thesis adopts typical representative days to represent the complete planning year, considering uncertainties is even more important than for other approaches. For developing countries, forecasting electricity demand is even more difficult because of emulation factors to be considered.

Variable generation form RESs is another source of uncertainties in microgrid. A high degree of RESs, commonly wind and solar energy, are utilized in microgrids. Generation from these sources is subject to uncertainty in the their primary resources and thus would produce variable power. Typically, the RESs generation does not always follow a repetitive pattern in the daily operation of microgrids. Accurate forecasting of variable generation is challenging as it highly depends on site and weather conditions. In forecasting generation from WT, it is possible to adopt methods which forecast wind power directly or methods which forecast wind speed and convert it to wind power. Wind forecasts are created using statistical models, physical models, or a hybrid of both. However, the results from forecasting models are mostly applied in planning the operation of the system. For long-term planning, it is difficult to obtain on-site wind speed data, thus most planning studies and softwares rely on data from meteorological models. To model uncertainty, one can use historical or meteorological data to generate plausible scenarios of wind speed and wind power generation [151].

Uncertainty in solar irradiance data results from the atmospheric condition of the site and measurement error in collection of historical or meteorological data. Also, variations of temperature has significant effect on the PV systems conversion efficiency. Uncertainties in technological parameters may results from technological advancement such as improvement of existing technology performance, e.g. efficiency of PV panels, new innovation in production methods and thus change in technology cost (specifically for PV), adoption of new technologies such as micro CHP, and drop in the cost of expensive technology such as PVs, WTs and Fuel Cells (FCs).

Uncertainties in economic parameters include the volatility in fuel cost, natural gas cost, price of electricity (for grid connected microgrid), carbon price, incentives for diesel, and different risks associated to different technologies that result in different costs. These uncertainty will affect long-term operation of microgrid, particulary the commitment and dispatch of DER. For example, a method to determine optimal investment strategies in a microgrid with an uncertainty in electricity price and fuel cost is presented in [152]. That paper applies a real options approach to analyze the investment and operational decisions.

Operational uncertainty results from unforeseen generator outages and the overall change of microgrid operation mode such as microgrid islanding. Islanding mode occurs when a grid-connected microgrid disconnects itself from the maingrid due to a disturbance on the main grid. The microgrid is expected re-synchronized with the utility system when the disturbance is removed. However, the time and duration of such disturbances are not known to microgrids and therefore present a form of uncertainty. Depending on the level of system reliability considered during the planning stage, modeling operational uncertainty may be necessary part of microgrid planning problem.

5.3 Uncertainties Modelling Techniques

The decision making process for microgrid planning problem under uncertainty is summarised as follow. The planning problem aims at obtaining the optimal design plan, that is, the number of component of different types, capacities, and technologies to be installed in the microgrid. It is further required to select components that will ensure continuous supply of electricity demand at minimum cost. Assuming that the components characteristics can be modeled by linear functions, the above description suggests that the problem at hand is a MILP problem modeling simultaneous determination of the planning and long-term operation variables. If the future demand and renewable resources are assumed to be known with certainty, the problem is modeled and solved as described in Chapter 3 and 4 respectively.

Considering uncertainty in electricity demand and renewable resources data, the above problem can be modeled using various formulations, depending on the quality, robustness, and flexibility of the desired solution. This problem has two inherent stages of decision making. The planning decisions are made first and fixed for long-term. The operational decisions, which define the optimal use of the installed components in order to approximate the long-term operational costs, are made after the realization of uncertain electricity demand and renewable resources data. In this case, what kinds of demand and renewable resources profiles will be realized in each day of the planning year cannot be anticipated. However, since the planning decisions are made before the realization of uncertainties, the optimal values of these planning decisions should be the ones which minimize total investment cost and the total expected operation cost. Two most common frameworks for modeling uncertainty are presented in the following subsections.

5.3.1 Stochastic Optimization

5.3.1.1 Introduction to Stochastic Optimization

Contrary to the classical deterministic optimization which assumes perfect knowledge of the input data, SO deals with a more practical case in which input data are uncertain. Usually, in SO the uncertainty is described by using Probability Distribution Functions (PDFs). SO models can be divided into two primary classes: SO problems with recourse and SO with chance/probability-constraints. In the recourse models, a set of decisions have to be made a priori in a context when the related environmental information is not completely available. These decisions are usually called *first-stage* decisions. Given the first-stage decisions, later stage decision variables (also called *recourse variables*) can be made based on the realization of a number of random events. These recourse variables are also interpreted as "correction actions" if they are used to compensate any infeasibility from the first-stage decisions. On the other hand, stochastic models with chance-constraints allow occasional infeasibility and require that the constraints be satisfied with some specified probability.

SO models with recourse can be further classified into single-stage, two-stage, and multi-stage models. In SO, stages define a collection of consecutive periods of time such that during each stage, one or more stochastic (i.e. uncertain) events take place, and at the end of each stage, decisions are made taking into account the specific outcomes of the stochastic events of this and previous stages. For a single-stage SO model, decisions are made with no subsequent recourse. For the two-stage SO model, the first-stage or here-and-now decisions are made before the realization of the stochastic process and thus these decision variables do not depend on the realization of the stochastic process. Second-stage or wait-and-see decisions are made after knowing the actual realization of the stochastic process. Consequently, these decisions depend on each realization of the stochastic process. If the stochastic process is represented by a set of scenarios, a second stage decision variable is defined for each single scenario considered. In the multi-stage setting, the uncertain data is revealed gradually over time, in a number of periods, and a sequence of decisions are made in each stage such that the first stage decisions are independent of each future realization of the stochastic processes, and the following stages are dependent on each realization of the stochastic process in the previous stage, but they are independent on all possible values of the stochastic processes that are realized in the future. For example, the second stage decisions are considered as wait-and-see decisions with respect to the first stochastic process and here-and-now decisions with respect to subsequent stochastic processes.

Modelling a two stage SO problem in which some of the first and second stage decision variables have integrality restrictions leads to a Two-Stage Stochastic Integer Programming (2SSIP) model. This type of problem is hard to solve since it combines the difficulty of stochastic and integer programming [153]. However, most engineering design and operational planning problems under uncertainty have inherent features which fit very well to the 2SSIP formulation. In this research, the 2SSIP formulation is adopted to model microgrid planning problem.

5.3.1.2 Two-Stage Stochastic Integer Programming

The first framework for modeling uncertainty in microgrid planning problem is by using SO [154]. This approach has a long and active history dating at least as far back as Dantzig's original paper [155]. Within the SO framework, microgrid planning problem falls naturally under the 2SSIP framework. In 2SSIP, the planning decision variables are considered as the first stage “here-and-now” variables that are decided prior to the realization of uncertain parameters, whereas operational decision variables are considered as the second stage "wait-and-see" variables, which are decided when the uncertain parameters have been observed. A standard form of a 2SSIP is given by:

$$
\begin{aligned}
\min_{\mathbf{x},\mathbf{y}_s(\boldsymbol{\omega})} \quad & \left\{ \mathbf{c}^T\mathbf{x} + \sum_s \pi_s \mathbf{q}_s^T(\boldsymbol{\omega})\mathbf{y}_s(\boldsymbol{\omega}) \right\} \\
\text{s. t.} \quad & \mathbf{A}\mathbf{x} = \mathbf{b}, \\
\text{s. t.} \quad & \mathbf{T}_s(\boldsymbol{\omega})\mathbf{x} + \mathbf{W}_s(\boldsymbol{\omega})\mathbf{y}_s(\boldsymbol{\omega}) = \mathbf{h}_s(\boldsymbol{\omega}) \\
& \mathbf{x} \in \mathbf{X},\ \mathbf{y}_s(\boldsymbol{\omega}) \in \mathbf{Y} \quad s = 1 \dots S,
\end{aligned}
\tag{5.1}
$$

where the first and second stage variable vectors $\mathbf{x}$ and $\mathbf{y}(\boldsymbol{\omega})$ belong to polyhedral sets $\mathbf{X}$ and $\mathbf{Y}$ with integrality requirements. The first stage matrix is represented by $\mathbf{A}$ and its right hand side vector by $\mathbf{b}$. Vectors $\mathbf{c}^T$ and $\mathbf{q}_s^T(\boldsymbol{\omega})$ represent the first and second stage objective vectors respectively. the uncertain data is denoted by $\boldsymbol{\omega}$, whereas the parameter s represents the index of the number of scenarios S with corresponding probabilities π_s. The constraints are formulated by means of the *technology matrix* $\mathbf{T}(\boldsymbol{\omega})$, *recourse matrix* $\mathbf{W}(\boldsymbol{\omega})$, which is assumed to be deterministic, and the right hand side vector $\mathbf{h}(\boldsymbol{\omega})$.

Problem (5.1) seeks the first-stage decisions that minimize the first stage costs and the expected cost of the second-stage (recourse) decisions. Note that a sub set of the first stage variables and the second stage variables are restricted to be integers. Also, note that for the 2SSIP problem, the value function defined by:

$$
\begin{aligned}
Q_s(\mathbf{x},\boldsymbol{\omega}) = \quad \min_{\mathbf{y}_s(\boldsymbol{\omega})} \quad & \mathbf{q}_s^T(\boldsymbol{\omega})\mathbf{y}_s(\boldsymbol{\omega}) \\
\text{s. t.} \quad & \mathbf{W}_s(\boldsymbol{\omega})\mathbf{y}_s(\boldsymbol{\omega}) = \mathbf{h}_s(\boldsymbol{\omega}) - \mathbf{T}_s(\boldsymbol{\omega})\mathbf{x} \\
& \mathbf{y}_s(\boldsymbol{\omega}) \in \mathbf{Y}
\end{aligned}
\tag{5.2}
$$

In general, the value function (5.2) is non-convex and non-differentiable in $\mathbf{x}$ and exhibits the same properties as the value function in integer programming [156]

5.3.1.3 Solution Methods

If a finite number of discrete scenarios is considered, then simplest approach to solve (5.1) is to consider it as a large scale monolithic MILP and apply a commercial standard MIP solvers.The deterministic equivalent MILP of problem (5.1) is given by:

$$
\begin{aligned}
\min_{\mathbf{x},\mathbf{y}_s(\boldsymbol{\omega})} \quad & \left\{ \mathbf{c}^T\mathbf{x} + \sum_s \pi_s \mathbf{q}_s^T(\boldsymbol{\omega})\mathbf{y}_s(\boldsymbol{\omega}) \right\} \\
\text{s. t.} \quad & \mathbf{A}\mathbf{x} = \mathbf{b}, \\
& \mathbf{T}_s(\boldsymbol{\omega})\mathbf{x} + \mathbf{W}_s(\boldsymbol{\omega})\mathbf{y}_s(\boldsymbol{\omega}) = \mathbf{h}_s(\boldsymbol{\omega}) \quad s = 1 \dots S \\
& \mathbf{x} \in \mathbf{X},\ \mathbf{y}_s(\boldsymbol{\omega}) \in \mathbf{Y} \qquad\qquad\qquad\quad s = 1 \dots S
\end{aligned}
\tag{5.3}
$$

Another approach which rely on the case which the constraint matrix of (5.1) exhibits a characteristic block-angular structure is called *scenario (dual) decomposition approach* [157]. Again, assuming a finite discrete scenarios, the 2SSIP problem (5.1) is re-formulated as:

$$\begin{aligned}
\min_{\mathbf{x},\mathbf{y}_s(\boldsymbol{\omega})} \quad & \sum_s \pi_s \Big\{ \mathbf{c}^T\mathbf{x} + \mathbf{q}_s^T(\boldsymbol{\omega})\mathbf{y}_s(\boldsymbol{\omega}) \Big\} & \\
\text{s. t.} \quad & \mathbf{A}\mathbf{x}_s = \mathbf{b}, & s = 1\dots S \\
& \mathbf{T}_s(\boldsymbol{\omega})\mathbf{x} + \mathbf{W}_s(\boldsymbol{\omega})\mathbf{y}_s(\boldsymbol{\omega}) = \mathbf{h}_s(\boldsymbol{\omega}) & s = 1\dots S \\
& \mathbf{x}_1 = \mathbf{x}_2 \dots = \mathbf{x}_S & s = 1\dots S \\
& \mathbf{x} \in \mathbf{X},\ \mathbf{y}_s(\boldsymbol{\omega}) \in \mathbf{Y} & s = 1\dots S
\end{aligned} \tag{5.4}$$

The first stage decision $\mathbf{x}$ cannot anticipate which scenario realizes and must be feasible for each scenario. For this reason, copies of the first-stage variable have been introduced for each scenario as expressed in the last constraint of (5.4). This constraint, known as the *non-anticipativity* constraint, guarantees that the first-stage variables are identical across the different scenarios. In summary, applying scenario decomposition approach proceeds by considering the Lagrangian dual problem obtained by relaxing the non-anticipativity constraints through the introduction of Lagrange multipliers. This makes the problem separable by scenarios, for a given set of multipliers, and thus the dual function can be evaluated in a decomposed manner. Optimization of the dual function can be performed using standard non-smooth optimization techniques. Note that, due to the non-convexities, a duality gap exists. Also, the Lagrangian decomposition find a near-optimal primal feasible solution from which a feasible solution canbe recovered by using some heuristic procedures. However, in order to reestablish non-anticipativity and to prove the optimality, the branch-and-bound algorithm is required [158].

5.3.1.4 Scenario Generation and Reduction

In SO the decision process is conveniently visualized through a scenario tree. The structure of the scenario tree represents the flow of information in the problem and the timing of when new information becomes available for decision making process. A scenario tree comprises a set of nodes and branches. The nodes represent states of the problem at a particular instant, i.e., the points where decisions are made. Each node has a single predecessor and can have several successors. The first node is called the root node, and it corresponds to the beginning of the planning horizon. In the root node, first-stage decisions are made. The nodes connected to the root node are the second-stage nodes and represent the points where the second-stage decisions are made. An arc or branch emanating from a node indicates a possible realization of the uncertain variables from that node, i.e. a scenario. Each arc has a probability of occurrence. The probability of a scenario is therefore determined by the product of all arcs probability in that scenario. For the two stage SO problem, like the one at hand, the second stage nodes are equal to the scenarios and are referred to as leaves [159]. In this study, a single scenario consists of 24 hours data triplets with random variables representing uncertainty in electricity demand, irradiance and wind speed for a given each hour of a typical day. Generation of input scenarios for the 2SSIP model is summarised in the following steps:

(i) Processing of the input data

Depending of the geographical location of the site under study, and in order to retain seasonal variations, the typical planning year is divided into four or two seasons. The site considered in this thesis is located in tropical region which has mainly two seasons: rainy and dry season. Each season is represented by one typical day with 24-h segments each representing a particular hourly

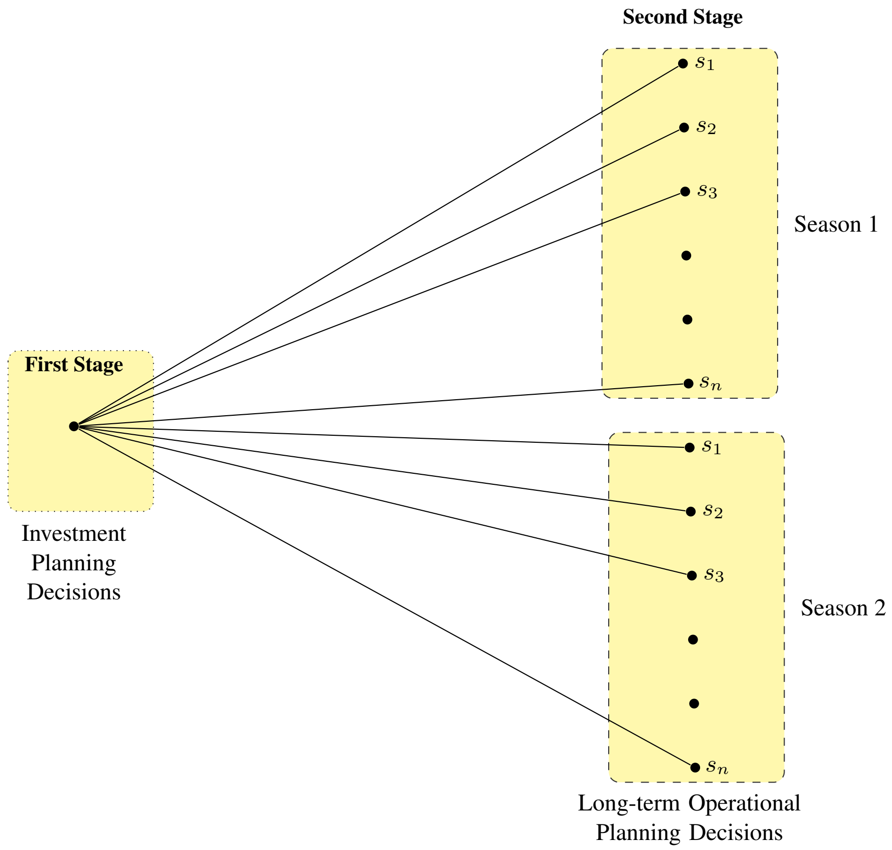

Figure 5.1: *Scenario trees depicting decision making process in 2SSIP*

interval for that season. Hourly input data profiles for the days in the historical data are grouped according to their respective seasons. Using these data the mean and standard deviation for each hour are calculated. For each hour of each typical day, electricity demand is assumed to follow Normal PDF, solar irradiance Beta PDF, and wind speed Weibull PDF. Hourly Normal PDFs for electricity demand are determined by:

$$f_n(D_h) = \frac{1}{\sqrt{2\pi(\sigma_h^D)^2}} \left(-\frac{(D_h - \mu_h^D)^2}{2\pi(\sigma_h^D)^2} \right) \tag{5.5}$$

where σ_h^D and μ_h^D are the mean and standard deviation of electricity demand in hour h.

This thesis models uncertainty in irradiance data following the approach presented in [160], [161]. For each hour of the typical day, irradiance data have shown to follow bimodal distribution function. The irradiance data are divided into two groups, each group having a unimodal distribution function. To describe the random phenomenon of the irradiance data, a Beta PDF is utilized for each unimodal as follows.

$$f_b(G_h) = \begin{cases} \frac{\Gamma(\alpha_h+\beta_h)}{\Gamma(\alpha_h)\Gamma(\beta_h)} G_h^{(\alpha_h-1)}(1-G_h)^{(\beta_h-1)} & \text{for } 0 \leq G_h \leq 1, \alpha_h, \beta_h \geq 0 \\ 0 & \text{otherwise} \end{cases} \tag{5.6}$$

where G_h is the solar irradiance in hour h, $f_b(G_h)$ is the Beta PDF of G_h, and α_h and β_h are parameters of the Beta PDF in hour h. The parameters of the Beta PDFs for each hour are calculated from the hourly mean and standard deviation of the irradiance as follows:

$$\alpha_h = \frac{\mu_h^G \sigma_h^G}{1-\mu_h^G} \qquad \forall h \tag{5.7a}$$

$$\beta_h = (1-\mu_h^G)\frac{\mu_h^G(1+\mu_h^G)}{(\sigma_h^G)^2} - 1 \qquad \forall h \tag{5.7b}$$

A common way to characterize the statistics of wind speeds is by using the Weibull PDF (5.8) [162]:

$$f_w(V) = \frac{k}{c}\left(\frac{V}{c}\right)^{k-1} \exp\left[-\left(\frac{V}{c}\right)^k\right] \tag{5.8}$$

where k is called the shape index, and c is called the scale index. When the shape index equals 2, the PDF is called a Rayleigh PDF as given in (5.9).

$$f_w(V) = \left(\frac{2V}{c^2}\right) \exp\left[-\left(\frac{V}{c}\right)^2\right] \tag{5.9}$$

This is the most common PDF which has been used to model most wind speed profiles particularly when little detail is known about the wind regime at a site. The relationship between scaling factor c and average wind speed $\bar{V}$ can be approximated by:

$$\bar{V} = \frac{\sqrt{\pi}}{2}c \cong 0.886c \tag{5.10}$$

(ii) Scenario generation

From the hourly PDFs, scenarios of for electricity demand, irradiance, and wind speed are generated by using Latin Hypercube Sampling (LHS) [163]. LHS is a stratified random procedure, which provides an efficient way of sampling variables from their distributions. Work in [164] has shown that LHS method can offer great benefits in terms of increased sampling efficiency and faster run time compared to the traditional Monte Carlo sampling method. For each hour in the typical day, 4000 scenarios of the profiles of input data are generated as follows:

- 4000 values are sampled according to the PDF of each random variables, i.e. electricity demand, irradiance, and wind speed, at that hour. This is achieved by diving the cumulative distribution for each variable into 4000 intervals with equal probability 1/4000. In order to obtain specific values for each parameter, 4000 random number are randomly selected from the standard uniformly distribution.
- Each of these random number r_i is scaled in order to obtain cumulative probability P_i, such that each P_i lies within the i^{th} interval, i.e,

$$P_i = \frac{1}{4000}r_i + \frac{(i-1)}{4000} \tag{5.11}$$

where r_i is uniformly distributed random number ranging from 0 to 1;

- Map the cumulative probability values into a value of random variables using the inverse of cumulative distribution function.

$$x_i = F_n^{-1}(P_i) \tag{5.12}$$

- The 4000 values obtained for each uncertain variable x, i.e. electricity demand, solar irradiance, and wind speed, are paired randomly (equally likely combinations) with the values of the other variables.

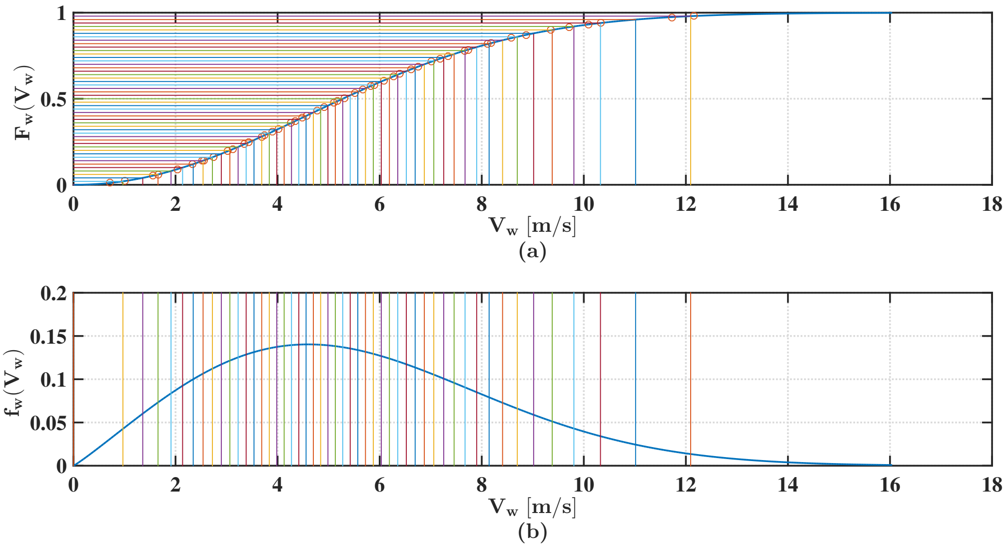

Figure 5.2: *Illustration of LHS for wind speed data for hour 20 (a) CDF generated using mean and standard deviation of wind speed data for hour 20 (b) PDF generated using mean and standard deviation of wind speed*

Advantages of LHS method are:

- LHS yields a stratified sample with smaller variance than that from Monte Carlo sampling [165].
- LHS constraints the sampling within regions such that for each sample a value is generated at the tail of the distribution.
- The stratification in LHS ensures that the sample points are always well spread out over the unit cube [166].
- Increased sampling efficiency, and
- Faster run time

Some disadvantages of LHS method include: difficulty to increase the size of an already generated sample while simultaneously preserving the stratification properties, and dimensionality problem [167] . For simplicity it is assumed that random variables are independent and not correlated. However LHS algorithm can be modified to consider correlation of random variables [168], [169].

(iii) Scenario reduction

The computational time required to solve the SO problem depends mainly on the number of scenarios used to model uncertainty. The higher the number of scenarios, the higher the computation time and the possibility to encounter out of memory error due to the growing size of the problem. This is even more of concern for the problem with integer variables like the planning problem addressed in this thesis. Therefore, it is necessary to determine a finite and manageable number of representative scenarios that can closely approximate the original scenarios. This research did not engage in detailed development of scenario reduction algorithm but only select and apply a suitable scenario reduction tools. For this purpose, a scenario reduction tool Scenred2 in GAMS is applied.

Scenred2 implements the classical scenario reduction approach for two-stage SO models. The most popular and accurate reduction algorithms of fast forward and backward type are maintained in Scenred2 [170]. The tool offers options which make it possible to to control scenario reduction process by different type of probability distances such as Transport, Fortet-Mourier, and Wasserstein. Altogether the three distances can be selected with an assigned order. The fast forward reduction algorithm based on Kantorovich distance is recommended for strong reduction in which the number of preserved scenarios is small [171]. Kantorovich distance metric is selected because is one of the most common probability distance used in stochastic optimization [172]. Figure 5.3 illustrate data of the output from the SCENRED2 for the sample of four scenarios obtained after scenario reduction.

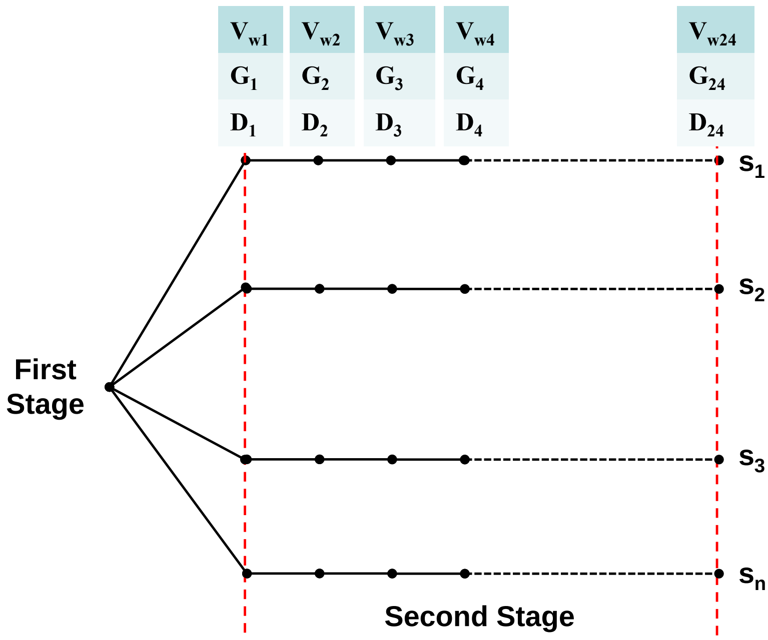

Figure 5.3: *Reduced scenario tree 4 scenarios from Scenred2, each scenario contains 24 triplets with random data for electricity demand, solar irradiance, and wind speed*

Figure 5.3 saves for visualization purpose only. Data from the reduced tree which are obtained as output of Scenred2 include: the set of ancestor relations of the reduced tree, the parameter containing the node probabilities for the reduced tree, and the parameters containing random values of the nodes.

5.3.2 Robust Optimization

Another approach to include uncertainties in microgrid planning is by adopting RO framework. Contrary to the SO framework, which require *a priori* knowledge of the PDFs of the input parameters in order to obtain solutions with the minimum expected cost (or risk), RO needs minimum information on the uncertain parameters. Absence of enough information about input data is very common in planning and designing a new microgrid, particulary for rural ares, in which the input data are not known or are partially known at the time when the planning problem needs to be solved. It is therefore difficult to employ PDFs to model uncertainties in the input data. In this case, RO, which is a distribution-free approach, has proved to be very promising optimization techniques and has attracted many researchers [173], [174]. The main idea in RO approach is to protect the solution against all possible realizations belonging to a so-called *uncertainty set* [175]. Uncertainty set contains the descriptions of all possible values which the uncertain parameter may realize. The size of the uncertainty set is determined by the level of desired robustness. Clearly, the choice of an uncertainty set is crucial from the point of view of both the uncertainty modeling and the tractability of the resulting formulation. Thus, one must avoid begin too conservative while guaranteeing sufficient robustness by making a trade-off between robustness against each realization of uncertain parameter and the size of the uncertainty set.

RO dates back to the work of Soyster [176] which formulated a convex mathematical programming problem in which the use of convex inequalities to define the feasible region was replaced by a convex resource set. Theories on RO have been developed starting from the 90s, in particular due to the work of Ben-Tal and Nemirovski reported in [177], [178]. In [177], a comparison between optimal solution of original deterministic problem and the solution of RO problem for 90 LP problems selected from the NETLIB collection is presented. In most cases optimal solutions of these LPs were found to be completely infeasible if the nominal data were slightly perturbed, whereas the robust solutions were immune against those perturbations. Furthermore, it was demonstrated that the robust solutions do not necessarily lose a lot in optimality and more importantly, in many cases, these robust solutions cannot be obtained by a moderately small correction of the optimal solution. This places the RO as a distinguished research field which must be understood to be completely different from the post-optimization sensitivity analysis. Work in [178] laid the foundation of robust convex optimization and showed that for ellipsoidal uncertainty set, most generic convex optimization problems have a corresponding robust counterpart which can be solved in polynomial time by interior point methods.

An approach in RO that has gained considerable attention in recent years is the so-called Γ-robustness, originated from the work of Bertsimas and Sim [179]. This approach characterizes the uncertainty set via a parameter Γ, the so-called *budget of uncertainty*, which bounds the number of deviations of the parameters from their nominal values. This approach offers full control on the degree of conservatism for every constraint. Another attractive feature of Γ-robustness is that the robust counterpart of a problem maintains the same computational class of the deterministic formulation. Contrary to the notions of robustness of Ben-Tal and Nemirovski, which yield problems that are often too hard to solve as compared to their original deterministic problems, Γ-robustness offers a possibility to have a robust counterpart which maintains their classification of the original problem. For example, in [179], the robust counterpart of a LP problem is shown to be still LP problem. Furthermore, if the uncertainty set is constructed in a specific way, one can derive probabilistic guarantees on the feasibility of the obtained solution, similar to the approach adopted in chance-constrained optimization.

Regarding the applications of RO in power system planning under uncertainty, a detailed report is presented in [180]. The report shows that RO, particularly the two-stage RO techniques which has been applied to solve unit commitment problems, has gained a great deal of attention in the electrical power system sector. Solutions obtained by the RO models are guaranteed to be feasible and optimal even for the worst-case realization of uncertain parameters in the uncertainty sets. The conservative nature of RO, which may not be preferred in other applications, is in accordance with the power system industry in regards to maintaining high level of reliability. RO models for planning power system capacity expansion under uncertain electricity demand and for planning of corrective transmission switching schemes under uncertain operating states are presented in [181] and [182] respectively. In the area of electricity markets, a robust MILP model for building hourly offering curves for a price-taker producer participating in a pool is proposed in [183]. Instead of using price predictions as input data, price confidence intervals are considered to derive optimal offering curves.

Various formulations of the UC problem which have been solved by using RO method are presented in [184]–[187]. A common feature shared by all these studies is that their solution method is mostly based on decomposition techniques such as BD. In particular, [184] presents a two-stage adaptive RO model for Security Constrained Unit Commitment (SCUC) problem in the presence of nodal net injection uncertainty. That paper applies BD and outer approximations to solve the SCUC problem for the case of large power system operated by the ISO New England. Another work, which applies Column-and-Constraint Generation (CCG) method to solve a two stage RO model for optimal placement of dispatchable and intermittent distributed generators in a microgrid considering uncertainties in their generations and in load consumptions, is presented in [188]. The model, which is formulated as a min-max-min problem, is decomposed into a master problem and bi-level subproblem which is reformulated to a MILP problem prior to the application of the CCG method. Since the master problem yields a lower bound and the subproblem yields the upper bound, the proposed algorithm requires a specified optimality gap to be terminated. Similar work, which applies an exact BD approach for robust transmission network expansion planning with uncertain renewable generation and loads, is presented in [189]. That paper adopt a specialized implementation of two-stage RO with right-hand side uncertainty.

A key and recent paper in which RO is applied to model uncertainties in electricity demand, renewable resources, and market prices in microgrid planning is presented in [147]. The authors apply a BD algorithm, which consists of an investment master problem, solved annually, and operational subproblems, which are solved hourly and are used to generate optimality cuts. In [190], RO is applied to determine the optimal mix of power generation and storage components in an autonomous system for supplying power to a remote telecommunication station. The work in [190] does not consider DGs and assumes the component capacities to be continuous variables, and both [190] and [147] neglect all combinatorial aspects of the operational problem. It is important to note that maintaining integrality of operational decision variables does not allow the use of decomposition methods and thus forces one to adopt a single stage min-max RO formulation. Another work which applies RO to obtain robust daily and weekly scheduling of virtual power plant under uncertain electricity price is presented in [191]. That paper adopts MILP formulation which maintains discrete operational decision variables but consider uncertainty in electricity market price which appears in the objective function only.

5.3.2.1 Robustness Concepts

Before presenting the general mathematical formulation of RO problem it is important to give an overview of the main robustness concepts which govern these formulations. The most important robustness concepts are:

- **Strict Robustness**: Requires that a solution RO problem is is feasible for all realizations of uncertain parameters or scenarios in the uncertainty set [175], [176]. This concept adopts very pessimistic view of minimizing the worst-case over all scenarios. It is sometimes also known as classic robust optimization, single-stage robustness, min-max optimization, absolute deviation, or simply robust optimization, and can be seen as the pivotal starting point in the field of robustness.

- **Γ-Robustness**: Requires a solution of RO problem to hedge only against scenarios in which at most Γ uncertain parameters per constraint change to their worst-case values. The aim is to overcome high degree of conservatism of the strict robustness by setting a budget of uncertainty. This concept was introduced by Bertsimas and Sim in [192] for LP problems. Due to this reason, it is sometimes also known as the approach of "Bertsimas and Sim", or "Γ-robustness". Bertsimas and Sim show that "Γ-robustness" provides probabilistic bounds on constraints violations.
- **Adjustable Robustness**: This concept is similar to the two-stage stochastic optimization approach in which the decision variables are decomposed into two stages [193]. The first stage variables for the here-and-now decisions have to be found by the RO algorithm in advance, while the second stage decisions or wait-and-see variables can wait until the worst realization of uncertainty set becomes known.
- **Light Robustness**: This concept requires that a solution of RO problem must not be too bad in the nominal case with a certain nominal fixed standard. The aim is to determine, among all solutions satisfying this standard, the most "reliable" solution with respect to constraint violation [194].
- **Recovery Robustness**: This is similar to the two-stage adjustable robustness with additional requirement that for any possible scenario in the uncertainty set and a given solution, there exists an algorithm which can construct another feasible solution for that particular scenario [195].
- **Regret Robustness**: This robustness concept usually considers uncertainty in the objective function only [196], [197]. Instead of minimizing the worst-case performance of a solution, it minimizes the difference to the objective function of the best solution that would have been possible in a scenario.
- **Soft Robustness**: The basic idea of soft robustness as introduced in [198] is to handle the conservatism of the strict robust approach by considering a nested family of uncertainty sets, and allowing more deviation in the constraints for larger uncertainties.
- **Comprehensive Robustness**: This is similar to the adjustable robustness but it removes the assumption that only scenarios defined in the uncertainty set need to be considered. However, this concept introduces additional measure of a controlled deterioration in performance when the data is outside the uncertainty set [199].

This thesis adopt **Γ-Robustness** approach for optimizing the plan of a new microgrid. To avoid over-conservatism in planning, the underlying assumption is that it is unlikely for all 24 hours data in the profiles of electricity demand and generations from each type of PV panels and WTs for the typical representatives days to change simultaneously to their worst-case values.

5.3.2.2 Uncertainty Sets

The formulation of a robust counterpart optimization model is connected with the selection of the uncertainty set $\mathcal{U}$. To define the uncertainty set, consider the uncertain parameters a_i with $i = 1, \ldots, h$, where h is the index of hours. Their probability distribution is unknown, but each parameter is assumed to belong to the support interval $[\tilde{a}_i - \widehat{a}_i,\ \tilde{a}_i + \widehat{a}_i]$, where $\tilde{a}_i$ is the nominal value, and $\widehat{a}_i$ the maximum deviation. Also consider a variable, $\zeta_i \in [-1, 1]$, which defines the scaled deviation of each parameter in period i, then the three common types of uncertainty sets used to model uncertainty in RO are defined as:

(1) Box uncertainty set

$$\boldsymbol{\mathcal{U}}_{\infty} = \{\mathbf{a}\ : a_i\ =\ \tilde{a}_i\ +\ \hat{a}_i\,\zeta_i \quad \forall i, \quad \|\boldsymbol{\zeta}\|_{\infty} \leq \Psi\} \tag{5.13}$$

(2) Ellipsoidal Uncertainty Set

$$\boldsymbol{\mathcal{U}}_{2} = \{\mathbf{a}\ : a_i\ =\ \tilde{a}_i\ +\ \hat{a}_i\,\zeta_i \quad \forall i, \quad \|\boldsymbol{\zeta}\|_{\infty} \leq 1, \quad \|\boldsymbol{\zeta}\|_{2} \leq \Omega\} \tag{5.14}$$

(3) Polyhedral Uncertainty Set

$$\boldsymbol{\mathcal{U}}_{1} = \{\mathbf{a}\ : a_i\ =\ \tilde{a}_i\ +\ \hat{a}_i\,\zeta_i \quad \forall i, \quad \|\boldsymbol{\zeta}\|_{\infty} \leq 1, \quad \|\boldsymbol{\zeta}\|_{1} \leq \Gamma\} \tag{5.15}$$

where Ψ, Ω, and Γ are adjustable parameters controlling the size of the uncertainty sets. Note that the above classification is not exclusive, i.e., it is possible to formulate uncertainty sets which belong to multiple types at the same time.

The question of choosing uncertainty sets that yield a good trade-off between performance and conservatism is central to RO. In this thesis, the polyhedral uncertainty set is selected to model uncertainties in electricity demand, and generation from RESs. This offers a simple way to set different uncertainty budgets for electricity demand, PV generations, and WTs generations, in order to avoid overprotecting the planning results. Polyhedral uncertainty set is selected because is one of the most common type of uncertainty sets, with additional advantage that it retains the classifications of the original MILP problem. The next section presents two generic formulations of RO problems.

5.3.2.3 General formulation of RO model

The general MILP model for microgrid planning problem considered in this thesis can be writtern as:

$$\begin{aligned}
\min_{\mathbf{x},\mathbf{y}} \max_{\boldsymbol{u}} \quad & \left\{\boldsymbol{c}'(\boldsymbol{u})\boldsymbol{x}\ +\ \boldsymbol{d}'(\boldsymbol{u})\boldsymbol{y}\right\} \\
\text{s.t.} \quad & \boldsymbol{A}(\boldsymbol{u})\boldsymbol{x}\ +\ \boldsymbol{O}(\boldsymbol{u})\boldsymbol{y} \leq \boldsymbol{b}(\boldsymbol{u}) \\
& \boldsymbol{x},\ \boldsymbol{y} \geq 0 \\
& \boldsymbol{x},\ \boldsymbol{y} \in \ \mathbb{Z} \text{ or } \mathbb{R}
\end{aligned} \tag{5.16}$$

where vector $\boldsymbol{x}$ consists of discrete variables indicating the selection of optimal planning alternative for each type of component in the search space, and vector $\boldsymbol{y}$ operational variables which include continuous, binary, and integer variables. Vector $\boldsymbol{c}(\boldsymbol{u})$ and $\boldsymbol{d}(\boldsymbol{u})$, and matrices $\boldsymbol{A}(\boldsymbol{u})$ and $\boldsymbol{O}(\boldsymbol{u})$ represent value of the model input parameters which are subject to uncertainty. In order to move all uncertain parameters to the LHS of constraints, problem (5.16) can be recast as:

$$
\begin{aligned}
\min_{\mathbf{x},\mathbf{y},z} \quad & z \\
\text{s.t.} \ \max_{\boldsymbol{u}} \quad & \left\{ \boldsymbol{c}'(\boldsymbol{u})\boldsymbol{x} \ + \ \boldsymbol{d}'(\boldsymbol{u})\boldsymbol{y} \leq z \right\} \\
\max_{\boldsymbol{u}} \quad & \left\{ \boldsymbol{A}(\boldsymbol{u})\boldsymbol{x} \ + \ \boldsymbol{O}(\boldsymbol{u})\boldsymbol{y} - \boldsymbol{b}(\boldsymbol{u}) \ \leq \ \boldsymbol{0} \right\} \\
& \boldsymbol{x}, \ \boldsymbol{y} \geq 0 \\
& \boldsymbol{x}, \ \boldsymbol{y} \in \ \mathbb{Z} \text{ or } \mathbb{R}
\end{aligned}
\tag{5.17}
$$

Note that uncertainty in the RO problem data can be modelled constraint-wise (For the general proof, see [175, p. 11]). Assuming that uncertainty are in the coefficients matrix $\boldsymbol{A}$ only, without loss of generality, one can focus on i^{th} constraint from problem (5.17) and derive its Robust Counterpart (RC). The formulation of RC is explained in the following subsection. Note that the RC of the RO problem depends on the selected uncertainty set $\boldsymbol{\mathcal{U}}$. Also, note that the variable x_j can be either a continuous or an integer variable. In the following section, reformulation of RC is derived for the case of a simple LP problem and extended to the problem with discrete variable.

5.3.2.4 Robust Counterpart and Solution Methods

The two most frequently described methods in the literature for solving RO problems are the reformulation approach and the so-called cutting plane approach. The first approach involves a reformulation of RO problem into a tractable RC of the same class of the original deterministic problem. The adversarial approach involves solving the RO problem with a subset of the uncertainty set using an iterative cutting plane method [200]. Reformulation of a tractable RC require rigorous application of duality theorem in order to convert inner maximization problem to the equivalent minimization problem. A computational study by Fischetti and Monaci [201] compares the two methods for robust LP problems and robust MILP problems with a polyhedral uncertainty set. The study suggests that the cutting-plane approach is superior for robust LP problems and that reformulation approach is superior for robust MILP problems. However, another recent work found that, for robust MILP problems with polyhedral uncertainty sets, there was no clear winner between the two approaches [202].

In this work, a reformulation approach is adopted. To illustrate the formulation into RC, consider the following nominal MILP on a set of n variables $\boldsymbol{x}$, the first k of which are integral:

$$
\begin{aligned}
\min_{\mathbf{x},\mathbf{y}} \max_{\boldsymbol{u}} \quad & \boldsymbol{c}'\boldsymbol{x} \\
\text{s.t.} \quad & \boldsymbol{A}(\boldsymbol{u})\boldsymbol{x} \leq \boldsymbol{b} \\
& \boldsymbol{lb} \leq \boldsymbol{x} \leq \boldsymbol{ub} \\
& x_i \in \ \mathbb{Z} \text{ for } i \ = 1, \ldots, \ k,
\end{aligned}
\tag{5.18}
$$

where $\boldsymbol{c}$, $\boldsymbol{lb}$, and, $\boldsymbol{ub}$, are n vectors, $\boldsymbol{A}$ is an $m \times n$ matrix, and $\boldsymbol{b}$, is an m vector. Without loss of generality, data uncertainty is assumed to affects only the elements of matrix $\boldsymbol{A}$, but not vector $\boldsymbol{c}$ and $\boldsymbol{b}$. Three main steps to derive the RC of RO problem in (5.18) with the polyhedral uncertainty set are as follow.

(1) *Worst case reformulation*

Adopting the polyhedral uncertainty set $\boldsymbol{\mathcal{U}}_1$, a single constraint taken out of the RO problem (5.18) is rewritten as:

$$\max_{\boldsymbol{A}\in\boldsymbol{\mathcal{U}}_1} \sum_j a_{ij}x_j \;\leq\; b_i \tag{5.19}$$

A small problem associated with the i^{th} constraints is:

$$\begin{aligned}
\max_{\boldsymbol{A}\in\boldsymbol{\mathcal{U}}_1} \quad & \sum_j (\tilde{a}_{ij} \;+\; \hat{a}_{ij}\;\zeta_{ij})x_j \\
\text{s.t.} \quad & \sum_{j\in J} |\zeta_{ij}| \;\leq\; \Gamma, \\
& 0 \;\leq\; |\zeta_{ij}| \;\leq\; 1, \qquad \forall i, j \in J
\end{aligned} \tag{5.20}$$

(2) *Formulating the dual of the inner maximization problem*
This involves the reformulation of the maximization problem (5.20) as a minimization problem using strong duality. Since the feasible set is non-empty and bounded, applying the strong duality principle on (5.20) gives its dual form (5.21)

$$\begin{aligned}
\min \quad & \Big\{ q_i\Gamma \;+\; \sum_{j:i,j\in J} r_{ij} \Big\} \\
\text{s.t.} \quad & q_i \;+\; r_{ij} \geq \hat{a}_{ij}|x_j| && \forall j : i,\; j \in J \\
& q_i \geq 0 && \forall j : i,\; j \in J \\
& r_{ij} \geq 0 && \forall j : i,\; j \in J
\end{aligned} \tag{5.21}$$

(3) *Writing the Robust Counterpart*
The final RC can be obtained by substituting (5.21) into the original problem (5.18), and omitting the minimization term:

$$\begin{aligned}
\min \quad & \boldsymbol{c}'\,\boldsymbol{x} \\
\text{s.t.} \quad & \sum_j \tilde{a}_{ij}x_j \;+\; q_i\Gamma \;+\; \sum_{j:i,j\in J} r_{ij} \;\leq b_i && \forall i \\
& q_i \;+\; r_{ij} \geq \hat{a}_{ij}y_j && \forall i,\; j \in J_i \\
& -y_j \leq x_j \leq y_j && \forall j \\
& lb_j \leq x_j \leq ub_j && \forall j \\
& q_i \geq 0 && \forall i \\
& r_{ij} \geq 0 && \forall i,\; j \in J_i \\
& y_j \geq 0 && \forall j
\end{aligned} \tag{5.22}$$

The above reformulation (5.22) is derived assuming LP problem with uncertainty in matrix $\boldsymbol{A}$. Uncertainties in the objective function coefficient vector $\boldsymbol{c}$ or in the right hand side vector $\boldsymbol{b}$ can be treated in the same way (see for example [203]).

5.4 Two-Stage Stochastic Integer Programming Model for Microgrid Planning

5.4.1 Objective function

In the stochastic model, the objective function minimizes the total annualized life cycle investment cost and the expected operation cost computed over a number of suitable selected scenarios. To account for uncertainties and still maintaining seasonal variations, each season is represented by one typical day. Instead of using typical days with one deterministic profile for solar irradiance, wind speed, and electricity demand, a set of scenarios of input data profiles for each typical representative day are considered. The objective function is given by:

$$\min_{\mathbf{x},\mathbf{y}_s} \quad \left\{ TAIC(\mathbf{x}) + \sum_s \pi_{d,s} AEOC(\mathbf{x}, \mathbf{y}_s) \right\} \tag{5.23}$$

where $TAIC$ is the total annualized investment cost, which is independent of the realization of stochastic scenarios, and $AEOC$ is the expected annualized operational cost calculated after the realization of s discrete scenarios with probabilities $\pi_{d,s}$. Vector $\mathbf{x}$ consists of binary variables indicating the selection of optimal planning alternative for each type of component in the search space. Vector $\mathbf{y}$ consists of the second stage decision variables: integer variables for number of committed, start-up, and shutdown DGs, binary variables to indicate operational modes of BCs, binary variable to control charging and discharging of SBB, positive continuous variables representing output power from each technology, charging power, discharging power, and SOC of the SBB.

The total annualised fixed investment cost is given by:

$$\begin{aligned} FAIC(\mathrm{x}) = & \sum_p \sum_{n_p} x_{p,n_p} N^{par}_{p,n_p} N^{ser}_p AC_p \; + \sum_w \sum_{n_w} x_{w,n_w} N_{w,n_w} AC_w \; + \\ & \sum_b \sum_{n_b} x_{b,n_b} N^{par}_{b,n_b} N^{ser}_b AC_b \; + \sum_c \sum_{n_c} x_{c,n_c} N_{c,n_c} AC_c \; + \\ & \sum_g \sum_{n_g} x_{g,n_g} N_{g,n_g} AC_g \end{aligned} \tag{5.24}$$

where the terms represent annualized investment costs for PV arrays, WT, SBB, BC, and DG respectively. The binary variable x_{p,n_p} indicates the selection of n^{th}_p solution from search space of PV of type p, Similarly, x_{w,n_w} is the binary variable indicating selection of n^{th}_w solution from search space of WT of type w, x_{b,n_b} is the binary variable indicating selection of n^{th}_b solution from search space of SB of type b, x_{c,n_c} is the binary variable indicating selection of n^{th}_c solution from search space of BC of type c, and x_{g,n_g} is the binary variable indicating selection of n^{th}_g solution from search space of DG of type g. Parameter N^{par}_{p,n_p} presents the number of parallel connected PV panels of type p specified in the n^{th}_p solution of the search space, whereas parameter N^{ser}_p is the number of series strings of PV panels of type p. N_{w,n_w} is the number of WT of type w specified in the n^{th}_w solution of the search space. N^{par}_{b,n_b} is the number of parallel connected SB of type b specified in the n^{th}_b solution of the search space, whereas N^{ser}_b is the number of series strings of SB panels of type b. N_{c,n_c} is the number of BC of type c specified in the n^{th}_c solution of the search space, and N_{g,n_g} is the number of DG of type g specified in the n^{th}_g solution of the search space. AC_p is the annualized installation cost of PV panel of type p, AC_w is the annualized installation cost of WT of type w, AC_b is the annualized installation cost of SB of type b, AC_c is the annualized installation cost of BC of type c, AC_g is the annualized installation cost of DG of type g,

The total annualised expected operational cost for each scenario is given by:

$$\begin{aligned} AEOC(\mathbf{x},\mathbf{y},s) = & \sum_d \sum_h \sum_g f_d U_{d,h,g,s} RC_g / Y_g \ + \ \sum_d \sum_h \sum_b f_d C_{bw,b} P^{dch}_{d,h,b,s} + \\ & \sum_d \sum_h \sum_g f_d U_{d,h,g,s} OMC_g + \\ & \sum_d \sum_h \sum_g f_d C_{fuel} FC_{d,h,g,s} + \\ & \sum_d \sum_h \sum_g f_d \left(V_{d,h,g,s} SUC_g + Z_{d,h,g,s} SDC_g \right) \end{aligned} \tag{5.25}$$

where the the first two terms express replacement costs for DGs and SBBs respectively, the third term represents O&M costs for DG, the fourth term represents fuel cost for DG, and the fifth term expresses start-up and shut down costs for DG. Parameter f_d represents the weight of the typical day d, RC_g, replacement cost for DG of type g [€/h], Y_g, lifetime of DG of type g [h], $C_{bw,b}$, operational wear cost for SBB of type b [€/kWh], OMC_g, operational and maintenance cost for DG of type g [€/h], $FC_{d,h,g}$ is the fuel consumption for DGs of type g in hour h of day d, [ł], and C_{fuel} the fuel cost [€/l]. The slope and y-intercept for each PWLA of input-output characteristics of DGs are given by parameters $B_{q,g}$ and $A_{q,g}$ respectively. Start-up and shut-down costs for DG of type g are represented by SUC_g and SDC_g respectively. Variable $U_{d,h,g,s}$ represents the number of online DG of type g in hour h and scenario s of typical day d. Variables $P^{dch}_{d,h,b,s}$ and $P_{d,h,g,s}$ represent total discharging power from the SBB of type b and the total power from DGs of type g in hour h and scenario s of typical day s, respectively. The number of started-up and shut-down DGs of type g at the beginning of hour h and scenario s of typical day d are represented by integer variables $V_{d,h,g,s}$ and $Z_{d,h,g,s}$ respectively.

5.4.2 Constraints

The objective function 5.23 is minimized subject to the following constraints:

- The discrete search space is made, for each type of component, by n_ℓ different alternative. The binary variable x_{ℓ,n_ℓ} defines if the n_ℓ^{th} alternative is selected or not. Only one alternative can be chosen, so:

$$\sum_{n_\ell} x_{\ell,n_\ell} \leq 1 \qquad \forall \ell \in \{g,p,w,b,c\} \tag{5.26}$$

- For each scenarios, the power balance constraint at the AC bus bar of Fig. **??** in Chapter 4, is expressed by:

$$P^{dg,tot}_{d,h,s} + \left(P^{dch}_{d,h,s} + P^{ren,L}_{d,h,s} \right) \eta_{inv} - P^{dg,ch}_{d,h,s} - P^{dg,exc}_{d,h,s} = D_{d,h,s} \quad \forall d,h,s \tag{5.27}$$

where $P^{dg,tot}_{d,h,s}$ is the total power from online DGs in hour h and scenario s of typical day d, $P^{dch}_{d,h,s}$ the total discharging from SBBs in hour h and scenario s of typical day d, $P^{ren,L}_{d,h,s}$ the total power from RESs which is supplied directly to the load in hour h and scenario s of typical day d, η_{inv}

the BC inversion efficiency, $P_{d,h,s}^{dg,ch}$ the total charging power from DGs in hour h and scenario s of typical day d, $P_{d,h,s}^{dg,exc}$ the total excess power from DGs in hour h and scenario s of typical day d, and $D_{d,h,s}$ the total electricity demand in hour h and scenario s of typical day d. Constraint (5.27) implies that that the demand can be supplied by any combination of DGs, SBBs, PV array, and WTs.

- The part of the total generation from RESs which is supplied directly to the load is equal to the difference between the total RESs generation and the sum of charging and spilled power from RESs, (5.28).

$$P_{d,h,s}^{ren,L} = P_{d,h,s}^{ren,tot} - P_{d,h,s}^{ren,ch} - P_{d,h,s}^{ren,spl} \quad \forall d,h,s \tag{5.28}$$

where $P_{d,h,s}^{ren,tot}$ is the total generation from RESs in hour h and scenario s of typical day d, $P_{d,h,s}^{ren,ch}$ the total charging power from RESs in hour h and scenario s of typical day d, and $P_{d,h,s}^{ren,spl}$ the total RESs power which is spilled in hour h and scenario s of typical day d.

- The total RESs generation is given by sum of generation from PV array and WTs (5.29a).

$$P_{d,h,s}^{ren,tot} = P_{d,h,s}^{pv,tot} + P_{d,h,s}^{wt,tot} \quad \forall d,h,s \tag{5.29a}$$

$$P_{d,h,s}^{pv,tot} = \sum_{p}\sum_{n_p} x_{p,n_p} N_{p,n_p}^{par} N_p^{ser} \overline{P_{d,h,s,p}} \quad \forall d,h,s \tag{5.29b}$$

$$P_{d,h,s}^{wt,tot} = \sum_{w}\sum_{n_w} x_{w,n_w} N_{w,n_w} \overline{P_{d,h,s,w}} \quad \forall d,h,s \tag{5.29c}$$

where $P_{d,h,s}^{pv,tot}$ is the total generation from PV arrays in hour h of scenario s of typical day d, $P_{d,h,s}^{wt,tot}$ is the total generation from WTs in hour h of scenario s of typical day d, $\overline{P}_{d,h,s,p}$ is the MPP generation from a single PV panel of type p in hour h and scenario s of typical day d, and $\overline{P}_{d,h,s,w}$ is the MPP generation from a single WT of type w in hour h and scenario s of typical day d.

- The total power from the DGs is the sum of generation from all types of DGs which are online at a particular period (5.30a). Similarly, the total discharging power is the sum of discharging power from all types of SBBs installed (5.30b).

$$P_{d,h,s}^{dg,tot} = \sum_{g} P_{d,h,g,s} \quad \forall d,h,s \tag{5.30a}$$

$$P_{d,h,s}^{dch} = \sum_{b} P_{d,h,b,s}^{dch} \quad \forall d,h,s \tag{5.30b}$$

where $P_{d,h,g,s}$ is the generation from the group of DGs of type g in in hour h and scenario s of typical day d, and $P_{d,h,b,s}^{dch}$ is the discharging power from SBB of type b in hour h and scenario s of typical day d.

- Total charging power to the SBBs is the sum of charging power from RESs and DGs.

$$\sum_{b} P_{d,h,b,s}^{ch} = P_{d,h,s}^{ren,ch} + P_{d,h,s}^{dg,ch} \eta_{rec} \quad \forall d,h,s \tag{5.31}$$

where $P_{d,h,b,s}^{ch}$ is the charging power to the SBB of type b in hour h and scenario s of typical day d, $P_{d,h,s}^{ren,ch}$ and $P_{d,h,s}^{dg,ch}$ are the total charging power from RESs and DGs in hour h and scenario s

of typical day d respectively, and η_{rec} is the rectification efficiency.

- Total amount of power which can flow from the DC bus to the AC bus during the inversion mode is limited by the total inversion capacity of the installed BCs (5.32a). Similarly, the amount of charging power from DGs flowing from the AC to the DC bus bar during the rectification mode is limited by the total rectification capacity of installed BCs (5.32b).

$$\left(P^{dch}_{d,h,s} + P^{ren,L}_{d,h,s}\right) \leq \sum_{c}\sum_{n_c} x_{c,n_c} N_{c,n_c} \overline{P^{inv}_{c}} \qquad \forall d,h,s \tag{5.32a}$$

$$P^{dg,ch}_{d,h,s} \leq \sum_{c}\sum_{n_c} x_{c,n_c} N_{c,n_c} \overline{P^{rec}_{c}} \qquad \forall d,h,s \tag{5.32b}$$

where $\overline{P}^{inv}_{c}$ and $\overline{P}^{rec}_{c}$ are the maximum inversion and rectification capacities of a single BC of type c.

- Power flow from the AC bus bar to the DC bus bar occurs only during the rectification mode, whereas power flow from the DC to AC bus bar occurs only during the inversion mode. This complementarity condition is enforced by (5.33a) and (5.33b) respectively.

$$\left(P^{dch}_{d,h,s} + P^{ren,L}_{d,h,s}\right) \leq w^{inv}_{d,h,s} M \qquad \forall d,h,s \tag{5.33a}$$

$$P^{dg,ch}_{d,h,s} \leq w^{rec}_{d,h,s} M \qquad \forall d,h,s \tag{5.33b}$$

where $w^{inv}_{d,h,s}$ is the binary variable equal to 1 when the BCs operate as invertors and 0 otherwise, and $w^{rec}_{d,h,s}$ is the binary variables equal to 1 when the BCs operate as rectifiers and 0 otherwise. Parameter M is a big number which is set to enforce the complementarity constraint.

- The BCs cannot operate in inversion and rectification mode at the same time (5.34):

$$w^{inv}_{d,h,s} + w^{rec}_{d,h,s} \leq 1 \quad \forall d,h,s \tag{5.34}$$

- The rectification mode can occur only when at least one DG is online (5.35):

$$w^{rec}_{d,h,s} \leq \sum_{g} U_{d,h,g,s} \quad \forall d,h,s \tag{5.35}$$

- Any online DGs may charge the SBB only when they operates at their minimum limits and the demand is less than these DGs minimum limits (5.36).

$$P^{dg,ch}_{d,h,s} \leq \sum_{g} U_{d,h,g,s} \underline{P}_{g} - P^{dg,exc}_{d,h,s} - w^{rec}_{d,h,s} D_{d,h,s} \quad \forall d,h,s \tag{5.36}$$

where $\underline{P}_{g}$ is the minimum output power limit for a single DG of type g.

DGs operation constraints are formulated based on the CUCs method described in Chapter 3.

- Fuel consumption is modeled by PWLA as:

$$FC_{d,h,g,s} = \max_{q=1,2,3}\{B_{q,g} P_{d,h,g,s} + U_{d,h,g,s} A_{q,g}\} \qquad \forall d,h,g,s \qquad \forall d,h,g,s \tag{5.37}$$

- DGs output power limits are specified by (5.38).

$$U_{d,h,g,s}\underline{P}_g \leq P_{d,h,g,s} \leq U_{d,h,g,s}\overline{P_g} \qquad \forall d,h,g,s \tag{5.38}$$

where $\overline{P}_g$ is the maximum output power from a single DG of type g.

- The relationship between number of start-up, shut-down and online DGs is expressed by (5.39).

$$V_{d,h,g,s} - Z_{d,h,g,s} \leq U_{d,h,g,s} - U_{d,h-1,g,s} \qquad \forall d,h,g,s \tag{5.39}$$

- Constraint (5.40) imposes that the number of online DGs is not greater than the number of installed DGs.

$$U_{d,h,g,s} \leq \sum_{n_g} x_{g,n_g} N_{g,n_g} \qquad \forall d,h,g,s \tag{5.40}$$

- Constraint (5.41) relates the current energy in SBB to the energy stored in the previous hour and the current charging and discharging power.

$$E_{d,h,b,s} = E_{d,h-1,b,s} + \Delta h(\eta_b^{ch} P_{d,h,b,s}^{ch} - P_{d,h,b,s}^{dch}/\eta_b^{dch}) \quad \forall d,h,b,s \tag{5.41}$$

where $E_{d,h,b,s}$ is the energy in the SBB of type b in hour h of scenario s of day d, Δh is the time step, η_b^{ch} the charging efficiency for the SBB of type b, η_b^{ch} the discharging efficiency for the SBB of type b, and the rest of the variables are as defined before. Initial energy in the SBB, $E_{0,b}$, is defined by:

$$E_{0,b} = SOC_{0,b} C_b^{bb} \qquad \forall b \tag{5.42}$$

where $SOC_{0,b}$ is the relative initial SOC of SBB of type b and $\overline{C}_b$ is the capacity of SBB of type b given by:

$$C_b^{bb} = \sum_b \sum_{n_b} x_{b,n_b} N_{b,n_b}^{par} N_b^{ser} C_b V_b \quad \forall b \tag{5.43}$$

where C_b and V_b are nominal capacity and voltage of a single SBB of type b.

- Energy stored in the SBB must be not less than its minimum energy limit, and no greater than its maximum energy limit as described by (5.44a) - (5.44c).

$$\underline{E_b} \leq E_{d,h,b,s} \leq \overline{E_b} \qquad \forall d,h,b,s \tag{5.44a}$$

$$\overline{E_b} = C_b^{bb} \qquad \forall b \tag{5.44b}$$

$$\underline{E_b} = (1 - DOD_b) C_b^{bb} \qquad \forall b \tag{5.44c}$$

where $\overline{E}_b$ is the maximum energy limit of SBB of type b, $\underline{E}_b$ is the minimum energy limit of SBB of type b, and DOD_b is the depth of discharge of SBB of type b.

- Maximum limits for charging and discharging power of the SBB of type b are expressed in (5.45a) -(5.45c).

$$P_{d,h,b,s}^{ch} \leq x_{b,n_b} N_{b,n_b}^{par} N_b^{ser} \overline{P_b^{ch}} \qquad \forall d,h,b,s \tag{5.45a}$$

$$P_{d,h,b,s}^{ch} \leq \overline{Ch_b^r} \left(C_b^{bb} - E_{d,h,b,s}\right) \qquad \forall d,h,b,s \tag{5.45b}$$

$$P^{dch}_{d,h,b,s} \leq x_{b,n_b} N^{par}_{b,n_b} N^{ser}_{b} \overline{P^{dch}_{b}} \qquad \forall d,h,b,s \tag{5.45c}$$

where $\overline{P}^{ch}_{b}$ is the maximum charging power of the SB of type b , $\overline{Chr_b}$ the maximum charging rate for the SB of type b, and $\overline{P}^{dch}_{b}$ the maximum discharging power for the SB of type b.

- Complementarity condition to avoid simultaneous charging and discharging of SBB of type b is expressed by using the big M formulation.

$$P^{ch}_{d,h,b,s} \leq x^{ch}_{d,h,s} M \qquad \forall d,h,b,s \tag{5.46a}$$

$$P^{dch}_{d,h,b,s} \leq x^{dch}_{d,h,s} M \qquad \forall d,h,b,s \tag{5.46b}$$

$$x^{ch}_{d,h,s} + x^{dch}_{d,h,s} \leq 1 \qquad \forall d,h,b,s \tag{5.46c}$$

where for each hour h and scenario s of typical day d, $x^{ch}_{d,h,s}$ is the binary variable which is equal to 1 when the SBBs are charged and 0 otherwise, while $x^{ch}_{d,h,s}$ is the binary variable which is equal to 1 when SBBs are discharged and 0 otherwise, and $P^{ch}_{d,h,b,s}$, $P^{dch}_{d,h,b,s}$ and M are as defined before.

- Generation from a single PV panel of type p, is a function of incident solar irradiance and ambient temperature [102].

$$\overline{P_{d,h,p}} = f_{der} \tfrac{G_{d,h}}{G^{STC}} \overline{P^{STC}_{p}} \left[1 + \gamma \left(T^{a}_{d,h} + \tfrac{NOCT-20}{800} G_{d,h} - T^{STC}\right)\right] \tag{5.47}$$

- Generation from each WT is estimated by interpolation of the power curve of each type of turbine considered in the planning in order to obtain the output power corresponding to the hub height wind speed. The hub height wind speed used in the interpolation is calculated by using Logarithmic law and the effect of air density is modelled by using the air density ratio **windpinpsys3rded**

5.5 Robust Optimization Model for Microgrid Planning

Similarly to the 2SSIP model, the robust model consider uncertainty for each season. However, the RO model does not consider a discrete number of scenarios, but a single representative day for each season, whose parameters are *uncertain*. The RO is aimed at computing the minimum cost planning solution that is robust against all possible realizations of the parameters within the uncertainty sets. In other words, the objective is to determine the planning decision vector $\mathbf{x}$ that ensures feasibility for all realizations of the parameters within the uncertainty sets, and optimizes the objective function in the worst case realizations of these parameters.

5.5.1 Objective function

The objective function for the RO model is similar to that of 2SSIP model presented in section 5.4, except that the subscript s for the scenarios is dropped: The objective function minimizes the fixed annualized investment cost, while also taking into account the operational costs. Instead of a different operational schedule for each scenario, this case has only one robust operational schedule per season, whose cost has to be weighted in the objective function according to the estimated number of days in each season, f_d. It is also important to stress that, while 2SSIP model aimed at approximating (thus, optimizing) the expected operational cost, the RO model provides an upper bound on the annual operation cost, optimizing the worst-case in a min-max fashion. The objective function is given by:

$$\min_{\mathbf{x},\mathbf{y}} \max_{\boldsymbol{u} \in \boldsymbol{\mathcal{U}}^d, \boldsymbol{\mathcal{U}}^p, \boldsymbol{\mathcal{U}}^w,} \{TAIC(\mathbf{x}) + AEOC(\mathbf{x}, \mathbf{y})\} \tag{5.48}$$

where $\mathbf{x}$ and $\mathbf{y}$ are as defined before, and $\boldsymbol{\mathcal{U}}_d^d$, $\boldsymbol{\mathcal{U}}_d^p$, and $\boldsymbol{\mathcal{U}}_d^w$ are uncertainty sets for electricity demand, generation from PV panel of type p, and generation from WT of type w. $TAIC$ is the total annualized investment cost while $AEOC$ is the annualized operational cost. For the sake of completeness, these functions are repeated below:

$$\begin{aligned} FAIC(\mathbf{x}) = & \sum_p \sum_{n_p} x_{p,n_p} N_{p,n_p}^{par} N_p^{ser} AC_p + \sum_w \sum_{n_w} x_{w,n_w} N_{w,n_w} AC_w + \\ & \sum_b \sum_{n_b} x_{b,n_b} N_{b,n_b}^{par} N_b^{ser} AC_b + \sum_c \sum_{n_c} x_{c,n_c} N_{c,n_c} AC_c + \\ & \sum_g \sum_{n_g} x_{g,n_g} N_{g,n_g} AC_g \end{aligned} \tag{5.49}$$

$$\begin{aligned} AEOC(\mathbf{x}, \mathbf{y}) = & \sum_d \sum_h \sum_g f_d U_{d,h,g} RC_g / Y_g + \sum_d \sum_h \sum_b f_d C_{bw,b} P_{d,h,b}^{dch} + \\ & \sum_d \sum_h \sum_g f_d U_{d,h,g} OMC_g + \\ & \sum_d \sum_h \sum_g f_d C_{fuel} FC_{d,h,g} + \\ & \sum_d \sum_h \sum_g f_d \left(V_{d,h,g} SUC_g + Z_{d,h,g} SDC_g \right) \end{aligned} \tag{5.50}$$

Note that for the planning problem considered in this thesis, uncertainty parameters do not appear in the objective function even though their effect are accounted for through other operation variables.

5.5.2 Description of uncertainty sets

This section presents the description of the uncertainty sets used to model uncertainties in the RO model. The uncertainties arise from intermittent generations from PV arrays and WTs, and the electricity demand. In the 2SSIP model, PDFs for the forecasted generation from PV arrays and WTs, and the forecasted electricity demand were applied to model forecasting errors. Conversely, the RO model presented in this section models uncertainties in PV arrays and WTs, and the electricity demand by using polyhedral uncertainty sets as defined by (5.15) in Section 5.3 For simplicity, it is assumed that the worst case solution occurs at the extreme points of uncertain parameters, thus:

$$\boldsymbol{\mathcal{U}}_d^d = \{D_d : D_{d,h} = \widetilde{D}_{d,h}^d \pm \sigma_{d,h}^d \zeta_{d,h}^d \; \forall h, \|\zeta^d\|_\infty \leq 1, \|\zeta^d\|_1 \leq \Gamma_d^d\} \tag{5.51a}$$

$$\boldsymbol{\mathcal{U}}_d^p = \{P_d^p : P_{d,h}^p = \widetilde{P}_{d,h}^p \pm \sigma_{d,h}^p \zeta_{d,h}^p \; \forall h, \|\zeta^p\|_\infty \leq 1, \|\zeta^p\|_1 \leq \Gamma_d^p\} \tag{5.51b}$$

$$\boldsymbol{\mathcal{U}}_d^w = \{P_d^w : P_{d,h}^w = \widetilde{P}_{d,h}^w \pm \sigma_{d,h}^w \zeta_{d,h}^w \; \forall h, \|\zeta^w\|_\infty \leq 1, \|\zeta^w\|_1 \leq \Gamma_d^w\} \tag{5.51c}$$

where $\boldsymbol{\mathcal{U}}_d^d$, $\boldsymbol{\mathcal{U}}_d^p$, and $\boldsymbol{\mathcal{U}}_d^w$ are uncertainty sets for electricity demand, generation from PV panel of type p, and generation from WT of type w, in hour h of typical day d. Variables $\zeta_{d,h}^d$, $\zeta_{d,h}^p$, and $\zeta_{d,h}^w$ represent the occurrence of deviations in electricity demand, generation from PV panel of type p, and generation from WT of type w, in hour h of typical day d. The uncertainty sets consider parameters belonging to a support interval $\widetilde{D}^d_{d,h} \pm \sigma^d_{d,h}$, for the electricity demand, $\widetilde{P}^p_{d,h} \pm \sigma^p_{d,h}$, for the generation from PVs, and $\widetilde{P}^w_{d,h} \pm \sigma^w_{d,h}$, for the generation from WTs in which $D^d_{d,h}$, $P^p_{d,h}$, and $P^w_{d,h}$ are the average forecasted electricity demand, generation from PV array of type p, and the generation from WTs of type w in hour h of typical day d. Parameters $\sigma^p_{d,h}$, $\sigma^w_{d,h}$, and $\sigma^d_{d,h}$ are the standard deviation of the electricity demand, generation from PV panel of type p, and generation from WT of type w in hour h of typical day d. Parameters Γ^d_d, Γ^p_d, and Γ^w_d represent the *budgets of uncertainties*, that controls the conservatism of the approach, as they impose upper bounds on the number of worst-case deviations in electricity demand, generation from PV array of type p, and the generation from WTs of type w that can occur in the time horizon. From a theoretical standpoint, the value of Γ also gives probabilistic guarantees on the satisfaction of a constraint, thanks to the bounds described in [192]. These probabilistic bounds can be used to guide the choice of the correct Γ.

The robust counterpart can also be seen as a semi-infinite programming problem, since the robust constraints must be satisfied for all the (infinitely many) parameters in the uncertainty sets. However, for polyhedral uncertainty sets such as that described in (5.51a)–(5.51c), the problem can be easily reformulated exploiting duality theory, obtaining a robust formulation that is of the same class as the deterministic problem (in this case, MILP), except for a (manageable) number of additional continuous variables and constraints. Detailed discussion on the reformulation presented in [192], [204]. However, note that to formulate the robust counterpart of the planning model, it is necessary to adopt reformulation of the constraints presented in the 2SSIP model as described in the following section.

5.5.3 Constraints for RO model

The constraints for the RO model are formulated from those in the 2SSIP by dropping the subscript s for scenarios and change the position of indices d, p, and w to superscript for succinct representation of the model. Note that index d appears as superscript in parameter $D^d_{d,h}$ to stress that this parameter refers to the average forecasted demand otherwise when index d appears as a subscript it represents the typical day. In formulating the RO constraints, it is necessary to observe that [205]:

(i) All redundant variables (whose values are completely determined by the remaining ones) are eliminated by substitution.

(ii) All equality constraints in which the uncertain parameters $D_{d,h},\ P^{pv}_{d,h},\ P^{wt}_{d,h}$ appear are converted into inequality constraints.

(iii) All definition variables are eliminated in order to avoid splitting the uncertainty in one constraint over more constraints.

(iv) No slack variable is introduced in the uncertain constraints, unless they are adjustable and that the equality constraint can be avoided.

With this in mind, the objective function is minimized subject to maximization over $\boldsymbol{u} \in \boldsymbol{\mathcal{U}}^d$, $\boldsymbol{\mathcal{U}}^p$, $\boldsymbol{\mathcal{U}}^w$ of all constraints in which the uncertain parameters appear, and subject to the uncertainty budgets described in (5.51a) – (5.51c), and the remaining constraints. Note to obtain the equivalent MILP model, each constraint which has term(s) with uncertain parameter(s) is subject to a rigorous reformulation demonstrated in Section above. Following this, constraints for the RO model are now listed below:

- It is required to ensure that only one alternative in the design search space is chosen. Thus constraint 5.26 remains unchanged.

$$\sum_{n_\ell} x_{\ell,n_\ell} \leq 1 \qquad \forall \ell \in \{g,p,w,b,c\} \tag{5.52}$$

- The power balance constraint contains all uncertain parameters and thus needs to be recast to properly model the uncertainties in these input parameters. Therefore, power balance constraint for the RO model is given by:

$$\begin{aligned}
&\sum_{g} P_{d,h,g} + \Bigg[\sum_{b} P^{dch}_{d,h,b} \; + \sum_{p}\sum_{n_p} x_{p,n_p} N^{par}_{p,n_p} N^{ser}_{p} (\widetilde{P}^{p}_{d,h} \pm \sigma^{p}_{d,h}\zeta^{p}_{d,h}) + \\
&\sum_{w}\sum_{n_w} x_{w,n_w} N_{w,n_w} (\widetilde{P}^{w}_{d,h} \pm \sigma^{w}_{d,h}\zeta^{w}_{d,h}) \; - \; \sum_{b} P^{ren,ch}_{d,h,b}\Bigg] \eta_{inv} + \\
&\sum_{b} P^{dg,ch}_{d,h,b} \; + \; \sum_{g} P^{exc}_{d,h,g} \;\; \geq \;\; (\widetilde{D}^{d}_{d,h} \pm \sigma^{d}_{d,h}\zeta^{d}_{d,h}) \\
&\forall d,h
\end{aligned} \tag{5.53}$$

where $P^{dg,ch}_{d,h}$ is the charging power from online DGs used to charge SBB of type b in hour h of typical day d, $P^{exc}_{d,h,g}$ the excess power from the single online DG in hour h of typical day d, and the remaining symbols are as defined in previously. Note that constraints (5.28) to (5.31) of the 2SSIP model are all included in the power balance constraint (5.53) of the RO model.

- Constraint (5.32a) which limits flow of power from the DC to AC bus bar during the inversion mode of BCs is included in the RO model after reformulation as follows.

$$\begin{aligned}
&\Bigg[\sum_{b} P^{dch}_{d,h,b} \; + \; \sum_{p}\sum_{n_p} x_{p,n_p} N^{par}_{p,n_p} N^{ser}_{p} (\widetilde{P}^{p}_{d,h} \pm \sigma^{p}_{d,h}\zeta^{p}_{d,h}) + \\
&\sum_{w}\sum_{n_w} x_{w,n_w} N_{w,n_w} (\widetilde{P}^{w}_{d,h} \pm \sigma^{w}_{d,h}\zeta^{w}_{d,h}) \; - \; \sum_{b} P^{ren,ch}_{d,h,b}\Bigg] \; + \\
&\leq \sum_{c}\sum_{n_c} x_{c,n_c} N_{c,n_c} \overline{P^{inv}_{c}} \\
&\forall d,h
\end{aligned} \tag{5.54}$$

- Similarly constraint (5.32b) of the 2SSIP model, which limits flow of power from the AC to DC bus bar during rectification mode of BCs, is reformulated as follows.

$$\sum_{b} P^{dg,ch}_{d,h,b} \leq \sum_{c}\sum_{n_c} x_{c,n_c} N_{c,n_c} \overline{P^{rec}_{c}} \qquad \forall d,h \tag{5.55}$$

- Power flow from the AC bus bar to the DC bus bar occurs only during the rectification mode, thus

(5.33a) becomes:

$$\left[\sum_b P^{dch}_{d,h,b} + \sum_p \sum_{n_p} x_{p,n_p} N^{par}_{p,n_p} N^{ser}_p (\widetilde{P}^p_{d,h} \pm \sigma^p_{d,h}\zeta^p_{d,h}) + \right.$$
$$\left. \sum_w \sum_{n_w} x_{w,n_w} N_{w,n_w} (\widetilde{P}^w_{d,h} \pm \sigma^w_{d,h}\zeta^w_{d,h}) - \sum_b P^{ren,ch}_{d,h,b} \right] + \tag{5.56}$$
$$\leq w^{inv}_{d,h,s} M$$
$$\forall d, h$$

- Power flow from the DC to AC bus bar occurs only during the inversion mode. Therefore, (5.33b) is modified to:

$$\sum_b P^{dg,ch}_{d,h,b} \leq w^{rec}_{d,h} M \qquad \forall d, h \tag{5.57}$$

- The BCs cannot operate in inversion and rectification mode at the same time (5.58).

$$w^{inv}_{d,h} + w^{rec}_{d,h} \leq 1 \qquad \forall d, h \tag{5.58}$$

- The rectification mode can occur only when at least one DG is online (5.59).

$$w^{rec}_{d,h} \leq \sum_g U_{d,h,g} \qquad \forall d, h \tag{5.59}$$

- Any online DGs may charge the SBB only when they operates at their minimum limits and the demand is less than these DGs minimum limits.

$$\sum_b P^{dg,ch}_{d,h,b} \leq \sum_g U_{d,h,g} \underline{P}_g - \sum_g P^{exc}_{d,h,g} - w^{rec}_{d,h} (\widetilde{D}^d_{d,h} \pm \sigma^d_{d,h}\zeta^d_{d,h}) \;\; \forall d, h \tag{5.60}$$

- DGs output power limits are enforced by (5.61).

$$U_{d,h,g} \underline{P}_g \leq P_{d,h,g} \leq U_{d,h,g} \overline{P_g} \qquad \forall d, h, g \tag{5.61}$$

- The relationship between number of start-up, shut-down and online DGs is expressed by (5.62).

$$V_{d,h,g} - Z_{d,h,g} \leq U_{d,h,g} - U_{d,h-1,g} \qquad \forall d, h, g \tag{5.62}$$

- The number of online DGs is no greater than the number of installed DGs.

$$U_{d,h,g} \leq \sum_{n_g} x_{g,n_g} N_{g,n_g} \qquad \forall d, h, g \tag{5.63}$$

- Constraints (5.41) which relates the current energy in SBB to the energy stored in the previous hour and the current charging and discharging power, and (5.44a) which enforces the upper and lower limits for the energy in the SBB are replaced by (5.64)

$$\underline{E}_b \leq E_{0,b} + \Delta h \sum_{\tau=1}^{h} \left[\frac{(P^{ren,ch}_{d,h,b} + P^{dg,ch}_{d,h,b}\eta_{rec})}{\eta^{ch}_b} - \frac{P^{dch}_{d,\tau,b}}{\eta^{dch}_b} \right] \leq \overline{E}_b \;\; \forall d,h,b \tag{5.64}$$

Note that the aggregated formulation of energy conservation constraints for the SBB in the RO model, i.e. (5.64), combines all definition variables in equality constraints (5.42) to (5.44c) which appear in the 2SSIP model.

- Other inequality constraints which enforce maximum charging and discharging power limits for the SBB remain unchanged.

$$(P^{ren,ch}_{d,h,b} + P^{dg,ch}_{d,h,b}\eta_{rec}) \leq x_{b,n_b} N^{par}_{b,n_b} N^{ser}_b \overline{P^{ch}_b} \qquad \forall d,h,b \tag{5.65a}$$
$$P^{dch}_{d,h,b} \leq x_{b,n_b} N^{par}_{b,n_b} N^{ser}_b \overline{P^{dch}_b} \qquad \forall d,h,b \tag{5.65b}$$
$$(P^{ren,ch}_{d,h,b} + P^{dg,ch}_{d,h,b}\eta_{rec}) \leq x^{ch}_{d,h} M \qquad \forall d,h,b \tag{5.65c}$$
$$P^{dch}_{d,h,b} \leq x^{dch}_{d,h} M \qquad \forall d,h,b \tag{5.65d}$$
$$x^{ch}_{d,h} + x^{dch}_{d,h} \leq 1 \qquad \forall d,h,b \tag{5.65e}$$

- If the charging rate is considered, then constraint (5.45b) becomes

$$(P^{ren,ch}_{d,h,b} + P^{dg,ch}_{d,h,b}\eta_{rec}) \leq \overline{Chr_b} \left(C^{bb}_b - E_{0,b} + \Delta h \sum_{\tau=1}^{h} \left[\frac{(P^{ren,ch}_{d,h,b} + P^{dg,ch}_{d,h,b}\eta_{rec})}{\eta^{ch}_b} - \frac{P^{dch}_{d,\tau,b}}{\eta^{dch}_b} \right] \right) \;\; \forall d,h,b \tag{5.66}$$

where the $\overline{C}_b$ is the capacity of SBB of type b given should be substituted by its definition in (5.43).

5.5.4 Model Reformulation and Size

In order to solve the above RO model with MILP solvers such as Cplex or Gurobi in GAMS, reformulation to its tractable RC problem is required. A review on reformulation library for RO problem is presented in [196] In this thesis, a JuMP extension for RO (JuMPeR) is applied to reformulate the RO model. This tool can take polyhedral and ellipsoidal constraints on the uncertain parameters and reformulate them using duality approach as explained in Subsection 5.3.2.3, or generate cutting planes by solving LP problems or Second Order Cone Problems (SOCPs). Table **??** summarizes the size of 2SSIP model with 100 scenarios and the resulted RC of the RO model.

Model	Number of Constraints	Number of Variables				CPU Time [s]
		Integer	Binary	Continuous	Total	
2SSIP†	86,739	14,400	9,630	33,603	57,633	5,024.85
RO♯	167,000	288	78	338,000	338,366	73.9

† 2SSIP model solved with 100 scenarios, ♯ Robust counterpart of the RO model (Obtained after reformulation) solved with uncertainty budgets $\mathbf{\Gamma_D = 8}$, $\mathbf{\Gamma_{PV} = 4}$, and $\mathbf{\Gamma_{WT} = 8}$.

5.6 Case: Microgrid Planning using 2SSIP and RO Model

The proposed 2SSIP and RO models are applied to optimize the plan of a community microgrid considering PVs, WTs, SBBs, and DGs. For the 2SSIP model, uncertainties in solar irradiance, wind speed, and electricity demand are modeled by Beta, Rayleigh, and Normal PDFs, respectively. Since the site is located in a tropical region (a village located in $5.5°S$, $34.5°E$, Singida, Tanzania), annual hourly input data are classified into dry and rainy seasons in order to generate scenarios which retain seasonal variations. Then, probability distributions for irradiance, wind speed, and electricity demand for each hour of the days falling in the dry and rainy seasons are estimated. Using these distributions, LHS is applied to generate 4000 discrete scenarios. Each season is represented by a subset of reduced scenarios obtained by applying the fast forward algorithm in GAMS/Scenred2. Reduced scenarios for irradiance and wind speed are used in calculation of per unit generation of each type of PV panel and WT considered in this study. Fig. 5.6 shows 50 reduced scenarios for electricity demand, power from PV of type PV1, and power from WT of type WT1, for each typical day representing the dry and rainy season.

For the RO model, the input data simply consists of hourly support intervals for each uncertain parameter, namely, electricity demand, and PV and WT generation. We first compute the hourly mean $\mu_{d,h}$ and standard deviation $\sigma_{d,h}$ over the raw data (shown in Fig. 5.4). Then, the support intervals are defined as $1.2\mu_{d,h} \pm \sigma_{d,h}$, where the factor 1.2 is chosen so to include the yearly peaks.

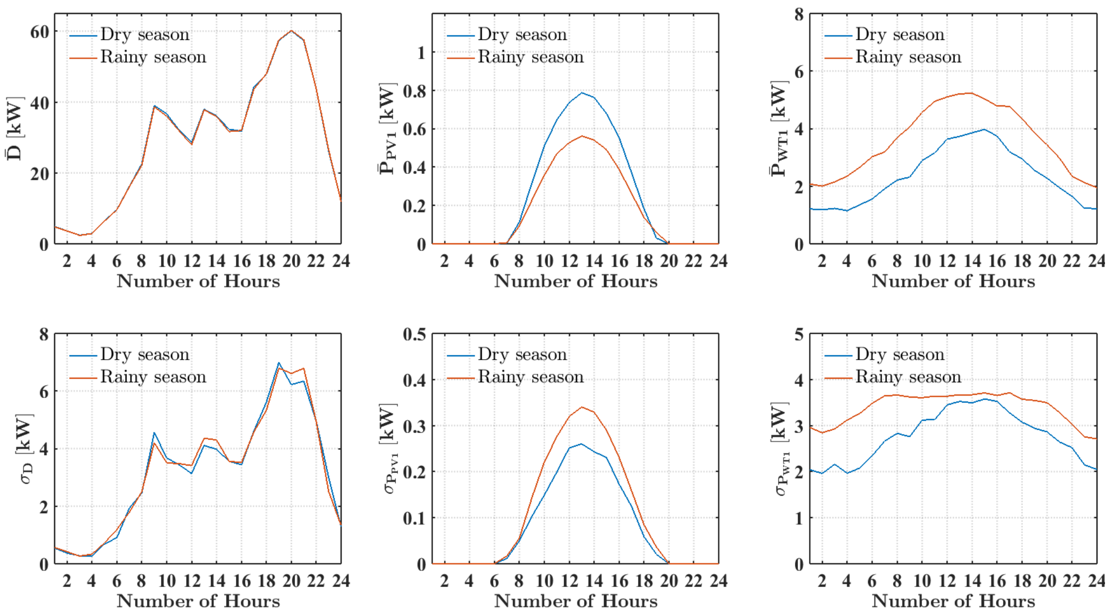

Figure 5.4: *Sample input data for RO model, average electricity demand ($\bar{D}$), power from PV1($\bar{P}_{PV1}$) and WT1($\bar{P}_{WT1}$), and their corresponding standard deviations*

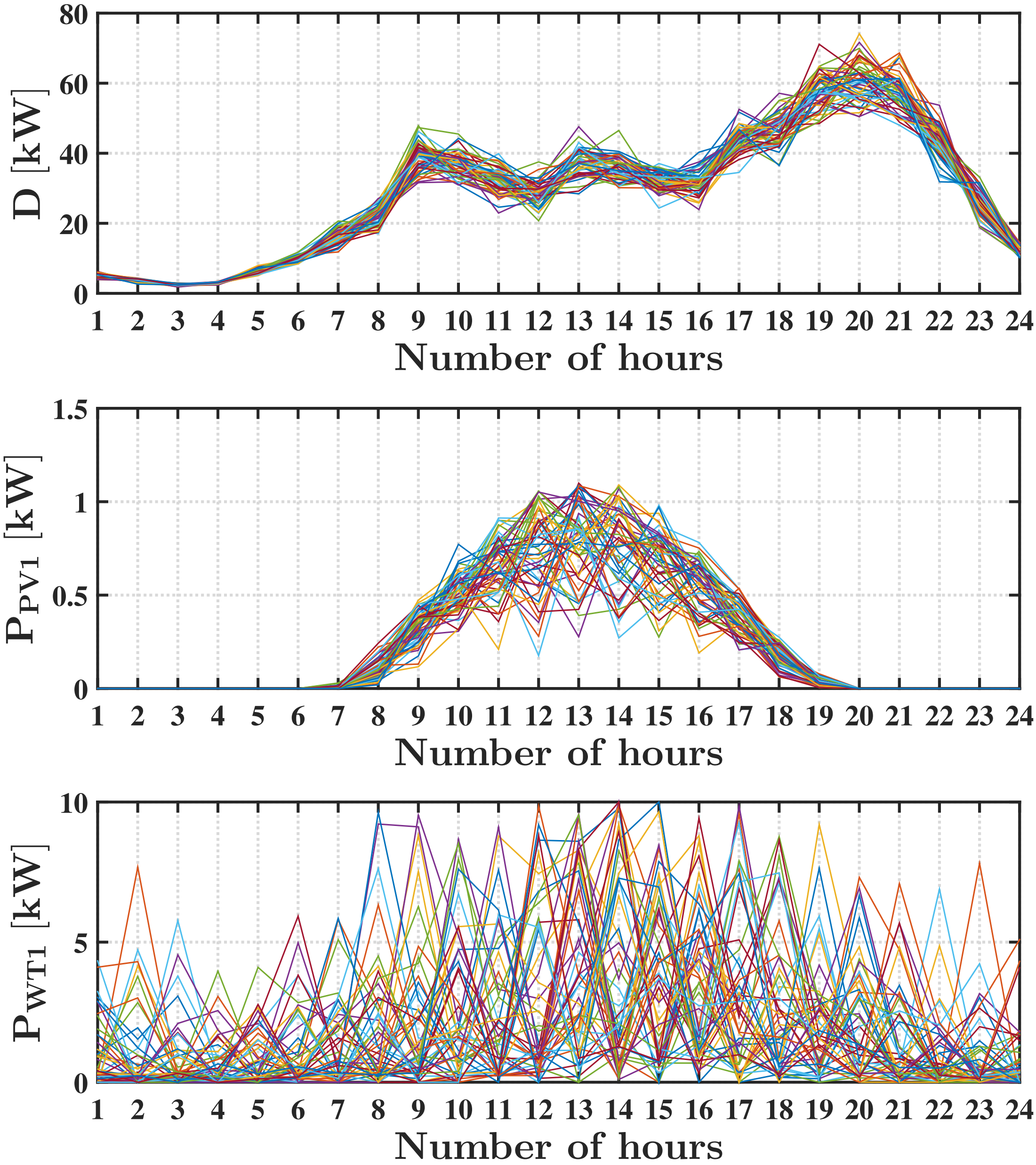

Figure 5.5: *Scenarios for electricity demand ($\bar{\boldsymbol{D}}$), power from PV1($\bar{\boldsymbol{P}}_{PV1}$) and WT1($\bar{\boldsymbol{P}}_{WT1}$) for the typical day of the dry season*

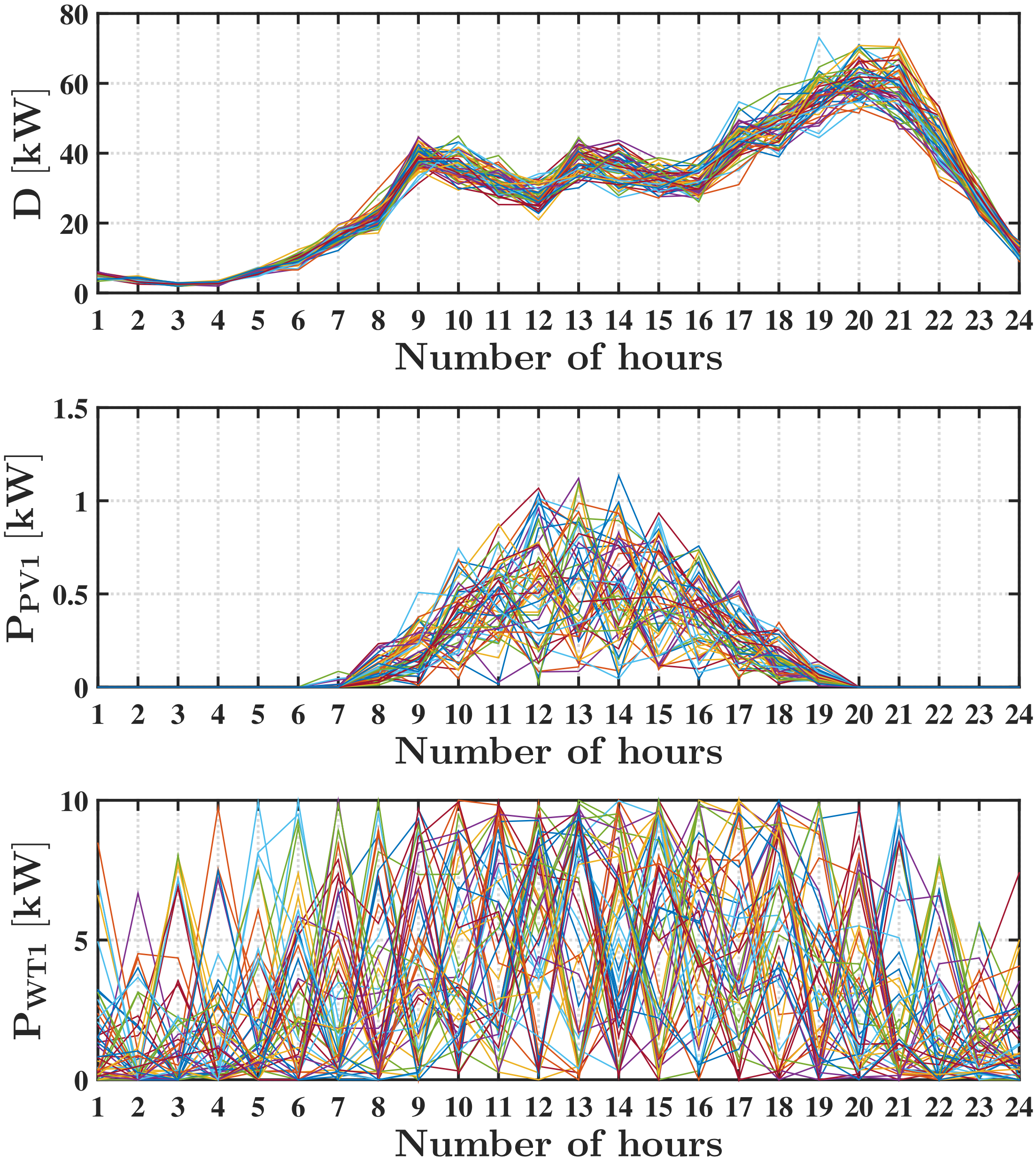

Figure 5.6: *Scenarios for electricity demand ($\bar{\boldsymbol{D}}$), power from PV1($\bar{\boldsymbol{P}}_{PV1}$) and WT1($\bar{\boldsymbol{P}}_{WT1}$) for the typical day of the rainy season (right)*

5.6.0.1 Component input data

These tests were performed by using similar component with technical and economic specifications specified in Section 4.7 of Chapter 4.

5.7 Tests and Results

This section presents the comparison and discussion of the results from the two models. The 2SSIP and RO models were implemented in GAMS and solved with Gurobi 6.0 with an optimality gap tolerance of 10^{-4} on an Intel i7-3770 @3.40GhZ with a 8 GB memory. Table 5.1 shows the optimal number of each type of components obtained by the 2SSIP model, with different number of scenarios, and RO with different settings of budget of uncertainty. From a computational point of view, it is interesting to observe that the computing time for the 2SSIP model grows very quickly as the number of scenarios is increased, although the solutions are similar, indicating that a relatively small number of scenarios is sufficient to obtain an accurate solution for this case. The largest instance, with 100 scenarios, required almost 2 days of computing time and gave the same results as obtained with 40 scenarios. On the contrary, the computational time for the RO model vary slightly with the size of uncertainty sets.

The solutions obtained with the RO model are significantly different. The model can be solved very quickly if the budget of uncertainty is set to 0 for all uncertain parameters: indeed, this case is equivalent to solving a deterministic model with only two representative days, which can be solved in very few seconds. If Γs are nonzero, the model is significantly more challenging to solve, although the optimal solution can be obtained in a few minutes. From a point of view of the solution, it is easy to observe that the RO model favors renewable energies when no uncertainty is considered: indeed, RES are extremely cost efficient, if their volatility is neglected. When Γ is increased, the number of installed RESs is decreased. In particular, WTs have very large deviations, thus a RO approach tends to favor the more expensive, but less volatile, generation sources, namely the DGs. The trend is clear: increasing the level of protection brings to a smaller fraction of RESs. It is also worth noting that the storage batteries are crucial as a buffer against uncertainty, with both approaches. The RO model selects the maximum number of SBB(15 units) in all cases with nonzero Γ.

While the total investment costs is fixed, once a solution has been determined, the actual operational costs may differ from what was considered in the planning model. The is due to the fact that operational planning costs are accounted for in a different way by the two models, i.e. the RO costs account for the worst case operational planning with the degree of conservatism specified by Γ, whereas the 2SSIP cost account for the planning solution considering operation costs approximated by the most probable realization of the input renewable energy resource and electricity demand scenarios. It is therefore reasonable to ask how the solutions in Table 5.1 would behave in a practical setting, and, specifically, what would be the actual cost of operating such system over a year. A complete comparison of the results from the 2SSIP model and the RO model was carried out by running an operational optimization model with planning results summarized in Table 5.1. In order to do so, 365 daily scenarios are sampled from the hourly distributions used to generate scenarios for the 2SSIP model. For each day with its sampled scenarios, an optimal operational planning problem (similarly to [124]) with the configuration of the system as obtained by the 2SSIP and the RO model, is solved. The aim is to assess the performance of each planning results by comparing the total annualized operational cost and unmet demand. It is found that the RO model is able to give competitive results.

Note, since the 2SSIP model used scenarios that were sampled from exactly the same input data (perfect information), it is expected that the value of operational cost from the operational simulation model will be close to the expected cost approximated by the 2SSIP planning model. On the other hand, note that no distribution information has been used for the RO, except for the sample mean and standard

Table 5.1: *Optimal components mix from 2SSIP and RO models*

Components			Number of Installed Components								Installed Capacity by Technology [kW] or [kWh]							
			2SSIP Model				RO model				2SSIP Model				RO model			
Name	Type	Capacity	$s = 10$	$s = 20$	$s = 40$	$s = 100$	$\Gamma_D = 0$, $\Gamma_{PV} = 0$, $\Gamma_{WT} = 0$	$\Gamma_D = 2$, $\Gamma_{PV} = 1$, $\Gamma_{WT} = 2$	$\Gamma_D = 4$, $\Gamma_{PV} = 3$, $\Gamma_{WT} = 4$	$\Gamma_D = 8$, $\Gamma_{PV} = 4$, $\Gamma_{WT} = 8$	$s = 10$	$s = 20$	$s = 40$	$s = 100$	$\Gamma_D = 0$, $\Gamma_{PV} = 0$, $\Gamma_{WT} = 0$	$\Gamma_D = 2$, $\Gamma_{PV} = 1$, $\Gamma_{WT} = 2$	$\Gamma_D = 4$, $\Gamma_{PV} = 3$, $\Gamma_{WT} = 4$	$\Gamma_D = 8$, $\Gamma_{PV} = 4$, $\Gamma_{WT} = 8$
DGs	$DG1$	16.0 kW	3	3	3	3	3	3	4	4	62.4	62.4	69.6	69.6	48	55.2	64	64
	$DG2$	7.2 kW	2	2	3	3	0	1	0	1								
PVs	$PV1$	1.0 kW	20	30	30	30	30	30	10	20	20	30	30	30	30	30	10	20
WTs	$WT1$	10.0 kW	4	4	4	4	4	4	2	0	40	40	40	40	40	40	20	0
	$WT2$	3.0 kW	0	0	0	0	4	1	0	0								
SB	$SB1$	4.92 kWh	15	15	12	12	4	15	15	15	73.8	73.8	59.04	59.04	19.68	59.04	59.04	59.04
BC	$BC1$	10.0 kW	4	4	4	4	2	5	2	2	40	40	40	40	20	50	20	20
CPU Time [s]			22.75	473.68	5024.85	172366.4	2.9	249.2	106.3	73.9	22.75	473.68	5024.85	172366.4	2.9	249.2	106.3	73.9

deviation from the raw data. Figure 5.7 shows the total annualized investment (in blue), the (estimated) operation costs given by the optimum of the 2SSIP and RO models (in pink), and the (simulated) operation costs of the corresponding systems computed over the 365 generated scenarios (in yellow).

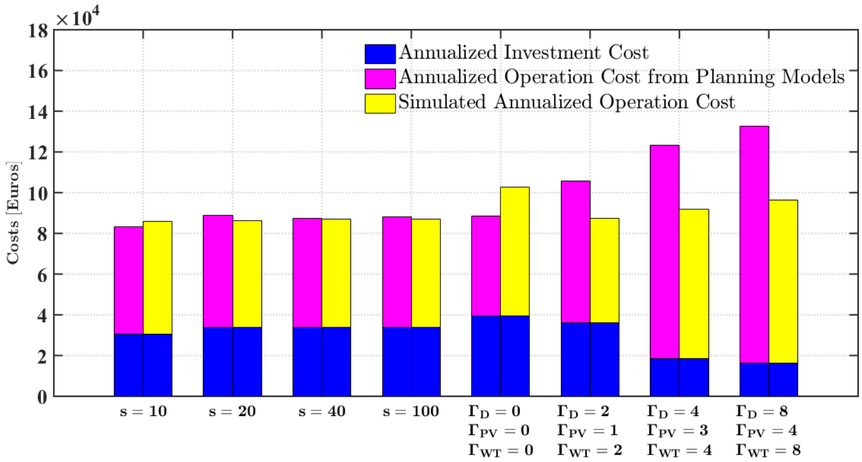

Figure 5.7: *Evaluation of the planning solutions: total annualized investment and operation cost*

As expected, the 2SSIP formulation, even with a small number of scenarios, yields a solution that has a simulated operational cost which is very close to the expected one. This is not surprising, as the 2SSIP had perfect information: the 2SSIP model used discrete scenarios that were sampled from the very same distributions used to generate the 365 validation scenarios. However, using fewer scenarios results in a (small) quantity of unmet demand, see Fig.5.8, that is reduced nearly to 0 if at least 40 scenarios are used.

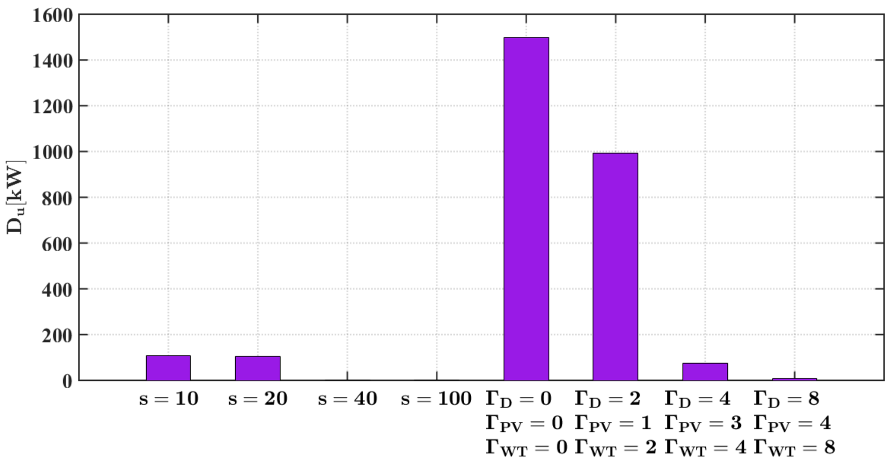

Figure 5.8: *Evaluation of the planning solution: annual unmet demand*

On the other hand, the RO model shows significant differences depending on the level of protection that we impose. For $\Gamma = 0$, the solution is clearly not robust: the actual operational cost is higher than the cost in the planning model, and there is a rather large quantity of unmet demand. Increasing Γ has the effect of increasing the operational cost in the planning model, since the solution is protecting against a larger uncertainty set. This, however, allows for better results in the simulation, both regarding the costs and the unmet demand, which is negligible for $\Gamma_D = 8, \Gamma_{PV} = 4, \Gamma_{WT} = 8$. This comes at a price: although the investment cost is smaller, the robust solutions are more expensive to operate (see Fig. 5.7). Indeed, they rely more on the DGs, due to the lack of information on the probability distributions of RESs generation, and the less accurate estimate of the operational costs in the planning model. In addition, results from the RO model without uncertainty budget confirm that the use of mean data for microgrid planning results in significant underestimation of the required components to install in the microgrid which in turn results to a very high operational costs and unmet demand.

Model	Number of Constraints	Number of Variables				CPU Time [s]
		Integer	Binary	Continuous	Total	
2SSIP†	86,739	14,400	9,630	33,603	57,633	5,024.85
RO♯	167,000	288	78	338,000	338,366	73.9

*Deterministic MILP model solved for the complete year, **Deterministic MILP model solved for 36 typical days, † 2SSIP model solved with 100 scenarios, ♯ Robust counterpart of the RO model (Obtained after reformulation) solved with uncertainty budgets $\boldsymbol{\Gamma_D = 8}$, $\boldsymbol{\Gamma_{PV} = 4}$, and $\boldsymbol{\Gamma_{WT} = 8}$.

5.8 Summary

This chapter has presented 2SSIP and RO models for microgrid planning under uncertainties in electricity demand, solar irradiance and wind speed. The model are formulated with discrete planning and operational decision variables which reflect the real-world application in which component capacities are not continuous and operational decisions are discrete. Using annual hourly historical data, a number of scenarios of electricity demand, solar irradiance and wind speed for the 2SSIP model were generated. Computational experiments show that the 2SSIP model provides good planning solutions in a reasonable computing time. A simulation on 365 generated scenarios shows that the 2SSIP solutions have small operational costs, and small quantity of unmet demand. On the other hand, the RO model aims at providing a solution which guarantees operational feasibility for all the realizations of the uncertain parameters in the uncertainty sets. The RO model is smaller and can be solved more efficiently, but it provides plans with usually larger operation costs. This research recommend the use of all three model proposed so far: the determinist planning model, 2SSIP model, and the RO model in the planning of new microgrid. Our finding show that these model complements each other and reveals different information which are valuable for the planner based on different planning requirement. For example, the RO model gives valuable planning results with regards to reliability of the solution. For preliminary studies RO model is arguably better complement to the deterministic model because at this stage often there are no enough real data available to allow the description of PDFs for the uncertain parameters. In order to obtain good results from the RO model, it is necessary to choose the correct shape of uncertainty sets and properly calibrate the parameters which define these sets. One of the potential limitations of the 2SSIP model is the long computation time which increase with number of scenarios considered. However, for planning problems, such long computational time can be accepted since the problem is solved off-line and only once during the planning stage.

CHAPTER 6

Conclusion and Future Work

6.1 Conclusions and Future Work

6.1.1 Conclusions

This thesis concentrates on the planning of hybrid microgrid for electrification of rural or remote areas. The microgrid is considered under isolated or off-grid condition in which the connection to the main grid is not yet available. The planning consider uncertainty associated with renewable resources and electric demand input data . A detailed MILP deterministic model of the microgrid planning problem is developed. The model adopts discrete planning and operational decision variables which reflect real-world application in which component capacities are not continuous and operational decisions are discrete. This enables a more realistic and accurate approximation of the long term system operation costs. Solving the deterministic MILP model for the complete planning problem requires very long computational time and memory. Two techniques are proposed to tackle this problem: first, a CUC approach is developed and applied to model the operation of DGs, and second, a modified K-medoid clustering algorithm is applied to select typical representative days over which the long term operation planning is approximated. These techniques have led to a significant reduction in computational times, thus enabling the planning problem to be applied for the real case studies.

The deterministic MILP model was applied for two case studies on microgrid planning. In the first case, the model results were compared with results obtained by using HOMER Pro 3.3 planning tool. In this case the model installed similar components as HOMER, but it gave minimum total annualized cost of the system due to the fact that microgrid long term operation is optimized for the entire planning period. HOMER approximates the long term operational planning on each individual hour based the past operational history of the system storage. This was the base case study to confirm the accuracy of the proposed MILP model.

In the second planning case study, applications of the MILP model with different formulations and constraints for the dispatching of SBB were investigated. The first formulation employs charging and discharging cost in the the objective function in order to avoid the use of binary variables to implement complementarity condition for SBB operation. Contrary to expectations, the results did not show any significant improvement in the computation time as compared to the MILP planning model with binary variables. This finding suggested that the difficult in locating optimal planning solution does not rely on the binary control variable but rather on the complex interaction between system planning and operation constraints.

The second formulation replaces integer planning decision variables with binary variable to select among the alternative planning solution specified in the search space. The search space was provided as an input to the model. This test showed that the computation time is significantly reduced. The reason for this is that this approach simplifies the planning problem leaving the solver with the task of optimal selection of the planning solution among the specified planning alternatives which have already fixed the number of components to install. This approach is acceptable, considering the fact that system planning is carried out by experienced planner who can provide close to optimal planning alternatives to the model. This finding confirmed that the proposed planning model can determine the optimal solution, if it is among the specified search space, much faster and thus simplifying the planning task.

Moreover, the extension of the deterministic model to the 2SSIP and RO models for microgrid planning under uncertainties in solar irradiance, wind speed and electric demand, is presented. These formulations consider discrete planning and operational decision variables which reflect the real-world application in which component capacities are not continuous and operational decisions are discrete. Using annual hourly historical data, a number of scenarios for solar irradiance, wind speed and electric demand for the 2SSIP model were generated. Computational experiments show that the 2SSIP model provides good planning solutions in a reasonable computing time. A simulation on 365 generated scenarios shows that the 2SSIP solutions have small operational costs, and lower unmet demand. One of the potential limitations of the 2SSIP model is the long computation time which increases with number of scenarios considered. However, for planning problems, moderately long computational time can be accepted since the problem is solved off-line and only once during the planning stage. Another limitation is that the 2SSIP model requires knowledge of PDF of input data which may not be available in some cases. However data from the nearby electrified village can be used for the planning study and still provide good results due to some similarities in demand consumption patterns.

On the other hand, the RO model aims at providing a solution which guarantees operational feasibility for all the realizations of the uncertain parameters in the uncertainty sets. The RO model is smaller and can be solved more efficiently, but it provides plans with usually larger operation costs. However, solutions from the RO model guarantee operational feasibility for the worst case realizations of uncertain parameters in the uncertainty sets. The RO approach is arguably better when planning a new microgrid, when often there are not enough real data available to allow the description of PDF for the uncertain parameters. In order to obtain good results from the RO model, it is necessary to choose the correct shape of uncertainty sets and properly calibrate the parameters which define these sets.

6.1.2 Future Work

Based on the work presented in this thesis, further research in the area of microgrid planning may be pursued on the following:

- Due to economic reasons it might be of interest to adopt multistage incremental planning approach. This will enable adopting microgrid planning to future conditions with increased demand, diversified market structures or under arrival of the grid extensions. Considering multistage can also save as a risk hedging strategy, i.e. the owner is not obliged to invest large capital today due to a number of foreseen scenarios. Another important motives to consider incremental planning approach is due to the fact the construction period for microgrid is shorter than the time it would take to build up a conventional power system. Also, for private owned microgrid cases, the investor may wish not to wait for 20 years to realise the ROI. Therefore, it may be required to consider only planning for the current demand requirements while considering future expansion scenarios.

- This study adopt a LCCA which assumes similar condition for all planning horizon. An approach similar to the capacity expansion problem in power system planning can be adopted to formulate a multistage optimization model. The main challenge here is to ensure sufficient level of planning details are maintained. Such types of problems usually results into very big models which are difficult to solve.

- Future research should focus on testing the proposed model on planning cases with available data, and evaluating the impact of the discrete operational variables on the planning decision. Furthermore, methods to speed up the 2SSIP optimization and analysis of the RO model with different uncertainty sets should be considered.

- Improvement of the clustering algorithm by developing hybrid clustering algorithms which combines artificial intelligence clustering methods with conventional clustering methods may be beneficial for selection of typical representative days. The aim should be to extract rare features of resources and demand profiles, particularly those which are important for the planning studies.

- A technique to assess the sensitivity of the the solution towards different types of risks should be developed. This will give the ability to quantify and manage the different elements of risk associated with microgrid planning projects and thus easy the financing. For example, even though DGs have higher operation costs, they may have lower risk, considering the fact that they can be easily shifted to another village which may not be the case for WTs and PVs.

Appendices

APPENDIX A

General Algebraic Modeling System (GAMS)

A.1 Introduction to GAMS

The General Algebraic Modeling System (GAMS) is a high-level algebraic modeling system for large scale optimization. GAMS is specifically designed for modeling linear, nonlinear and mixed integer optimization problems. The system is especially useful with large, complex problems. GAMS is available for use on personal computers, workstations, mainframes and supercomputers. It allows the user to concentrate on the modeling problem by making the setup simple. The system takes care of the time-consuming details of the specific machine and system software implementation.

GAMS is especially useful for handling large, complex, one-of-a-kind problems which may require many revisions to establish an accurate model. The system models problems in a highly compact and natural way. One of the reason this GAMS was selected for this research is that any change in the architecture of the microgrid requires modification of the model constraints. In GAMS, it is possible to change the formulation quickly and easily, change from one solver to another, convert from linear to nonlinear model, and adding new constraints.

A.2 System Features

GAMS lets the user concentrate on modeling. By eliminating the need to think about purely technical machine-specific problems such as address calculations, storage assignments, subroutine linkage, and input-output and flow control, GAMS increases the time available for conceptualizing and running the model, and analyzing the results. GAMS structures good modeling habits itself by requiring concise and exact specification of entities and relationships. The GAMS language is formally similar to commonly used programming languages. It is therefore familiar to anyone with programming experience.

Using GAMS, data are entered only once in familiar list and table form. Models are described in concise algebraic statements which are easy for both humans and machines to read. Whole sets of closely related constraints are entered in one statement. GAMS automatically generates each constraint equation, and lets the user make exceptions in cases where generality is not desired. Statements in models can be reused without having to change the algebra when other instances of the same or related problems arise. The location and type of errors are pinpointed before a solution is attempted. GAMS handles dynamic models involving time sequences, lags and leads and treatment of temporal endpoints.

GAMS is flexible and powerful. Models are fully portable from one computer platform to another when GAMS is loaded to each platform. GAMS facilitates sensitivity analysis. The user can easily program a model to solve for different values of an element and then generate an output report listing the solution characteristics for each case. Models can be developed and documented simultaneously because GAMS allows the user to include explanatory text as part of the definition of any symbol or equation. GAMS is being enhanced and expanded on a continuing basis.

The key features of GAMS are:

- Robust, scalable state-of-the-art modeling technology
- Tailored for complex, large-scale modeling applications
- Productivity gains through rapid development environment
- Broad academic and commercial network
- More than 30 years of experience in industry and academia

Basic types of models which can be handled by GAMS includes:Mixed Integer Linear/Quadratic Programs (MIP/MIQCP), Mixed Integer Nonlinear Programs (MINLP), Mixed Complementarity Problems (MCP), Mathematical Programs with Equilibrium Constraints (MPEC), Constrained Nonlinear Systems (CNS), and Extended Mathematical Programming (EMP).

GAMS offers an open architecture which assures a smooth integration of optimization models into all kinds of application environments. GAMS can be interfaced with various tools such as MATLAB, and has a huge bank of libraries for different applications. This thesis applies the interfacing between GAMS and MATLAB, Scenred2 [170], and robust optimization modelling language in JuMPeR.

A.3 Structure of GAMS project

Description of the model in GAMS includes the declaration and assignment of sets with indices of types of components, index of hours and typical days, and other indices employed in the formulation of the model. Input data are introduced in the model in form of scalars (e.g. fuel price), parameters (e.g. electricity demand, solar irradiation and wind speed each period) and tables consisting of technical and economic specifications of each component. Then follows the declaration and assignment of types, bounds and initial values for decision variables. The decision variables in the optimal planning model are discrete variables for planning and operation scheduling, and continuous variables to model the generation, storage, spilling or shortage of power, and the SOC of the SBB. Since GAMS does not use an explicitly entity called the objective function, it is necessary to declare a free objective function variable which is scalar-valued in the equation definition **rosenthal2004gams** All the constraints and objective function are declared and defined as equations in the GAMS model. In GAMS, the model is specified using the *Model Statement* while appropriate solver is assigned by using the *Solve statement*. The structure of GAMS model is summarised in Table A.1. Figure A.1 summarises the optimization

Table A.1: *Structure of a GAMS Model*

1.	**SETS**	Structures consisting of indices or names
2.	**DATA**	SCALARS (zero-dimentional),
		PARAMETERS (one-dimentional)
		TABLES (multi-dimensional)
		Pre-Processing to obtain values of some input parameters
3.	**VARIABLES**	Variables or arrays of variables
		Declaration with assigning a type of variable
		Declaration of limits for possible changes, initial level
4.	**EQUATIONS**	Equations or complexes and arrays of equations (includes both declaration and definition)
5.	**MODEL**	Model declaration (which equations to include)
6.	**SOLVE**	Method of solution (which algorithm to use)
7.	**OUTPUT**	Output of information to files

process in GAMS.

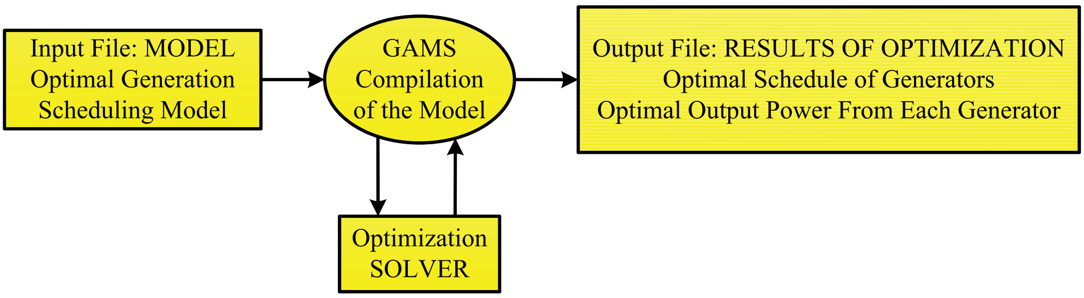

Figure A.1: *Optimization process in GAMS*

Interfacing GAMS and MATLAB aimed at simplifying the pre-processing of model input data and enabling the use of visualization tools of MATLAB. The interfacing is achieved by using GDXMRW, a tool for moving data between GAMS and MATLAB as described in **ferris2011gdxmrw**

Notation

Indices

g	Index of types of diesel generators (DG).
p	Index of types of photovoltaic (PV) arrays.
w	Index of types of wind turbines (WT).
b	Index of types of storage battery (SB).
c	Index of types of bidirectional converters (BC).
h	Index of number of hours.
d	Index of number of typical days (one per season).
s	Index of scenarios.
ℓ	index set of components and types to be considered $\ell \in \{g, p, w, b, c\}$.

Sets

$\boldsymbol{\mathcal{U}}_d^d$	Uncertainty set for electric demand in hour h of typical day d.
$\boldsymbol{\mathcal{U}}_d^p$	Uncertainty set for the generation from PV panel of type p in hour h of typical day d.
$\boldsymbol{\mathcal{U}}_d^w$	Uncertainty set for generation from WT turbine of type w in hour h of typical day d.

Variables

$TAIC$	total annualized investment cost.
$AEOC$	Expected annualized operational cost.
x_{p,n_p}	binary variable indicating the selection of n_p^{th} solution from search space of PV of type p.
x_{w,n_w}	binary variable indicating selection of n_w^{th} solution from search space of WT of type w.
x_{b,n_b}	binary variable indicating the selection of n_b^{th} solution from search space of SB of type b.
x_{c,n_c}	binary variable indicating selection of n_c^{th} solution from search space of BC of type c.
x_{g,n_g}	binary variable indicating the selection of n_g^{th} solution from search space of DG of type g.
$P_{d,h,b,s}^{dch}$	discharging power from the SBB of type b in scenario s.
$P_{d,h}^{dg,tot}$	total power from online DGs.
$P_{d,h,s}^{dg,tot}$	total power from online DGs in scenario s.
$P_{d,h}^{dch}$	total discharging from the SBBs.
$P_{d,h,s}^{dch}$	total discharging from the SBBs in scenario s.

$P_{d,h}^{ren,L}$	total power from RES supplied directly to the load.
$P_{d,h,s}^{ren,L}$	total power from RES supplied directly to the load in scenario s.
$P_{d,h}^{dg,ch}$	total charging power from DGs.
$P_{d,h,s}^{dg,ch}$	total charging power from DGs in scenario s.
$P_{d,h}^{ren,tot}$	total generation from RESs.
$P_{d,h,s}^{ren,tot}$	total generation from RESs in scenario s.
$P_{d,h}^{ren,ch}$	total charging power from RESs.
$P_{d,h,s}^{ren,ch}$	total charging power from RESs in scenario s.
$P_{d,h,g}$	generation from a group of DGs of type g.
$P_{d,h,g,s}$	generation from a group of DGs of type g in scenario s.
$P_{d,h,b}^{ch}$	charging power to the SBB of type b.
$P_{d,h,b,s}^{ch}$	charging power to the SBB of type b in scenario s.
$w_{d,h}^{inv}$	binary variable indicating BCs inversion mode.
$w_{d,h,s}^{inv}$	binary variable indicating BCs inversion mode in scenario s.
$w_{d,h}^{rec}$	binary variable indicating the BCs rectification mode.
$w_{d,h,s}^{rec}$	binary variable indicating the BCs rectification mode in scenario s.
$E_{d,h,b}$	energy in the SBB of type b.
$E_{d,h,b,s}$	energy in the SBB of type b in scenario s.
$E_{0,b}$	initial energy in the SBB of type b.
$\overline{C}_b$	total capacity of SBB of type b.
$\overline{E}_b$	maximum energy limit of SBB of type b.
$\underline{E}_b$	minimum energy limit for SBB of type b.
$x_{d,h}^{ch}$	binary variable indicating that the SBB is charging.
$x_{d,h,s}^{ch}$	binary variable indicating the charging of SBBs in scenario s.
$x_{d,h}^{ch}$	binary variable indicating the discharging of SBBs.
$x_{d,h,s}^{ch}$	binary variable indicating the discharging of SBBs in scenario s.
$P_{d,h}^{pv,tot}$	total generation from PV arrays.
$P_{d,h,s}^{pv,tot}$	total generation from PV arrays in scenario s.
$P_{d,h,s}^{wt,tot}$	total generation from WTs in scenario s.
$\zeta_{d,h}^{d}$	binary variable indicating deviation in electric demand in hour h of typical day d.
$\zeta_{d,h}^{p}$	binary variable indicating deviation in the generation from PV panel of type p in hour h of typical day d.
$\zeta_{d,h}^{w}$	binary variable indicating deviation in the generation from WT turbine of type w, in hour h of typical day d.
$P_{d,h,g}^{exc}$	excess power from online DG of type g.
N_p	number of installed PVs.
N_c	number of installed BCs.
N_b	number of installed SBs.
N_g	number of installed DGs.
N_w	number of installed WTs.
$U_{d,h,g}$	number of online DGs.
$V_{d,h,g}$	number of DGs started-up.
$Z_{d,h,g}$	number of DGs shut-down.

$U_{d,h,g,s}$	number of online in scenario s.
$V_{d,h,g,s}$	number of started-up DG in scenario s.
$Z_{d,h,g,s}$	number of shut-down DG in scenario s.
$P_{d,h,b}^{dch}$	discharging power from the SBB of type b.
$P_{d,h,b,s}^{dch}$	discharging power from the SBB b in scenario s.
$FC_{d,h,g}$	fuel consumption for DGs of type g in hour h of day d.
$P_{d,h}^{dg,exc}$	total excess power from DGs.
$P_{d,h,s}^{dg,exc}$	total excess power from DGs in scenario s.
$P_{d,h}^{ren,spl}$	total spilled power from RESs.
$P_{d,h,s}^{ren,spl}$	total spilled power from RESs in scenario s.
y_q	binary variable indicating the selection of segment q in PWLA function.
N_p^{par}	number of parallel connected PV panels.
N_b^{par}	number of parallel connected batteries in a string of SB of type b.
$E_{1,0,b}^{tot}$	total initial energy in the SBB of type b.
$E_{1,0,b}^{a}$	available initial energy in the SBB of type b.
$E_{1,0,b}^{b}$	bound initial energy in the SBB of type b.
$E_{d,h,b}^{tot}$	total energy in the SBB of type b.
$E_{d,h,b}^{a}$	available energy in the SBB of type b.
$E_{d,h,b}^{b}$	bound energy in the SBB of type b.
c_b	capacity ratio parameter for the SBB of type b.
k_b	rate constant parameter for the SBB of type b.
$P_{d,h,b}^{net}$	net power of the SBB of type b.

Parameters

$ACIC_\ell$	annualized capital and installation cost.
ARC_ℓ	annualized replacement cost.
SFF_ℓ	sinking fund factor.
$AOMC_\ell$	annuallized operation and maintenance cost.
CC_ℓ	capital cost.
IC_ℓ	Installation costs.
CRF	capital recovery factor.
r_{real}	real interest rate.
Y_{proj}	project lifetime.
r_{nom}	nominal interest rate.
r_{infl}	inflation rate.
RC_ℓ	replacement cost.
$f_{rep,\ell}$	replacement factor.
Y_ℓ	lifetime of component.
SV_ℓ	salvage value.
$Y_{rem,\ell}$	remaining lifetime.
AC_ℓ	annualized cost of component.
$Y_{rep,\ell}$	number of replacement of component.
f_d	weight of the typical day d.
RC_g	replacement cost for DG of type g.

List of Symbols

$C_{bw,b}$	SBB wear cost.
C_{fuel}	fuel cost.
OMC_g	operational and maintenance cost for DG of type g.
SUC_g	start-up cost for DG of type g.
SDC_g	shut-down cost for DG of type g.
C_{exc}	penalty cost for excess DG power.
C_{spl}	penalty cost for spilling RES generation.
RC_b	replacement cost of a SB of type b.
Q_{life_b}	lifetime throughput of a single battery.
η_b^{rt}	round trip efficiency of SB of type b.
η_b^{ch}	charging efficiency of SB of type b.
η_b^{ch}	discharging efficiency of SB of type b.
$\pi_{d,s}$	probability of scenario s in typical day d.
N_{p,n_p}^{par}	number of parallel connected PV panels of type p specified in the n_p^{th} solution of the search space.
N_p^{ser}	number of series strings of PV panels of type p.
N_{w,n_w}	number of WTs of type w specified in the n_w^{th} solution of the search space.
N_{b,n_b}^{par}	number of parallel connected SB of type b specified in the n_b^{th} solution of the search space.
N_b^{ser}	number of series strings of SB of type b.
N_{c,n_c}	number of BC of type c specified in the n_c^{th} solution of the search space.
N_{g,n_g}	number of DG of type g specified in the n_g^{th} solution of the search space.
AC_p	annualized installation cost of PV panel of type p.
AC_w	annualized installation cost of WT of type w.
AC_b	annualized installation cost of SB of type b.
AC_c	annualized installation cost of BC of type b.
AC_g	annualized installation cost of DG of type g.
Y_g	lifetime of DG of type g.
$B_{q,g}$	slope of linear segment q of PWLA of input-output characteristic of DG of type g.
$A_{q,g}$	y-intercept of linear segment q of PWLA of input-output characteristic of DG of type g.
η_{inv}	BC inversion efficiency.
η_{rec}	BC rectification efficiency.
$D_{d,h}$	electric demand.
$D_{d,h,s}$	electric demand in scenario s.
$D_{d,h}^u$	unmet demand.
$\overline{P}_{d,h,p}$	per unit MPP generation from PV panel of type p.
$\overline{P}_{d,h,s,p}$	per unit MPP generation from PV panel of type p in scenario s.
$\overline{P}_{d,h,w}$	per unit MPP generation from WT of type w.
$\overline{P}_{d,h,s,w}$	per unit MPP generation from WT of type w in scenario s.
$\overline{P}_c^{inv}$	maximum inversion capacity of a BC of type c.
$\overline{P}_c^{rec}$	maximum rectification capacity of a BC of type c.
M	Big number.
$\underline{P}_g$	minimum power from DG of type g.
$\overline{P}_g$	maximum power from DG of type g.

Δh	time step.
$SOC_{0,b}$	relative initial SOC of SBB of type b.
C_b	nominal capacity of a single SB of type b.
V_b	nominal voltage of a SB of type b.
DOD_b	depth of discharge of SBB of type b.
$\overline{P}_b^{ch}$	maximum charging power for the SB of type b.
$\overline{Chr}_b$	maximum charging rate for the SB of type b.
$\overline{P}_b^{dch}$	maximum discharging power for the SB of type b.
$D_{d,h}^d$	average electric demand in hour h of typical day d.
$P_{d,h}^p$	average generation from PV panel of type p in hour h of typical day d.
$P_{d,h}^w$	average forecasted generation from WT of type w in hour h of typical day d.
$\sigma_{d,h}^p$	standard deviation for electric demand in hour h of typical day d.
$\sigma_{d,h}^w$	standard deviation for generation from PV panel of type p in hour h of typical day d.
$\sigma_{d,h}^d$	standard deviation for generation from WT of type w in hour h of typical day d.
Γ_d^d	budget of uncertainty for the electric demand in typical day d.
Γ_d^p	budget of uncertainty for the generation from PVs in typical day d.
Γ_d^w	budget of uncertainty for the generation from WTs in typical day d.
$MAUE$	maximum allowable unmet energy.
E_{total}	total energy energy.
f_{ren}	renewable fraction.
UT_g	minimum up-time for DG of type g.
DT_g	minimum down-time for DG of type g.
H	time length of a day, i.e. hour 24.
$\bar{I}_b^{ch}$	maximum charging current of the SBB of type b.
f_{der}	derating factor.
$G_{d,h}$	irradiance at hour h of typical day d.
G^{STC}	irradiance at STC.
P_p^{STC}	output power of PV of type p at STC.
T^{STC}	temprature at STC.
$NOCT_p$	Nominal Operating Cell Temperature.
γ_p	temperature coefficient for output power from PV of type p.

Bibliography

[1] Q. Fu, A. Hamidi, A. Nasiri, V. Bhavaraju, S. Krstic, and P. Theisen, "The role of energy storage in a microgrid concept: Examining the opportunities and promise of microgrids.," *Electrification Magazine, IEEE*, vol. 1, no. 2, pp. 21–29, 2013, ISSN: 2325-5897. DOI: 10.1109/MELE.2013.2294736 (cit. on p. 1).

[2] R. Lasseter, A. Akhil, C. Marnay, J. Stephens, J. Dagle, R. Guttromson, A Meliopoulous, R. Yinger, and J. Eto, "The certs microgrid concept, white paper on integration of distributed energy resources," *California Energy Commission, Office of Power Technologies-US Department of Energy, LBNL-50829, http://certs. lbl. gov*, 2002 (cit. on p. 1).

[3] EERE, DOE, "Summary report: 2012 DOE microgrid workshop," *Chicago, Illinois, Jul*, 2012 (cit. on p. 1).

[4] R. L. Dohn, "The business case for microgrids," *Siemens AG White paper*, 2011 (cit. on p. 1).

[5] J. Driesen and F. Katiraei, "Design for distributed energy resources," *Power and Energy Magazine, IEEE*, vol. 6, no. 3, pp. 30–40, 2008, ISSN: 1540-7977. DOI: 10.1109/MPE.2008.918703 (cit. on p. 2).

[6] R Alford, M Dean, P Hoontrakul, and P Smith, "Power systems of the future: The case for energy storage, distributed generation, and microgrids," *Zpryme Research & Consulting, Tech. Rep*, 2012 (cit. on p. 2).

[7] S. Chowdhury, *Microgrids and Active Distribution Networks*, ser. Energy Engineering. Institution of Engineering and Technology, 2009. [Online]. Available: http://digital-library.theiet.org/content/books/po/pbrn006e (cit. on pp. 2, 28, 29).

[8] F. Birol *et al.*, "World energy outlook 2014," *Paris: International Energy Agency (IEA)*, 2014. [Online]. Available: http://www.worldenergyoutlook.org/resources/energydevelopment/energyaccessdatabase/ (cit. on p. 2).

[9] S. Bhattacharyya, "Introduction," English, in *Rural Electrification Through Decentralised Off-grid Systems in Developing Countries*, ser. Green Energy and Technology, S. Bhattacharyya, Ed., Springer London, 2013, pp. 3–12, ISBN: 978-1-4471-4672-8. DOI: 10.1007/978-1-4471-4673-5_1. [Online]. Available: http://dx.doi.org/10.1007/978-1-4471-4673-5_1 (cit. on p. 2).

[10] N. Jenkins, *Distributed Generation*, ser. Energy Engineering. Institution of Engineering and Technology, 2010. [Online]. Available: http://digital-library.theiet.org/content/books/po/pbrn001e (cit. on p. 2).

[11] D. Tagare, "Distributed generation (dg) and distributed resources (dr)," in *Electricity Power Generation:The Changing Dimensions*. Wiley-IEEE Press, 2011, pp. 275–299, ISBN: 9780470872659. DOI: 10.1002/9780470872659.ch14. [Online]. Available: http://ieeexplore.ieee.org/xpl/articleDetails.jsp?arnumber=5713333 (cit. on p. 2).

[12] A Shortt, J. Kiviluoma, and M. ÓMalley, "Accommodating variability in generation planning," *Power Systems, IEEE Transactions on*, vol. 28, no. 1, pp. 158–169, 2013, ISSN: 0885-8950. DOI: 10.1109/TPWRS.2012.2202925 (cit. on pp. 3, 13).

[13] P. Liu, M. C. Georgiadis, and E. N. Pistikopoulos, "An energy systems engineering approach for the design and operation of microgrids in residential applications," *Chemical Engineering Research and Design*, vol. 91, no. 10, pp. 2054 –2069, 2013, The 60th Anniversary of the European Federation of Chemical Engineering (EFCE), ISSN: 0263-8762. DOI: http://dx.doi.org/10.1016/j.cherd.2013.08.016. [Online]. Available: http://www.sciencedirect.com/science/article/pii/S0263876213003456 (cit. on pp. 3, 68).

[14] M. Stadler, M. Groissbock, G. Cardoso, and C. Marnay, "Optimizing distributed energy resources and building retrofits with the strategic der-camodel," *Applied Energy*, vol. 132, pp. 557 –567, 2014, ISSN: 0306-2619. DOI: http://dx.doi.org/10.1016/j.apenergy.2014.07.041. [Online]. Available: http://www.sciencedirect.com/science/article/pii/S0306261914007235 (cit. on p. 3).

[15] S. Giglmayr, A. C. Brent, P. Gauché, and H. Fechner, "Utility-scale {pv} power and energy supply outlook for south africa in 2015," *Renewable Energy*, vol. 83, pp. 779 –785, 2015, ISSN: 0960-1481. DOI: http://dx.doi.org/10.1016/j.renene.2015.04.058. [Online]. Available: http://www.sciencedirect.com/science/article/pii/S096014811500347X (cit. on p. 3).

[16] A. Malheiro, P. M. Castro, R. M. Lima, and A. Estanqueiro, "Integrated sizing and scheduling of wind/pv/diesel/battery isolated systems," *Renewable Energy*, vol. 83, pp. 646 –657, 2015, ISSN: 0960-1481. DOI: http://dx.doi.org/10.1016/j.renene.2015.04.066. [Online]. Available: http://www.sciencedirect.com/science/article/pii/S0960148115003559 (cit. on pp. 3, 22).

[17] H. G. Stoll and L. J. Garver, *Least-cost electric utility planning*. J. Wiley, 1989 (cit. on p. 8).

[18] D Phillips, F. Jenkin, J. Pritchard, and K Rybicki, "A mathematical model for determining generating plant mix," *Proceedings of the Third IEEE PSCC*, 1969 (cit. on p. 8).

[19] T. Zhang, R. Baldick, and T. Deetjen, “Optimized generation capacity expansion using a further improved screening curve method,” *Electric Power Systems Research*, vol. 124, pp. 47–54, 2015, cited By 0. DOI: 10.1016/j.epsr.2015.02.017. [Online]. Available: http://www.scopus.com/inward/record.url?eid=2-s2.0-84925360154&partnerID=40&md5=a30e978634fe14a7dbe73c3e7bf6bd0e (cit. on p. 10).

[20] C. Batlle and P. Rodilla, “An enhanced screening curves method for considering thermal cycling operation costs in generation expansion planning,” *Power Systems, IEEE Transactions on*, vol. 28, no. 4, pp. 3683–3691, 2013, ISSN: 0885-8950. DOI: 10.1109/TPWRS.2013.2249540 (cit. on p. 10).

[21] T. Levin, V. Thomas, and A. Lee, “A markal model of state electricity generation,” in *Sustainable Systems and Technology (ISSST), 2010 IEEE International Symposium on*, 2010, pp. 1–5. DOI: 10.1109/ISSST.2010.5507755 (cit. on p. 10).

[22] W. Buehring, C Huber, and J. M. de Souza, “Expansion planning for electrical generating systems: A guidebook,” *International Atomic Energy Agency, Tech. Rep*, 1984 (cit. on p. 10).

[23] International Atomic Energy Agency (IAEA), “Wien automatic system planning (WASP) package: A computer code for power generating system expansion planning,” International Atomic Energy Agency, Vienna, Austria, User’s Manual, 2001, Version WASP-IV (cit. on p. 10).

[24] T. Epperly, T. Edmunds, A. Lamont, C. Meyers, S. Smith, Y. Yao, and G. Drayton, “High-performance computing for electric grid planning and operations,” in *Power and Energy Society General Meeting, 2012 IEEE*, 2012, pp. 1–4. DOI: 10.1109/PESGM.2012.6345086 (cit. on p. 10).

[25] B. Hadzi-Kostova, L. Oprea, V. Popescu, and T. Veselka, “Simulation of regional power markets in the planning of trans-border interconnections,” in *PowerTech, 2009 IEEE Bucharest*, 2009, pp. 1–6. DOI: 10.1109/PTC.2009.5282191 (cit. on p. 10).

[26] J. Apt and P. Jaramillo, *Variable Renewable Energy and the Electricity Grid*. Taylor & Francis, 2014, ISBN: 9781317907671. [Online]. Available: https://books.google.co.uk/books?id=_Z3OAwAAQBAJ (cit. on p. 10).

[27] I. P. Power Costs, *TextscPCI-gentrader*, http://www.powercosts.com/wp-content/uploads/PCI-GenTrader.pdf, Accessed: 2015-08-15 (cit. on p. 10).

[28] P. Denholm, R. M. Margolis, and J. Milford, *Production cost modeling for high levels of photovoltaics penetration*. National Renewable Energy Laboratory Golden, CO, 2008 (cit. on p. 10).

[29] A. Pina, C. A. Silva, and P. Ferrao, “High-resolution modeling framework for planning electricity systems with high penetration of renewables,” *Applied Energy*, vol. 112, pp. 215 –223, 2013, ISSN: 0306-2619. DOI: http://dx.doi.org/10.1016/j.apenergy.2013.05.074. [Online]. Available: http://www.sciencedirect.com/science/article/pii/S030626191300487X (cit. on p. 10).

[30] J. Bebic, *Power system planning: Emerging practices suitable for evaluating the impact of high-penetration photovoltaics*. National Renewable Energy Laboratory, 2008 (cit. on p. 11).

[31] S. Gómez, J. Solano, L. Castellanos, and M. Quintana, "Tunneling and genetic algorithms for global optimization," English, in *Advances in Convex Analysis and Global Optimization*, ser. Nonconvex Optimization and Its Applications, N. Hadjisavvas and P. Pardalos, Eds., vol. 54, Springer US, 2001, pp. 553–567, ISBN: 978-0-7923-6942-4. DOI: `10.1007/978-1-4613-0279-7_36`. [Online]. Available: `http://dx.doi.org/10.1007/978-1-4613-0279-7_36` (cit. on p. 11).

[32] K. Lee and M. El-Sharkawi, *Modern Heuristic Optimization Techniques: Theory and Applications to Power Systems*, ser. IEEE Press Series on Power Engineering. Wiley, 2008, ISBN: 9780470225851. [Online]. Available: `https://books.google.co.uk/books?id=ZHRTmJfyeVYC` (cit. on p. 11).

[33] S. Kannan, S. Slochanal, and N. Padhy, "Application and comparison of metaheuristic techniques to generation expansion planning problem," *Power Systems, IEEE Transactions on*, vol. 20, no. 1, pp. 466–475, 2005, ISSN: 0885-8950. DOI: `10.1109/TPWRS.2004.840451` (cit. on p. 11).

[34] J.-B. Park, Y.-M. Park, J.-R. Won, and K. Lee, "An improved genetic algorithm for generation expansion planning," *Power Systems, IEEE Transactions on*, vol. 15, no. 3, pp. 916–922, 2000, ISSN: 0885-8950. DOI: `10.1109/59.871713` (cit. on p. 12).

[35] S. Kannan, S. Baskar, J. McCalley, and P. Murugan, "Application of nsga-ii algorithm to generation expansion planning," *Power Systems, IEEE Transactions on*, vol. 24, no. 1, pp. 454–461, 2009, ISSN: 0885-8950. DOI: `10.1109/TPWRS.2008.2004737` (cit. on p. 12).

[36] G. A. Bakirtzis, P. N. Biskas, and V. Chatziathanasiou, "Generation expansion planning by {milp} considering mid-term scheduling decisions," *Electric Power Systems Research*, vol. 86, pp. 98 –112, 2012, ISSN: 0378-7796. DOI: `http://dx.doi.org/10.1016/j.epsr.2011.12.008`. [Online]. Available: `http://www.sciencedirect.com/science/article/pii/S0378779611003178` (cit. on p. 12).

[37] L. Mari and N. Nabona, "Renewable energies in medium-term power planning," *Power Systems, IEEE Transactions on*, vol. 30, no. 1, pp. 88–97, 2015, ISSN: 0885-8950. DOI: `10.1109/TPWRS.2014.2328033` (cit. on p. 12).

[38] F. Noonan and R. J. Giglio, "Planning electric power generation: A nonlinear mixed integer model employing benders decomposition," *Management Science*, vol. 23, no. 9, pp. 946–956, 1977. DOI: `10.1287/mnsc.23.9.946`. eprint: `http://dx.doi.org/10.1287/mnsc.23.9.946`. [Online]. Available: `http://dx.doi.org/10.1287/mnsc.23.9.946` (cit. on p. 12).

[39] F. Careri, C. Genesi, P. Marannino, M. Montagna, S. Rossi, and I. Siviero, "Generation expansion planning in the age of green economy," *Power Systems, IEEE Transactions on*, vol. 26, no. 4, pp. 2214–2223, 2011, ISSN: 0885-8950. DOI: `10.1109/TPWRS.2011.2107753` (cit. on p. 12).

[40] J. A. Bloom, "Solving an electricity generating capacity expansion planning problem by generalized benders' decomposition," English, *Operations Research*, vol. 31, no. 1, pp. 84–100, 1983, ISSN: 0030364X. [Online]. Available: `http://www.jstor.org/stable/170276` (cit. on p. 12).

[41] R. Doherty, H. Outhred, and M. O'Malley, "Establishing the role that wind generation may have in future generation portfolios," *Power Systems, IEEE Transactions on*, vol. 21, no. 3, pp. 1415–1422, 2006, ISSN: 0885-8950. DOI: 10.1109/TPWRS.2006.879258 (cit. on p. 12).

[42] M. Welsch, M. Howells, M. R. Hesamzadeh, B. Ó Gallachóir, P. Deane, N. Strachan, M. Bazilian, D. M. Kammen, L. Jones, G. Strbac, and H. Rogner, "Supporting security and adequacy in future energy systems: The need to enhance long-term energy system models to better treat issues related to variability," *International Journal of Energy Research*, vol. 39, no. 3, pp. 377–396, 2015, ISSN: 1099-114X. DOI: 10.1002/er.3250. [Online]. Available: http://dx.doi.org/10.1002/er.3250 (cit. on p. 13).

[43] M. Welsch, P. Deane, M. Howells, B. O. Gallachóir, F. Rogan, M. Bazilian, and H.-H. Rogner, "Incorporating flexibility requirements into long-term energy system models – a case study on high levels of renewable electricity penetration in ireland," *Applied Energy*, vol. 135, pp. 600 –615, 2014, ISSN: 0306-2619. DOI: http://dx.doi.org/10.1016/j.apenergy.2014.08.072. [Online]. Available: http://www.sciencedirect.com/science/article/pii/S0306261914008836 (cit. on p. 13).

[44] P. Vithayasrichareon and I. MacGill, "Impacts of generation-cycling costs on future electricity generation portfolio investment," in *PES General Meeting | Conference Exposition, 2014 IEEE*, 2014, pp. 1–5. DOI: 10.1109/PESGM.2014.6938915 (cit. on p. 13).

[45] B. Palmintier and M. Webster, "Impact of unit commitment constraints on generation expansion planning with renewables," in *Power and Energy Society General Meeting, 2011 IEEE*, 2011, pp. 1–7. DOI: 10.1109/PES.2011.6038963 (cit. on pp. 13, 50).

[46] P. Vithayasrichareon and I. F. MacGill, "A monte carlo based decision-support tool for assessing generation portfolios in future carbon constrained electricity industries," *Energy Policy*, vol. 41, pp. 374 –392, 2012, Modeling Transport (Energy) Demand and Policies, ISSN: 0301-4215. DOI: http://dx.doi.org/10.1016/j.enpol.2011.10.060. [Online]. Available: http://www.sciencedirect.com/science/article/pii/S0301421511008755 (cit. on p. 13).

[47] F. Farzan, F. Farzan, M. Jafari, K. Gharieh, and R. Masiello, "Closing the loop between short-term operational volatilities and long-term investment risks in microgrids," in *Innovative Smart Grid Technologies Conference (ISGT), 2014 IEEE PES*, 2014, pp. 1–5. DOI: 10.1109/ISGT.2014.6816368 (cit. on p. 14).

[48] B. Borowy and Z. Salameh, "Methodology for optimally sizing the combination of a battery bank and pv array in a wind/pv hybrid system," *Energy Conversion, IEEE Transactions on*, vol. 11, no. 2, pp. 367–375, 1996, ISSN: 0885-8969. DOI: 10.1109/60.507648 (cit. on p. 14).

[49] M. Lee, D. Soto, and V. Modi, "Cost versus reliability sizing strategy for isolated photovoltaic micro-grids in the developing world," *Renewable Energy*, vol. 69, no. 0, pp. 16 –24, 2014, ISSN: 0960-1481. DOI: http://dx.doi.org/10.1016/j.renene.2014.03.019 (cit. on p. 14).

[50] A. Kaabeche and R. Ibtiouen, "Techno-economic optimization of hybrid photovoltaic/wind/diesel/-battery generation in a stand-alone power system," *Solar Energy*, vol. 103, pp. 171 –182, 2014, ISSN: 0038-092X. DOI: `http://dx.doi.org/10.1016/j.solener.2014.02.017`. [Online]. Available: `http://www.sciencedirect.com/science/article/pii/S0038092X14000954` (cit. on p. 15).

[51] H. Belmili, M. Haddadi, S. Bacha, M. F. Almi, and B. Bendib, "Sizing stand-alone photovoltaic–wind hybrid system: Techno-economic analysis and optimization," *Renewable and Sustainable Energy Reviews*, vol. 30, pp. 821 –832, 2014, ISSN: 1364-0321. DOI: `http://dx.doi.org/10.1016/j.rser.2013.11.011`. [Online]. Available: `http://www.sciencedirect.com/science/article/pii/S1364032113007600` (cit. on p. 15).

[52] T. Orhan, G. Shafiullah, A. Stojcevski, and A. Oo, "A feasibility study on microgrid for various islands in australia," in *Power Engineering Conference (AUPEC), 2014 Australasian Universities*, 2014, pp. 1–8. DOI: `10.1109/AUPEC.2014.6966604` (cit. on p. 15).

[53] K. Tanaka and K. Maeda, "Simulation-based design of microgrid system for a resort community," in *Clean Electrical Power (ICCEP), 2011 International Conference on*, 2011, pp. 28–34. DOI: `10.1109/ICCEP.2011.6036324` (cit. on p. 15).

[54] C. D. Barley, C. Winn, L Flowers, and H. Green, "Optimal control of remote hybrid power systems. part 1: Simplified model," National Renewable Energy Lab., Golden, CO (United States), Tech. Rep., 1995 (cit. on p. 15).

[55] F. Bhuiyan, A. Yazdani, and S. Primak, "Optimal sizing approach for islanded microgrids," *Renewable Power Generation, IET*, vol. 9, no. 2, pp. 166–175, 2015, ISSN: 1752-1416. DOI: `10.1049/iet-rpg.2013.0416` (cit. on p. 15).

[56] F. A. Bhuiyan, A. Yazdani, and S. L. Primak, "Modeling, simulation, and performance analysis of power management strategies for an islanded microgrid," *International Journal of Energy Science*, vol. 3, no. 6, pp. 383–394, 2013, ISSN: 2304-3679. DOI: `10.14355/ijes.2013.0306.02` (cit. on pp. 15, 47).

[57] L. Zhang, G. Barakat, and A. Yassine, "Design and optimal sizing of hybrid pv/wind/diesel system with battery storage by using direct search algorithm," in *Power Electronics and Motion Control Conference (EPE/PEMC), 2012 15th International*, 2012, DS3b.19–1–DS3b.19–7. DOI: `10.1109/EPEPEMC.2012.6397335` (cit. on p. 15).

[58] K.-H. Chang and G. Lin, "Optimal design of hybrid renewable energy systems using simulation optimization," *Simulation Modelling Practice and Theory*, vol. 52, pp. 40 –51, 2015, ISSN: 1569-190X. DOI: `http://dx.doi.org/10.1016/j.simpat.2014.12.002`. [Online]. Available: `http://www.sciencedirect.com/science/article/pii/S1569190X14001890` (cit. on p. 17).

[59] J. Xiao, L. Bai, F. Li, H. Liang, and C. Wang, "Sizing of energy storage and diesel generators in an isolated microgrid using discrete fourier transform (dft)," *Sustainable Energy, IEEE Transactions on*, vol. 5, no. 3, pp. 907–916, 2014, ISSN: 1949-3029. DOI: `10.1109/TSTE.2014.2312328` (cit. on p. 17).

[60] D. Goldberg, *Genetic Algorithms in Search, Optimization, and Machine Learning*, ser. Artificial Intelligence. Addison-Wesley Publishing Company, 1989, ISBN: 9780201157673. [Online]. Available: `https://books.google.co.uk/books?id=3\_RQAAAAMAAJ` (cit. on p. 17).

[61] R. Dufo-López and J. L. Bernal-Agustín, "Design and control strategies of pv-diesel systems using genetic algorithms," *Solar Energy*, vol. 79, no. 1, pp. 33 –46, 2005, ISSN: 0038-092X. DOI: `http://dx.doi.org/10.1016/j.solener.2004.10.004`. [Online]. Available: `http://www.sciencedirect.com/science/article/pii/S0038092X04003020` (cit. on p. 18).

[62] R. Dufo-López, *Software ihoga*, `http://personal.unizar.es/rdufo/index.php?option=com_content&view=article&id=2&Itemid=104&lang=en`, Accessed: 2015-08-13 (cit. on p. 18).

[63] E. Koutroulis, D. Kolokotsa, A. Potirakis, and K. Kalaitzakis, "Methodology for optimal sizing of stand-alone photovoltaic/wind-generator systems using genetic algorithms," *Solar Energy*, vol. 80, no. 9, pp. 1072 –1088, 2006, ISSN: 0038-092X. DOI: `http://dx.doi.org/10.1016/j.solener.2005.11.002`. [Online]. Available: `http://www.sciencedirect.com/science/article/pii/S0038092X05003713` (cit. on p. 18).

[64] B. Zhao, X. Zhang, P. Li, K. Wang, M. Xue, and C. Wang, "Optimal sizing, operating strategy and operational experience of a stand-alone microgrid on dongfushan island," *Applied Energy*, vol. 113, pp. 1656 –1666, 2014, ISSN: 0306-2619. DOI: `http://dx.doi.org/10.1016/j.apenergy.2013.09.015`. [Online]. Available: `http://www.sciencedirect.com/science/article/pii/S0306261913007629` (cit. on p. 19).

[65] M. A. Marin, "Long-term renewable energy electricity planning for remote communities," PhD thesis, University of Waterloo, Ontario, Canada, 2015 (cit. on pp. 19, 21).

[66] M. Shadmand and R. Balog, "Multi-objective optimization and design of photovoltaic-wind hybrid system for community smart dc microgrid," *Smart Grid, IEEE Transactions on*, vol. 5, no. 5, pp. 2635–2643, 2014, ISSN: 1949-3053. DOI: `10.1109/TSG.2014.2315043` (cit. on p. 19).

[67] A. Navaeefard, S. Tafreshi, M. Barzegari, and A. Shahrood, "Optimal sizing of distributed energy resources in microgrid considering wind energy uncertainty with respect to reliability," in *Energy Conference and Exhibition (EnergyCon), 2010 IEEE International*, 2010, pp. 820–825. DOI: `10.1109/ENERGYCON.2010.5771795` (cit. on p. 19).

[68] S. Avril, G. Arnaud, A. Florentin, and M. Vinard, "Multi-objective optimization of batteries and hydrogen storage technologies for remote photovoltaic systems," *Energy*, vol. 35, no. 12, pp. 5300 –5308, 2010, The 3rd International Conference on Sustainable Energy and Environmental Protection, {SEEP} 2009, ISSN: 0360-5442. DOI: `http://dx.doi.org/10.1016/j.energy.2010.07.033`. [Online]. Available: `http://www.sciencedirect.com/science/article/pii/S0360544210004081` (cit. on p. 19).

[69] S. Kahrobaee, S. Asgarpoor, and W. Qiao, "Optimum sizing of distributed generation and storage capacity in smart households," *Smart Grid, IEEE Transactions on*, vol. 4, no. 4, pp. 1791–1801, 2013, ISSN: 1949-3053. DOI: `10.1109/TSG.2013.2278783` (cit. on p. 19).

[70] A. Hassan, M. Saadawi, M. Kandil, and M. Saeed, “Modified particle swarm optimisation technique for optimal design of small renewable energy system supplying a specific load at mansoura university,” *Renewable Power Generation, IET*, vol. 9, no. 5, pp. 474–483, 2015, ISSN: 1752-1416. DOI: 10.1049/iet-rpg.2014.0170 (cit. on p. 19).

[71] O. Ekren and B. Y. Ekren, “Size optimization of a pv/wind hybrid energy conversion system with battery storage using simulated annealing,” *Applied Energy*, vol. 87, no. 2, pp. 592 –598, 2010, ISSN: 0306-2619. DOI: http://dx.doi.org/10.1016/j.apenergy.2009.05.022. [Online]. Available: http://www.sciencedirect.com/science/article/pii/S0306261909002177 (cit. on p. 19).

[72] Y. Katsigiannis, P. Georgilakis, and E. Karapidakis, “Hybrid simulated annealing-tabu search method for optimal sizing of autonomous power systems with renewables,” *Sustainable Energy, IEEE Transactions on*, vol. 3, no. 3, pp. 330–338, 2012, ISSN: 1949-3029. DOI: 10.1109/TSTE.2012.2184840 (cit. on p. 19).

[73] B. Korte and J. Vygen, “Np-completeness,” English, in *Combinatorial Optimization*, ser. Algorithms and Combinatorics, vol. 21, Springer Berlin Heidelberg, 2012, pp. 377–412, ISBN: 978-3-642-24487-2. DOI: 10.1007/978-3-642-24488-9_15. [Online]. Available: http://dx.doi.org/10.1007/978-3-642-24488-9_15 (cit. on p. 21).

[74] I. Grossmann and J. Ruiz, “Generalized disjunctive programming: A framework for formulation and alternative algorithms for minlp optimization,” English, in *Mixed Integer Nonlinear Programming*, ser. The IMA Volumes in Mathematics and its Applications, J. Lee and S. Leyffer, Eds., vol. 154, Springer New York, 2012, pp. 93–115, ISBN: 978-1-4614-1926-6. DOI: 10.1007/978-1-4614-1927-3_4. [Online]. Available: http://dx.doi.org/10.1007/978-1-4614-1927-3_4 (cit. on p. 21).

[75] P. Liu, E. Pistikopoulos, and Z. Li, “Energy systems engineering: Methodologies and applications,” English, *Frontiers of Energy and Power Engineering in China*, vol. 4, no. 2, pp. 131–142, 2010, ISSN: 1673-7393. DOI: 10.1007/s11708-010-0035-8. [Online]. Available: http://dx.doi.org/10.1007/s11708-010-0035-8 (cit. on p. 21).

[76] H. Ren and W. Gao, “A {milp} model for integrated plan and evaluation of distributed energy systems,” *Applied Energy*, vol. 87, no. 3, pp. 1001 –1014, 2010, ISSN: 0306-2619. DOI: http://dx.doi.org/10.1016/j.apenergy.2009.09.023. [Online]. Available: http://www.sciencedirect.com/science/article/pii/S0306261909004152 (cit. on p. 21).

[77] P. Liu, E. N. Pistikopoulos, and Z. Li, “An energy systems engineering approach to the optimal design of energy systems in commercial buildings,” *Energy Policy*, vol. 38, no. 8, pp. 4224 –4231, 2010, ISSN: 0301-4215. DOI: http://dx.doi.org/10.1016/j.enpol.2010.03.051. [Online]. Available: http://www.sciencedirect.com/science/article/pii/S0301421510002144 (cit. on p. 21).

[78] Z. Zhou, P. Liu, Z. Li, and W. Ni, “An engineering approach to the optimal design of distributed energy systems in china,” *Applied Thermal Engineering*, vol. 53, no. 2, pp. 387 –396, 2013, Includes Special Issue: PRO-TEM Special Issue, ISSN: 1359-4311. DOI: http://dx.doi.org/10.1016/j.applthermaleng.2012.01.067. [Online]. Available: http:

//www.sciencedirect.com/science/article/pii/S135943111200097X (cit. on p. 21).

[79] Y. Han, P. Young, and D. Zimmerle, "Optimal selection of generators in a microgrid for fuel usage minimization," in *Power and Energy Society General Meeting (PES), 2013 IEEE*, 2013, pp. 1–5. DOI: 10.1109/PESMG.2013.6672746 (cit. on p. 22).

[80] S. Chen, H. Gooi, and M. Wang, "Sizing of energy storage for microgrids," *Smart Grid, IEEE Transactions on*, vol. 3, no. 1, pp. 142–151, 2012, ISSN: 1949-3053. DOI: 10.1109/TSG.2011.2160745 (cit. on p. 22).

[81] M. Vafaei and M. Kazerani, "Optimal unit-sizing of a wind-hydrogen-diesel microgrid system for a remote community," in *PowerTech, 2011 IEEE Trondheim*, 2011, pp. 1–7. DOI: 10.1109/PTC.2011.6019412 (cit. on p. 22).

[82] D. Nelson, M. Nehrir, and C. Wang, "Unit sizing and cost analysis of stand-alone hybrid wind/pv/-fuel cell power generation systems," *Renewable Energy*, vol. 31, no. 10, pp. 1641 –1656, 2006, ISSN: 0960-1481. DOI: http://dx.doi.org/10.1016/j.renene.2005.08.031. [Online]. Available: http://www.sciencedirect.com/science/article/pii/S0960148105002600 (cit. on p. 22).

[83] E. Sfikas, Y. Katsigiannis, and P. Georgilakis, "Simultaneous capacity optimization of distributed generation and storage in medium voltage microgrids," *International Journal of Electrical Power & Energy Systems*, vol. 67, pp. 101 –113, 2015, ISSN: 0142-0615. DOI: http://dx.doi.org/10.1016/j.ijepes.2014.11.009. [Online]. Available: http://www.sciencedirect.com/science/article/pii/S0142061514006917 (cit. on p. 22).

[84] T. Lambert, P. Gilman, and P. Lilienthal, "Micropower system modeling with homer," in *Integration of Alternative Sources of Energy*. John Wiley & Sons, Inc., 2006, pp. 379–418, ISBN: 9780471755623. DOI: 10.1002/0471755621.ch15. [Online]. Available: http://dx.doi.org/10.1002/0471755621.ch15 (cit. on pp. 23, 57, 58).

[85] C. Marnay, G. Venkataramanan, M. Stadler, A. Siddiqui, R. Firestone, and B. Chandran, "Optimal technology selection and operation of commercial-building microgrids," *Power Systems, IEEE Transactions on*, vol. 23, no. 3, pp. 975–982, 2008, ISSN: 0885-8950. DOI: 10.1109/TPWRS.2008.922654 (cit. on pp. 23, 24).

[86] O. Hafez and K. Bhattacharya, "Optimal planning and design of a renewable energy based supply system for microgrids," *Renewable Energy*, vol. 45, pp. 7 –15, 2012, ISSN: 0960-1481. DOI: http://dx.doi.org/10.1016/j.renene.2012.01.087. [Online]. Available: http://www.sciencedirect.com/science/article/pii/S0960148112000985 (cit. on p. 23).

[87] A. S. Siddiqui, C. Marnay, R. M. Firestone, and N. Zhou, "Distributed generation with heat recovery and storage," *Journal of Energy Engineering*, vol. 133, no. 3, pp. 181–210, 2007 (cit. on p. 24).

[88] Microgrids at Berkeley Lab, D*istributed* E*nergy* R*esources* C*ustomer* A*doption* M*odel* (DER-CAM), https://building-microgrid.lbl.gov/projects/der-cam, Accessed: 2015-08-19 (cit. on pp. 24, 25).

[89] D. Steen, M. Stadler, G. Cardoso, M. Groissböck, N. DeForest, and C. Marnay, "Modeling of thermal storage systems in {milp} distributed energy resource models," *Applied Energy*, vol. 137, pp. 782 –792, 2015, ISSN: 0306-2619. DOI: `http://dx.doi.org/10.1016/j.apenergy.2014.07.036`. [Online]. Available: `http://www.sciencedirect.com/science/article/pii/S0306261914007181` (cit. on p. 24).

[90] S. Beer, T. Gomez, D. Dallinger, I. Momber, C. Marnay, M. Stadler, and J. Lai, "An economic analysis of used electric vehicle batteries integrated into commercial building microgrids," *Smart Grid, IEEE Transactions on*, vol. 3, no. 1, pp. 517–525, 2012, ISSN: 1949-3053. DOI: `10.1109/TSG.2011.2163091` (cit. on p. 24).

[91] A. Litchy, C. Young, S. Pourmousavi, and M. Nehrir, "Technology selection and unit sizing for a combined heat and power microgrid: Comparison of webopt and homer application programs," in *North American Power Symposium (NAPS), 2012*, 2012, pp. 1–6. DOI: `10.1109/NAPS.2012.6336337` (cit. on p. 24).

[92] C. D. Barley and C. B. Winn, "Optimal dispatch strategy in remote hybrid power systems," *Solar Energy*, vol. 58, no. 4–6, pp. 165 –179, 1996, Selected Proceedings of the {ISES} 1995: Solar World Congress. Part {II}, ISSN: 0038-092X. DOI: `http://dx.doi.org/10.1016/S0038-092X(96)00087-4` (cit. on p. 25).

[93] J. McGowan, J. Manwell, C. Avelar, and C. Warner, "Hybrid wind/pv/diesel hybrid power systems modeling and south american applications," *Renewable Energy*, vol. 9, no. 1–4, pp. 836 –847, 1996, World Renewable Energy Congress Renewable Energy, Energy Efficiency and the Environment, ISSN: 0960-1481. DOI: `http://dx.doi.org/10.1016/0960-1481(96)88412-6`. [Online]. Available: `http://www.sciencedirect.com/science/article/pii/0960148196884126` (cit. on p. 25).

[94] Ministry Natural Resources Canada: RETScreen® International, RETS*creen* S*oftware* S*uite* - D*ownload* F*ree*, `http://www.retscreen.net/ang/home.php`, Accessed: 2015-08-19 (cit. on p. 25).

[95] S. Sinha and S. Chandel, "Review of software tools for hybrid renewable energy systems," *Renewable and Sustainable Energy Reviews*, vol. 32, pp. 192 –205, 2014, ISSN: 1364-0321. DOI: `http://dx.doi.org/10.1016/j.rser.2014.01.035`. [Online]. Available: `http://www.sciencedirect.com/science/article/pii/S136403211400046X` (cit. on p. 25).

[96] C. Schwaegerl and L. Tao, *Microgrids: Architectures and Control*. John Wiley and Sons Ltd, 2013, pp. 1–24, ISBN: 9781118720677. DOI: `10.1002/9781118720677.ch01`. [Online]. Available: `http://dx.doi.org/10.1002/9781118720677.ch01` (cit. on pp. 28, 29).

[97] A. Tsikalakis and N. Hatziargyriou, "Centralized control for optimizing microgrids operation," *Energy Conversion, IEEE Transactions on*, vol. 23, no. 1, pp. 241–248, 2008, ISSN: 0885-8969. DOI: `10.1109/TEC.2007.914686` (cit. on p. 28).

[98] ELVI SPA, *Elvi spa - energy and automation system*, `http://www.elvi-italia.com/en/applications/energy/`, Accessed: 2015-11-12 (cit. on p. 28).

[99] ABB S.A., *Renewable microgrid controller mgc600*, `http://new.abb.com/docs/default-source/ewea-doc/microgrid-controller-600_en_lr(dic2013).pdf?sfvrsn=2`, Accessed: 2015-11-12 (cit. on p. 28).

[100] O. Skarstein and K. Uhlen, "Design considerations with respect to long-term diesel saving in wind/diesel plants," *Wind Eng*, vol. 13, no. 2, pp. 72–87, 1989 (cit. on p. 29).

[101] N. Femia, G. Petrone, G. Spagnuolo, and M. Vitelli, *Power Electronics and Control Techniques for Maximum Energy Harvesting in Photovoltaic Systems*. CRC Press, 2012, vol. 11 (cit. on p. 31).

[102] J. Momoh, *Smart grid: Fundamentals of design and analysis*. Hoboken NJ : Wiley ; Piscataway : IEEE Press, 2012, 2012, vol. 63 (cit. on pp. 31, 65, 107).

[103] J. A. Duffie and W. A. Beckman, "Available solar radiation," in *Solar Engineering of Thermal Processes*. John Wiley & Sons, Inc., 2013, pp. 43–137, ISBN: 9781118671603. DOI: `10.1002/9781118671603.ch2`. [Online]. Available: `http://dx.doi.org/10.1002/9781118671603.ch2` (cit. on p. 32).

[104] All Small Wind Turbines, *Portal to the world of small wind turbines*, `http://www.allsmallwindturbines.com/`, Accessed: 2015-10-14 (cit. on p. 32).

[105] J. F. Manwell, J. G. McGowan, and A. L. Rogers, "Wind turbine design and testing," in *Wind Energy Explained*. John Wiley & Sons, Ltd, 2009, pp. 311–357, ISBN: 9781119994367. DOI: `10.1002/9781119994367.ch7`. [Online]. Available: `http://dx.doi.org/10.1002/9781119994367.ch7` (cit. on p. 32).

[106] T. Burton, D. Sharpe, N. Jenkins, and E. Bossanyi, "Wind-turbine performance," in *Wind Energy Handbook*, John Wiley & Sons, Ltd, 2002, pp. 173–207, ISBN: 9780470846063. DOI: `10.1002/0470846062.ch1`. [Online]. Available: `http://dx.doi.org/10.1002/0470846062.ch1` (cit. on p. 33).

[107] S. Al-Hallaj and K. Kiszynski, "Renewable energy sources and energy conversion devices," English, in *Hybrid Hydrogen Systems*, ser. Green Energy and Technology, Springer London, 2011, pp. 9–29, ISBN: 978-1-84628-466-3. DOI: `10.1007/978-1-84628-467-0_2`. [Online]. Available: `http://dx.doi.org/10.1007/978-1-84628-467-0_2` (cit. on p. 33).

[108] G. G. Moshi, A. Berizzi, and C. Bovo, "Grid connected systems for access to electricity: From microgrid to grid extension," English, in *Renewable Energy for Unleashing Sustainable Development*, E. Colombo, S. Bologna, and D. Masera, Eds., Springer International Publishing, 2013, pp. 99–132, ISBN: 978-3-319-00283-5. DOI: `10.1007/978-3-319-00284-2_5`. [Online]. Available: `http://dx.doi.org/10.1007/978-3-319-00284-2_5` (cit. on pp. 34, 42, 44).

[109] D. Rekioua and E. Matagne, *Optimization of photovoltaic power systems*. Springer, 2012 (cit. on p. 34).

[110] D. Olivares, C. Cañizares, and M. Kazerani, "A centralized energy management system for isolated microgrids," *Smart Grid, IEEE Transactions on*, vol. 5, no. 4, pp. 1864–1875, 2014, ISSN: 1949-3053. DOI: `10.1109/TSG.2013.2294187` (cit. on pp. 37, 62).

[111] J. F. Manwell and J. G. McGowan, “Lead acid battery storage model for hybrid energy systems,” *Solar Energy*, vol. 50, no. 5, pp. 399 –405, 1993, ISSN: 0038-092X. DOI: `http://dx.doi.org/10.1016/0038-092X(93)90060-2`. [Online]. Available: `http://www.sciencedirect.com/science/article/pii/0038092X93900602` (cit. on pp. 38, 39, 64).

[112] E. Vrettos and S. Papathanassiou, “Operating policy and optimal sizing of a high penetration res-bess system for small isolated grids,” *Energy Conversion, IEEE Transactions on*, vol. 26, no. 3, pp. 744–756, 2011, ISSN: 0885-8969. DOI: `10.1109/TEC.2011.2129571` (cit. on pp. 38, 64).

[113] H. Bindner, T. Cronin, P. Lundsager, J. F. Manwell, U. Abdulwahid, and I. Baring-Gould, *Lifetime modelling of lead acid batteries*. 2005 (cit. on p. 40).

[114] R. Kaiser *et al.*, “Development of battery lifetime models for energy storage systems in renewable energy systems (res).,” 2003 (cit. on p. 40).

[115] R. Dufo-López, J. M. Lujano-Rojas, and J. L. Bernal-Agustín, “Comparison of different lead–acid battery lifetime prediction models for use in simulation of stand-alone photovoltaic systems,” *Applied Energy*, vol. 115, pp. 242 –253, 2014, ISSN: 0306-2619. DOI: `http://dx.doi.org/10.1016/j.apenergy.2013.11.021`. [Online]. Available: `http://www.sciencedirect.com/science/article/pii/S0306261913009148` (cit. on p. 40).

[116] M. Nehrir, C. Wang, K. Strunz, H. Aki, R. Ramakumar, J. Bing, Z. Miao, and Z. Salameh, “A review of hybrid renewable/alternative energy systems for electric power generation: Configurations, control, and applications,” *Sustainable Energy, IEEE Transactions on*, vol. 2, no. 4, pp. 392–403, 2011, ISSN: 1949-3029. DOI: `10.1109/TSTE.2011.2157540` (cit. on pp. 42, 44).

[117] M. S. Carmeli, F. Castelli-Dezza, M. Mauri, G. Marchegiani, and D. Rosati, “Control strategies and configurations of hybrid distributed generation systems,” *Renewable Energy*, vol. 41, pp. 294 –305, 2012, ISSN: 0960-1481. DOI: `http://dx.doi.org/10.1016/j.renene.2011.11.010`. [Online]. Available: `http://www.sciencedirect.com/science/article/pii/S0960148111006124` (cit. on p. 42).

[118] E. Hossain, Z. Han, and H. V. Poor, Eds., *Smart Grid Communications and Networking*. Cambridge University Press, 2012, Cambridge Books Online, ISBN: 9781139013468. [Online]. Available: `http://dx.doi.org/10.1017/CBO9781139013468` (cit. on p. 44).

[119] Z. Wang, B. Chen, J. Wang, and J. Kim, “Decentralized energy management system for networked microgrids in grid-connected and islanded modes,” *Smart Grid, IEEE Transactions on*, vol. PP, no. 99, pp. 1–1, 2015, ISSN: 1949-3053. DOI: `10.1109/TSG.2015.2427371` (cit. on p. 44).

[120] B. Chowdhury and S. Rahman, “A review of recent advances in economic dispatch,” *Power Systems, IEEE Transactions on*, vol. 5, no. 4, pp. 1248–1259, 1990, ISSN: 0885-8950. DOI: `10.1109/59.99376` (cit. on p. 45).

[121] H. Happ, “Optimal power dispatch-a comprehensive survey,” *Power Apparatus and Systems, IEEE Transactions on*, vol. 96, no. 3, pp. 841–854, 1977, ISSN: 0018-9510. DOI: `10.1109/T-PAS.1977.32397` (cit. on p. 45).

[122] C. D. Barley and C. B. Winn, "Optimal dispatch strategy in remote hybrid power systems," *Solar Energy*, vol. 58, no. 4, pp. 165–179, 1996 (cit. on p. 47).

[123] R. Dufo-Lopez and J. L. Bernal-Agustín, "Design and control strategies of pv-diesel systems using genetic algorithms," *Solar energy*, vol. 79, no. 1, pp. 33–46, 2005 (cit. on p. 47).

[124] G. Moshi, C. Bovo, and A. Berizzi, "Optimal operational planning for pv-wind-diesel-battery microgrid," in *PowerTech, 2015 IEEE Eindhoven*, 2015, pp. 1–6. DOI: `10.1109/PTC.2015.7232461` (cit. on pp. 47, 116).

[125] S. Sen and D. Kothari, "An equivalencing technique for solving the large-scale thermal unit commitment problem," in *The Next Generation of Electric Power Unit Commitment Models*, ser. International Series in Operations Research & Management Science, B. F. Hobbs, M. H. Rothkopf, R. P. Ó Neill, and H.-p. Chao, Eds., vol. 36, Springer US, 2001, pp. 211–225, ISBN: 978-0-7923-7334-6. DOI: `10.1007/0-306-47663-0_12` (cit. on p. 50).

[126] S. Takriti, B. Krasenbrink, and L. S.-Y. Wu, "Incorporating fuel constraints and electricity spot prices into the stochastic unit commitment problem," *Operations Research*, vol. 48, no. 2, pp. 268–280, 2000 (cit. on pp. 51, 62).

[127] A. B. Lovins, *Small is profitable*. Rocky Mountain Institute, 2002 (cit. on p. 55).

[128] C. Nayar, S. Phillips, W. James, T. Pryor, and D. Remmer, "Novel wind/diesel/battery hybrid energy system," *Solar Energy*, vol. 51, no. 1, pp. 65 –78, 1993, ISSN: 0038-092X. DOI: `http://dx.doi.org/10.1016/0038-092X(93)90043-N` (cit. on p. 55).

[129] L. T. Blank and A. J. Tarquin, *Engineering Economy*, 6th. New York : McGraw-Hill, 2005, ISBN: 9780073205342. [Online]. Available: `http://trove.nla.gov.au/work/16654191` (cit. on p. 56).

[130] P. Groumpos and G. Papageorgiou, "An optimal sizing method for stand-alone photovoltaic power systems," *Solar Energy*, vol. 38, no. 5, pp. 341 –351, 1987, ISSN: 0038-092X. DOI: `http://dx.doi.org/10.1016/0038-092X(87)90006-5` (cit. on p. 56).

[131] E. S. Prassas and R. P. Roess, "Use of banking formulae in engineering economics," in *Engineering Economics and Finance for Transportation Infrastructure*, ser. Springer Tracts on Transportation and Traffic, vol. 3, Springer Berlin Heidelberg, 2013, pp. 29–71, ISBN: 978-3-642-38579-7. DOI: `10.1007/978-3-642-38580-3_3` (cit. on p. 56).

[132] Z. Wei and Y. Hongxing, "One optimal sizing method for designing hybrid solar-wind-diesel power generation systems," in *Proceedings of ISES World Congress 2007 (Vol. I–Vol. V)*, Springer, 2009, pp. 1489–1494 (cit. on p. 58).

[133] G. Mavrotas, D. Diakoulaki, K. Florios, and P. Georgiou, "A mathematical programming framework for energy planning in services' sector buildings under uncertainty in load demand: The case of a hospital in athens," *Energy Policy*, vol. 36, no. 7, pp. 2415 –2429, 2008, ISSN: 0301-4215. DOI: `http://dx.doi.org/10.1016/j.enpol.2008.01.011`. [Online]. Available: `http://www.sciencedirect.com/science/article/pii/S0301421508000104` (cit. on p. 68).

[134] M. Carvalho, M. A. Lozano, and L. M. Serra, "Multicriteria synthesis of trigeneration systems considering economic and environmental aspects," *Applied Energy*, vol. 91, no. 1, pp. 245 – 254, 2012, ISSN: 0306-2619. DOI: http://dx.doi.org/10.1016/j.apenergy.2011.09.029. [Online]. Available: http://www.sciencedirect.com/science/article/pii/S0306261911006325 (cit. on p. 68).

[135] J. Ortiga, J. Bruno, and A. Coronas, "Selection of typical days for the characterisation of energy demand in cogeneration and trigeneration optimisation models for buildings," *Energy Conversion and Management*, vol. 52, no. 4, pp. 1934 –1942, 2011, ISSN: 0196-8904. DOI: http://dx.doi.org/10.1016/j.enconman.2010.11.022. [Online]. Available: http://www.sciencedirect.com/science/article/pii/S0196890410005315 (cit. on p. 68).

[136] F. J. De Sisternes and M. D. Webster, "Optimal selection of sample weeks for approximating the net load in generation planning problems," Citeseer, Tech. Rep., 2013 (cit. on p. 68).

[137] J. Lee and S. Leyffer, *Mixed integer nonlinear programming*. Springer Science & Business Media, 2011, vol. 154 (cit. on p. 69).

[138] L. Kaufman and P. J. Rousseeuw, "Partitioning around medoids (program pam)," in *Finding Groups in Data*. John Wiley & Sons, Inc., 2008, pp. 68–125, ISBN: 9780470316801. DOI: 10.1002/9780470316801.ch2. [Online]. Available: http://dx.doi.org/10.1002/9780470316801.ch2 (cit. on p. 69).

[139] G. Gan, C. Ma, and J. Wu, *Data Clustering: Theory, Algorithms, and Applications*, ser. ASA-SIAM Series on Statistics and Applied Probability. Society for Industrial and Applied Mathematics, 2007, ISBN: 9780898716238. [Online]. Available: https://books.google.co.uk/books?id=ZXLSVPN1X1sC (cit. on p. 69).

[140] H.-S. Park and C.-H. Jun, "A simple and fast algorithm for k-medoids clustering," *Expert Systems with Applications*, vol. 36, no. 2, Part 2, pp. 3336 –3341, 2009, ISSN: 0957-4174. DOI: http://dx.doi.org/10.1016/j.eswa.2008.01.039. [Online]. Available: http://www.sciencedirect.com/science/article/pii/S095741740800081X (cit. on p. 72).

[141] F. Domínguez-Muñoz, J. M. Cejudo-López, A. Carrillo-Andrés, and M. Gallardo-Salazar, "Selection of typical demand days for chp optimization," *Energy and buildings*, vol. 43, no. 11, pp. 3036–3043, 2011 (cit. on p. 72).

[142] J. A. Duffie and W. A. Beckman, "Solar engineering of thermal processes," 2013 (cit. on p. 72).

[143] HOMER Energy, *Sample data files for homer pro:philippine village of sicud*, https://users.homerenergy.com/pages/file_download_pro, Accessed: 2015-07-14 (cit. on p. 74).

[144] H. Blennow, "Method for rural load estimations," (cit. on p. 76).

[145] G. Lena, "Rural electrification with pv hybrid systems," *International Energy Agency Photovoltaic Power Systems Programme, St. Ursen*, 2013 (cit. on p. 76).

[146] HOMER Energy, *Finding data to run homer*, http://support.homerenergy.com/index.php?/Knowledgebase/Article/View/487/113/10485, Accessed: 2015-06-5 (cit. on p. 77).

[147] A. Khodaei, S. Bahramirad, and M. Shahidehpour, "Microgrid planning under uncertainty," *Power Systems, IEEE Transactions on*, vol. 30, no. 5, pp. 2417–2425, 2015, ISSN: 0885-8950. DOI: 10.1109/TPWRS.2014.2361094 (cit. on pp. 87, 97).

[148] S. Soliman and A. Al-Kandari, *Electrical Load Forecasting: Modeling and Model Construction*. Elsevier Science, 2010, ISBN: 9780123815446. [Online]. Available: https://books.google.co.uk/books?id=a2Ty0O4r-uAC (cit. on p. 87).

[149] W.-C. Hong, "Introduction," English, in *Intelligent Energy Demand Forecasting*, ser. Lecture Notes in Energy, vol. 10, Springer London, 2013, pp. 1–20, ISBN: 978-1-4471-4967-5. DOI: 10.1007/978-1-4471-4968-2_1. [Online]. Available: http://dx.doi.org/10.1007/978-1-4471-4968-2_1 (cit. on p. 87).

[150] H. Al-Hamadi and S. Soliman, "Long-term/mid-term electric load forecasting based on short-term correlation and annual growth," *Electric Power Systems Research*, vol. 74, no. 3, pp. 353 – 361, 2005, ISSN: 0378-7796. DOI: http://dx.doi.org/10.1016/j.epsr.2004.10.015. [Online]. Available: http://www.sciencedirect.com/science/article/pii/S0378779605000817 (cit. on p. 87).

[151] J. King, A. Clifton, B.-M. Hodge, and L. RePPAE, *Validation of Power Output for the WIND Toolkit*. National Renewable Energy Laboratory, 2014 (cit. on p. 87).

[152] H. Asano, W. Ariki, and S. Bando, "Value of investment in a microgrid under uncertainty in the fuel price," in *Power and Energy Society General Meeting, 2010 IEEE*, 2010, pp. 1–5. DOI: 10.1109/PES.2010.5589804 (cit. on p. 88).

[153] S. Ahmed, "Two-stage stochastic integer programming: A brief introduction," in *Wiley Encyclopedia of Operations Research and Management Science*. John Wiley & Sons, Inc., 2010, ISBN: 9780470400531. DOI: 10.1002/9780470400531.eorms0092. [Online]. Available: http://dx.doi.org/10.1002/9780470400531.eorms0092 (cit. on p. 89).

[154] J. Birge and F. Louveaux, "Stochastic integer programs," English, in *Introduction to Stochastic Programming*, ser. Springer Series in Operations Research and Financial Engineering, Springer New York, 2011, pp. 289–338, ISBN: 978-1-4614-0236-7. DOI: 10.1007/978-1-4614-0237-4_7. [Online]. Available: http://dx.doi.org/10.1007/978-1-4614-0237-4_7 (cit. on p. 89).

[155] G. B. Dantzig, "Linear programming under uncertainty," *Management Science*, vol. 1, no. 3-4, pp. 197–206, 1955. DOI: 10.1287/mnsc.1.3-4.197. [Online]. Available: http://dx.doi.org/10.1287/mnsc.1.3-4.197 (cit. on p. 89).

[156] G. L. Nemhauser and L. A. Wolsey, *Integer and Combinatorial Optimization*. New York, NY, USA: Wiley-Interscience, 1988, ISBN: 0-471-82819-X (cit. on p. 90).

[157] R. Schultz, "Stochastic programming with integer variables," English, *Mathematical Programming*, vol. 97, no. 1-2, pp. 285–309, 2003, ISSN: 0025-5610. DOI: 10.1007/s10107-003-0445-z. [Online]. Available: http://dx.doi.org/10.1007/s10107-003-0445-z (cit. on p. 90).

[158] C. C. CarøE and R. Schultz, "Dual decomposition in stochastic integer programming," *Oper. Res. Lett.*, vol. 24, no. 1-2, pp. 37–45, Feb. 1999, ISSN: 0167-6377. DOI: `10.1016/S0167-6377(98)00050-9`. [Online]. Available: `http://dx.doi.org/10.1016/S0167-6377(98)00050-9` (cit. on p. 91).

[159] A. Conejo, M. Carrión, and J. Morales, "Stochastic programming fundamentals," English, in *Decision Making Under Uncertainty in Electricity Markets*, ser. International Series in Operations Research & Management Science, vol. 153, Springer US, 2010, pp. 27–62, ISBN: 978-1-4419-7420-4. DOI: `10.1007/978-1-4419-7421-1_2`. [Online]. Available: `http://dx.doi.org/10.1007/978-1-4419-7421-1_2` (cit. on p. 91).

[160] Z. Salameh, B. Borowy, and A. Amin, "Photovoltaic module-site matching based on the capacity factors," *Energy Conversion, IEEE Transactions on*, vol. 10, no. 2, pp. 326–332, 1995, ISSN: 0885-8969. DOI: `10.1109/60.391899` (cit. on p. 92).

[161] B. Borowy and Z. Salameh, "Optimum photovoltaic array size for a hybrid wind/pv system," *Energy Conversion, IEEE Transactions on*, vol. 9, no. 3, pp. 482–488, 1994, ISSN: 0885-8969. DOI: `10.1109/60.326466` (cit. on p. 92).

[162] G. M. Masters, "Wind power systems," in *Renewable and Efficient Electric Power Systems*. John Wiley & Sons, Inc., 2005, pp. 307–383, ISBN: 9780471668824. DOI: `10.1002/0471668826.ch6`. [Online]. Available: `http://dx.doi.org/10.1002/0471668826.ch6` (cit. on p. 93).

[163] M. Mazidi, A. Zakariazadeh, S. Jadid, and P. Siano, "Integrated scheduling of renewable generation and demand response programs in a microgrid," *Energy Conversion and Management*, vol. 86, pp. 1118 –1127, 2014, ISSN: 0196-8904. DOI: `http://dx.doi.org/10.1016/j.enconman.2014.06.078`. [Online]. Available: `http://www.sciencedirect.com/science/article/pii/S0196890414006037` (cit. on p. 93).

[164] H. Yu, C. Chung, K. Wong, H. Lee, and J. Zhang, "Probabilistic load flow evaluation with hybrid latin hypercube sampling and cholesky decomposition," *Power Systems, IEEE Transactions on*, vol. 24, no. 2, pp. 661–667, 2009, ISSN: 0885-8950. DOI: `10.1109/TPWRS.2009.2016589` (cit. on p. 93).

[165] P. Jirutitijaroen and C. Singh, "Reliability constrained multi-area adequacy planning using stochastic programming with sample-average approximations," *Power Systems, IEEE Transactions on*, vol. 23, no. 2, pp. 504–513, 2008, ISSN: 0885-8950. DOI: `10.1109/TPWRS.2008.919422` (cit. on p. 94).

[166] A. Singhee and R. Rutenbar, "Why quasi-monte carlo is better than monte carlo or latin hypercube sampling for statistical circuit analysis," *Computer-Aided Design of Integrated Circuits and Systems, IEEE Transactions on*, vol. 29, no. 11, pp. 1763–1776, 2010, ISSN: 0278-0070. DOI: `10.1109/TCAD.2010.2062750` (cit. on p. 94).

[167] D. P. Kroese, T. Taimre, and Z. I. Botev, "Variance reduction," in *Handbook of Monte Carlo Methods*. John Wiley & Sons, Inc., 2011, pp. 347–380, ISBN: 9781118014967. DOI: `10.1002/9781118014967.ch9`. [Online]. Available: `http://dx.doi.org/10.1002/9781118014967.ch9` (cit. on p. 94).

[168] Z. Shu and P. Jirutitijaroen, "Latin hypercube sampling techniques for power systems reliability analysis with renewable energy sources," *Power Systems, IEEE Transactions on*, vol. 26, no. 4, pp. 2066–2073, 2011, ISSN: 0885-8950. DOI: 10.1109/TPWRS.2011.2113380 (cit. on p. 94).

[169] X. Xu and Z. Yan, "Probabilistic load flow evaluation with hybrid latin hypercube sampling and multiple linear regression," in *Power Energy Society General Meeting, 2015 IEEE*, 2015, pp. 1–5. DOI: 10.1109/PESGM.2015.7285724 (cit. on p. 94).

[170] GAMS Development Corporation, *Gams documentation 24.5 scenred2*, https://www.gams.com/help/index.jsp?topic=%2Fgams.doc%2Ftools%2Fscenred2%2Findex.html, Accessed: 2015-10-15 (cit. on pp. 95, 127).

[171] N. Growe-Kuska, H. Heitsch, and W. Romisch, "Scenario reduction and scenario tree construction for power management problems," in *Power Tech Conference Proceedings, 2003 IEEE Bologna*, vol. 3, 2003, 7 pp. Vol.3–. DOI: 10.1109/PTC.2003.1304379 (cit. on p. 95).

[172] T. Follestad, O. Wolfgang, and M. M. Belsnes, "An approach for assessing the effect of scenario tree approximations in stochastic hydropower scheduling models," *17th PSCC Proceedings*, 2011 (cit. on p. 95).

[173] D. Bertsimas, D. B. Brown, and C. Caramanis, "Theory and applications of robust optimization," *SIAM Review*, vol. 53, no. 3, pp. 464–501, 2011. DOI: 10.1137/080734510. eprint: http://dx.doi.org/10.1137/080734510. [Online]. Available: http://dx.doi.org/10.1137/080734510 (cit. on p. 96).

[174] V. Gabrel, C. Murat, and A. Thiele, "Recent advances in robust optimization: An overview," *European Journal of Operational Research*, vol. 235, no. 3, pp. 471 –483, 2014, ISSN: 0377-2217. DOI: http://dx.doi.org/10.1016/j.ejor.2013.09.036. [Online]. Available: http://www.sciencedirect.com/science/article/pii/S0377221713007911 (cit. on p. 96).

[175] A. Ben-Tal, L. El Ghaoui, and A. Nemirovski, *Robust optimization*. Princeton University Press, 2009 (cit. on pp. 96, 97, 100).

[176] A. L. Soyster, "Convex programming with set-inclusive constraints and applications to inexact linear programming," *Operations Research*, vol. 21, no. 5, pp. 1154–1157, 1973, ISSN: 0030364X. [Online]. Available: http://www.jstor.org/stable/168933 (cit. on pp. 96, 97).

[177] A. Ben-Tal and A. Nemirovski, "Robust solutions of linear programming problems contaminated with uncertain data," *Mathematical programming*, vol. 88, no. 3, pp. 411–424, 2000 (cit. on p. 96).

[178] A. Ben-Tal and A. Nemirovski, "Robust convex optimization," *Mathematics of Operations Research*, vol. 23, no. 4, pp. 769–805, 1998 (cit. on p. 96).

[179] D. Bertsimas and M. Sim, "The price of robustness," *Operations research*, vol. 52, no. 1, pp. 35–53, 2004 (cit. on p. 96).

[180] K. Hedman, M. Zhang, A. Dominguez-Garcia, K. Moslehi, X. Wang, and K. Cheung, "The application of robust optimization in power systems," Power Systems Engineering Research Center, Tech. Rep., Aug. 2014 (cit. on p. 96).

[181] S. A. Malcolm and S. A. Zenios, “Robust optimization for power systems capacity expansion under uncertainty,” *The Journal of the Operational Research Society*, vol. 45, no. 9, pp. 1040–1049, 1994, ISSN: 01605682. [Online]. Available: `http://www.jstor.org/stable/2584145` (cit. on p. 97).

[182] A. Korad and K. Hedman, “Robust corrective topology control for system reliability,” *Power Systems, IEEE Transactions on*, vol. 28, no. 4, pp. 4042–4051, 2013, ISSN: 0885-8950. DOI: `10.1109/TPWRS.2013.2267751` (cit. on p. 97).

[183] L. Baringo and A. Conejo, “Offering strategy via robust optimization,” *Power Systems, IEEE Transactions on*, vol. 26, no. 3, pp. 1418–1425, 2011, ISSN: 0885-8950. DOI: `10.1109/TPWRS.2010.2092793` (cit. on p. 97).

[184] D. Bertsimas, E. Litvinov, X. Sun, J. Zhao, and T. Zheng, “Adaptive robust optimization for the security constrained unit commitment problem,” *Power Systems, IEEE Transactions on*, vol. 28, no. 1, pp. 52–63, 2013, ISSN: 0885-8950. DOI: `10.1109/TPWRS.2012.2205021` (cit. on p. 97).

[185] L. Zhao and B. Zeng, “Robust unit commitment problem with demand response and wind energy,” in *Power and Energy Society General Meeting, 2012 IEEE*, 2012, pp. 1–8. DOI: `10.1109/PESGM.2012.6344860` (cit. on p. 97).

[186] R. Jiang, J. Wang, and Y. Guan, “Robust unit commitment with wind power and pumped storage hydro,” *Power Systems, IEEE Transactions on*, vol. 27, no. 2, pp. 800–810, 2012, ISSN: 0885-8950. DOI: `10.1109/TPWRS.2011.2169817` (cit. on p. 97).

[187] R. Jiang, J. Wang, M. Zhang, and Y. Guan, “Two-stage minimax regret robust unit commitment,” *Power Systems, IEEE Transactions on*, vol. 28, no. 3, pp. 2271–2282, 2013, ISSN: 0885-8950. DOI: `10.1109/TPWRS.2013.2250530` (cit. on p. 97).

[188] Z. Wang, B. Chen, J. Wang, J. Kim, and M. Begovic, “Robust optimization based optimal dg placement in microgrids,” *Smart Grid, IEEE Transactions on*, vol. 5, no. 5, pp. 2173–2182, 2014, ISSN: 1949-3053. DOI: `10.1109/TSG.2014.2321748` (cit. on p. 97).

[189] R. Jabr, “Robust transmission network expansion planning with uncertain renewable generation and loads,” *Power Systems, IEEE Transactions on*, vol. 28, no. 4, pp. 4558–4567, 2013, ISSN: 0885-8950. DOI: `10.1109/TPWRS.2013.2267058` (cit. on p. 97).

[190] T. Dragicevic, H. Pandzic, D. Skrlec, I. Kuzle, J. Guerrero, and D. Kirschen, “Capacity optimization of renewable energy sources and battery storage in an autonomous telecommunication facility,” *Sustainable Energy, IEEE Transactions on*, vol. 5, no. 4, pp. 1367–1378, 2014 (cit. on p. 97).

[191] M. Shabanzadeh, M.-K. Sheikh-El-Eslami, and M.-R. Haghifam, “The design of a risk-hedging tool for virtual power plants via robust optimization approach,” *Applied Energy*, vol. 155, pp. 766 –777, 2015, ISSN: 0306-2619. DOI: `http://dx.doi.org/10.1016/j.apenergy.2015.06.059`. [Online]. Available: `http://www.sciencedirect.com/science/article/pii/S030626191500817X` (cit. on p. 97).

[192] D. Bertsimas and M. Sim, “The price of robustness,” *Operations research*, vol. 52, no. 1, pp. 35–53, 2004 (cit. on pp. 98, 109).

[193] A. Ben-Tal, A. Goryashko, E. Guslitzer, and A. Nemirovski, “Adjustable robust solutions of uncertain linear programs,” English, *Mathematical Programming*, vol. 99, no. 2, pp. 351–376, 2004, ISSN: 0025-5610. DOI: 10.1007/s10107-003-0454-y. [Online]. Available: http://dx.doi.org/10.1007/s10107-003-0454-y (cit. on p. 98).

[194] A. Schöbel, “Generalized light robustness and the trade-off between robustness and nominal quality,” English, *Mathematical Methods of Operations Research*, vol. 80, no. 2, pp. 161–191, 2014, ISSN: 1432-2994. DOI: 10.1007/s00186-014-0474-9. [Online]. Available: http://dx.doi.org/10.1007/s00186-014-0474-9 (cit. on p. 98).

[195] S. Cicerone, G. D’Angelo, G. Di Stefano, D. Frigioni, A. Navarra, M. Schachtebeck, and A. Schöbel, “Recoverable robustness in shunting and timetabling,” English, in *Robust and Online Large-Scale Optimization*, ser. Lecture Notes in Computer Science, R. Ahuja, R. Möhring, and C. Zaroliagis, Eds., vol. 5868, Springer Berlin Heidelberg, 2009, pp. 28–60, ISBN: 978-3-642-05464-8. DOI: 10.1007/978-3-642-05465-5_2. [Online]. Available: http://dx.doi.org/10.1007/978-3-642-05465-5_2 (cit. on p. 98).

[196] M. Goerigk and A. Schöbel, “Algorithm engineering in robust optimization,” *ArXiv preprint arXiv:1505.04901*, 2015 (cit. on pp. 98, 112).

[197] P. Kouvelis and G. Yu, *Robust Discrete Optimization and Its Applications*, ser. Nonconvex Optimization and Its Applications. Springer US, 1996, ISBN: 9780792342915. [Online]. Available: https://books.google.co.uk/books?id=58qr2Dx1iIkC (cit. on p. 98).

[198] A. Ben-Tal, D. Bertsimas, and D. B. Brown, “A soft robust model for optimization under ambiguity,” *Operations Research*, vol. 58, no. 4-part-2, pp. 1220–1234, 2010. DOI: 10.1287/opre.1100.0821. eprint: http://dx.doi.org/10.1287/opre.1100.0821. [Online]. Available: http://dx.doi.org/10.1287/opre.1100.0821 (cit. on p. 98).

[199] A. Ben-Tal, S. Boyd, and A. Nemirovski, “Extending scope of robust optimization: Comprehensive robust counterparts of uncertain problems,” English, *Mathematical Programming*, vol. 107, no. 1-2, pp. 63–89, 2006, ISSN: 0025-5610. DOI: 10.1007/s10107-005-0679-z. [Online]. Available: http://dx.doi.org/10.1007/s10107-005-0679-z (cit. on p. 98).

[200] D. Bienstock and N. Özbay, “Computing robust basestock levels,” *Discrete Optimization*, vol. 5, no. 2, pp. 389 –414, 2008, In Memory of George B. Dantzig, ISSN: 1572-5286. DOI: http://dx.doi.org/10.1016/j.disopt.2006.12.002. [Online]. Available: http://www.sciencedirect.com/science/article/pii/S1572528607000382 (cit. on p. 100).

[201] M. Fischetti and M. Monaci, “Cutting plane versus compact formulations for uncertain (integer) linear programs,” English, *Mathematical Programming Computation*, vol. 4, no. 3, pp. 239–273, 2012, ISSN: 1867-2949. DOI: 10.1007/s12532-012-0039-y. [Online]. Available: http://dx.doi.org/10.1007/s12532-012-0039-y (cit. on p. 100).

[202] D. Bertsimas, I. Dunning, and M. Lubin, “Reformulation versus cutting-planes for robust optimization,” English, *Computational Management Science*, pp. 1–23, 2015, ISSN: 1619-697X. DOI: 10.1007/s10287-015-0236-z. [Online]. Available: http://dx.doi.org/10.1007/s10287-015-0236-z (cit. on p. 100).

[203] D. Bertsimas and M. Sim, "Robust discrete optimization and network flows," English, *Mathematical Programming*, vol. 98, no. 1-3, pp. 49–71, 2003, ISSN: 0025-5610. DOI: 10.1007/s10107-003-0396-4. [Online]. Available: http://dx.doi.org/10.1007/s10107-003-0396-4 (cit. on p. 101).

[204] D. Bertsimas and A. Thiele, "A robust optimization approach to inventory theory," *Operations Research*, vol. 54, no. 1, pp. 150–168, 2006 (cit. on p. 109).

[205] B. L. Gorissen, İhsan Yanıkoğlu, and D. den Hertog, "A practical guide to robust optimization," *Omega*, vol. 53, pp. 124 –137, 2015, ISSN: 0305-0483. DOI: http://dx.doi.org/10.1016/j.omega.2014.12.006. [Online]. Available: http://www.sciencedirect.com/science/article/pii/S0305048314001698 (cit. on p. 109).